Distribution Agreement

In presenting this thesis or dissertation as a partial fulfillment of the requirements for an advanced degree from Emory University, I hereby grant to Emory University and its agents the non-exclusive license to archive, make accessible, and display my thesis or dissertation in whole or in part in all forms of media, now or hereafter known, including display on the world wide web. I understand that I may select some access restrictions as part of the online submission of this thesis or dissertation. I retain all ownership rights to the copyright of the thesis or dissertation. I also retain the right to use in future works (such as articles or books) all or part of this thesis or dissertation.

_____ _____

Ana Cheng Jaramillo Date

Targeting Bacterial Tolerance and Resistance with Small Molecules

Ana Victoria Cheng Jaramillo

Doctor of Philosophy
Chemistry

_____

William M. Wuest, Ph.D.
Advisor

_____

Simon B. Blakey
Committee Member

_____

Dennis C. Liotta
Committee Member

Accepted:

_____

Kimberly J. Arriola
Dean of the Laney Graduate School

_____

Date

Targeting Bacterial Tolerance and Resistance with Small Molecules

Ana Victoria Cheng Jaramillo
B.A., New College of Florida, 2017

William M. Wuest, Ph.D.
Advisor

An abstract of a dissertation submitted to the faculty of the James T. Laney School of Graduate Studies of Emory University in partial fulfillment of the requirements for the degree of Doctor of Philosophy in Chemistry.

2021

Abstract

Targeting Bacterial Tolerance and Resistance with Small Molecules

Ana Victoria Cheng Jaramillo

The overuse and misuse of antibiotics has put evolutionary pressure on bacteria to alter or bypass the targets of drugs or otherwise develop resistance, rendering a large percentage of our available medicines and pesticides ineffective. Novel antibiotics are quickly met with resistance, and treatment efforts are further complicated by bacterial tolerance mechanisms. Altogether we are facing a perfect storm of resistance and tolerance which threatens to kill millions and unravel our current approach to medicine in the process. I have focused my research efforts on two classes of molecules: 1) synthetic retinoids that can kill bacterial persisters with low resistance development potential, and 2) small molecule inhibitors of LexA, the gatekeeper of the bacterial SOS response.

Targeting Bacterial Tolerance and Resistance with Small Molecules

Ana Victoria Cheng Jaramillo
B.A., New College of Florida, 2017

William M. Wuest, Ph.D.
Advisor

A dissertation submitted to the faculty of the James T. Laney School of Graduate Studies of Emory University in partial fulfillment of the requirements for the degree of Doctor of Philosophy in Chemistry.

2021

Table of Contents

Figures and Tables

Chapter 1. Introduction

1.1 A Brief History

Human use of antibiotics predates modern drugs by thousands of years.[1] Various herbs, plants, and minerals such as St. John's Wort (*Hypericum perforatum*), aloe, and malachite have been used throughout history to treat burns, wounds, and other infections.[2,3] For example, multiple cultures and texts recommend molds as treatments for surface wounds. It is likely that the healers in these communities kept cultures of *Penicillium* or *Aspergillus* species which produce multiple antibiotic compounds such as penicillin, though they might not have known the exact mechanism(s) of antibacterial action.

In one famous example of an "ancientbiotic," a 10th century Anglo-Saxon leechbook details the careful preparation of a salve for the treatment of a sty caused by the bacterium *Staphylococcus aureus*. The recipe includes multiple ingredients known to have antibacterial activity—garlic, onion, wine, and oxgall combined in a brass or bronze (copper alloys) vessel and left to stand for nine days. In 2015 researchers empirically tested this recipe and verified its ability to kill methicillin-resistant *S. aureus* (MRSA).[4] Although each individual component was not wholly effective in killing bacteria, the combination proved synergistic. Another investigation identified some molecules belonging to the flavonoid family in traditional Chinese medicinal plants used to treat infectious gastroenteritis.[5] These and other recent studies have served to corroborate the knowledge passed down through folklore and medical texts, speaking to the advanced expertise and careful trial-and-error performed by past civilizations and demonstrating the rich history of antibiotic use predating modern-day drugs.

It wasn't until the early 1900s that the first modern antibiotic was discovered. Many histories of antibiotics mistakenly begin with the tale of penicillin, but it is a common misconception that it was the first modern antibiotic. Paul Ehrlich (University of Göttingen) beat penicillin to the punch in 1907 with his development of the syphilis drug Salvarsan (or arsphenamine, as it is known today), introduced in clinics in 1910. He referred to his discovery as a *magic bullet* for its ability to selectively target infection, with little toxic effect on the human host.

Figure 1.1: World War II era penicillin poster. (Source: Science History Institute. Public Domain.)

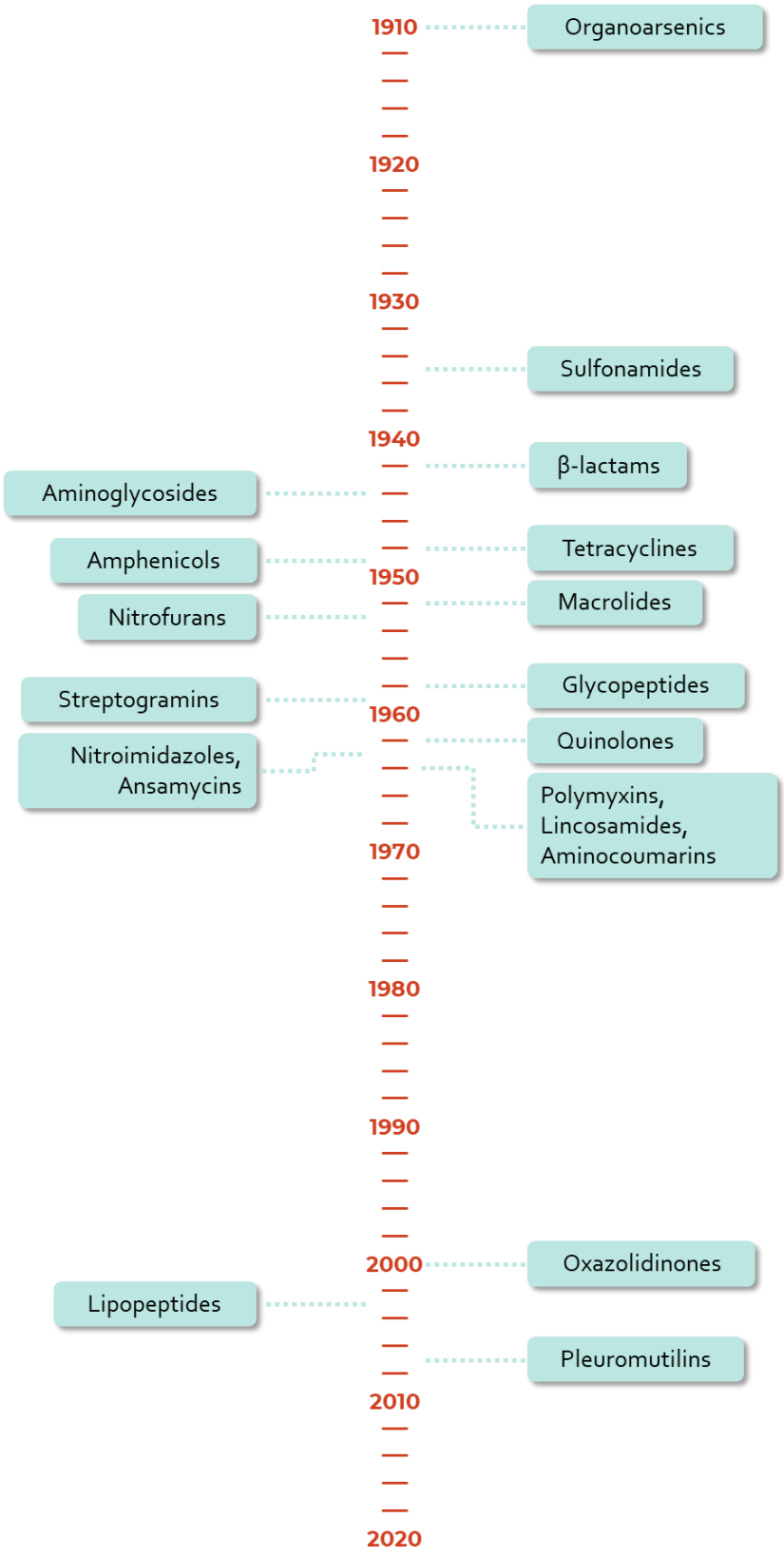

Figure 1.2: Timeline of antibiotic commercial application.

Some years later the first natural product antibiotic, penicillin, was (re)discovered by Alexander Fleming. Though multiple researchers between 1870 and 1920 had observed the ability of *Penicillium* species to prevent the growth of bacteria, their findings received little attention. Fleming observed the effect of mold on *S. aureus* in 1928, but it was not until 1938 that Howard Florey and his team at Oxford University (including Ernst Chain, who later shared the Nobel Prize in Medicine with Fleming and Florey) identified penicillin as the active antibacterial compound in the mold, leading to its clinical application in 1942 (Figure 1.1). It was followed by a flurry of discovery: between the 1940s and 1970s, over 20 new classes of antibiotics were approved by the United States Food and Drug Administration (FDA), a time commonly referred to as the "Golden Age" or "Golden Era" of antibiotics (Figure 1.2).

1.2 Antibiotic Overview

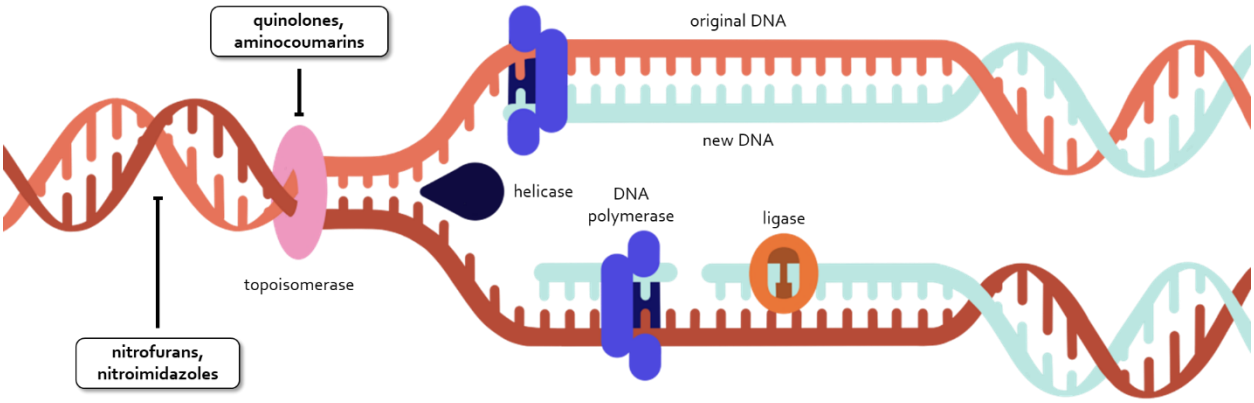

Figure 1.3: DNA synthesis-targeting antibiotics. Not shown: folate acid inhibitors (sulfonamides).

In general, antibiotics disrupt the normal function of a bacterial cell, rendering it unable to divide properly or damaging it so severely that it dies. Typically, this is done through the binding of a small molecule inhibitor to an enzyme, though some bind to or damage cell structures directly. Although there exist at least 200 conserved essential

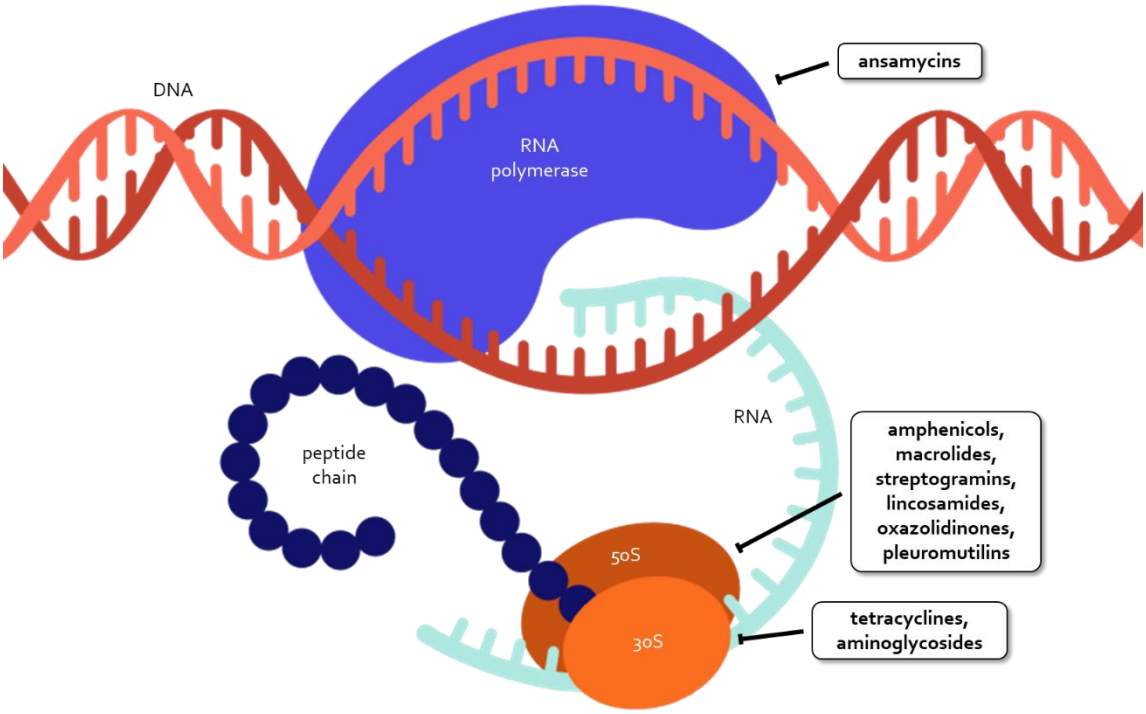

Figure 1.4: RNA and protein synthesis-targeting antibiotics.

proteins in bacteria, most antibiotics target one of just four processes: DNA synthesis (Figure 1.3), ribonucleic acid (RNA) synthesis, protein synthesis (Figure 1.4), or cell wall synthesis (Figure 1.5).[6] The enzymes involved in these systems are structurally different from their counterparts in eukaryotic cells or are totally nonexistent in eukaryotes, enabling their inhibitors to disrupt bacteria while leaving the host undisturbed.

Antibiotics vary widely in structure, function, and effects, necessitating multiple methods of classification. For example, antibacterials are commonly categorized as either bactericidal or bacteriostatic depending on whether they kill bacteria or simply inhibit their growth (respectively). The words stem from the Latin *-cida* (to kill) and *-statica* (to stand, balance). This designation is somewhat fuzzy, as there are bactericidal antibiotics that exhibit a bacteriostatic effect at lower concentrations and bacteriostatic antibiotics that exhibit a bactericidal effect at higher concentrations. Additionally, it is not predictive of the

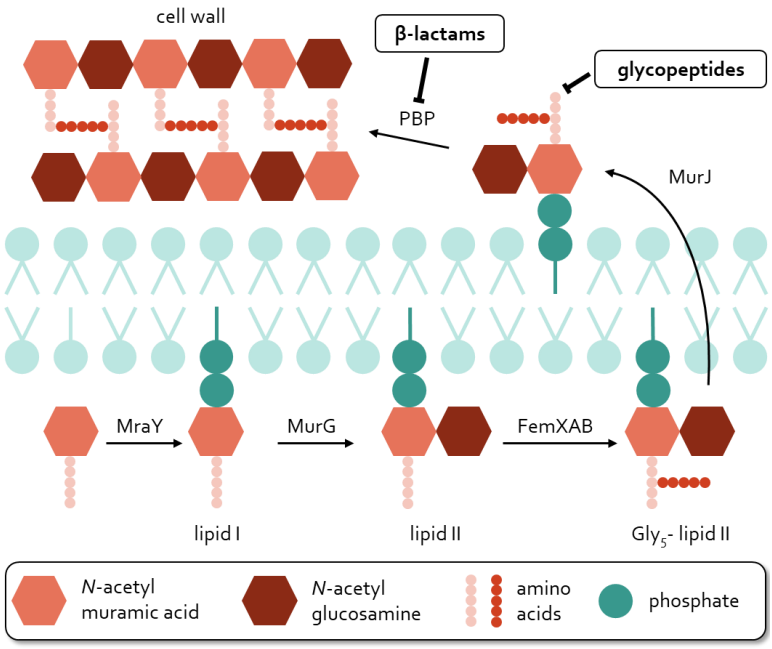

Figure 1.5: Cell wall synthesis-targeting antibiotics.

action of an antibiotic in the human body—a complicated system prone to fluctuations in infection site conditions and drug concentrations, as well as variation from person to person. There is an argument that concentration- vs. time-dependent killing may be a more useful classification since bacteriostatic drugs display bactericidal properties if given more time, while other drugs (like penicillin) appear to reach a concentration of peak activity.[7] However, this measure is not yet standard and thus lacks enough evidence to support clinical relevance.

Another common categorization of antibiotics specifies the range of species of bacteria they are effective against. The term broad-spectrum is typically applied to antibiotics with activity against both Gram-positive and Gram-negative bacteria (though this does not necessarily mean they are effective against *all* species). In contrast, narrow-spectrum agents are effective against a smaller group of bacteria—sometimes as small as a single species.[8] Prescription of broad-spectrum antibiotics does not require a diagnostic test

to ascertain the species causing a patient's illness, unlike narrow-spectrum drugs. However, they are accompanied by certain risks. Broad-spectrum agents place antibiotic pressure on not only the cause of an infection, but also on other species of bacteria present in a patient's body, potentially contributing to antibiotic resistance (discussed in section 1.3). They can also kill commensal bacteria in the microbiome, leading to dysbiosis. Narrow-spectrum antibiotics, in comparison, mostly eschew these risks due to their enhanced ability to target the cause of an infection while leaving the microbiome largely undisturbed. Unfortunately, there is a cultural preference within the pharmaceutical industry and medicine for broad-spectrum drugs since they can be prescribed more easily and have a comparatively larger market due to their broad applicability. Since narrow-spectrum agents can be prescribed in fewer cases, there is less incentive to develop and prescribe them, despite their advantages in decreasing side effects and resistance.

Finally, all antibiotics fall within one of three groups based on their origin: natural products, synthetics, or semi-synthetics. Natural products are compounds produced by living organisms. While some are derived from plants and herbs, a majority of natural product antibiotics come from bacteria themselves. In nature, microbes wage biological warfare on each other as they compete for space and resources. One of the main mechanisms they employ is the production and excretion of antimicrobial compounds to eliminate their competition. As a result, we have been able to exploit these compounds for medicinal use. Over 200 antibiotic drugs are direct natural products.[9] These natural antibiotics often feature intricate polycyclic carbon systems with multiple chiral centers which are easily synthesized by enzymes. In comparison, synthetic compounds are completely human-designed and typically primarily contain aromatic rings and heterocycles. However, many

drugs (some 250) are semi-synthetic, meaning that medicinal chemists have optimized a natural product through trial-and-error modifications of the chemical structure.[9] Antibiotics with related structures derived from similar origins are organized into groups called classes.

1.3 Resistance

Resistance is the ability of a bacterium to survive antibiotic treatment due to an advantageous genetic change, quantified in the laboratory by a corresponding increase in the effective MIC of the applied antibiotic. It is a manifestation of natural selection: antibiotic pressure stifles the growth of or eliminates susceptible cells in a population, enriching those with beneficial resistant mutations in the gene pool. And though the rule of natural selection holds true for all life, the evolutionary clock is dramatically faster for bacteria than for organisms that reproduce at slower rates. If their success has proven anything, it is that they are nature's most adaptive machines.

Paradoxically, the advent of modern antibiotics has seemingly expedited the spread of resistance due to improper use. The attitude toward antibiotics as "cure-all" solutions rather than precious resources to be used sparingly is one of the main causes of antibiotic resistance. The CDC estimates that 47 million courses of antibiotics are unnecessarily prescribed each year, accounting for 30% of all antibiotic prescriptions.[10] Accurate diagnosis and proper prescription require a diagnostic test, but few rapid tests exist. Thus, a blood test is usually required to identify the cause of an infection. This leaves sick patients waiting several days for test results. Instead, many clinicians default to prescribing broad-spectrum drugs to offer an immediate solution. However, unnecessary exposure to antibiotics can have deleterious effects on a patient's microbiome and lead to resistance among commensal species—which can later be transferred to pathogenic bacteria. Many patients are also

mislabeled with β-lactam allergies and are prescribed alternate antibiotics often associated with lower efficacy or increased side effects, such as glycopeptides or fluoroquinolones.[11] Subsequently, these patients are at higher risk for adverse outcomes and infection by resistant bacteria.

Perhaps the most egregious misuse of antibiotics is in the context of animal husbandry. Every year, 73% of all manufactured antibiotics are used for this purpose, including some of the most important classes of antibiotics in human healthcare.[12] Though

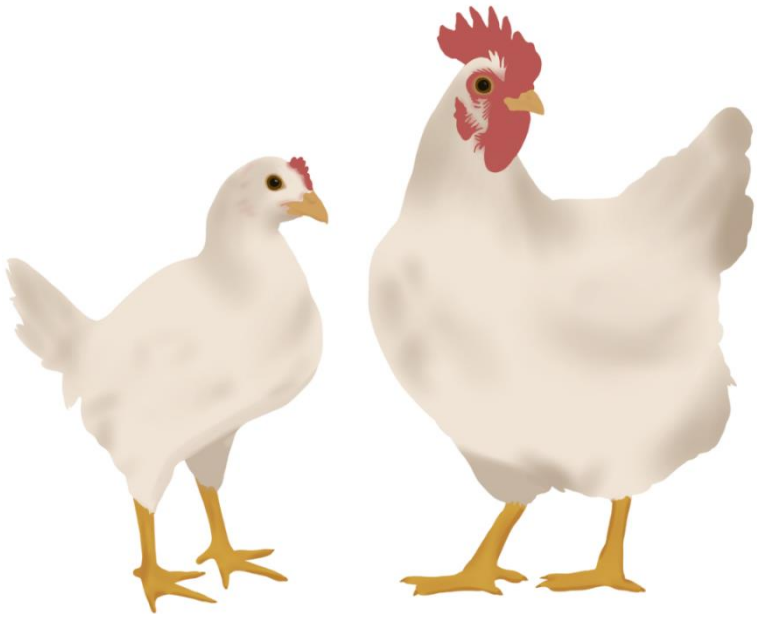

Figure 1.6: Antibiotic food additives. Chickens fed *Streptomyces aureofaciens* mash supplement (right) grow up to 2.5x the size of those fed no supplements.[14]

they are sometimes necessary for veterinary medicine should an animal fall ill, they have primarily been used as feed additives in the rearing of livestock to improve growth (Figure 1.6) and as prophylactics.[13,14] Medicated feed is also used in fish farming, and in some instances, antibiotics are even sprayed directly onto the surface of the water. As a consequence of this exposure, farmed animals' gastrointestinal tracts are bustling breeding grounds for resistant bacteria. These resistant strains as well as undigested antibiotics

themselves[15] are then spread through animal urine and feces, contaminated meat, and animal byproducts to consumers and the environment.

Campylobacter is a genus of Gram-negative bacteria most often transmitted through ingestion of contaminated poultry and raw dairy products (a result of antibiotic animal feed additives). However, they do not easily survive stomach acid so serious illness is only observed in cases of exposure to a large number of bacteria. *Campylobacter jejuni* and *Campylobacter coli* are the most common causes of these infections. Altogether, the genus causes 1.5 million infections a year (in the United States), 448,400 of which are fluoroquinolone or macrolide resistant.[10]

In 2017, the FDA asked pharmaceutical companies to relabel antibiotics used in human medicine to remove livestock feed as an approved usage. However, this call was voluntary and, though it was accompanied by a decrease in livestock-related antibiotic sales, an alarming number of drugs are still used as feed additives. Additionally, the global use of antibiotics in farming has risen every year as the practice gains popularity in more countries. Pesticides and pharmaceutical waste are two other sources of environmental antibiotic exposure which follow trajectories like those of feed additives—spreading through either food crops or the water supply. It is through this constant, low-dosage exposure to so much of our antibiotic arsenal that the bacterial gene pool in our bodies, food, and the environment is being constantly strengthened under evolutionary pressure.

Though antibiotic-producing microbes possess intrinsic resistance, clinically relevant antibiotic resistance arises either from mutagenesis or through transfer of genes from one bacterium to another. Mutations occur due to mistakes made by typical DNA polymerases or through the action of repair mechanisms triggered by environmental stress. When met with

DNA damage, a lack of nutrients, or other extreme conditions, established stress responses deploy a host of enzymes to alleviate and prevent damage. These enzymes include error-prone polymerases which introduce mutations at a higher rate than those responsible for normal DNA synthesis.[16]

Resistance genes (acquired or intrinsic) can be disseminated to other bacteria through a phenomenon known as horizontal gene transfer (HGT). HGT enables the lateral sharing of genes between species of bacteria and is the primary culprit in the spread of antibiotic resistance. It does not require the transfer of the genome in its entirety—as few as a single gene may be transferred at a time—though it can. A reasonably complex process, HGT can happen through multiple mechanisms: conjugation, transduction, or

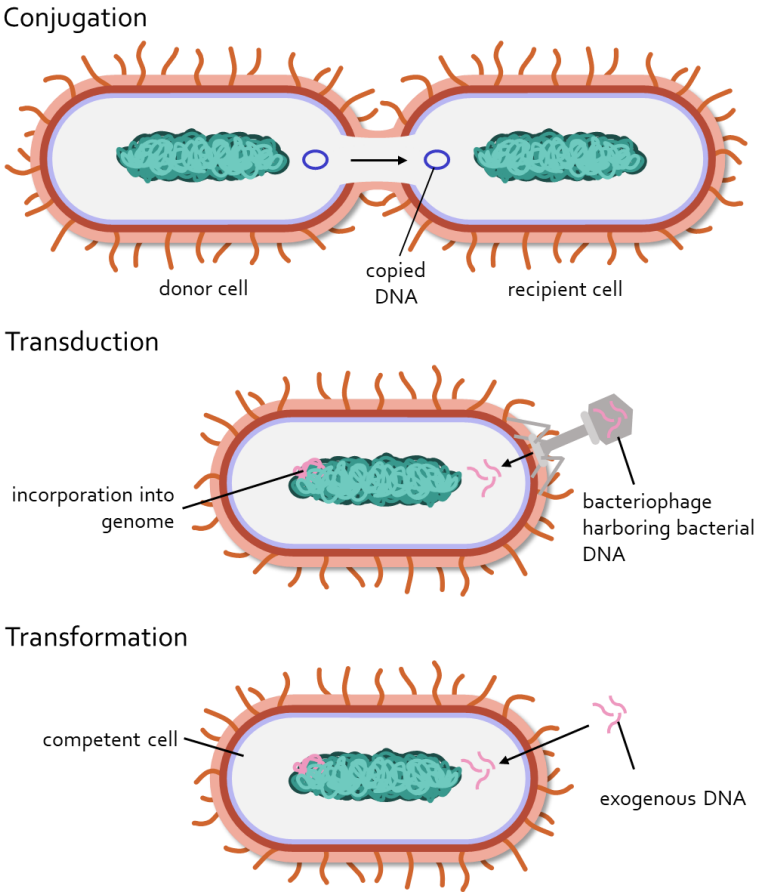

Figure 1.7: Horizontal gene transfer mechanisms

transformation (Figure 1.7).[17] The mobile genetic elements transferred in these processes are commonly termed pathogenicity islands or gene cassettes and play roles in both resistance and virulence.

Several islands and cassettes have been shown to confer resistance to antibiotics, such as the staphylococcal cassette chromosome *mec* (SCC*mec*). SCC*mec* is the hallmark of MRSA strains (Table 4.1). It contains the *mecA* gene which encodes an alternative penicillin binding protein with low affinity for ß-lactam antibiotics (PBP2a). This cassette may have been transferred to *S. aureus* from the human commensal bacterium *Staphylococcus epidermis*, though researchers are yet uncertain.[18] Inter-genus transfers are also possible, like in the case of vancomycin-resistant *S. aureus*, which is believed to have acquired the resistant *vanA* gene from vancomycin-resistant *Enterococcus*.[19]

Bacteria can also develop cross-resistance, or resistance to one drug as a result of resistance to a similarly acting drug conferred by a single genetic determinant. It has the highest potential of occurring when two antibiotics share a common binding site, target, or other pathway of action and is most common within a class of antibiotics. Researchers have voiced concerns about cross-resistance since during the antibiotic Golden Era.[20]

On a biochemical level, there are a few ways that bacteria may resist the effects of an antibiotic. These mechanisms are not mutually exclusive and may cumulatively contribute to heightened levels of resistance in a bacterium. The first is through direct drug modification: bacteria can produce enzymes that remove an active moiety from a drug or append a group to reduce its ability to bind to its target.[21–23] Other resistance mechanisms involve altering the other participant in a drug–target interaction—the enzyme or substrate target. Enzyme alteration often arises from point mutations in the binding site of an

antibiotic to decrease its affinity for the target without substantially affecting enzyme activity, or through modification of a target enzyme by another enzyme. It may also mean production of an alternative enzyme with similar catalytic activity altogether.[24–26] Bacteria may also resist antibiotics by overproducing or completely circumventing the drug target.[27,28]

ß-lactamases are an ancient group of enzymes that deactivate ß-lactam antibiotics. They have no apparent function other than to hydrolyze the ß-lactam ring which is integral to the antibiotics' ability to inhibit the transpeptidases involved in cell wall synthesis. A large class of enzymes with several subtypes, ß-lactamases are most commonly produced by Gram-negative bacteria, although a few instances of expression by Gram-positive species such as *S. aureus* and *Enterococcus faecalis* have been reported.[21] Typical ß-lactamases do not hydrolyze expanded-spectrum cephalosporins. However, in the past 40 years or so, new extended-spectrum ß-lactamase (ESBL)-producing Enterobacteriaceae have emerged with this capability.[22] Genes encoding ESBLs are often found on plasmids shared via HGT and are increasingly associated with co-transfer of aminoglycoside resistance: some bacteria possess HGT-associated *N*-acetyltransferases, *O*-nucleotidyltransferases, and *O*-phosphotransferases that acetylate or phosphorylate different amino and hydroxyl sites of antibiotics, such as aminoglycosides.[23] These modified drugs have a marked decrease in binding affinity to the ribosome due to added steric hindrance.

Because most antibiotic targets are intracellular, cell permeability plays an important role in drug efficacy. While some antibiotics can passively diffuse through cells, others rely on the help of membrane porins to gain entry. However, under antibiotic pressure, bacteria may evolve modified porins designed to exclude the offending molecule or downregulate

production of porins.[29] Permeability is also affected by the degree and type of efflux activity in a cell. Efflux pumps are a broad family of membrane transporters whose function is to remove molecules, including signaling molecules, metabolites, metals, and antibiotics, from a cell.[30] Although in many species, efflux plays a role in regular cellular upkeep unrelated to resistance, the mutation of these pumps to remove non-native antibiotic substrates or the horizontal acquisition of a pump from another species falls under the definition of resistance. Due to the cumulative breadth of these transporters, their upregulation is implicated in cross-resistance to multiple classes of antibiotics, making them a desirable target for the design of inhibitors to treat multidrug-resistant bacteria.[31]

Bacteria's ability to adjust to virtually any environment does not come free of cost. Acquiring and deploying the aforementioned resistance mechanisms drains the limited energetic and biosynthetic resources in a cell that would otherwise contribute to metabolism and reproduction. This concept, known as fitness cost, manifests as a reduced rate of growth in a resistant strain compared to the wild-type strain.[32] Recall that there are several paths through which a bacterium may grow resistant to antibiotics (drug or target alteration, circumvention, etc.). The fitness cost of a resistance mutation informs the success and prevalence of that mutation compared to the other possibilities. While some mutations appear cost-free, others drastically affect a cell's ability to reproduce and infect. However, the observed slowing of growth due to fitness cost is a temporary state to afford resistant strains the luxury of survival until they are able to resume normal growth rates. This can be accomplished through compensatory mutations, or secondary mutations that partially or fully restore cellular function to pre-resistance efficiency. Once these mutations are introduced, reversion to a susceptible phenotype is unlikely. Thus, resistant bacteria with

compensatory mutations can go on to acquire resistance to other drugs without losing resistance to the initial drug, resulting in multidrug-resistant pathogens.[33]

1.4 Tolerance and Persistence

Antibiotic tolerance can also complicate the treatment of bacterial infections. Tolerance is the ability of bacteria to withstand high concentrations of antibiotics due to a transient physiological state, usually (but not always) in which cells are slow-growing or even fully dormant. Because most antibiotics target processes important for cell division, growth arrest reduces or removes the target, rendering bacteria tolerant of the drug. Indeed, the killing rates of several antibiotics are directly proportional to the growth rates of the bacteria they eradicate.[34] Tolerance may also reduce the efficacy of drugs which require active transport to gain intracellular entry since this process may also be halted in slow-growing cells.

There is agreement among researchers that both resistance and tolerance exist and differ from each other, but the precise line which divides them exists in a philosophical gray area. For the purposes of this dissertation, I separate the two on the basis of genetic differences between antibiotic-susceptible and unsusceptible cells. Tolerance differs from resistance in that the former is a transient state stemming from epigenetics rather than mutations. In fact, tolerant cells are genetically identical to their drug-susceptible counterparts. In contrast, resistance stems from a genetic difference and may be quantified by a change in MIC. Colonies regrown from a resistant population maintain the resistance of their predecessors, whereas a population borne of tolerant cells may easily revert to a susceptible state with no observed change in MIC. Furthermore, a tolerant bacterium may be unaffected by multiple classes of antibiotics, while resistance mutations typically only confer

immunity to one class. However, confusing the matter is the fact that the two phenomena are closely intertwined. They can be triggered through the same mechanisms and may lead to one another. For instance, the DNA damage-induced SOS response not only triggers various tolerant phenotypes, but it also results in expression of error-prone DNA polymerases which increase the likelihood of resistance development.[35] In the reverse, mutations can enhance a cell's time in dormancy by 10 times, increasing its capacity for tolerance.[36]

Compared to antibiotic resistance, tolerance has received little attention, though it is by no means new—tolerance has been observed since 1944.[37] However, it remains difficult to study in the lab because it is difficult to quantify, and consequently lacks a universal standard measurement. Tolerant cells must undergo antibiotic therapy for a longer time before being killed, so some researchers have taken to assessing the minimum time duration required to kill 99% of a bacterial population, or minimum duration for killing (MDK), measured from a time-kill curve.[34] Others instead use the MBC/MIC ratio to quantify tolerance.

Persistence is sometimes used interchangeably with tolerance, though many use it strictly to refer to tolerance observed only in a small subpopulation of bacteria as opposed to in the population as a whole. The difference between the two may be visualized in a time-kill curve, as the presence of persister cells results in a bimodal curve, whereas a fully tolerant population exhibits a simple decay curve (Figure 1.8). However, on a unicellular

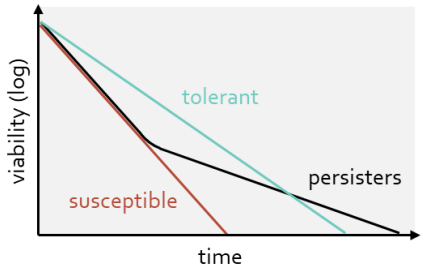

Figure 1.8: Time-kill curves for susceptible, tolerant, and persister populations.

phenotypic level, tolerance and persistence are one and the same. For the most part, the cause of tolerance/persister formation remains a mystery with a few proposed hypotheses. Some researchers have hypothesized that there is no actual mechanism of persister formation and that it results from accidental protein misfolding or stochastic overexpression of specific genes.[38,39] However, the proportion of persisters in a population seems to be connected to growth phases—tolerance may be naturally enhanced while a bacterial population is in the lag and stationary phases, when conditions do not encourage explosive growth. Together these observations indicate that tolerance depends on a mix of stochastic and deterministic factors.

A tolerant state may also be produced by environmental conditions such as a lack of nutrients or by antibiotic stress. For example, some studies indicate that the stringent response, which induces transient growth arrest as a response to the accumulation of the signal molecule guanosine tetraphosphate (ppGpp), can trigger dormancy in nutrient-depleted conditions.[40] Thus far, several gene knockouts have been connected to a decrease in persisters, but they are mostly global regulators and genes involved in nucleotide synthesis and metabolism. There are still many questions surrounding the actual mechanism of persister formation.[41] One informative gene that has been repeatedly connected to

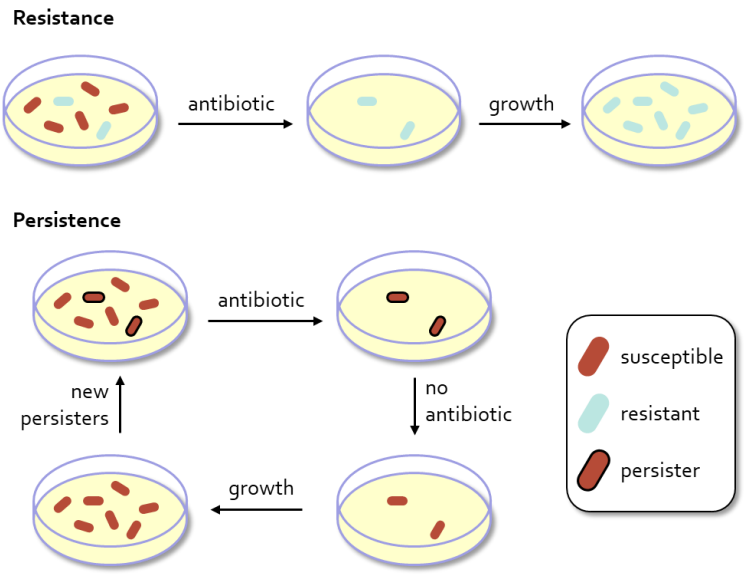

Figure 1.9: Resistance vs. persistence.

persister formation, however, is *hipA.*[42–45] It encodes a toxic kinase that, left unchecked, induces stasis. It is part of a toxin-antitoxin (TA) module, and is typically neutralized by its antitoxin, *hipB.* While deletion of *hipBA* leads to a sharp decrease in persisters, it does not fully abolish persister formation, both lending credence to the TA theory of formation and indicating that there is redundancy in tolerance mechanisms.

Even though it only affects a small number of cells, persistence is a useful survival strategy for bacteria—it is the bacterial equivalent of a diverse investment portfolio. Although some growth is sacrificed, the formation of at least some persisters ensures the survival of a few cells whose progeny may go on to repopulate an environment in the event of antibiotic exposure or lack of nutrients (Figure 1.9). In healthcare, persistence manifests as chronic infections which are difficult to eradicate using available antibiotics. Several recurring diseases are suspected to be perpetuated by persister cells, such as syphilis, which is known to have secondary and tertiary presentations. In addition, persisters may play a role in the recalcitrance of Lyme disease and tuberculosis[46] as well as in *Pseudomonas*

aeruginosa infections in patients with cystic fibrosis.[47] Persisters can also withstand the harsh environment of human macrophages. Once engulfed, these intracellular infections may be transported in the bloodstream away from the initial site of colonization, subsequently establishing infections in other tissues. *Salmonella* infections, which are mainly contracted through ingestion of contaminated food products, are intracellular. These species employ a number of immune evasion strategies in order to take up residence in various host cell types, including macrophages, epithelial cells, and dendritic cells.[48]

Virulence refers to a bacterium's pathogenicity, or its ability to cause disease. It takes many forms, including colonization, immunoevasion, immunosuppression, toxin production, and nutrient acquisition by bacteria within a host, among other effects. The specific molecules important to these processes are called virulence factors. Virulence factors may be native to a bacterium or may be acquired through HGT in the form of pathogenicity islands. Mechanisms that contribute to virulence but are not technically virulence factors are sometimes informally called "virulence behaviors." Like other concepts we have discussed, virulence is sometimes difficult to define because the interplay between resistance, tolerance, and virulence can be rather complex. Some virulence factors and behaviors also contribute to normal bacterial survival, so the line between life-sustaining processes and virulence becomes similarly blurred. Thus, in many cases, because resistance and tolerance enhance survivability, both contribute to virulence either indirectly through increased survival or directly through mutations in virulence genes. However, they may also theoretically decrease the virulence of a bacterium if there is an associated fitness cost or if a resistance mutation inadvertently disrupts virulence genes. It may be said that commensal bacteria are avirulent.

1.5 Current Outlook

> "There may be a danger, though, in underdosage. It is not difficult to make microbes resistant to penicillin in the laboratory by exposing them to concentrations not sufficient to kill them, and the same thing has occasionally happened in the body. The time may come when penicillin can be bought by anyone in the shops. Then there is the danger that the ignorant man may easily underdose himself and by exposing his microbes to non-lethal quantities of the drug make them resistant…. If you use penicillin, use enough."
>
> - Alexander Fleming in his Nobel Prize acceptance speech, 1945

The future appeared bright in the Golden Era of antibiotics. In 1962, after decades of rapid drug discovery, Nobel laureate Sir Frank Macfarlane Burnet wrote, "One can think of the middle of the twentieth century as the end of one of the most important social revolutions in history, the virtual elimination of the infectious diseases as a significant factor in social life."[49] Unfortunately, it may have been this attitude that led to the decline in antibiotic research and the predicament we find ourselves in today. Because of our brash overconfidence, we shrugged off the looming issue of resistance despite Fleming's warning in 1945. As a result, the rate of introduction of novel classes of antibiotics has significantly slowed. New antibiotics from existing classes have been developed, but they typically provide only temporary relief since they almost always have the same biological targets as their predecessors. Worsening the issue, the number of pharmaceutical companies with devoted antibiotic divisions has plummeted from 20 in the 1980s to just 4 in 2018.[50] The driving force behind these cutbacks is largely economic—a 1 to 2 week course of antibiotics brings in meager profits compared to treatments for long-term diseases like chronic hepatitis C or cancer, which are among the most expensive medications. Additionally, it is

financially unappealing to develop a pharmaceutical which will be limited in sales by antibiotic conservation efforts. This reduction in industrial research has left the bulk of the work in the hands of academic labs and startups with fewer resources, creating a discovery void in the field. In 2020, there were just 42 antibiotics at any stage of the drug development process, only a quarter of which possess a new mechanism of action.[10] Although resistance certainly precedes modern medicine (recall that bacteria have used antibiotics against each other long before humans began to), we are experiencing an unprecedented spike in the number of antibiotic resistant bacterial strains. This spike has accompanied the increased manufacture and widespread use of antibiotics for both medical and nonmedical applications. The quest to address resistance is only further confounded by tolerance and persistence, which boost resistance and are relatively poorly understood.

Fully addressing the resistance crisis would also require tightening regulations around antibiotic use by limiting access for uses other than life-saving medical treatments—something which also takes years to change. Though some states like California and Maryland have banned the use of antibiotics in livestock at the state level, global action is required. Further, despite some potentially promising discoveries and re-education initiatives such as the U.S. National Strategy for Combating Antibiotic-Resistant Bacteria, no new antibiotic classes have been approved by the FDA since 2007 and there has been only modest improvement in national statistics.[51]

As a result of these impediments, the situation has become critical. Today, antibiotic resistant bacteria and fungi cause nearly 3 million infections in the United States each year, killing 35,900 patients and incurring billions in healthcare costs.[10] Previously treatable infections are no longer responsive to typical antibiotics, forcing clinicians to resort to more

extreme “last-defense” drugs. It has been estimated that by 2050, 10 million people will die each year due to resistant infections.[52] This trajectory of resistant and tolerant infections threatens to undo most of the achievements of modern medicine, rendering even simple procedures life-threatening. Without breakthroughs on multiple fronts in the near future, the outlook is bleak.

Chapter 2. Anti-MRSA Retinoids

2.1 Methicillin-resistant *Staphylococcus aureus*

In recent decades, several pathogens have emerged as serious global health risks, including *Staphylococcus aureus*—more specifically, methicillin-resistant *S. aureus* (MRSA). *S. aureus* is a gram-positive bacterium commonly found in the upper respiratory tract and on the skin of up to 50% of the human population.[53] It was first identified in 1884 when Friedrich Julius Rosenbach differentiated it from *Staphylococcus albus* (now *Staphylococcus epidermidis*).[54] He named it *aureus* from the Latin *aurum* (gold) for its yellow pigmentation.

Active infections of *S. aureus* can cause minor skin issues such as impetigo, boils, cellulitis, folliculitis, carbuncles, scalded skin syndrome, and abscesses, while more serious infections can lead to pneumonia, meningitis, osteomyelitis, endocarditis, toxic shock syndrome, bacteremia, and sepsis.[55] A variety of virulence factors in *S. aureus* contribute to this pathology. Primary among these is alpha-hemolysin (also known as alpha-toxin), a pore-forming beta-barrel toxin that lyses host cells with a special affinity for platelets and monocytes.[54] It is so critical to virulence that alpha-hemolysin expression levels directly correlate with virulence of a given *S. aureus* strain.[56] In addition to toxins, *S. aureus* also produces surface proteins called adhesins which facilitate adhesion to host cells and eventual biofilm formation or intracellular infections.[55,57]

Although cases of MRSA have decreased over the past 15 years, it still infects 323,700 Americans, leading to 10,600 deaths and $1.7 billion in healthcare costs each year.[10] Counterintuitively, one of the more common settings to acquire a MRSA or other resistant infection is during a hospital or other healthcare visit. These infections are referred to as

healthcare-associated infections (HAI) or nosocomial infections. Patients who see a doctor for a resistant infection are liable to spread the bacterium through contact with medical personnel or contamination of common surfaces and equipment. Infections may then be transmitted to other patients who are at a high risk due to their immunocompromised status, including babies, the elderly, those with chronic conditions, those taking immunosuppressive medications or other antibiotics, or those undergoing invasive procedures such as surgery. Concerns about transmission of these infections has led some clinics to introduce strict isolation and disinfection procedures such as cohorting patients and nurses, daily antiseptic baths, hydrogen peroxide vapor disinfection of equipment, and use of disposable materials wherever possible.[58] Between 2005 and 2008, 17,508 of 21,503 (81%) invasive MRSA infections were HAI.[59] The rest were spread through less common routes—through community contact (community-associated infection, CAI) or through interaction with livestock (livestock-associated infection, LAI).[60]

The primary therapies for *S. aureus* infection are β-lactam antibiotics, but production of β-lactamases by *S. aureus* enables the hydrolysis and resultant deactivation of β-lactam antibiotics.[61,62] Additionally, the mobile genetic element staphylococcal cassette chromosome mec (SCC*mec*) contains the *mecA* gene (the hallmark of MRSA), which encodes penicillin-binding protein (PBP) 2a, an altered PBP with decreased affinity for all β-lactam antibiotics.[18,63,64] Resistance to vancomycin, a glycopeptide antibiotic and the next line of defense against MRSA, has also emerged as a result of acquisition of the *vanA* gene cluster from vancomycin-resistant enterococci (VRE).[65] Today, clinicians may opt for last-line of defense drugs such as linezolid to treat MRSA and VRSA infections. However, resistance to linezolid has also been observed.[66]

2.2 *Staphylococcus aureus* Persistence

In addition to resistance, *S. aureus* is also a concern due to its ability to assume tolerant states. In liquid culture, *S. aureus* persisters have been shown to tolerate aminoglycosides, fluoroquinolones, and β-lactams.[67] Persisters are also present in high concentration within *S. aureus* biofilms, which have been implicated in osteomyelitis, periodontitis, endocarditis, chronic rhinosinusitis, ocular infections, chronic wound infections, and medical device infections (more detail on biofilms in section 4.1.1).[68,69] Further, *S. aureus* is known to form small colony variants (SCVs)—slow-growing, abnormal subpopulations of bacteria that are particularly suited to invade host cells and form intracellular infections.[70] SCVs commonly invade osteoblasts, fibroblasts, keratinocytes, and endothelial and epithelial cells to evade antibiotic treatment only to later re-emerge and re-establish infection, contributing to many latent and chronic infections.[57,71] Altogether, *S. aureus* tolerance makes some infections virtually untouchable, posing a major problem in healthcare.[72]

Because bacteria in a tolerant state are frequently dormant or have unique physiology, treatments for these infections cannot rely on active transport to gain intracellular entry and cannot act on traditional, metabolically active antibiotic targets. Thus, standard antibiotics are ineffective, requiring creative solutions. One such approach is the activation of the caseinolytic protease system (Clp), which plays a role in bacterial homeostasis through the degradation of misfolded or short-lived peptides. While its action is typically ATP-dependent, agonism by small molecules results in indiscriminate degradation of large peptides, leading to persister cell death. This has been accomplished in a research setting with various acyldepsipeptides and the natural product sclerotiamide.[73,74]

Researchers have also seen some anti-persister success by co-dosing antibiotics with metabolic stimuli as a means to "wake up" the antibiotic target. In one study, addition of fructose induced gentamicin susceptibility in *S. aureus* persisters.[67]

Membrane-targeting antibiotics can also eradicate persister cells (both planktonic and in biofilm).[73] Unlike the targets of traditional antibiotics, the bacterial membrane is accessible regardless of persister status. These antibiotics are also unconstrained by issues of cell permeability that plague many other would-be antibiotics and are less likely to be met by resistance due to their rapid bactericidal activity and the general conservation of bacterial membranes. Unfortunately, they are difficult to develop due to their risk of toxicity to mammalian cells. However, there exist key differences in the characteristics and composition of bacterial and mammalian cells that permit some directed selectivity for one over the other. Bacterial membranes are covered with negatively charged teichoic acids (Gram-positive) or lipopolysaccharides (Gram-negative), neither of which are present in mammalian membranes. Instead, the mammalian cell membrane is populated by neutral lipids. Subsequently, membrane-perturbing efforts have focused on linear and cyclic cationic peptides, quaternary ammonium compounds, and other positively charged small molecules.[75–77]

2.3 Retinoids and CD437

Retinoids are molecules derived from the vitamin A family, stored in our bodies as retinyl esters (primarily retinyl palmitate) in the liver, intestine, eyes, lungs, adipose tissue, testes, skin, and spleen, where they perform essential functions.[78] In the eye, 11-*cis*-retinal binds to the protein opsin to form rhodopsin and iodopsin complexes. It dissociates from the complexes upon light-mediated isomerization to the *trans* form, triggering a signal to the

optic nerve in the brain. Lack of sufficient vitamin A to power this process results in night blindness and, eventually, total blindness.[79] Throughout our bodies, retinoic acid (produced by retinaldehyde dehydrogenases) binds to nuclear receptors that regulate the expression of specific genes, including the well-studied gene for phosphoenolpyruvate carboxykinase, which plays a crucial role in gluconeogenesis.[80] Retinoids also contribute to immunity—retinoic acid regulates the differentiation of T cells and dormancy of hematopoietic stem cells, among other functions.[81,82]

The retinoids are separated into three generations according to structure (Figure 2.1).[83] The first generation comprises cyclohexene-containing scaffolds with a polyene side chain and terminal polar groups. These are found in nature and include vitamin A and its metabolites (retinol, retinal, retinoic acid, tretinoin, etc.). The second generation is a group of synthetic vitamin A derivatives which replace the cyclohexene ring with a benzene ring. The third generation of retinoids have polyaromatic scaffolds that confer them with more rigid structures, resulting in higher receptor specificity.

Retinoids are commonly used as topicals in the skin-care and beauty industry due to their ability to slow signs of aging.[83] They are also used clinically for the treatment of various skin disorders—second-generation retinoids acitretin and etretinate are used for severe psoriasis and adapalene, a third-generation synthetic retinoid, is used to treat acne and keratosis pilaris.[83] Topical retinoids also enhance the efficacy of other topical applications when used together.[84]

CD437 (also sometimes called AHPN), a third generation retinoid, was first studied in 1992 when it was developed as a selective inhibitor of the gamma isoform of retinoic acid receptor (RARγ).[85] Since, it has been studied for its RAR binding and its pro-apoptotic

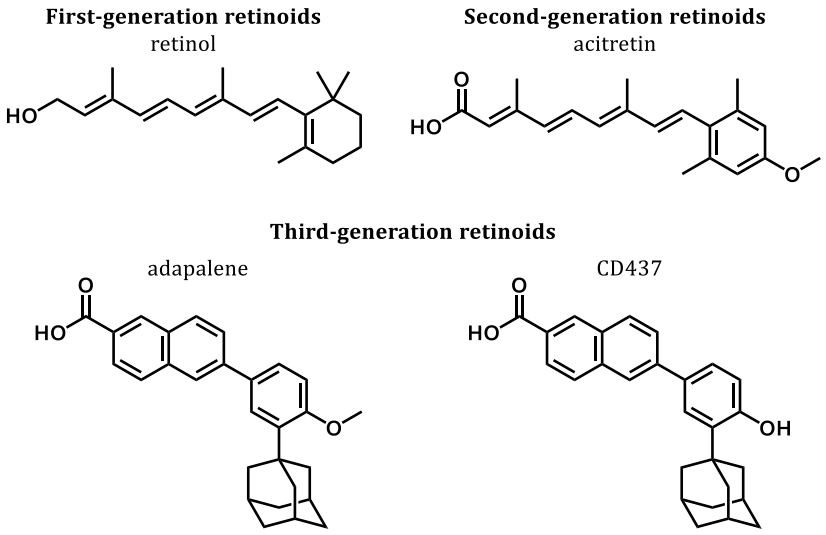

Figure 2.1: Selected retinoid structures.

activity, making it a promising anticancer therapy.[86–89] However, the mechanism of action in cancer long eluded researchers. It wasn't until 2016 that Han and co-workers showed that CD437 exerts its anticancer activity by directly binding to POLA1, a subunit of DNA polymerase α that initiates DNA synthesis.[90] Through a seemingly selective mechanism that has yet to be elucidated, this promotes apoptosis in cancer cells but not in healthy cells. More recently, CD437 has also been studied in aortic valve calcification and as an adjuvant in other therapies.[91,92]

2.4 Anti-MRSA Retinoids

In pursuit of a new class of *S. aureus* drugs, our collaborators in the Mylonakis group performed a high throughput screen of 82,000 FDA-approved molecules using a whole animal *C. elegans-S. aureus* infection model, which supplies preliminary toxicity information concurrently with initial activity results.[93,94] Two of the 185 hits, the synthetic retinoids CD437 and CD1530, shared a common scaffold and were thus further investigated. These retinoids not only killed MW2, a community-associated MRSA strain, with a minimum

inhibitory concentration (MIC) of 1 μg/mL in just two hours, but they also killed persister cells from 13 clinical isolates at 8-10x MIC in 1-4 hours and showed synergy with gentamicin.[93] Further, they killed persisters of VRS1 (a multi-drug resistant strain) at 10x MIC as well as those in biofilms at 16-32x MIC. A resistance assay revealed mutations in *graS, yjbH,* and *manA* (membrane physiology genes), implicating the membrane in the retinoid mechanism of action. A SYTOX green uptake assay and biomembrane-mimicking giant unilamellar vesicle experiments further confirmed that the retinoids target the bacterial membrane.[93] All-atom molecular dynamics simulations predicted that they do so through a multi-step process: the phenol and acid groups first attract the molecule to the polar phosphate heads of the membrane before the greasy adamantyl group intercalates into the lipid tails. The embedded retinoid disrupts the membrane, inducing cell death (Figure 2.2). Although we remain healthily skeptical of this precise step-by-step mechanism, the simulation suggests the importance of the terminal groups and the adamantane.

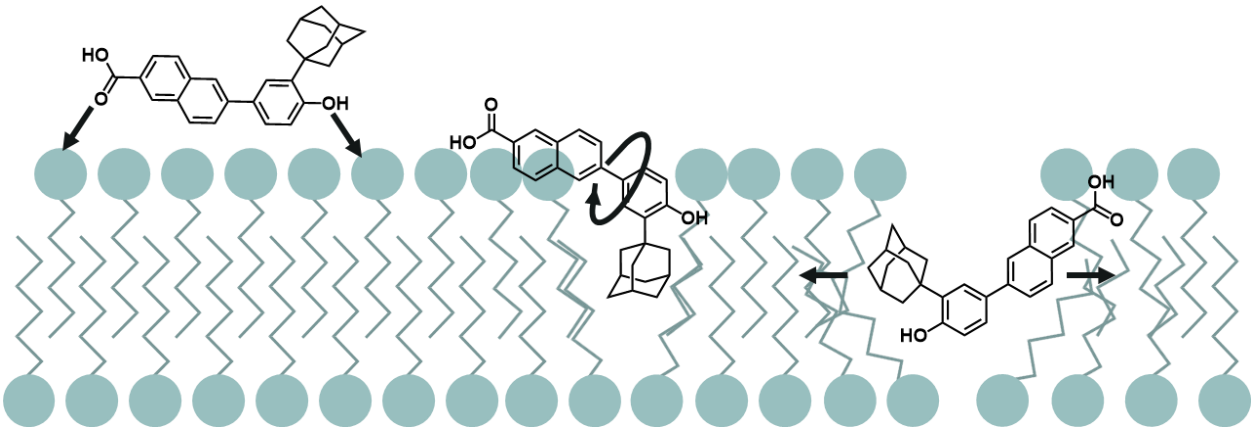

Figure 2.2: Cartoon representation of molecular dynamics simulation of CD437 activity.

A preliminary structure-activity relationship (SAR) study conducted by our group probed the acid and phenol anchor points in CD437, which displayed faster killing of MW2 persisters than CD1530. Methylation of the phenol resulted in loss of activity, as did

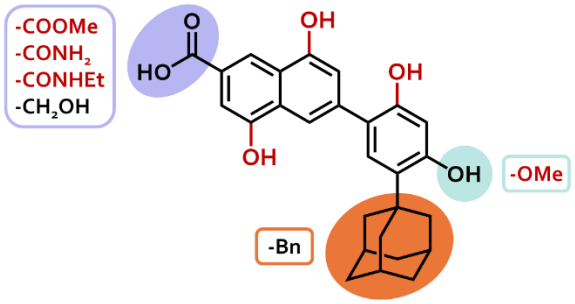

Figure 2.3: Previous SAR study findings.

replacing the acid with a methyl ester or amide.[93] Repositioning of the phenol and addition of second and third phenols were also disfavored. However, substitution of adamantane with benzyl was tolerated and reduction of the acid to a primary alcohol resulted in a highly potent (MIC 2 μg/mL) analogue with reduced hemolytic activity and cytotoxicity.

2.5 Role of Globularity in Anti-MRSA Activity

Antibacterial mechanism of action studies indicated that the retinoids target bacterial membranes. Based on the aforementioned all-atom molecular dynamics simulations and SAR study,[93] I hypothesized that the hydrophobic adamantyl moiety is essential to this action and functions by interacting with the lipid tails in the membrane. Further, previous SAR studies of a related scaffold (ST1926) in various cancer cell lines determined that removal of adamantane or replacement with other hydrophobic groups led to a decrease in anticancer activity.[95,96] Thus, I chose the hydrophobic adamantane as the focal point of my SAR study. To explore its role in both MRSA and cancer, I synthesized analogues with varied substitutions at this position. I probed the role of globularity with analogues featuring both smaller and larger hydrophobic groups than the adamantane present in CD437. I also synthesized a group of lipid-mimicking analogues with unsaturated and saturated alkyl chains of varying lengths with the goal of altering protein binding in polymerase α while inducing a stronger interaction between the alkyl chains and the lipid tails in bacterial

membranes. For all analogues, both the carboxylic acid and primary alcohol derivatives were synthesized to investigate whether the decreased toxicity of the primary alcohol derivative of CD437 was a trend, and whether it resulted in lowered anticancer potency as previously observed in similar retinoids.[96] To this end I synthesized and our collaborators tested 20 analogues.[97]

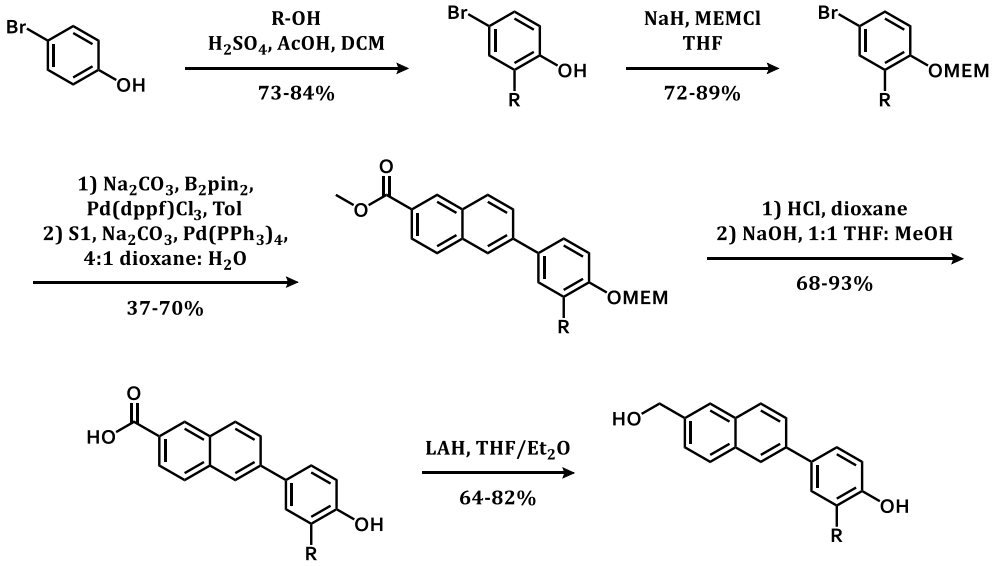

Figure 2.4: General synthesis of retinoid globularity panel.

Each analogue was made in 3–5 steps following the same general synthesis (Figure 2.4): the 2-substituted 4-bromophenols were assembled and protected, Miyaura borylated for use in a Suzuki cross coupling, then deprotected. Each analogue's acid was also reduced to yield the primary alcohol derivatives. My sole departure from the route previously used by our group was the replacement of an electrophilic borylation using n-butyllithium and trimethyl borate, which resulted in several oligomers in low yield and had to be carried on as a crude mixture. Instead, I opted for the milder Miyaura borylation which eliminated the need to use sensitive and harsh reagents like n-BuLi and could be carried through without hydrolysis of the boronic ester. For the first group, commercially available 4-bromophenol, 4-bromo-2-methylphenol, and 4-bromo-2-(tert-butyl)phenol were protected with 2-

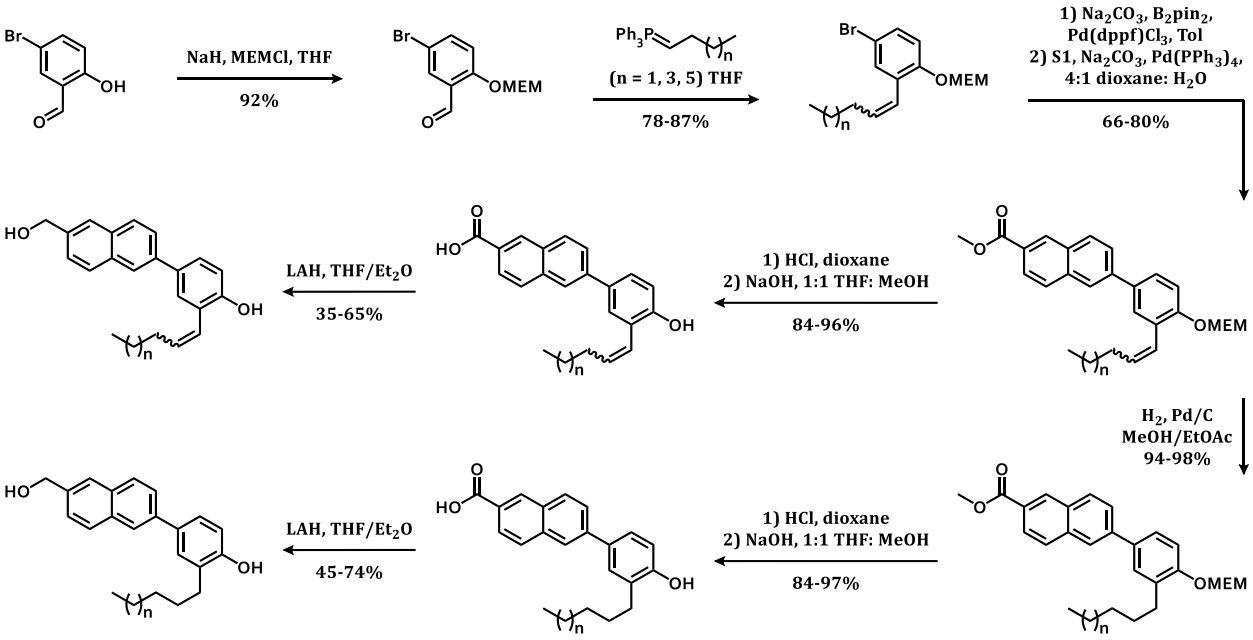

Figure 2.5: General synthesis of lipid mimics.

methoxyethoxymethyl ether (MEM) before Miyaura borylation and subsequent Suzuki coupling to methyl-6-bromo-2-naphthoate. The phenol and acid were deprotected, and a portion of each was reduced to yield analogues **2.1–2.3** and **2.5–2.7**. Similarly, 4-bromo-2-(3,5-dimethyl-1- adamantyl)phenol was synthesized first using a Friedel–Crafts alkylation, then was carried through the aforementioned route. For the lipid-mimics, 5-bromosalicylaldehyde was MEM-protected before Wittig reactions were used to append ylides with 4-, 6-, and 8-carbon length chains, yielding analogues **2.9-2.14**. A further hydrogenation provided fully saturated analogues **2.15–2.20** (Figure 2.5). Full synthetic details are provided in the Supporting Information.

Antimicrobial and antineoplastic activity of the analogues were tested using MRSA MW2 and a human liver cancer cell line, HepG2 (Table 2.1). This testing confirmed the importance of a bulky hydrophobic moiety to antibacterial action as analogues **2.1**, **2.2**, **2.5**, and **6**, which featured either no substitution or a methyl, exert no killing against MW2 cells.

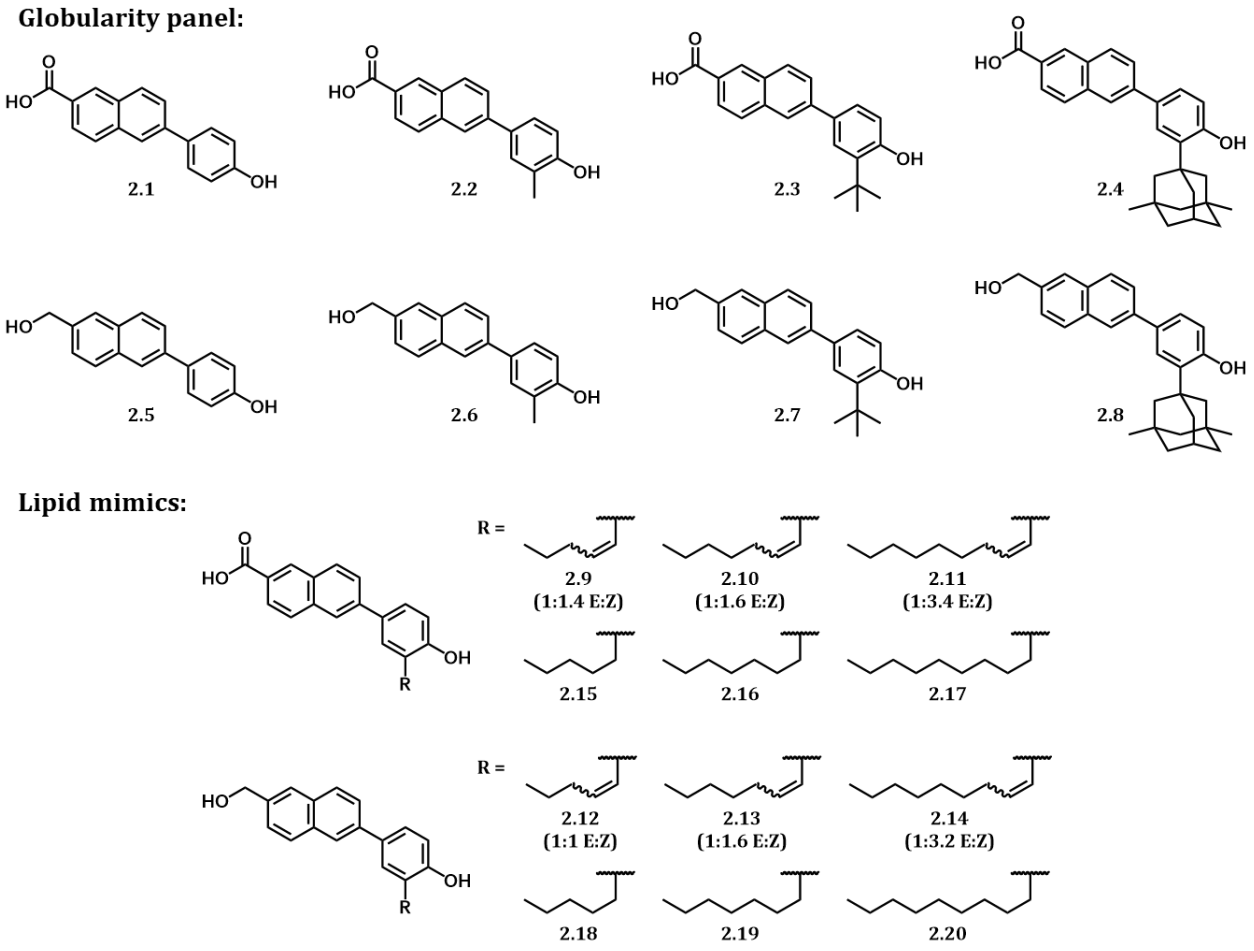

Figure 2.6: SAR panel.

This finding provides further evidence for the putative method of membrane disruption: previous simulations suggest that the hydrophobic group intercalates into the membrane, facilitating retinoid embedment.[93] Analogues possessed cLogP values between 3.75 and 8.75, with **2.1** and **2.5** the lowest, making them the least likely to be localized in the lipid bilayer. The larger substitutions in analogues **2.3**, **2.4**, **2.7**, and **2.8** displayed modest activity against MRSA, indicating that increased steric bulk leads to increased antibacterial activity. However, none were more active and less toxic than CD437 and its alcohol derivative, confirming the putative role of adamantane in CD437—without a sufficiently bulky hydrophobic group, the retinoids are unable to effectively burrow into the membrane.

Table 2.1: Retinoid biological testing: minimum inhibitory concentration (MIC) against MW2 MRSA cells, median lethal concentration (LC50) in human hepatoma cells (HepG2), and median hemolytic concentration (HC50).

Analogue	MW2 MIC (μg/mL)	HepG2 LC_{50} (μg/mL)	Hemolytic HC_{50} (μg/mL)
CD437	1	1.02 ± 0.13	>64
2.1	>64	>32	>64
2.2	>64	>32	>64
2.3	16	9.80 ± 1.33	>64
2.4	2	1.84 ± 0.09	15.4
2.5	>64	>32	>64
2.6	>64	>32	>64
2.7	8	7.50 ± 2.56E6	>64
2.8	8	11.65 ± 1.42	>64
2.9	16	5.38 ± 0.32	>64
2.10	8	2.44 ± 0.26	45.41
2.11	4	2.60 ± 0.20	51.54
2.12	4	3.89 ± 6.25E4	>64
2.13	4	4.19 ± 0.28	>64
2.14	>64	5.51 ± 0.39	>64
2.15	8	3.26 ± 0.37	>64
2.16	4	1.89 ± 0.08	>64
2.17	4	1.73 ± 0.12	22.8
2.18	4	3.27 ± 0.25	>64
2.19	4	3.61 ± 0.16	>64
2.20	>64	7.25 ± 0.50	>64

In the case of the lipid-mimics, I was curious about whether the (albeit slight) increased rigidity of the unsaturated analogues had any effect since we had previously observed favorable results with a benzyl substitution.[93] I also sought to observe what effect chain length might have on anti-MRSA activity. It has been previously shown that small molecules that function by lysing bacterial cells benefit from a 10–12 carbon length chain mimicking the phospholipid composition.[98] However, we have shown that retinoids do not lyse bacterial cells, thus shorter carbon chains were used.[93] Again, modest activity (in comparison to CD437) was observed. From analogues **2.9–2.11** it might be deduced that increased chain length correlates with antibacterial activity. However, this trend is less

pronounced between analogues **2.15–2.17** and in the primary alcohol analogues. Analogues **2.12–2.14** and **2.18–2.20** instead exhibit a steep drop-off in bacterial killing with the longest length chains. I imagine that the acid analogues might anchor the retinoids to the bacterial membrane more rigidly, enforcing this chain length trend, while the primary alcohol analogues are more flexible, rendering the chain length less important. These results indicate that, although the lipid mimics exert anti-MRSA activity, a more globular substitution is better able to disrupt the bacterial lipid bilayer.

We further tested our most active analogue, **2.4**, in another common MRSA strain (JE2), a healthcare-associated MRSA strain (ATCC 33591), and a vancomycin-resistant strain (VRS1). Analogue **2.4** maintained a similar activity profile to CD437, with a MIC of 2 μg/mL in all strains. Likewise, **2.4** killed MW2 persister cells with almost identical speed to CD437, eradicating 5×10^7 CFU/mL MRSA persisters within 1 h. Unfortunately, all analogues (including CD437) lose activity in media with 10% fetal bovine serum due to high serum protein binding. This binding is detrimental to the bioavailability of the drug in an *in vivo* system—protein-bound drug cannot exert its effects on the bacterial target. Addressing this problem is crucial for the advancement of these retinoids to *in vivo* studies.

Table 2.2: Minimum inhibitory concentration (MIC) of analogue **4** in additional MRSA strains (μg/ mL).

MRSA Strain	Analogue 2.4	CD437	Vancomycin
JE2	2	1	1
ATCC 33591	2	1	2
VRS1	2	1	>64

In most cases, anti-MRSA activity loosely correlates with HepG2 killing. However, primary alcohol analogues **2.14** and **2.20** appear to be selective for HepG2 killing over MRSA killing. No trends can be extrapolated on the basis of primary alcohols since the primary alcohol derivative of CD437, which we previously reported, showed the reverse selectivity.[93]

We further examined the anticancer activity of **2.4**, **2.14**, and **2.20** as well as that of **2.16**, our most active nontoxic analogue, in HeLa cells. In all cases, we observed lower LC_{50} values than in HepG2 cells. Most active were **2.4** (LC_{50} = 0.49 μg/mL) and **2.16** (LC_{50} = 0.60 μg/mL), two carboxylic acid analogues. However, CD437 remained the most potent (LC_{50} = 0.21 μg/mL), supporting a previous study of a similar scaffold, which observed decreased apoptotic activity in analogues lacking a carboxylic acid or with different hydrophobic groups.[96]

These results verify the importance of a sterically large hydrophobic group to the anti-MRSA activity of synthetic retinoids. Adamantane was revealed to be the optimal size, as CD437 and its primary alcohol derivative are the most active compared to any other acid-alcohol pair tested, while complete removal of the hydrophobic group resulted in loss of antibacterial activity. Although analogues furnished with lipid-mimicking groups displayed modest bacterial killing, they did not have the activity I had hoped for. Generally, the carboxylic-primary alcohol analogue pairs show similar activity (with the exceptions of **2.11**/**2.14** and **2.17**/**2.20**). Perhaps most interestingly, almost all analogues show low or no hemolytic activity, despite their bacterial membrane disruption ability. However, no clear trend in toxicity or cancer killing can be gleaned. Overall, CD437 presents a possible solution to the problems of MRSA, VRSA, and *S. aureus* persistence in a landscape that otherwise leaves much to be desired.

Chapter 3. Expanding the Retinoid Spectrum

3.1 Targeting Gram-negative Bacteria

Like mammalian cells, bacterial cells are encased by a phospholipid bilayer membrane. This membrane protects cellular contents and allows for a difference in electric potential between the intracellular and extracellular spaces, created by differences in concentration of ions. A cell wall composed of peptidoglycan surrounds the cytoplasmic membrane and provides structural reinforcement and protection. But here we observe a split in bacteria—while some species possess a very thick, multilayered cell wall, others have a thinner cell wall as well as a second membrane surrounding it. These factions are referred to as Gram-positive (single membrane) and Gram-negative (double membrane) bacteria based on their susceptibility to Gram staining (Figure 3.1.) The differences between Gram-positive and Gram-negative bacteria make infections caused by the latter uniquely difficult to treat, though both present a challenge in the fight against antibiotic resistance.

The Gram-negative outer membrane is composed of a hybrid phospholipid-lipopolysaccharide complex containing lipoproteins and porins, unlike the cytoplasmic membrane (a simple phospholipid bilayer).[99] The lipopolysaccharide (LPS) covering the outer membrane of Gram-negatives is composed of a lipophilic anchor adorned with six or seven fatty acid chains (called lipid A) and a chain of oligosaccharides and polysaccharides (broken into segments called the core and O antigen). An abundance of hydroxy and phosphate groups, stabilized by divalent cations, gives LPS its anionic character. The negative charge and tight packing of the LPS make the outer membrane highly ordered in comparison to the cytoplasmic membrane.[100] Subsequently, it is incredibly hard for small

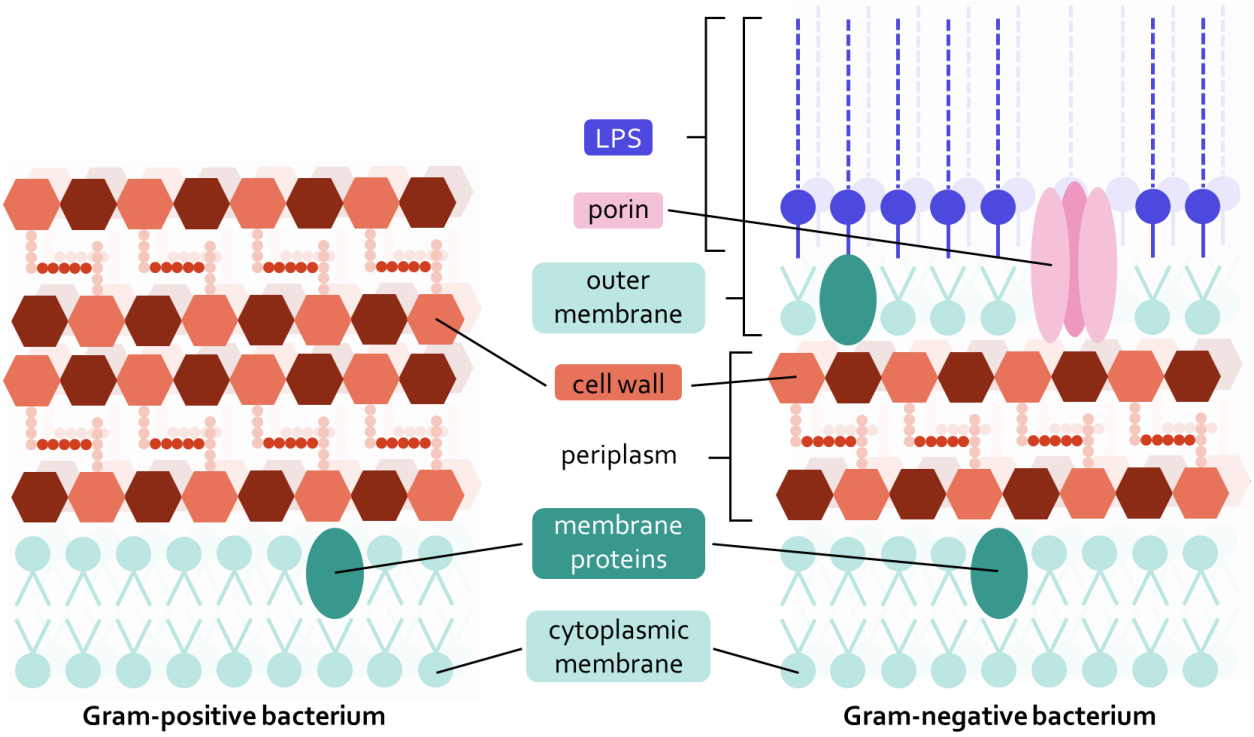

Figure 3.1: Gram-positive vs. Gram-negative bacterial membranes.

molecule antibiotics to diffuse through the outer membrane—in some cases even up to 100 times harder.[101] Drugs that do manage to penetrate these cells do so either through porins or through a self-promoted uptake process.[102] However, porins are narrow and lined with charged amino acids, making them similarly difficult for small molecules to traverse. Even if a compound makes it into the periplasmic space, it still has to contend with the inner membrane, which has orthogonal exclusion criteria to the outer membrane.[103] Even still, these antibiotics may be met by resistance upon cell entry, or may be foiled by mutations in porins and efflux pumps that decrease cell permeability and accumulation.[100,104]

This lack of cell permeability is largely responsible for the difference in antibiotic susceptibility between Gram-positive and Gram-negative species: even though common antibiotic targets are conserved across both groups, most antibiotics are simply unable to penetrate Gram-negative cells to reach their targets. Only some drugs are able to do so, such

as certain β-lactams, amphenicols, tetracyclines, fluoroquinolones, polymyxins, aminoglycosides, and macrolides.[102,103,105] Gram-negative species' impenetrability poses a major threat—in their 2019 antibiotic resistance report, the Centers for Disease Control and Prevention listed ten species or genera of Gram-negative bacteria as healthcare threats.[10] Altogether, the listed threats account for close to 1.5 million infections in the United States each year. Our antibiotic arsenal for Gram-negative pathogens is already smaller than that for Gram-positive, and these species display resistance to some or all available antibiotics. Troublingly, no new classes of Gram-negative antibiotics have been approved since 1964, spelling out a dire future unless researchers find solutions soon.[106]

In pursuit of guidance, researchers have sought to elucidate trends in compounds that accumulate intracellularly in Gram-negative bacteria. In a 2008 retrospective study of Gram-negative-active compounds à la Lipinski,[107] researchers examined the physicochemical characteristics of 147 antibacterial compounds (both commercial and under development) against those of Gram-positive and nonantibacterial compounds.[108] They found that Gram-negative active compounds tended to have a molecular weight below 600 Da and were more polar than Gram-positive and nonantibacterial drugs (as measured with relative polar surface area, $ClogD_{7.4}$, and hydrogen bond donor and acceptor numbers). In a similar study in 2014, analysis of roughly 3200 compounds with whole cell activity against any bacteria revealed that Gram-negative active compounds were either highly polar and low in molecular weight or zwitterionic and very large.[109] In 2018, the "eNTRy rules" narrowed this criteria even further.[103] The rules state that Gram-negative accumulating compounds possess a sterically unencumbered ionizable nitrogen 1°>2°>3°, low globularity, and few rotatable bonds (≤5). These rules have been validated by the conversion of multiple Gram-

positive therapies into broad-spectrum antibiotics, most famously in the conversion of penicillin G to ampicillin.[103,110] In a few instances, addition of an alkylamine was the only modification needed to unlock Gram-negative activity.[111–113]

3.2 Applying eNTRy Rules to Membrane Perturbing Antibiotics

Serial passaging, giant unilamellar vesicle experiments, SYTOX green uptake assays, and transmission electron microscopy indicate that CD437 kills MRSA by perturbing the cell membrane.[93] However, CD437 and another membrane perturbing compound studied in our lab (bithionol) lack compelling Gram-negative activity.[114] The difference in activity is compatible with the putative mechanism of action—to have an effect on Gram-negative bacteria, CD437 and bithionol would have to access the inner membrane or the inner leaflet of the outer membrane. Other membrane permeabilizing agents face similar issues.[115]

In theory, CD437 and bithionol are only hindered by their inability to penetrate the Gram-negative outer membrane. However, both meet two of the three criteria of the eNTRy rules: they are mostly planar and have few rotatable bonds. The only deficiency is their lack of an ionizable amine. Thus, addition of a primary amine might theoretically grant activity in Gram-negative bacteria. If these compounds could enter the periplasm, they could potentially disrupt the outer membrane or inner membrane, thereby releasing degradative periplasmic enzymes into the cytoplasm.[99]

As an initial exploration into this strategy, I decided that it would be synthetically simple to append an alkylamine to an existing phenol handle as opposed to installing a primary amine directly. I first designed analogues **3.1** and **3.2** based on a compound explored in a previous SAR campaign by our group. Then, fellow graduate student Cassandra Schrank joined the project and together, using the existing phenols in CD437 and bithionol,

we synthesized analogues **3.3** and **3.4**, while she alone synthesized analogue **3.5**. We reasoned that, although the phenols had been proven important to antibacterial activity, that appending a cationic amine might simply extend the polar anchor that the phenols provide. In any case, they were easily synthesized from intermediates already on hand. Taking inspiration from the arylomycins, we opted for ethylamine as our appendage.[116]

I synthesized analogues **3.1** and **3.2** as previously reported, beginning with preparation of an alkyl phosphonate for a Horner-Wadsworth-Emmons reaction with 4-bromobenzaldehyde.[93] The resultant alkene was then treated with trifluoroacetic acid and acetic anhydride to initiate a cyclization, forming the naphthalene core of the retinoid. A Suzuki coupling simultaneously completes the scaffold and removes the acetyl group. At this stage, the phenol was capped with Boc-protected ethylamine, leaving only deprotections and a reduction to yield the final analogues (see Supporting Information for synthetic details). Analogues **3.3-3.5** were prepared through the direct capping of CD437 and bithionol, followed by deprotection and, in the case of analogue **3.4**, a reduction to yield the primary

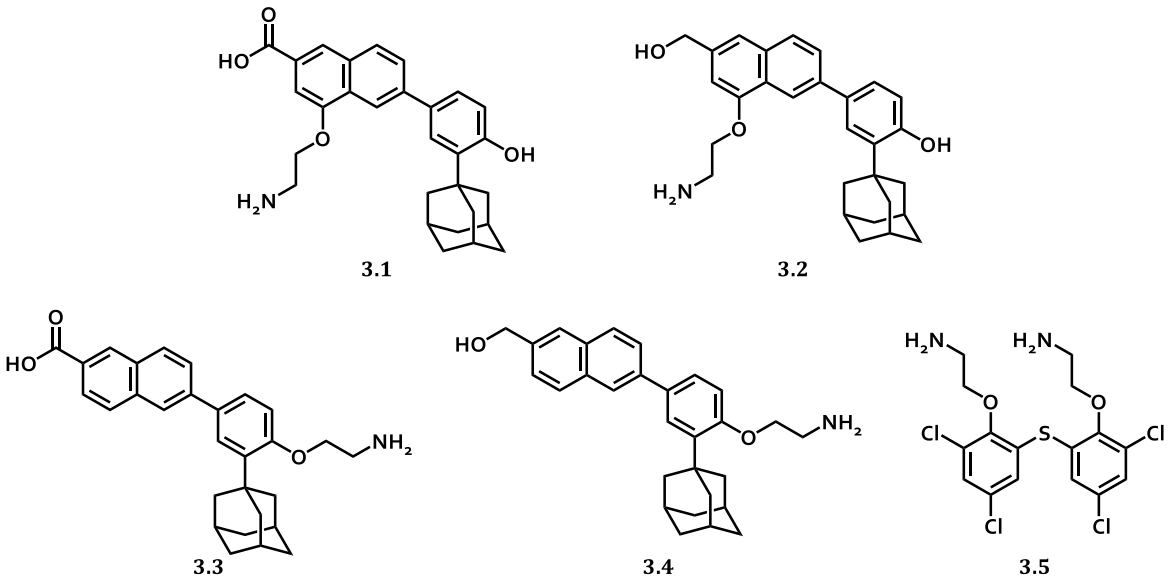

Figure 3.2: Analogue panel.

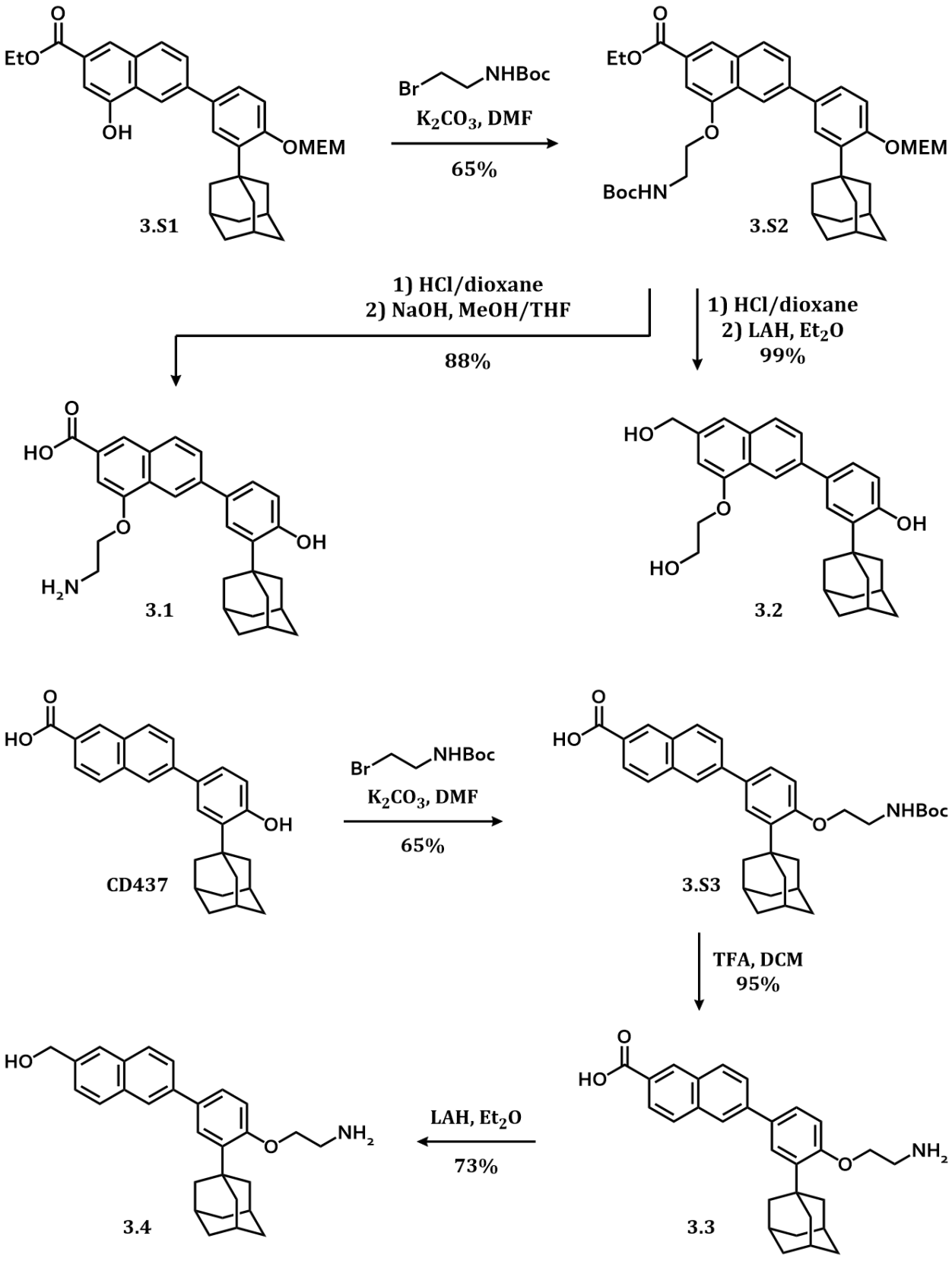

Figure 3.3: Synthesis of analogues 3.1-3.4.

alcohol. Due to synthetic difficulties, we were unable to synthesize an analogue with ethylamine appended to the primary alcohol of the reduced CD437 scaffold.

All analogues were tested for activity against four MRSA strains (MW2, BF1, BF2, and BF3) as well as Gram-negative pathogens *Pseudomonas aeruginosa* (PA14), *Klebsiella pneumoniae* (WGLW2), and *Acinetobacter baumannii* (ATCC 17978). Unfortunately, our modifications to CD437 and bithionol did not afford broad-spectrum activity. In fact, in the cases of analogues **3.3-3.5**, they abolished all activity, including that against MRSA. Analogues **3.1** and **3.2**, however, still displayed anti-MRSA activity comparable to that of the parent compound. This is unsurprising considering what we know of bithionol and the retinoids so far. Thus, these results reinforce what past studies have shown: the phenols are integral to antibacterial activity. Our attempt to elicit Gram-negative activity from our membrane perturbers via addition of alkylamines was unsuccessful.

Material in this chapter reprinted with permission from:

Bioorganic Med. Chem. Lett. **2020**, *30*, 127099. DOI: 10.1016/j.bmcl.2020.127099.

Chapter 4. Small Molecule Inhibitors of LexA

4.1 Stress Responses

Because bacteria live in a wide range of environments where they may encounter any number of conditions, they must remain dynamic and adaptable. To this end, bacteria have evolved several overlapping and conserved stress responses that regulate expression of specific genes in response to extreme stimuli, such as changes in temperature, pH, nutrients, salts, and oxidation. The genes controlled by these responses are often involved in mutagenesis and tolerance, providing means for bacteria to survive such conditions.

Most genetic mutations are detrimental, making constant mutation a poor strategy. However, a transient increase in mutation can be beneficial in dire situations. Thus, multiple stress responses induce the expression of error-prone polymerases. The SOS response (a DNA damage response) controls expression of low fidelity translesion repair polymerases Pol IV and Pol V from the Y family of polymerases.[117] Pol IV expression is also induced by the general stress response, the onset of which coincides with bacteria entering stationary phase. Other stress responses, including the heat-shock response and the stringent response, also induce mutagenesis.[16,118] Further, stress responses have been connected to the dissemination of mobile genetic elements.[119] Thus, they promote both the development and spread of resistance.

Stress responses have also been implicated in the formation of persisters and other tolerance phenotypes. It has even been suggested that all stress responses induce persister formation.[38] Specific responses, such as the oxidative stress response, the stringent response, and the SOS response, have been connected to increased persistence via ppGpp-

and cAMP-mediated mechanisms.[40,120] Stress responses can also initiate the formation of other tolerance phenotypes, such as biofilms, filaments, and spores.

4.1.1 Biofilms

Biofilms are among the most cunning tolerance strategies utilized by bacteria (Figure 5.3). They are matrices composed of polysaccharides, proteins, nucleic acids, and lipids that act as strongholds for communities of multiple species of bacteria on a variety of surfaces, both medical and industrial. The thick extracellular polymeric substance (EPS) which envelops the biofilm provides the colony with structural stability and enables adhesion to surfaces. It has also been speculated that, because cells are confined to such close quarters, biofilms facilitate intercellular coordination and recycling of dead cell material.[121] Moreover, EPS protects resident cells from host immune response, UV damage, metal toxicity, acid, dehydration, and antibiotics.[122–126] Depending on the biofilm density, diffusion of antibiotics may be hindered and bacterial growth rates may decrease, making biofilm infections particularly hard to eradicate. Additionally, biofilms contain high concentrations of persister cells, so much so that researchers have considered redefining biofilms as adherent persisters.[69] As with other tolerance mechanisms, cells may disperse from the biofilm and reassume a susceptible, planktonic (free-floating) state (Figure 4.1). Subsequently, biofilms are responsible for the majority of recalcitrant infections.[43] Due to the protective functions

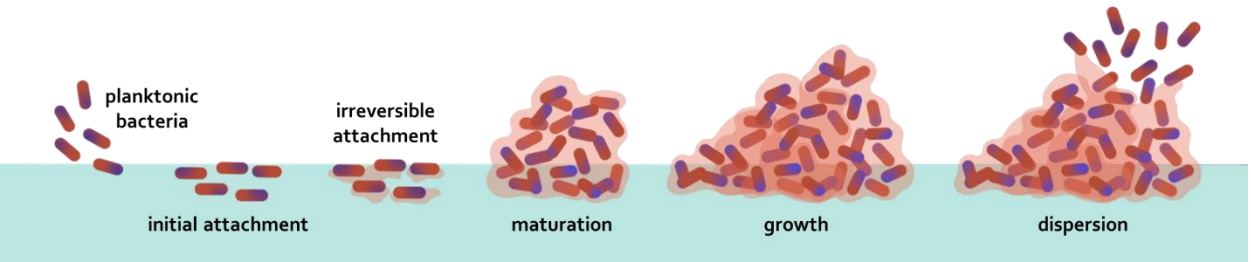

Figure 4.1: The life cycle of a bacterial biofilm.

of biofilms and their ability to enhance the spread of infection, they also greatly contribute to virulence. Indeed, knockouts of relevant genes lead to decreased virulence in several biofilm-producing pathogens.[127] Most commonly formed in high shear environments (environments with high velocity liquid movement), biofilms cause between 65% and 80% of human infections in the United States and are known to adhere to epithelial surfaces in the heart, the lungs of patients with cystic fibrosis (CF), and the gums, causing infective endocarditis, CF pneumonia, and periodontal disease (respectively).[127,128] They pose a unique threat in healthcare settings as they can contaminate medical surfaces such as catheters and implants. They are also responsible for biofouling, a huge problem in the shipping industry, as they provide a sticky and nutrient-rich surface for larger organisms to adhere to.[129] Despite the omnipresence of biofilm-based infections, only a few antibiofilm therapies have been successfully demonstrated in humans.[130]

4.1.2 Endospores

Certain species of (mostly Gram-positive) bacteria can alter their morphology to a reduced cellular form, called an endospore. These spores are tough, dormant forms of bacteria that are immune to ultraviolet light, heat, freezing, desiccation, and antibiotics. They are composed of just DNA and a few limited proteins encased in multiple protective layers (an inner membrane, a germ cell wall, a spore cortex, an outer membrane, and a spore coat).[131] The spore coat contains a variety of species-specific enzymes and acts as a sort of chemical defense by deactivating potentially harmful molecules. Large amounts of dipicolinic acid in the cytoplasm appear to stabilize the DNA and confer some of the spore's tolerant properties.

They are formally known as *endo*spores because they first form within a bacterial cell. The process begins when specialized sporulation proteins direct an asymmetrical cell division resulting in the engulfment of a pre-spore daughter cell by the mother cell. The peptidoglycan cortex and the spore coat are then formed. When the mother cell decomposes, a mature spore is released. The sporulation process is triggered by nutrient depletion. It is reversed through a process called germination in which receptors (embedded in the spore coat layers) bind to key signal molecules called germinants and signal to the spore that conditions are appropriate for growth. While many of the finer mechanistic details of sporulation and germination are still unknown, it is obvious that sporulation is a very successful tolerance strategy. Endospores are perhaps the most durable cells in existence, with reports of spores remaining viable for millions of years.[132] Destruction of spores requires extreme measures, such as burning, heating under pressure to 121 °C, or exposure to ionizing radiation. In the laboratory, they are typically sterilized using ethylene oxide or 10% bleach, or through cycles of heating in a method known as tyndallization.

For example, *Clostridioides difficile* is an urgent endospore forming bacterium that typically resides in the human colon. It is responsible for 223,900 infections and 12,800 deaths per year in the United States alone.[10] Its spores, which are spread via infected people's feces, can survive on a variety of surfaces and, if ingested, will traverse a new host's gastrointestinal tract, unaffected by stomach acid to settle in a new colon. The likelihood of contracting a serious C-diff infection is increased if a patient has recently received a course of antibiotics for another bacterial infection, with fluoroquinolones among the most implicated drugs. This allows *C. difficile*, which is typically a weak competitor for nutrients, to flourish, especially in clinical environments.

4.1.3 Filamentation

Certain rod-shaped bacteria grow in filaments—long strand-like forms which arise when bacteria grow without dividing. These are multinucleated cells, meaning that they contain multiple nucleoids evenly spaced along the filament, sometimes separated by septa. Some non-pathogenic species naturally prefer to form filaments, while others only do so under stress, such as DNA damage, high temperatures, or the presence of cell wall synthesis-targeting antibiotics.[133] For example, the DNA-damage SOS response induces expression of *sulA*, a cell division inhibitor.[134] In other cases, treatment with ß-lactam antibiotics (especially cefuroxime and ceftazidime) is believed to cause filamentation in *Escherichia coli* and *P. aeruginosa* through the inhibition of PBP3, which is responsible for peptidoglycan cross-linking at the septal wall.[135] Even in the absence of stress, filaments are usually present in small amounts. Release from the inducing stress results in resumption of cell division, splitting the filament into regular cells.

Filamentation, although it may be transient, can enhance the virulence of a bacterium. It promotes adherence both *in vitro* and *in vivo* to host epithelial cells through increased cellular surface area.[136] Filaments' larger size also impedes engulfment by neutrophils and phagocytes in the host immune system, as well as predation by protists in marine environments.[137] It has been observed that filamentation mediates the development of antibiotic resistance: in cases of SOS-induced filament formation, cells also experience a higher rate of mutagenesis. Concerted filamentation and mutation allows these cells to accumulate resistance mutations as the filament extends, and, upon SOS response cessation, leads to the release of the most drug-resistant cells from the ends of the filament.[138] It is also possible that adaptation results from chromosomal recombination within the filament.

4.2 The SOS Response

Several resistance and tolerance pathways have been connected to the bacterial SOS response. The response is triggered by DNA damage caused by UV exposure, reactive oxygen species, or antimicrobials. Damaged DNA stalls transcription, exposing single-stranded DNA. RecA, a DNA damage sensor protein, is then recruited to the ssDNA, which templates RecA's filamentation and activation, creating RecA*. Interaction between RecA* and LexA then induces a conformational change, moving one of LexA's β-turns into LexA's proteolytic site, which in turn causes the cleavage of LexA.[139] Ultimately, this leads to the disassociation of LexA from the SOS promoter region of the DNA, allowing the unrepressed transcription of the SOS genes—over 40 genes including low-fidelity DNA polymerases that promote mutagenesis and genes that induce persister cell formation, dissemination of mobile gene elements, and resistance determinants (Figure 4.2).[119,134,140–146]

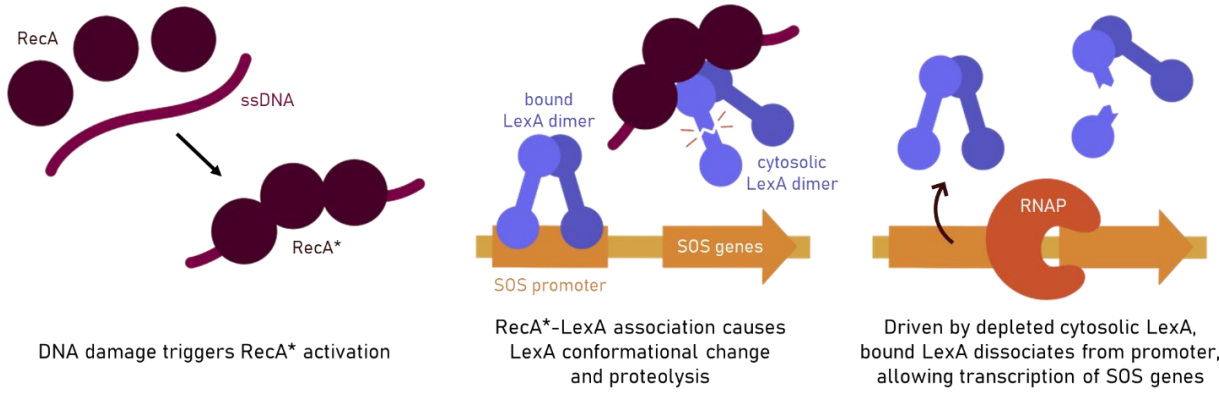

Figure 4.2: The SOS Response. The response is controlled by repressor-protease LexA.

Multiple commercial antibiotics increase resistance development through stress response induction. The SOS response has specifically been incriminated in this phenomenon. Indeed, interruption of the SOS response with a non-cleavable LexA mutant mitigates acquired resistance to fluoroquinolones.[147] Furthermore, attenuation of the SOS

response via *recA* inactivation not only reduces acquired resistance of *Escherichia coli* to several antibiotics, but also sensitizes the bacteria to some antibiotics.[148] Mutations in *recA* also decrease mutation rate in low-level quinolone-resistant *E. coli* strains and decrease biofilm production by 22-80%.[149] This is not the only time the SOS response has been connected to biofilm formation.[150,151] LexA represses transcription of *fnbB*, a fibronectin-binding protein important for adherence to extracellular matrix components and, as a result, biofilm formation.[152,153] As a result, *recA* mutants display diminished stress-induced biofilm formation (4x), whereas *recA*-complemented strains regain biofilm formation ability.[149,150]

SOS is integral to bacterial colonization—compared to a wildtype, an SOS-impaired strain of *E. coli* is less fit to colonize the gut in a mouse model.[154] It also contributes to the formation of filaments, spores, and persisters.[144,151,155] In fact, *tisB*, the first verified persister gene, is under SOS control.[38] These factors make the SOS response an attractive target for the abrogation of acquired resistance and biofilm formation, among other adaptive responses. An inhibitor of this stress response could be co-administered with traditional antibiotics to extend—perhaps indefinitely—their clinical shelf life.

Most investigations of the SOS response utilize genetic engineering to compare wildtype and SOS-interrupted bacteria. Only a handful of studies have attempted to use inhibitors, and those that have targeted RecA activity or filamentation.[156–162] However, RecA is homologous to the fundamental eukaryotic Rad51 recombinase family, making it a problematic antibiotic target.[163] Seeing as the key step of SOS response initiation is the RecA*-induced cleavage of LexA, LexA (which has no eukaryotic homologs) would be a more ideal target.[164]

4.3 Small Molecule Inhibitors of LexA

In 2018 our collaborators in the Kohli Group, who have been researching the SOS response for some time, designed a high-throughput screen to identify small molecule inhibitors of SOS.[165–168] In bacteria, LexA exists as a homodimer with each unit composed of a DNA-binding N-terminal domain and a proteolytic C-terminal domain. Our collaborators built a FlAsH-LexA construct in which the N-terminal domain was replaced with a tetracysteine tag that binds to the FlAsH fluorophore. This construct could then be used to measure RecA*-dependent LexA autoproteolytic activity as a function of fluorescence in a high throughput manner. In a partnership with GlaxoSmithKline, they used FlAsH-LexA to screen a library of approximately 1.8 million compounds and subsequently identified 144 potential lead compounds. These were further narrowed down on the basis of potency, cell permeability, and selectivity, leaving compound **GSK-1** (Figure 4.2) as the chosen lead for advancement.

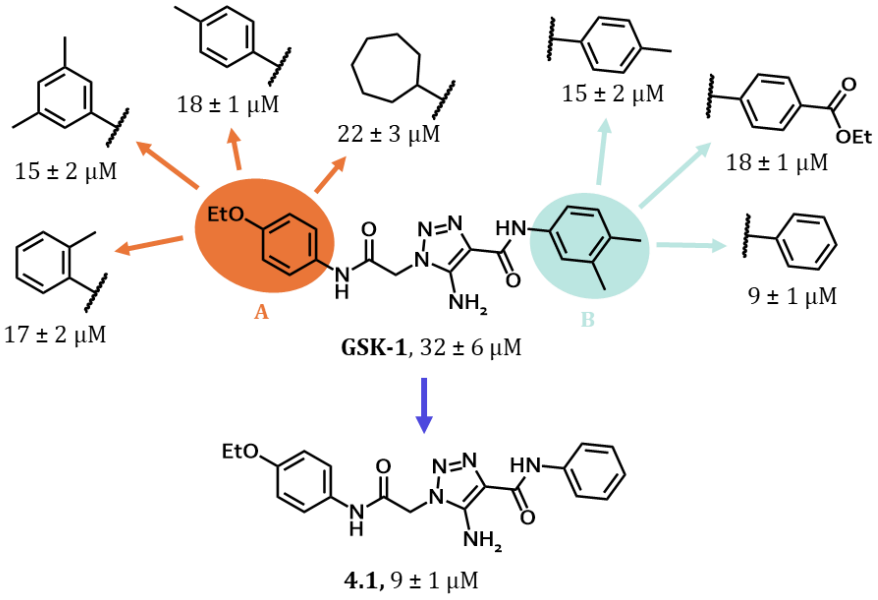

Figure 4.3: Previous SAR study.

Although **GSK-1** had shown potent activity in *in vitro* assays, there was room for improvement in whole cell testing. The Kohli group performed a preliminary SAR study which yielded some basic information about the functional groups adorning **GSK-1**.[169] Methylation of either amide nitrogen completely abolished activity, as did truncation or elongation of the B portion of the molecule. Removal or replacement of the primary amine with a hydrocarbon also resulted in a total loss of activity, while various other modifications were accompanied by decreases (but not loss) of activity. Ultimately, it was most beneficial to maintain the central scaffold while making modifications to the substitutions of the outer aryl rings (Figure 4.2). This strategy provided an inhibitor 4x more potent than **GSK-1**. While **GSK-1** appeared to inhibit the RecA*-LexA interaction, **4.1** inhibited low levels of proteolysis that LexA naturally undergoes in the absence of RecA*, indicating that it functions by specifically interacting with LexA.

4.4 Expanded SAR Library

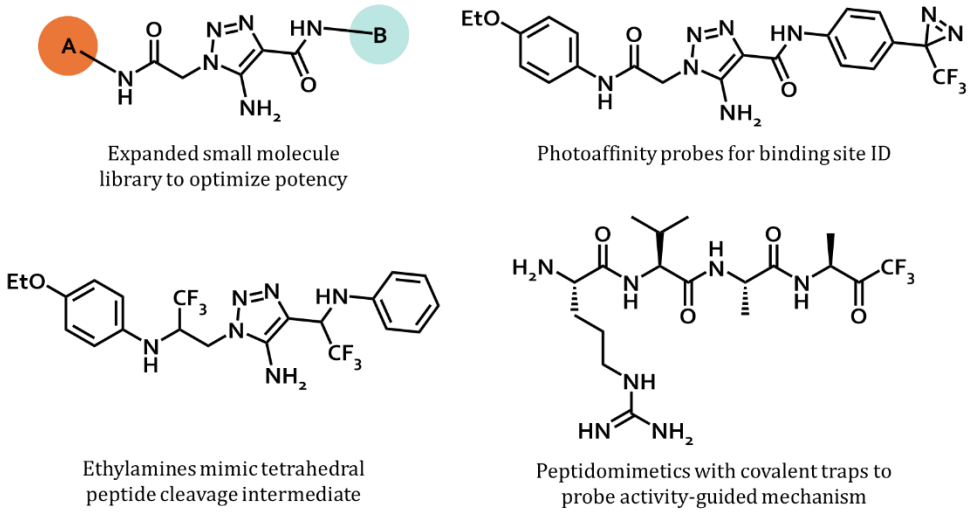

Figure 4.4: Original research proposal

Intrigued by LexA as a target, I proposed a collaboration with the Kohli group. Though they had conducted a SAR campaign, they had outsourced synthesis of their compounds to a

private company. I proposed to synthesize an expanded library of small molecule inhibitors with a wider array of substitutions on the outer rings as well as trifluoroethylamine analogues, proteomic probes, and peptidomimetic analogues (Figure 4.3). I also proposed some downstream biological assays, including measuring mutation rate and biofilm growth in the presence of inhibitors.

I began with the small molecule library, the potencies of which would inform the other analogues I had proposed. I envisioned assembling the analogues with a convergent synthesis: the relevant anilines would be amide coupled with 2-bromoacetyl bromide, followed by respective substitution with either a cyanide or azide nucleophile, and finally united with a base-catalyzed click reaction used in the previous SAR study.[169] However, the click reaction presented synthetic difficulties. None of the reported conditions yielded the desired product. In fact, I was only able to isolate an unexpected side product (a dihydropyrrolone) which I later purified for testing (**4.12**). In a dark twist of fate, my troubleshooting was interrupted by the COVID-19 pandemic. It wasn't until several months and many frustrations later that a simple solvent and base swap yielded the desired click product (troubleshooting information in the Supporting Information).

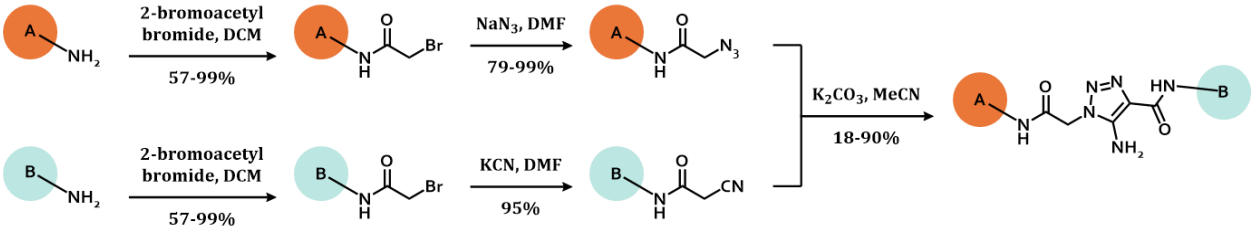

Figure 4.5: Synthesis of small molecule panel.

With the click reaction working, I synthesized a panel of 12 compounds, including **4.1**, the previous lead (Figure 4.5). Unfortunately, upon IC_{50} testing, none of the synthesized analogues improved LexA cleavage inhibition. Even in the case of analogues **4.2-4.5**, which

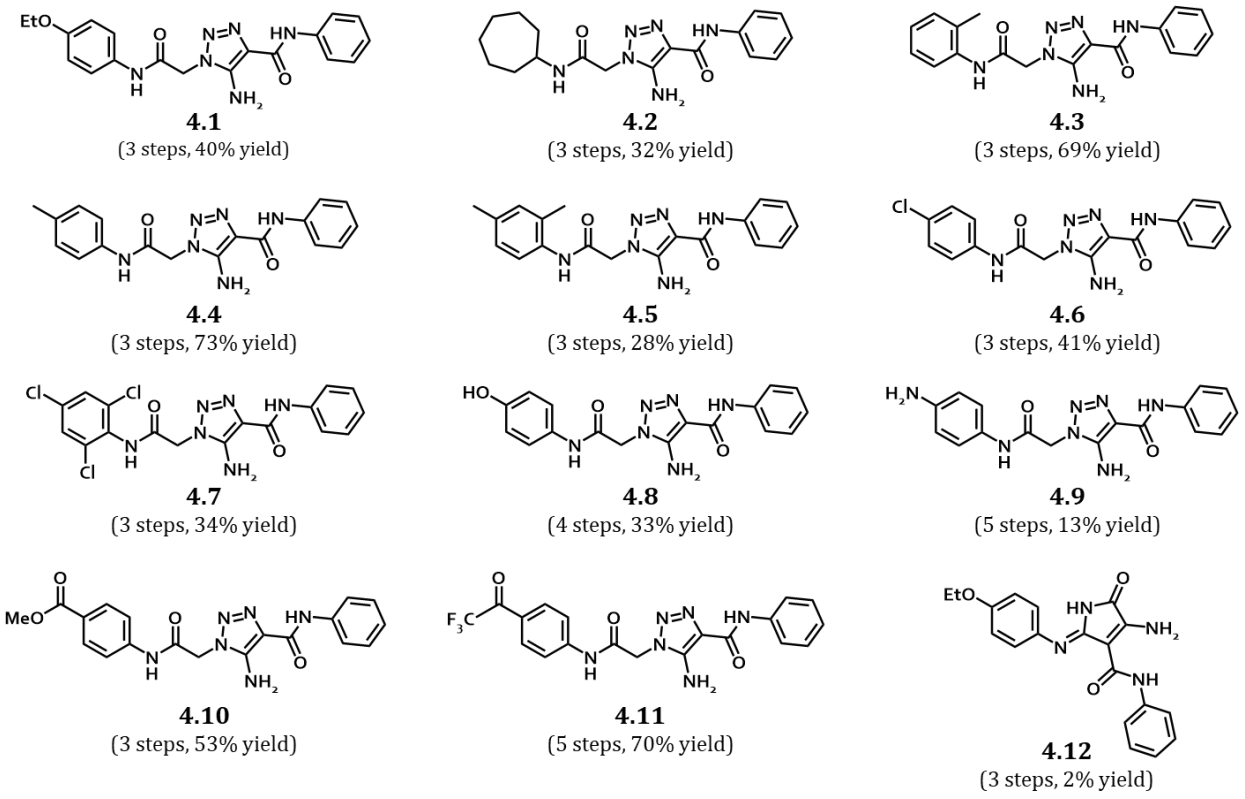

Figure 4.6: Small molecule panel.

combined the most potent A and B fragments from the previous SAR study, no improvement was observed. Further, addition of electron-withdrawing substitutions and heteroatoms also decreased inhibitor potency.

The counterintuitive bioactivity observed for analogues **4.2**-**4.5** might be explained by conformational similarities between our small molecules and the native cleavage region of LexA. In the active conformation of LexA, the cleavage loop adopts a β-turn shape. Our small molecules center a 1,2,3-triazole, which has been used in the past to mimic β-turn structures.[170,171] Thus, the inhibitors could be directly competing with the native cleavage loop for binding to the active site of LexA by adopting this shape, positioning the A and B rings proximal to each other. As a result, simultaneous changes in these two rings might be synergistic or antagonistic.

Alongside the small molecule panel, I had begun efforts toward the synthesis of the proteomic probes and peptidomimetics. However, due to differences in project goals between us and our collaborators as well as my graduation timeline, I ceased working on the other components of the proposal.

Table 4.1: LexA IC_{50} of small molecules.

Analog	IC_{50} (μM)	Analog	IC_{50} (μM)
1	37	**7**	>250
2	>250	**8**	>250
3	>250	**9**	>250
4	110	**10**	75
5	>250	**11**	>250
6	>250	**12**	>250

References

(1) Forrest, R. D. Early History of Wound Treatment. *J. R. Soc. Med.* **1982**, *75* (3), 198–205.

(2) W.J., L. Considerations for Determining If a Natural Product Is an Effective Wound-Healing Agent. *Int. J. Low. Extrem. Wounds* **2008**, *7* (2), 75–81. https://doi.org/10.1177/1534734608316028.

(3) Pirvu, L.; Nicorescu, I.; Hlevca, C.; Albu, B.; Nicorescu, V. Epilobi Hirsuti Herba Extracts Influence the In Vitro Activity of Common Antibiotics on Standard Bacteria. *Open Chem.* **2016**, *14*, 65–75. https://doi.org/10.1515/chem-2016-0004.

(4) Harrison, F.; Roberts, A. E. L.; Gabrilska, R.; Rumbaugh, K. P.; Lee, C.; Diggle, S. P. A 1,000-Year-Old Antimicrobial Remedy with Antistaphylococcal Activity. *MBio* **2015**, *6* (4), 1–7. https://doi.org/10.1128/mBio.01129-15.

(5) Tsou, L. K.; Lara-Tejero, M.; Rosefigura, J.; Zhang, Z. J.; Wang, Y. C.; Yount, J. S.; Lefebre, M.; Dossa, P. D.; Kato, J.; Guan, F.; Lam, W.; Cheng, Y. C.; Galán, J. E.; Hang, H. C. Antibacterial Flavonoids from Medicinal Plants Covalently Inactivate Type III Protein Secretion Substrates. *J. Am. Chem. Soc.* **2016**, *138*, 2209–2218. https://doi.org/10.1021/jacs.5b11575.

(6) Kohanski, M. A.; Dwyer, D. J.; Collins, J. J. How Antibiotics Kill Bacteria: From Targets to Networks. *Nat. Rev. Microbiol.* **2010**, *8* (6), 423–435. https://doi.org/10.1038/nrmicro2333.How.

(7) Pankey, G. A.; Sabath, L. D. Clinical Relevance of Bacteriostatic versus Bactericidal Activity in the Treatment of Gram-Positive Bacterial Infections. *Clin. Infect. Dis.* **2004**, *38*, 864–870. https://doi.org/10.1086/381972.

(8) Melander, R. J.; Zurawski, D. V.; Melander, C. Narrow-Spectrum Antibacterial Agents. *Med. Chem. Commun.* **2018**, *9*, 12–21. https://doi.org/10.1039/c7md00528h.

(9) Janos Berdy. Thoughts and Facts about Antibiotics: Where We Are Now and Where We Are Heading. *J. Antibiot. (Tokyo).* **2012**, *65*, 385–395. https://doi.org/10.1038/ja.2012.27.

(10) CDC. *Antibiotic Resistance Threats in the United States*; Centers for Disease Control and Prevention: Atlanta, GA, 2019. https://doi.org/10.15620/cdc:82532.

(11) Blumenthal, K. G.; Peter, J. G.; Trubiano, J. A.; Phillips, E. J. Antibiotic Allergy. *Lancet* **2019**, *393* (10167), 183–198. https://doi.org/10.1016/S0140-6736(18)32218-9.Antibiotic.

(12) Boeckel, T. P. Van; Pires, J.; Silvester, R.; Zhao, C.; Song, J.; Criscuolo, N. G.; Gilbert, M.; Bonhoeffer, S.; Laxminarayan, R. Global Trends in Antimicrobial Resistance in Animals in Low- and Middle-Income Countries. *Science (80-.).* **2019**, *365*, 1266. https://doi.org/10.1126/science.aaw1944.

(13) Moore, P. R.; Evenson, A.; Luckey, T. D.; McCoy, E.; Elvehjem, C. A.; Hart, E. B. Use of

Sulfasuxidine, Streptothricin, and Streptomycin in Nutritional Studies With the Chick. *J. Biol. Chem.* **1946**, *165*, 437–441.

(14) Stokstad, E. L. R.; Jukes, T. H.; Pierce, J.; Page, A. C.; Franklin, A. L. The Multiple Nature of the Animal Protein Factor. *J. Biol. Chem.* **1949**, *180* (2), 647–654.

(15) Halling-Sorensen, B.; Nielsen, S. N.; Lanzky, P. F.; Lutzhoft, H. C. H.; Jorgensen, S. E. Occurrence, Fate and Effects of Pharmaceutical Substances in the Environment - A Review. *Chemosphere* **1997**, *36* (2), 357–393. https://doi.org/10.1016/S0045-6535(97)00354-8.

(16) Foster, P. L. Stress Responses and Genetic Variation in Bacteria. *Mutat. Res.* **2005**, *569* (1–2), 3–11. https://doi.org/10.1016/j.mrfmmm.2004.07.017.

(17) Gyles, C.; Boerlin, P. Horizontally Transferred Genetic Elements and Their Role in Pathogenesis of Bacterial Disease. *Vet. Pathol.* **2014**, *51* (2), 328–340. https://doi.org/10.1177/0300985813511131.

(18) Hanssen, A.; Sollid, J. U. E. SCCmec in Staphylococci: Genes on the Move. *FEMS Immunol. Med. Microbiol.* **2006**, *46* (1), 8–20. https://doi.org/10.1111/j.1574-695X.2005.00009.x.

(19) Chang, S.; Sievert, D. M.; Hageman, J. C.; Boulton, M. L.; Tenover, F. C.; Downes, F. P.; Shah, S.; Rudrik, J. T.; Pupp, G. R.; Brown, W. J.; Cardo, D.; Fridkin, S. K. Infection with Vancomycin-Resistant Staphylococcus Aureus Containing the VanA Resistance Gene. *N. Engl. J. Med.* **2003**, *348*, 1342–1347. https://doi.org/10.1056/NEJMoa025025.

(20) Stapley, E. O. Cross-Resistance Studies and Antibiotic Identification. *Appl. Environ. Microbiol.* **1958**, *6*, 392–398.

(21) Bush, K. Past and Present Perspectives on β-Lactamases. *Antimicrob. Agents Chemother.* **2018**, *62* (10), e01076-18. https://doi.org/10.1128/AAC.01076-18.

(22) Rupp, M. E.; Fey, P. D. Extended Spectrum β-Lactamase (ESBL)-Producing Enterobacteriaceae. *Drugs* **2003**, *63* (4), 353–365.

(23) Mingeot-Leclercq, M.-P.; Glupczynski, Y.; Tulkens, P. M. Aminoglycosides: Activity and Resistance. *Antimicrob. Agents Chemother.* **1999**, *43* (4), 727–737. https://doi.org/10.1128/AAC.43.4.727.

(24) Aldred, K. J.; Kerns, R. J.; Osheroff, N. Mechanism of Quinolone Action and Resistance. *Biochemistry* **2014**, *53*, 1565–1574. https://doi.org/10.1021/bi5000564.

(25) Cetinkaya, Y.; Falk, P.; Mayhall, C. G. Vancomycin-Resistant Enterococci. *Clin. Microbiol. Rev.* **2000**, *13* (4), 686–707. https://doi.org/10.1128/cmr.13.4.686-707.2000.

(26) Butler, M. S.; Hansford, K. A.; Blaskovich, M. A. T.; Halai, R.; Cooper, M. A. Glycopeptide Antibiotics: Back to the Future. *J. Antibiot. (Tokyo).* **2014**, *67*, 631–644. https://doi.org/10.1038/ja.2014.111.

(27) Flensburg, J.; Skold, O. Massive Overproduction of Dihydrofolate Reductase in

Bacteria as a Response to the Use of Trimethoprim. *Eur. J. Biochem.* **1987**, *162*, 473–476. https://doi.org/10.1111/j.1432-1033.1987.tb10664.x.

(28) Zervos, M. J.; Schaberg, D. R. Reversal of the In Vitro Susceptibility of Enterococci to Trimethoprim-Sulfamethoxazole by Folinic Acid. *Antimicrob. Agents Chemother.* **1985**, *28* (3), 446–448. https://doi.org/10.1128/aac.28.3.446.

(29) De, E.; Basle, A.; Jaquinod, M.; Saint, N.; Mallea, M.; Molle, G.; Pages, J. A New Mechanism of Antibiotic Resistance in Enterobacteriaceae Induced by a Structural Modification of the Major Porin. *Mol. Microbiol.* **2001**, *41* (1), 189–198. https://doi.org/10.1046/j.1365-2958.2001.02501.x.

(30) Nikaido, H. Prevention of Drug Access to Bacterial Targets: Permeability Barriers and Active Efflux. *Science (80-.).* **1994**, *264* (5157), 382–388. https://doi.org/10.1126/science.8153625.

(31) Evans, B. A.; Hamouda, A.; Amyes, S. G. B. The Rise of Carbapenem-Resistant Acinetobacter Baumannii. *Curr. Pharm. Des.* **2013**, *19*, 223–238. https://doi.org/10.2174/13816128130204.

(32) Andersson, D. I.; Levin, B. R. The Biological Cost of Antibiotic Resistance. *Curr. Opin. Microbiol.* **1999**, *2*, 489–493. https://doi.org/10.1016/S1369-5274(99)00005-3.

(33) Jordt, H.; Stalder, T.; Kosterlitz, O.; Ponciano, J. M.; Top, E. M.; Kerr, B. Coevolution of Host–Plasmid Pairs Facilitates the Emergence of Novel Multidrug Resistance. *Nat. Ecol. Evol.* **2020**. https://doi.org/10.1038/s41559-020-1170-1.

(34) Brauner, A.; Fridman, O.; Gefen, O.; Balaban, N. Q. Distinguishing between Resistance, Tolerance and Persistence to Antibiotic Treatment. *Nat. Rev. Microbiol.* **2016**, *14*, 320–330. https://doi.org/10.1038/nrmicro.2016.34.

(35) Schlacher, K.; Goodman, M. F. Lessons from 50 Years of SOS DNA-Damage-Induced Mutagenesis. *Nat. Rev. Mol. Cell Biol.* **2007**, *8*, 587–594. https://doi.org/10.1038/nrm2198.

(36) Fridman, O.; Goldberg, A.; Ronin, I.; Shoresh, N.; Balaban, N. Q. Optimization of Lag Time Underlies Antibiotic Tolerance in Evolved Bacterial Populations. *Nature* **2014**, *513*, 418–421. https://doi.org/10.1038/nature13469.

(37) Bigger, J. W. Treatment of Staphylococcal Infections with Penicillin by Intermittent Sterilisation. *Lancet* **1944**, *244* (6320), 497–500.

(38) Lewis, K. Persister Cells. *Annu. Rev. Microbiol.* **2010**, *64*, 357–372. https://doi.org/10.1146/annurev.micro.112408.134306.

(39) Fisher, R. A.; Gollan, B.; Helaine, S. Persistent Bacterial Infections and Persister Cells. *Nat. Rev. Microbiol.* **2017**, *15*, 453–464. https://doi.org/10.1038/nrmicro.2017.42.

(40) Chatterji, D.; Kumar Ojha, A. Revisiting the Stringent Response, PpGpp and Starvation Signaling. *Curr. Opin. Microbiol.* **2001**, *4*, 160–165. https://doi.org/10.1016/S1369-5274(00)00182-X.

(41) Hansen, S.; Lewis, K.; Vulić, M. Role of Global Regulators and Nucleotide Metabolism in Antibiotic Tolerance in Escherichia Coli. *Antimicrob. Agents Chemother.* **2008**, *52* (8), 2718–2726. https://doi.org/10.1128/AAC.00144-08.

(42) Moyed, H. S.; Bertrand, K. P. HipA, a Newly Recognized Gene of Escherichia Coli K-12 That Affects Frequency of Persistence after Inhibition of Murein Synthesis. *J. Bacteriol.* **1983**, *155* (2), 768–775. https://doi.org/10.1128/jb.155.2.768-775.1983.

(43) Keren, I.; Shah, D.; Spoering, A.; Kaldalu, N.; Lewis, K. Specialized Persister Cells and the Mechanism of Multidrug Tolerance in Escherichia Coli. *J. Bacteriol.* **2004**, *186*, 8172–8180. https://doi.org/10.1128/JB.186.24.8172–8180.2004.

(44) Germain, E.; Castro-Roa, D.; Zenkin, N.; Gerdes, K. Molecular Mechanism of Bacterial Persistence by HipA. *Mol. Cell* **2013**, *52*, 248–254. https://doi.org/10.1016/j.molcel.2013.08.045.

(45) Huang, C. Y.; Gonzalez-Lopez, C.; Henry, C.; Mijakovic, I.; Ryan, K. R. HipBA Toxin-Antitoxin Systems Mediate Persistence in Caulobacter Crescentus. *Sci. Rep.* **2020**, *10*, 2865. https://doi.org/10.1038/s41598-020-59283-x.

(46) Lewis, K. Persister Cells, Dormancy and Infectious Disease. *Nat. Rev. Microbiol.* **2007**, *5*, 48–56. https://doi.org/10.1038/nrmicro1557.

(47) Mulcahy, L. R.; Burns, J. L.; Lory, S.; Lewis, K. Emergence of Pseudomonas Aeruginosa Strains Producing High Levels of Persister Cells in Patients with Cystic Fibrosis . *J. Bacteriol.* **2010**, *192* (23), 6191–6199. https://doi.org/10.1128/JB.01651-09.

(48) Jantsch, J.; Chikkaballi, D.; Hensel, M. Cellular Aspects of Immunity to Intracellular Salmonella Enterica. *Immunol. Rev.* **2011**, *240*, 185–195. https://doi.org/10.1111/j.1600-065X.2010.00981.x.

(49) Pier, G. B. On the Greatly Exaggerated Reports of the Death of Infectious Diseases. *Clin. Infect. Dis.* **2008**, *47*, 1113–1114. https://doi.org/10.1086/592123.

(50) Wanted: A Reward for Antibiotic Development. *Nat. Biotechnol.* **2018**, *36* (7), 555. https://doi.org/10.1038/nbt.4193.

(51) Paukner, S.; Riedl, R. Pleuromutilins: Potent Drugs for Resistant Bugs — Mode of Action and Resistance. *Cold Spring Harb Perspect Med* **2017**, *7*, a027110. https://doi.org/10.1101/cshperspect.a027110.

(52) O'Neill, J. Antimicrobial Resistance: Tackling a crisis for the health and wealth of nations https://amr-review.org/sites/default/files/AMR Review Paper - Tackling a crisis for the health and wealth of nations_1.pdf.

(53) Wertheim, H. F. L.; Melles, D. C.; Vos, M. C.; Leeuwen, W. Van; Belkum, A. Van; Verbrugh, H. A.; Nouwen, J. L. The Role of Nasal Carriage in Staphylococcus Aureus Infections. *Lancet Infect. Dis.* **2005**, *5* (12), 751–762. https://doi.org/10.1016/S1473-3099(05)70295-4.

(54) Todar, K. Staphylococcus aureus and Staphylococcal Disease

http://www.textbookofbacteriology.net/staph.html (accessed Sep 29, 2021).

(55) Tong, S. Y. C.; Davis, J. S.; Eichenberger, E.; Holland, T. L.; Fowler, V. G. Staphylococcus Aureus Infections : Epidemiology , Pathophysiology , Clinical Manifestations , and Management. *Clin. Microbiol. Rev.* **2015**, *28* (3), 603–661. https://doi.org/10.1128/CMR.00134-14.

(56) Wardenburg, J. B.; Schneewind, O. Vaccine Protection against Staphylococcus Aureus Pneumonia. *J. Exp. Med.* **2008**, *205* (2), 287–294. https://doi.org/10.1084/jem.20072208.

(57) Proctor, R. A.; von Eiff, C.; Kahl, B. C.; Becker, K.; McNamara, P.; Herrmann, M.; Peters, G. Small Colony Variants: A Pathogenic Form of Bacteria That Facilitates Persistent and Recurrent Infections. *Nat. Rev. Microbiol.* **2006**, *4*, 295–305. https://doi.org/10.1038/nrmicro1384.

(58) Palmore, T. N.; Henderson, D. K. Managing Transmission of Carbapenem-Resistant Enterobacteriaceae in Healthcare Settings: A View From the Trenches. *Clin. Infect. Dis.* **2013**, *57* (11), 1593–1599. https://doi.org/10.1093/cid/cit531.

(59) Kallen, A. J.; Mu, Y.; Bulens, S.; Reingold, A.; Petit, S.; Gershman, K.; Ray, S. M.; Harrison, L. H.; Lynfield, R.; Dumyati, G.; Townes, J. M.; Schaffner, W.; Patel, P. R.; Fridkin, S. K. Health Care-Associated Invasive MRSA Infections, 2005-2008. *J. Am. Med. Assoc.* **2010**, *304* (6), 641–648. https://doi.org/10.1001/jama.2010.1115.

(60) Otto, M. MRSA Virulence and Spread. *Cell. Microbiol.* **2012**, *14* (10), 1513–1521. https://doi.org/10.1111/j.1462-5822.2012.01832.x.

(61) Abraham, E. P.; Chain, E. An Enzyme from Bacteria Able to Destroy Penicillin.Pdf. *Nature* **1940**, *3713*, 837.

(62) Fuda, C. C. S.; Fisher, J. F.; Mobashery, S. β-Lactam Resistance in Staphylococcus Aureus: The Adaptive Resistance of a Plastic Genome. *Cell. Mol. Life Sci.* **2005**, *62*, 2617–2633. https://doi.org/10.1007/s00018-005-5148-6.

(63) Katayama, Y.; Ito, T.; Hiramatsu, K. A New Class of Genetic Element, Staphylococcus Cassette Chromosome Mec, Encodes Methicillin Resistance in Staphylococcus Aureus. *Antimicrob. Agents Chemother.* **2000**, *44* (6), 1549–1555.

(64) Hartman, B. J.; Tomasz, A. Low-Affinity Penicillin-Binding Protein Associated with β-Lactam Resistance in Staphylococcus Aureus. *J. Bacteriol.* **1984**, *158* (2), 513–516.

(65) Pupp, G. R.; Brown, W. J.; Ph, D.; Cardo, D.; Fridkin, S. K. Infection with Vancomycin-Resistant Staphylococcus Aureus Containing the VanA Resistance Gene. *N. Engl. J. Med.* **2003**, *348*, 1342–1347.

(66) Tsiodras, S.; Gold, H. S.; Sakoulas, G.; Eliopoulos, G. M.; Wennersten, C.; Venkataraman, L.; Moellering, R. C.; Ferraro, M. J. Linezolid Resistance in a Clinical Isolate of Staphylococcus Aureus. *Lancet* **2001**, *358*, 207–208. https://doi.org/10.1016/S0140-6736(01)05410-1.

(67) Allison, K. R.; Brynildsen, M. P.; Collins, J. J. Metabolite-Enabled Eradication of Bacterial Persisters by Aminoglycosides. *Nature* **2011**, *473*, 216–220. https://doi.org/10.1038/nature10069.

(68) Archer, N. K.; Mazaitis, M. J.; Costerton, J. W.; Leid, J. G.; Powers, M. E.; Shirtliff, M. E. osteomyeliti. Staphylococcus Aureus Biofilms: Properties, Regulation and Roles in Human Disease. *Virulence* **2011**, *2* (5), 445–459. https://doi.org/10.4161/viru.2.5.17724.

(69) Waters, E. M.; Rowe, S. E.; Gara, J. P. O.; Conlon, B. P. Convergence of Staphylococcus Aureus Persister and Biofilm Research : Can Biofilms Be Defined as Communities of Adherent Persister Cells ? *PLoS Pathog.* **2016**, *12* (12), e1006012. https://doi.org/10.1371/journal.ppat.1006012.

(70) Tuchscherr, L.; Heitmann, V.; Hussain, M.; Viemann, D.; Roth, J.; Von Eiff, C.; Peters, G.; Becker, K.; Löffler, B. Staphylococcus Aureus Small-Colony Variants Are Adapted Phenotypes for Intracellular Persistence. *J. Infect. Dis.* **2010**, *202* (7), 1031–1040. https://doi.org/10.1086/656047.

(71) Kalinka, J.; Hachmeister, M.; Geraci, J.; Sordelli, D.; Hansen, U.; Niemann, S.; Oetermann, S.; Peters, G.; Löffler, B.; Tuchscherr, L. Staphylococcus Aureus Isolates from Chronic Osteomyelitis Are Characterized by High Host Cell Invasion and Intracellular Adaptation, but Still Induce Inflammation. *Int. J. Med. Microbiol.* **2014**, *304*, 1038–1049. https://doi.org/10.1016/j.ijmm.2014.07.013.

(72) Chong, Y. P.; Park, S. J.; Kim, H. S.; Kim, E. S.; Kim, M. N.; Park, K. H.; Kim, S. H.; Lee, S. O.; Choi, S. H.; Jeong, J. Y.; Woo, J. H.; Kim, Y. S. Persistent Staphylococcus Aureus Bacteremia: A Prospective Analysis of Risk Factors, Outcomes, and Microbiologic and Genotypic Characteristics of Isolates. *Medicine (Baltimore).* **2013**, *92* (2), 98–108. https://doi.org/10.1097/MD.0b013e318289ff1e.

(73) Kim, W.; Hendricks, G. L.; Tori, K.; Fuchs, B. B.; Mylonakis, E. Strategies against Methicillin-Resistant Staphylococcus Aureus Persisters. *Future Med. Chem.* **2018**, *10* (7), 779–794. https://doi.org/10.4155/fmc-2017-0199.

(74) Lavey, N. P.; Coker, J. A.; Ruben, E. A.; Duerfeldt, A. S. Sclerotiamide: The First Non-Peptide-Based Natural Product Activator of Bacterial Caseinolytic Protease P. *J. Nat. Prod.* **2016**, *79*, 1193–1197. https://doi.org/10.1021/acs.jnatprod.5b01091.

(75) Epand, R. M.; Walker, C.; Epand, R. F.; Magarvey, N. A. Molecular Mechanisms of Membrane Targeting Antibiotics. *Biochim. Biophys. Acta* **2016**, *1858*, 980–987. https://doi.org/10.1016/j.bbamem.2015.10.018.

(76) Herzog, I. M.; Fridman, M. Design and Synthesis of Membrane-Targeting Antibiotics: From Peptides- to Aminosugar-Based Antimicrobial Cationic Amphiphiles. *Medchemcomm* **2014**, *5*, 1014–1026. https://doi.org/10.1039/c4md00012a.

(77) Morrison, K. R.; Allen, R. A.; Minbiole, K. P. C.; Wuest, W. M. More QACs , More Questions: Recent Advances in Structure Activity Relationships and Hurdles in Understanding Resistance Mechanisms. *Tetrahedron Lett.* **2019**, *60*, 150935.

https://doi.org/10.1016/j.tetlet.2019.07.026.

(78) O'Byrne, S. M.; Blaner, W. S. Retinol and Retinyl Esters: Biochemistry and Physiology. *J. Lipid Res.* **2013**, *54*, 1731–1743. https://doi.org/10.1194/jlr.R037648.

(79) Tanumihardjo, S. A. Vitamin A: Biomarkers of Nutrition for Development. *Am. J. Clin. Nutr.* **2011**, *94*, 658S-665S. https://doi.org/10.3945/ajcn.110.005777.

(80) McGrane, M. M. Vitamin A Regulation of Gene Expression: Molecular Mechanism of a Prototype Gene. *J. Nutr. Biochem.* **2007**, *18*, 497–508. https://doi.org/10.1016/j.jnutbio.2006.10.006.

(81) Mucida, D.; Park, Y.; Kim, G.; Turovskaya, O.; Scott, I.; Kronenberg, M.; Cheroutre, H. Reciprocal TH17 and Regulatory T Cell Differentiation by Retinoic Acid. *Science (80-.).* **32009BC**, *317*, 256–260. https://doi.org/10.1126/science.1145697.

(82) Cabezas-Wallscheid, N.; Buettner, F.; Sommerkamp, P.; Klimmeck, D.; Ladel, L.; Thalheimer, F. B.; Pastor-Flores, D.; Roma, L. P.; Renders, S.; Zeisberger, P.; Przybylla, A.; Schönberger, K.; Scognamiglio, R.; Altamura, S.; Florian, C. M.; Fawaz, M.; Vonficht, D.; Tesio, M.; Collier, P.; Pavlinic, D.; Geiger, H.; Schroeder, T.; Benes, V.; Dick, T. P.; Rieger, M. A.; Stegle, O.; Trumpp, A. Vitamin A-Retinoic Acid Signaling Regulates Hematopoietic Stem Cell Dormancy. *Cell* **2017**, *169*, 807–823. https://doi.org/10.1016/j.cell.2017.04.018.

(83) Zasada, M.; Budzisz, E. Retinoids: Active Molecules Influencing Skin Structure Formation in Cosmetic and Dermatological Treatments. *Adv Dermatol Allergol* **2019**, *36* (4), 392–397. https://doi.org/10.5114/ada.2019.87443.

(84) Rolewski, S. L. Clinical Review: Topical Retinoids. *Dermatology Nurs.* **2003**, *15* (5), 447–465.

(85) Martin, B.; Bernardon, J.-M.; Cavey, M.-T.; Bernard, B.; Carlavan, I.; Charpentier, B.; Pilgrim, W. R.; Shroot, B.; Reichert, U. Selective Synthetic Ligands for Human Nuclear Retinoic Acid Receptors. *Skin Pharmacol. Physiol.* **1992**, *5*, 57–65. https://doi.org/10.1159/000211018.

(86) Sun, S.; Yue, P.; Lotan, R. Implication of Multiple Mechanisms in Apoptosis Induced by the Synthetic Retinoid CD437 in Human Prostate Carcinoma Cells. *Oncogene* **2000**, *19*, 4513–4522.

(87) Zhao, X.; Spanjaard, R. A. The Apoptotic Action of the Retinoid CD437/AHPN: Diverse Effects, Common Basis. *J. Biomed. Sci.* **2003**, *10*, 44–49. https://doi.org/10.1159/000068087.

(88) Li, Y.; Lin, B.; Agadir, A.; Liu, R.; Dawson, M. I.; Reed, J. C.; Fontana, J. A.; Bost, F.; Hobbs, P. D.; Zheng, Y.; Chen, G.-Q.; Chroot, B.; Mercola, D.; Zhang, X.-K. Molecular Determinants of AHPN (CD437)-Induced Growth Arrest and Apoptosis in Human Lung Cancer Cell Lines. *Mol. Cell. Biol.* **1998**, *18* (8), 4719–4731. https://doi.org/10.1128/mcb.18.8.4719.

(89) Fontana, J. A.; Rishi, A. K. Classical and Novel Retinoids: Their Targets in Cancer

Therapy. *Leukemia* **2002**, *16*, 463–472. https://doi.org/10.1038/sj.leu.2402414.

(90) Han, T.; Goralski, M.; Capota, E.; Padrick, S. B.; Kim, J.; Xie, Y.; Nijhawan, D. The Antitumor Toxin CD437 Is a Direct Inhibitor of DNA Polymerase α. *Nat. Chem. Biol.* **2016**, *12* (7), 511–515. https://doi.org/10.1038/nchembio.2082.

(91) Susen, S.; Corseaux, D.; Sottejeau, Y.; Rosa, M.; Soquet, J.; Belle, E. Van; Staels, B.; Dupont, A. Use of Retinoic Acid Receptor (RAR) Agonists for Reversing, Preventing, or Delaying Calcification of Aortic Valve. WO 2021/064072 Al, 2021.

(92) McCoy, O. A. G. J. Minoxidil Adjuvant Therapies. US 2021/0059920 Al, 2021.

(93) Kim, W.; Zhu, W.; Hendricks, G. L.; Tyne, D. Van; Steele, A. D.; Keohane, C. E.; Fricke, N.; Conery, A. L.; Shen, S.; Pan, W.; Lee, K.; Rajamuthiah, R.; Fuchs, B. B.; Vlahovska, P. M.; Wuest, W. M.; Gilmore, M. S.; Gao, H.; Ausubel, F. M.; Mylonakis, E. A New Class of Synthetic Retinoid Antibiotics Effective against Bacterial Persisters. *Nature* **2018**, *556*, 103–107. https://doi.org/10.1038/nature26157.

(94) Rajamuthiah, R.; Fuchs, B. B.; Jayamani, E.; Kim, Y.; Larkins-ford, J.; Conery, A.; Ausubel, F. M.; Mylonakis, E. Whole Animal Automated Platform for Drug Discovery against Multi-Drug Resistant Staphylococcus Aureus. *PLoS One* **2014**, *9* (2), 1–11. https://doi.org/10.1371/journal.pone.0089189.

(95) Cincinelli, R.; Dallavalle, S.; Merlini, L.; Penco, S.; Pisano, C.; Carminati, P.; Giannini, G.; Vesci, L.; Gaetano, C.; Illy, B.; Zuco, V.; Supino, R.; Zunino, F. A Novel Atypical Retinoid Endowed with Proapoptotic and Antitumor Activity. *J. Med. Chem.* **2003**, *46*, 909–912. https://doi.org/10.1021/jm025593y.

(96) Cincinelli, R.; Dallavalle, S.; Nannei, R.; Carella, S.; De Zani, D.; Merlini, L.; Penco, S.; Garattini, E.; Giannini, G.; Pisano, C.; Vesci, L.; Carminati, P.; Zuco, V.; Zanchi, C.; Zunino, F. Synthesis and Structure-Activity Relationships of a New Series of Retinoid-Related Biphenyl-4-Ylacrylic Acids Endowed with Antiproliferative and Proapoptotic Activity. *J. Med. Chem.* **2005**, *48*, 4931–4946. https://doi.org/10.1021/jm049440h.

(97) Cheng, A. V.; Kim, W.; Escobar, I. E.; Mylonakis, E.; Wuest, W. M. Structure-Activity Relationship and Anticancer Profile of Second-Generation Anti-MRSA Synthetic Retinoids. *ACS Med. Chem. Lett.* **2019**, ASAP. https://doi.org/10.1021/acsmedchemlett.9b00159.

(98) Kontos, R. C.; Schallenhammer, S. A.; Bentley, B. S.; Morrison, K. R.; Feliciano, J. A.; Tasca, J. A.; Kaplan, A. R.; Bezpalko, M. W.; Kassel, W. S.; Wuest, W. M.; Minbiole, K. P. C. An Investigation into Rigidity–Activity Relationships in BisQAC Amphiphilic Antiseptics. *ChemMedChem* **2019**, *14*, 83–87. https://doi.org/10.1002/cmdc.201800622.

(99) Silhavy, T. J.; Kahne, D.; Walker, S. The Bacterial Cell Envelope. *Cold Spring Harb Perspect Biol* **2010**, *2*, a000414. https://doi.org/10.1101/cshperspect.a000414.

(100) Hiroshi, N. Prevention of Drug Access to Bacterial Targets: Permeability Barriers and Active Efflux. *Science (80-.).* **1994**, *264* (April), 382–388.

(101) Vaara, M.; Plachy, W. Z.; Nikaido, H. Partitioning of Hydrophobic Probes into Lipopolysaccharide Bilayers. *Biochim. Biophys. Acta* **1990**, *1024*, 152–158. https://doi.org/10.1016/0005-2736(90)90218-D.

(102) Nikaido, H. Molecular Basis of Bacterial Outer Membrane Permeability. *Microbiol. Mol. Biol. Rev.* **2003**, *67* (4), 593–656. https://doi.org/10.1128/MMBR.67.4.593–656.2003.

(103) Richter, M. F.; Hergenrother, P. J. The Challenge of Converting Gram-Positive-Only Compounds into Broad-Spectrum Antibiotics. *Ann. N. Y. Acad. Sci.* **2018**, *1435* (1), 18–38. https://doi.org/10.1111/nyas.13598.

(104) Piddock, L. J. V. Clinically Relevant Chromosomally Encoded Multidrug Resistance Efflux Pumps in Bacteria. *Clin. Microbiol. Rev.* **2006**, *19* (2), 382–402. https://doi.org/10.1128/CMR.19.2.382-402.2006.

(105) Silver, L. L. Challenges of Antibacterial Discovery. *Clin. Microbiol. Rev.* **2011**, *24* (1), 71–109. https://doi.org/10.1128/CMR.00030-10.

(106) Cheng Jaramillo, A. V.; Wuest, W. M. *Antibacterials*; American Chemical Society, 2021. https://doi.org/10.1021/acs.infocus.7e4006.

(107) Lipinski, C. A.; Lombardo, F.; Dominy, B. W.; Feeney, P. J. Experimental and Computational Approaches to Estimate Solubility and Permeability in Drug Discovery and Development Settings. *Adv. Drug Deliv. Rev.* **2001**, *46*, 3–26. https://doi.org/10.1016/S0169-409X(00)00129-0.

(108) O'Shea, R.; Moser, H. E. Physicochemical Properties of Antibacterial Compounds: Implications for Drug Discovery. *J. Med. Chem.* **2008**, *51* (10), 2871–2878. https://doi.org/10.1021/jm700967e.

(109) Brown, D. G.; May-Dracka, T. L.; Gagnon, M. M.; Tommasi, R. Trends and Exceptions of Physical Properties on Antibacterial Activity for Gram-Positive and Gram-Negative Pathogens. *J. Med. Chem.* **2014**, *57*, 10144–10161. https://doi.org/10.1021/jm501552x.

(110) Acred, P.; Brown, D. M.; Turner, D. H.; Wilson, M. J. Pharmacology and Chemotherapy of Ampicillin—a New Broad-Spectrum Penicillin. *Br. J. Pharmacol. Chemother.* **1962**, *18*, 356–369. https://doi.org/10.1111/j.1476-5381.1962.tb01416.x.

(111) Richter, M. F.; Drown, B. S.; Riley, A. P.; Garcia, A.; Shirai, T.; Svec, R. L.; Hergenrother, P. J. Predictive Rules for Compound Accumulation Yield a Broad-Spectrum Antibiotic. *Nature* **2017**, *545* (7654), 299–304. https://doi.org/10.1038/nature22308.

(112) Hernandez, V.; Crépin, T.; Palencia, A.; Cusack, S.; Akama, T.; Baker, S. J.; Bu, W.; Feng, L.; Freund, Y. R.; Liu, L.; Meewan, M.; Mohan, M.; Mao, W.; Rock, F. L.; Sexton, H.; Sheoran, A.; Zhang, Y.; Zhang, Y. K.; Zhou, Y.; Nieman, J. A.; Anugula, M. R.; Keramane, E. M.; Savariraj, K.; Shekhar Reddy, D.; Sharma, R.; Subedi, R.; Singh, R.; O'Leary, A.; Simon, N. L.; De Marsh, P. L.; Mushtaq, S.; Warner, M.; Livermore, D. M.; Alley, M. R. K.; Plattner, J. J. Discovery of a Novel Class of Boron-Based Antibacterials with Activity

against Gram-Negative Bacteria. *Antimicrob. Agents Chemother.* **2013**, *57* (3), 1394–1403. https://doi.org/10.1128/AAC.02058-12.

(113) Savage, V. J.; Charrier, C.; Salisbury, A. M.; Moyo, E.; Forward, H.; Chaffer-Malam, N.; Metzger, R.; Huxley, A.; Kirk, R.; Uosis-Martin, M.; Noonan, G.; Mohmed, S.; Best, S. A.; Ratcliffe, A. J.; Stokes, N. R. Biological Profiling of Novel Tricyclic Inhibitors of Bacterial DNA Gyrase and Topoisomerase IV. *J. Antimicrob. Chemother.* **2016**, *71*, 1905–1913. https://doi.org/10.1093/jac/dkw061.

(114) Kim, W.; Zou, G.; Hari, T. P. A.; Wilt, I. K.; Zhu, W.; Galle, N.; Faizi, H. A.; Hendricks, G. L.; Tori, K.; Pan, W.; Huang, X.; Steele, A. D.; Csatary, E. E.; Dekarske, M. M.; Rosen, J. L.; De Queiroz Ribeiro, N.; Lee, K.; Port, J.; Fuchs, B. B.; Vlahovska, P. M.; Wuest, W. M.; Gao, H.; Ausubel, F. M.; Mylonakis, E. A Selective Membrane-Targeting Repurposed Antibiotic with Activity against Persistent Methicillin-Resistant Staphylococcus Aureus. *Proc. Natl. Acad. Sci. U. S. A.* **2019**, *116* (33), 16529–16534. https://doi.org/10.1073/pnas.1904700116.

(115) Payne, D. J.; Gwynn, M. N.; Holmes, D. J.; Pompliano, D. L. Drugs for Bad Bugs: Confronting the Challenges of Antibacterial Discovery. *Nat. Rev. Drug Discov.* **2007**, *6*, 29–40. https://doi.org/10.1038/nrd2201.

(116) Smith, P. A.; Koehler, M. F. T.; Girgis, H. S.; Yan, D.; Chen, Y.; Chen, Y.; Crawford, J. J.; Durk, M. R.; Higuchi, R. I.; Kang, J.; Murray, J.; Paraselli, P.; Park, S.; Phung, W.; Quinn, J. G.; Roberts, T. C.; Rougé, L.; Schwarz, J. B.; Skippington, E.; Wai, J.; Xu, M.; Yu, Z.; Zhang, H.; Tan, M.-W.; Heise, C. E. Optimized Arylomycins Are a New Class of Gram-Negative Antibiotics. *Nature* **2018**, *561*, 189–194. https://doi.org/10.1038/s41586-018-0483-6.

(117) Walsh, J. M.; Hawver, L. A.; Beuning, P. J. Escherichia Coli Y Family DNA Polymerases. *Front. Biosci.* **2011**, *16*, 3164–3182. https://doi.org/10.2741/3904.

(118) Foster, P. L. Stress-Induced Mutagenesis in Bacteria. *Crit. Rev. Biochem. Mol. Biol.* **2007**, *42* (5), 373–397. https://doi.org/10.1080/10409230701648494.

(119) Beaber, J. W.; Hochhut, B.; Waldor, M. K. SOS Response Promotes Horizontal Dissemination of Antibiotic Resistance Genes. *Nature* **2004**, *427*, 72–74. https://doi.org/10.1038/nature02241.

(120) Molina-Quiroz, R. C.; Silva-Valenzuela, C.; Brewster, J.; Castro-Nallar, E.; Levy, S. B.; Camilli, A. Cyclic AMP Regulates Bacterial Persistence through Repression of the Oxidative Stress Response and SOS-Dependent DNA Repair in Uropathogenic Escherichia Coli. *MBio* **2018**, *9* (1), e02144-17. https://doi.org/10.1128/mBio.02144-17.

(121) Flemming, H. C.; Wingender, J. The Biofilm Matrix. *Nat. Rev. Microbiol.* **2010**, *8*, 623–633. https://doi.org/10.1038/nrmicro2415.

(122) Espeland, E. M.; Wetzel, R. G. Complexation, Stabilization, and UV Photolysis of Extracellular and Surface-Bound Glucosidase and Alkaline Phosphatase: Implications for Biofilm Microbiota. *Microb. Ecol.* **2001**, *42*, 572–585.

https://doi.org/10.1007/s00248-001-1023-7.

(123) Teitzel, G. M.; Parsek, M. R. Heavy Metal Resistance of Biofilm and Planktonic Pseudomonas Aeruginosa. *Appl. Environ. Micrbiology* **2003**, *69* (4), 2313–2320. https://doi.org/10.1128/AEM.69.4.2313.

(124) McNeill, K.; Hamilton, I. R. Acid Tolerance Response of Biofilm Cells of Streptococcus Mutans. *FEMS Microbiol. Lett.* **2003**, *221*, 25–30. https://doi.org/10.1016/S0378-1097(03)00164-2.

(125) Le Magrex-Debar, E.; Lemoine, J.; Gellé, M. P.; Jacquelin, L. F.; Choisy, C. Evaluation of Biohazards in Dehydrated Biofilms on Foodstuff Packaging. *Int. J. Food Microbiol.* **2000**, *55*, 239–243. https://doi.org/10.1016/S0168-1605(00)00177-X.

(126) Van Acker, H.; Van Dijck, P.; Coenye, T. Molecular Mechanisms of Antimicrobial Tolerance and Resistance in Bacterial and Fungal Biofilms. *Trends Microbiol.* **2014**, *22* (6), 326–333. https://doi.org/10.1016/j.tim.2014.02.001.

(127) Hall-Stoodley, L.; Costerton, J. W.; Stoodley, P. Bacterial Biofilms: From the Natural Environment to Infectious Diseases. *Nat. Rev. Microbiol.* **2004**, *2*, 95–108. https://doi.org/10.1038/nrmicro821.

(128) Joo, H.-S.; Otto, M. Molecular Basis of In-Vivo Biofilm Formation by Bacterial Pathogens. *Chem Biol* **2012**, *19* (12), 1503–1513. https://doi.org/10.1016/j.chembiol.2012.10.022.

(129) Banerjee, I.; Pangule, R. C.; Kane, R. S. Antifouling Coatings: Recent Developments in the Design of Surfaces That Prevent Fouling by Proteins, Bacteria, and Marine Organisms. *Adv. Mater.* **2011**, *23* (6), 690–718. https://doi.org/10.1002/adma.201001215.

(130) Wood, T. K. Strategies for Combating Persister Cell and Biofilm Infections. *Microb. Biotechnol.* **2017**, *10* (5), 1054–1056. https://doi.org/10.1111/1751-7915.12774.

(131) Henriques, A. O.; Moran, C. P. Structure, Assembly, and Function of the Spore Surface Layers. *Annu. Rev. Microbiol.* **2007**, *61*, 555–588. https://doi.org/10.1146/annurev.micro.61.080706.093224.

(132) Cano, R. J.; Borucki, M. K. Revival and Identification of Bacterial Spores in 25- to 40-Million-Year-Old Dominican Amber. *Science (80-.).* **1995**, *268*, 1060–1064. https://doi.org/10.1126/science.7538699.

(133) Cushnie, T. P. T.; O'Driscoll, N. H.; Lamb, A. J. Morphological and Ultrastructural Changes in Bacterial Cells as an Indicator of Antibacterial Mechanism of Action. *Cell. Mol. Life Sci.* **2016**, *73*, 4471–4492. https://doi.org/10.1007/s00018-016-2302-2.

(134) Bojer, M. S.; Wacnik, K.; Kjelgaard, P.; Gallay, C.; Bottomley, A. L.; Cohn, M. T.; Lindahl, G.; Frees, D.; Veening, J.-W.; Foster, S. J.; Ingmer, H. SosA Inhibits Cell Division in Staphylococcus Aureus in Response to DNA Damage. *Mol. Microbiol.* **2019**. https://doi.org/doi.org/10.1111/mmi.14350.

(135) Noguchi, H.; Matsuhashi, M.; Takaoka, M.; Mitsuhashi, S. New Antipseudomonal Penicillin , PC-904: Affinity to Penicillin-Binding Proteins and Inhibition of the Enzyme Cross-Linking Peptidoglycan. *Antimicrob. Agents Chemother.* **1978**, *14* (4), 617–624. https://doi.org/10.1128/aac.14.4.617.

(136) Rodriguez, J. L.; Dalia, A. B.; Weiser, J. N. Increased Chain Length Promotes Pneumococcal Adherence and Colonization. *Infect. Immun.* **2012**, *80* (10), 3454–3459. https://doi.org/10.1128/IAI.00587-12.

(137) Yang, D. C.; Blair, K. M.; Salamaa, N. R. Staying in Shape: The Impact of Cell Shape on Bacterial Survival in Diverse Environments. *Microbiol. Mol. Biol. Rev.* **2016**, *80* (1), 187–203. https://doi.org/10.1128/MMBR.00031-15.

(138) Bos, J.; Zhang, Q.; Vyawahare, S.; Rogers, E.; Rosenberg, S. M.; Austin, R. H. Emergence of Antibiotic Resistance from Multinucleated Bacterial Filaments. *Proc. Natl. Acad. Sci.* **2015**, *112* (1), 178–183. https://doi.org/10.1073/pnas.1420702111.

(139) Luo, Y.; Pfuetzner, R. A.; Mosimann, S.; Paetzel, M.; Frey, E. A.; Cherney, M.; Kim, B.; Little, J. W.; Strynadka, N. C. J. Crystal Structure of LexA: A Conformational Switch for Regulation of Self-Cleavage. *Cell* **2001**, *106*, 585–594. https://doi.org/10.1016/S0092-8674(01)00479-2.

(140) Tippin, B.; Pham, P.; Goodman, M. F. Error-Prone Replication for Better or Worse. *Trends Microbiol.* **2004**, *12* (6), 288–295. https://doi.org/10.1016/j.tim.2004.04.004.

(141) Galhardo, R. S.; Do, R.; Yamada, M.; Friedberg, E. C.; Hastings, P. J.; Nohmi, T.; Rosenberg, S. M. DinB Upregulation Is the Sole Role of the SOS Response in Stress-Induced Mutagenesis in Escherichia Coli. *Genetics* **2009**, *182*, 55–68. https://doi.org/10.1534/genetics.109.100735.

(142) Schlacher, K.; Pham, P.; Cox, M. M.; Goodman, M. F. Roles of DNA Polymerase V and RecA Protein in SOS Damage-Induced Mutation. *Chem. Rev.* **2006**, *106*, 406–419. https://doi.org/10.1021/cr0404951.

(143) McKenzie, G. J.; Harris, R. S.; Lee, P. L.; Rosenberg, S. M. The SOS Response Regulates Adaptive Mutation. *Proc. Natl. Acad. Sci.* **2000**, *97* (12), 6646–6651. https://doi.org/10.1073/pnas.120161797.

(144) Dorr, T.; Lewis, K.; Vulic, M. SOS Response Induces Persistence to Fluoroquinolones in Escherichia Coli. *PLoS Genet.* **2009**, *5* (12), e1000760. https://doi.org/10.1371/journal.pgen.1000760.

(145) Da Re, S.; Garnier, F.; Guérin, E.; Campoy, S.; Denis, F.; Ploy, M. C. The SOS Response Promotes QnrB Quinolone-Resistance Determinant Expression. *EMBO Rep.* **2009**, *10* (8), 929–933. https://doi.org/10.1038/embor.2009.99.

(146) Liu, P.; Wu, Z.; Xue, H.; Zhao, X. Antibiotics Trigger Initiation of SCCmectransfer by Inducing SOS Responses. *Nucleic Acids Res.* **2017**, *45* (7), 3944–3952. https://doi.org/10.1093/nar/gkx153.

(147) Cirz, R. T.; Chin, J. K.; Andes, D. R.; De Crécy-Lagard, V.; Craig, W. A.; Romesberg, F. E.

Inhibition of Mutation and Combating the Evolution of Antibiotic Resistance. *PLoS Biol.* **2005**, *3* (6), 1024–1033. https://doi.org/10.1371/journal.pbio.0030176.

(148) Thi, T. D.; Lopez, E.; Rodriguez-Rojas, A.; Rodriguez-Beltran, J.; Couce, A.; Guelfo, J. R.; Castaneda-Garcia, A.; Blazquez, J. Effect of RecA Inactivation on Mutagenesis of Escherichia Coli Exposed to Sublethal Concentrations of Antimicrobials. *J. Antimicrob. Chemother.* **2011**, *66*, 531–538. https://doi.org/10.1093/jac/dkq496.

(149) Recacha, E.; Machuca, J.; Díaz-Díaz, S.; García-Duque, A.; Ramos-Guelfo, M.; Docobo-Pérez, F.; Blázquez, J.; Pascual, A.; Rodríguez-Martínez, J. M. Suppression of the SOS Response Modifies Spatiotemporal Evolution, Post-Antibiotic Effect, Bacterial Fitness and Biofilm Formation in Quinolone-Resistant Escherichia Coli. *J. Antimicrob. Chemother.* **2019**, *74* (1), 66–73. https://doi.org/10.1093/jac/dky407.

(150) Gotoh, H.; Kasaraneni, N.; Devineni, N.; Dallo, S. F.; Weitao, T. SOS Involvement in Stress-Inducible Biofilm Formation. *Biofouling* **2010**, *26* (5), 603–611. https://doi.org/10.1080/08927014.2010.501895.

(151) Walter, B. M.; Cartman, S. T.; Minton, N. P.; Butala, M.; Rupnik, M. The SOS Response Master Regulator LexA Is Associated with Sporulation, Motility and Biofilm Formation in Clostridium Difficile. *PLoS One* **2015**, *10* (12), e0144763. https://doi.org/10.1371/journal.pone.0144763.

(152) Bisognano, C.; Kelley, W. L.; Estoppey, T.; Francois, P.; Schrenzel, J.; Li, D.; Lew, D. P.; Hooper, D. C.; Cheung, A. L.; Vaudaux, P. A RecA-LexA-Dependent Pathway Mediates Ciprofloxacin-Induced Fibronectin Binding in Staphylococcus Aureus. *J. Biol. Chem.* **2004**, *279* (10), 9064–9071. https://doi.org/10.1074/jbc.M309836200.

(153) Yeswanth, S.; Chaudhury, A.; Sarma, P. V. G. K. Quantitative Expression Analysis of SpA, FnbA and Rsp Genes in Staphylococcus Aureus: Actively Associated in the Formation of Biofilms. *Curr. Microbiol.* **2017**, *74*, 1394–1403. https://doi.org/10.1007/s00284-017-1331-x.

(154) Samuels, A. N.; Roggiani, M.; Zhu, J.; Goulian, M.; Kohli, R. M. The SOS Response Mediates Sustained Colonization of the Mammalian Gut. **2019**, *87* (2), 1–15. https://doi.org/10.1128/IAI.00711-18.

(155) Bojer, M. S.; Frees, D.; Ingmer, H. SosA in Staphylococci: An Addition to the Paradigm of Membrane-Localized, SOS-Induced Cell Division Inhibition in Bacteria. *Curr. Genet.* **2020**, *66* (3), 495–499. https://doi.org/10.1007/s00294-019-01052-z.

(156) Alam, M. K.; Alhhazmi, A.; Decoteau, J. F.; Luo, Y.; Geyer, C. R. RecA Inhibitors Potentiate Antibiotic Activity and Block Evolution of Antibiotic Resistance. *Cell Chem. Biol.* **2016**, *23*, 381–391. https://doi.org/10.1016/j.chembiol.2016.02.010.

(157) Lee, A. M.; Wigle, T. J.; Singleton, S. F. A Complementary Pair of Rapid Molecular Screening Assays for RecA Activities. *Anal. Biochem.* **2007**, *367*, 247–258. https://doi.org/10.1016/j.ab.2007.04.021.

(158) Peterson, E. J. R.; Janzen, W. P.; Kireev, D.; Singleton, S. F. High-Throughput Screening

for RecA Inhibitors Using a Transcreener Adenosine 5′-O-Diphosphate Assay. *Assay Drug Dev. Technol.* **2012**, *10* (3), 260–268. https://doi.org/10.1089/adt.2011.0409.

(159) Sexton, J. Z.; Wigle, T. J.; He, Q.; Hughes, M. A.; Smith, G. R.; Singleton, S. F.; Williams, A. L.; Yeh, L.-A. Novel Inhibitors of E. Coli RecA ATPase Activity. *Curr. Chem. Genomics* **2010**, *4*, 34–42. https://doi.org/10.2174/1875397301004010034.

(160) Wigle, T. J.; Lee, A. M.; Singleton, S. F. Conformationally Selective Binding of Nucleotide Analogues to Escherichia Coli RecA: A Ligand-Based Analysis of the RecA ATP Binding Site. *Biochemistry* **2006**, *45*, 4502–4513. https://doi.org/10.1021/bi052298h.

(161) Bellio, P.; Di Pietro, L.; Mancini, A.; Piovano, M.; Nicoletti, M.; Brisdelli, F.; Tondi, D.; Cendron, L.; Franceschini, N.; Amicosante, G.; Perilli, M.; Celenza, G. SOS Response in Bacteria: Inhibitory Activity of Lichen Secondary Metabolites against Escherichia Coli RecA Protein. *Phytomedicine* **2017**, *29*, 11–18. https://doi.org/10.1016/j.phymed.2017.04.001.

(162) Yakimov, A.; Pobegalov, G.; Bakhlanova, I.; Khodorkovskii, M.; Petukhov, M.; Baitin, D. Blocking the RecA Activity and SOS-Response in Bacteria with a Short α-Helical Peptide. *Nucleic Acids Res.* **2017**, *45* (16), 9788–9796. https://doi.org/10.1093/nar/gkx687.

(163) Huang, F.; Motlekar, N. A.; Burgwin, C. M.; Napper, A. D.; Diamond, S. L.; Mazin, A. V. Identification of Specific Inhibitors of Human RAD51 Recombinase Using High-Throughput Screening. *ACS Chem. Biol.* **2011**, *6*, 628–635. https://doi.org/10.1021/cb100428c.

(164) Butala, M.; Žgur-Bertok, D.; Busby, S. J. W. The Bacterial LexA Transcriptional Repressor. *Cell. Mol. Life Sci.* **2009**, *66*, 82–93. https://doi.org/10.1007/s00018-008-8378-6.

(165) Culyba, M. J.; Mo, C. Y.; Kohli, R. M. Targets for Combating the Evolution of Acquired Antibiotic Resistance. *Biochemistry* **2015**, *54* (23), 3573–3582. https://doi.org/10.1021/acs.biochem.5b00109.

(166) Mo, C. Y.; Manning, S. A.; Roggiani, M.; Culyba, M. J.; Samuels, A. N.; Sniegowski, P. D.; Goulian, M.; Kohli, R. M. Systematically Altering Bacterial SOS Activity under Stress Reveals Therapeutic Strategies for Potentiating Antibiotics. *Ther. Prev.* **2016**, *1* (4), e00163-16. https://doi.org/10.1128/mSphere.00163-16.

(167) Mo, C. Y.; Birdwell, L. D.; Kohli, R. M. Specificity Determinants for Autoproteolysis of Lexa, a Key Regulator of Bacterial SOS Mutagenesis. *Biochemistry* **2014**, *53*, 3158–3168. https://doi.org/10.1021/bi500026e.

(168) Mo, C. Y.; Culyba, M. J.; Selwood, T.; Kubiak, M.; Hostetler, Z. M.; Jurewicz, A. J.; Keller, P. M.; Pope, A. J.; Quinn, A.; Schneck, J.; Widdowson, K. L.; Kohli, R. M. Inhibitors of LexA Autoproteolysis and the Bacterial SOS Response Discovered by an Academic – Industry Partnership. *ACS Infect. Dis.* **2018**, *4*, 349–359. https://doi.org/10.1021/acsinfecdis.7b00122.

(169) Selwood, T.; Larsen, B. J.; Mo, C. Y.; Culyba, M. J.; Hostetler, Z. M.; Kohli, R. M.; Reitz, A. B.; Baugh, S. D. P. Advancement of the 5-Amino-1-(Carbamoylmethyl)-1H-1,2,3-Triazole-4-Carboxamide Scaffold to Disarm the Bacterial SOS Response. *Front. Microbiol.* **2018**, *9* (December). https://doi.org/10.3389/fmicb.2018.02961.

(170) Whitby, L. R.; Ando, Y.; Setola, V.; Vogt, P. K.; Roth, B. L.; Boger, D. L. Design, Synthesis, and Validation of a β-Turn Mimetic Library Targeting Protein-Protein and Peptide-Receptor Interactions. *J. Am. Chem. Soc.* **2011**, *133*, 10184–10194. https://doi.org/10.1021/ja201878v.

(171) Oh, K.; Guan, Z. A Convergent Synthesis of New β-Turn Mimics by Click Chemistry. *Chem. Commun.* **2006**, 3069–3071. https://doi.org/10.1039/b606185k.

(172) Xiong, B.; Wang, G.; Xiong, T.; Wan, L.; Zhou, C.; Liu, Y.; Zhang, P.; Yang, C.; Tang, K. Direct Synthesis of N-Arylamides via the Coupling of Aryl Diazonium Tetrafluoroborates and Nitriles under Transition-Metal-Free Conditions. *Tetrahedron Lett.* **2018**, *59*, 3139–3142. https://doi.org/10.1016/j.tetlet.2018.07.014.

(173) Jiang, C.; Shi, J.; Liao, L.; Zhang, L.; Liu, J.; Wang, Y.; Lao, Y.; Zhang, J. 5-[2-(N-(Substituted Phenyl)Acetamide)]Amino-1,3,4-Thiadiazole-2-Sulfonamides as Selective Carbonic Anhydrase II Inhibitors with Neuroprotective Effects. *ChemMedChem* **2020**, *15*, 705–715. https://doi.org/10.1002/cmdc.201900703.

(174) Xie, H.; Ng, D.; Savinov, S. N.; Dey, B.; Kwong, P. D.; Wyatt, R.; Smith, A. B.; Hendrickson, W. A. Structure-Activity Relationships in the Binding of Chemically Derivatized CD4 to Gp120 from Human Immunodeficiency Virus. *J. Med. Chem.* **2007**, *50*, 4898–4908. https://doi.org/10.1021/jm070564e.

(175) Cook, P. D.; Kawasaki, A. M.; Kung, P. P. Novel Heterocycle Compositions. WO 98/05332, 1998.

(176) Eirich, J.; Braig, S.; Schyschka, L.; Servatius, P.; Hoffmann, J.; Hecht, S.; Fulda, S.; Zahler, S.; Antes, I.; Kazmaier, U.; Sieber, S. A.; Vollmar, A. M. A Small Molecule Inhibits Protein Disulfide Isomerase and Triggers the Chemosensitization of Cancer Cells. *Angew. Chemie - Int. Ed.* **2014**, *53*, 12960–12965. https://doi.org/10.1002/anie.201406577.

(177) Ippoliti, J. T.; Kummer, R. L.; Honig-Schmidt, N. ANTI-DIABETIC COMPOUNDS, PHARMACEUTICAL COMPOSITIONS CONTAINING THEM, AND METHOD TO TREAT DIABETES. WO 2015/142670 Al, 2015.

(178) Zhang, J.; Zhang, J.; Hao, G.; Xin, W.; Yang, F.; Zhu, M.; Zhou, H. Design, Synthesis, and Structure-Activity Relationship of 7-Propanamide Benzoxaboroles as Potent Anticancer Agents. *J. Med. Chem.* **2019**, *62*, 6765–6784. https://doi.org/10.1021/acs.jmedchem.9b00736.

(179) Pombo-García, K.; Zarschler, K.; Barreto, J. A.; Hesse, J.; Spiccia, L.; Graham, B.; Stephan, H. Design, Synthesis, Characterisation and in Vitro Studies of Hydrophilic, Colloidally Stable, 64Cu(Ii)-Labelled, Ultra-Small Iron Oxide Nanoparticles in a Range

of Human Cell Lines. *RSC Adv.* **2013**, *3*, 22443–22454. https://doi.org/10.1039/c3ra43726d.

(180) Wallace, D. M.; Haramura, M.; Cheng, J. F.; Arrhenius, T.; Nadzan, A. M. Novel Trifluoroacetophenone Derivatives as Malonyl-CoA Decarboxylase Inhibitors. *Bioorganic Med. Chem. Lett.* **2007**, *17*, 1127–1130. https://doi.org/10.1016/j.bmcl.2006.09.023.

(181) Jöst, C.; Nitsche, C.; Scholz, T.; Roux, L.; Klein, C. D. Promiscuity and Selectivity in Covalent Enzyme Inhibition: A Systematic Study of Electrophilic Fragments. *J. Med. Chem.* **2014**, *57*, 7590–7599. https://doi.org/10.1021/jm5006918.

(182) Bajaj, K.; Pillai, G. G.; Sakhuja, R.; Kumar, D. Expansion of Phosphane Treasure Box for Staudinger Peptide Ligation. *J. Org. Chem.* **2020**, *85*, 12147–12159. https://doi.org/10.1021/acs.joc.0c01319.

(183) Reed, C. S.; Huigens, R. W.; Rogers, S. A.; Melander, C. Modulating the Development of E. Coli Biofilms with 2-Aminoimidazoles. *Bioorganic Med. Chem. Lett.* **2010**, *20*, 6310–6312. https://doi.org/10.1016/j.bmcl.2010.08.075.

Supporting Information

Chapter 2 Supporting Information

Biology Experimental Section

Biology completed by Wooseong Kim and Iliana E. Escobar.

Bacterial strains, growth conditions. Methicillin-resistant *S. aureus* strains MW2 BAA-1707, ATCC 33591, and JE2[1], and vancomycin-resistant *S. aureus* strain VRS1[2] were grown in tryptic soy broth (TSB) (BD, Franklin Lakes, NJ, USA).

Minimal inhibitory concentration (MIC) assay. The MICs of each analog were determined by the standard micro-dilution method recommended by the Clinical and Laboratory Standards Institute.[1] MIC assays were conducted in biological triplicate.

Persister killing assay. We have shown previously that MRSA MW2 become persisters that when grown to stationary phase are tolerant to conventional antibiotics such as gentamicin, ciprofloxacin and vancomycin.[3-5] We prepared MW2 persister cells by growing cultures overnight to stationary phase at 37°C at 225 rpm. The overnight cultures were washed three times with PBS and diluted to ~5×10^7 CFU/ml with the same buffer. 1 mL of ~10^8 CFU/mL MRSA persisters was added to 1 mL of PBS containing 2-fold of the desired concentration of antibiotics in a 96-well assay block (Corning Costar 3960). The assay block was incubated at 37 °C, with shaking at 200 rpm. At specific times, 400 µL aliquots were removed, washed once with PBS, serially diluted and spot-plated on TSA plates. Colonies were counted to enumerate the number of live cells after overnight incubation at 37 °C. These experiments were conducted in biological triplicate.

Human blood hemolysis. Hemolytic activity was evaluated as described in a previous study.[2] Briefly, 50 µL of 4% human erythrocytes (Rockland Immunochemicals, Limerick, PA, USA) was added to 50 µL of 2-fold serial dilutions of compounds in PBS, 0.2% DMSO (negative control), or 2% Triton-X 100 (positive control) in a U-bottom 96-well plate. The 96-well plate was incubated at 37 °C for 1 h and then centrifuged at 500×g for 5 min. 50 µL of the super-natant was transferred to a fresh flat-bottom 96-well plate, and absorbance of supernatants was measured at 540 nm. Percent hemolysis was calculated using the following equation: (A_{540nm} of compound treated sample − A_{540nm} of 0.1% DMSO treated sample) / (A_{540nm} of 1% Triton X-100 treated sample − A_{540nm} of 0.1% DMSO treated sample) × 100. The assay was conducted in triplicate. HC_{50} (median hemolytic concentrations) was determined using GraphPad Prism 7 (GraphPad Software, La Jolla, CA, USA).

Cytotoxicity against human cell lines. HepG2 (human hepatoma, ATCC HB-8065) and HeLa (human cervical adenocarcinoma ATCC CCL-2) cells were maintained in DMEM containing 10% fetal bovine serum in a humidified 5% CO_2 incubator at 37°C. For cytotoxicity tests, HepG2 and HeLa cells were plated at $1.0X10^6$, $0.3X10^6$, and $0.4X10^6$ cells/mL (respectively) in tissue culture treated 96-well plates in a volume of 50 µL/well of

corresponding serum free media. The cells were then treated with a range of concentrations of compounds in the serum-free culture media at a final volume of 100 µL for a total of 24 h. For the last 2 h of the 24 h period 10 µl of WST-1 (Roche, Mannheim, Germany) were added in each well of 96-well plates. WST-1 reduction was measured at 450 nm. The percent fluorescence relative to that of the no-treatment control was calculated. The assay was done in triplicate. LC_{50} (median lethal concentrations) was determined using GraphPad Prism 7 (GraphPad Software, La Jolla, CA, USA).

(1) Fey, P. D.; Endres, J. L.; Yajjala, V. K.; Widhelm, T. J.; Boissy, R. J.; Bose, J. L.; Bayles, K. W. A Genetic Resource for Rapid and Comprehensive Phenotype Screening of Nonessential *Staphylococcus Aureus* Genes. *MBio* **2013**, *4* (1), e00537–12–e00537–12.

(2) Weigel, L. M.; Clewell, D. B.; Gill, S. R.; Clark, N. C.; McDougal, L. K.; Flannagan, S. E.; Kolonay, J. F.; Shetty, J.; Killgore, G. E.; Tenover, F. C. Genetic Analysis of a High-Level Vancomycin-Resistant Isolate of *Staphylococcus Aureus*. *Science* **2003**, *302* (5650), 1569–1571.

(3) Kim, W.; Conery, A. L.; Rajamuthiah, R.; Fuchs, B. B.; Ausubel, F. M.; Mylonakis, E. Identification of an Antimicrobial Agent Effective Against Methicillin-Resistant *Staphylococcus Aureus* Persisters Using a Fluorescence-Based Screening Strategy. *PLoS ONE* **2015**, *10* (6), e0127640.

(4) Kim, W.; Zhu, W.; Hendricks, G. L.; Van Tyne, D.; Steele, A. D.; Keohane, C. E.; Fricke, N.; Conery, A. L.; Shen, S.; Pan, W.; Lee, K.; Rajamuthiah, R.; Fuchs, B. B.; Vlahovska, P. M.; Wuest, W. M.; Gilmore, M. S.; Gao, H.; Ausubel, F. M.; Mylonakis, E. A New Class of Synthetic Retinoid Antibiotics Effective Against Bacterial Persisters. *Nature* **2018**, *556*, 103–107.

(5) Kim, W.; Steele, A. D.; Zhu, W.; Csatary, E. E.; Fricke, N.; Dekarske, M. M.; Jayamani, E.; Pan, W.; Kwon, B.; Sinitsa, I. F.; Rosen, J. L.; Conery, A. L.; Fuchs, B. B.; Vlahovska, P. M.; Ausubel, F. M.; Gao, H.; Wuest, W. M.; Mylonakis, E. Discovery and Optimization of nTZDpa as an Antibiotic Effective Against Bacterial Persisters. *ACS Infect. Dis.* **2018**, *4* (11), 1540–1545.

Chemistry Experimental Section

Chemistry completed by Ana V. Cheng.

General Methods and Instrumentation

NMR spectra were recorded using the following spectrometers: Varian INOVA400, Varian INOVA500, VNMR400, and Bruker Ascend 600. Chemical shifts are quoted in ppm relative to the indicated solvents. The following abbreviations are used to describe splitting: br (broad), s (singlet), d (doublet), t (triplet), q (quartet), p (pentet), m (multiplet), dd (doublet of doublets), dt (doublet of triplets), etc.

Accurate mass spectra were recorded using a Thermo LTQ-FTMS.

Non-aqueous reactions were performed using flame-dried glassware under an atmosphere of Argon with HPLC-grade solvents purified on a Pure Process Technology solvent purification system. Brine refers to a saturated solution of sodium chloride, sat. Na_2CO3 to a saturated aqueous solution of sodium carbonate, sat. NH_4Cl to a saturated aqueous solution of ammonium chloride, etc. Column chromatography was performed using a Biotage® flash chromatography purification system. Chemicals were used as received from Oakwood, Sigma-Aldrich, Alfa Aesar, or AK Scientific. At least 95% purity of final compounds was assessed using ^1H NMR integrations and/or HPLC. LogP and topological polar surface area (TPSA) were calculated using Molinspiration Cheminformatics 2019 software.

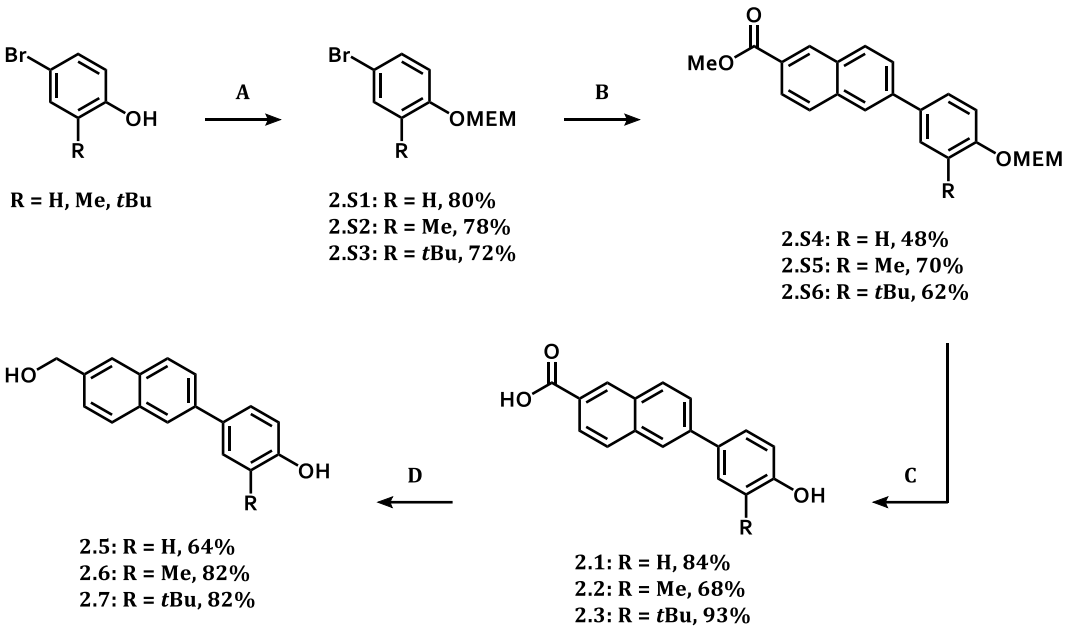

Figure S1. Synthesis of bulk panel (R = H, Me, or tBu).

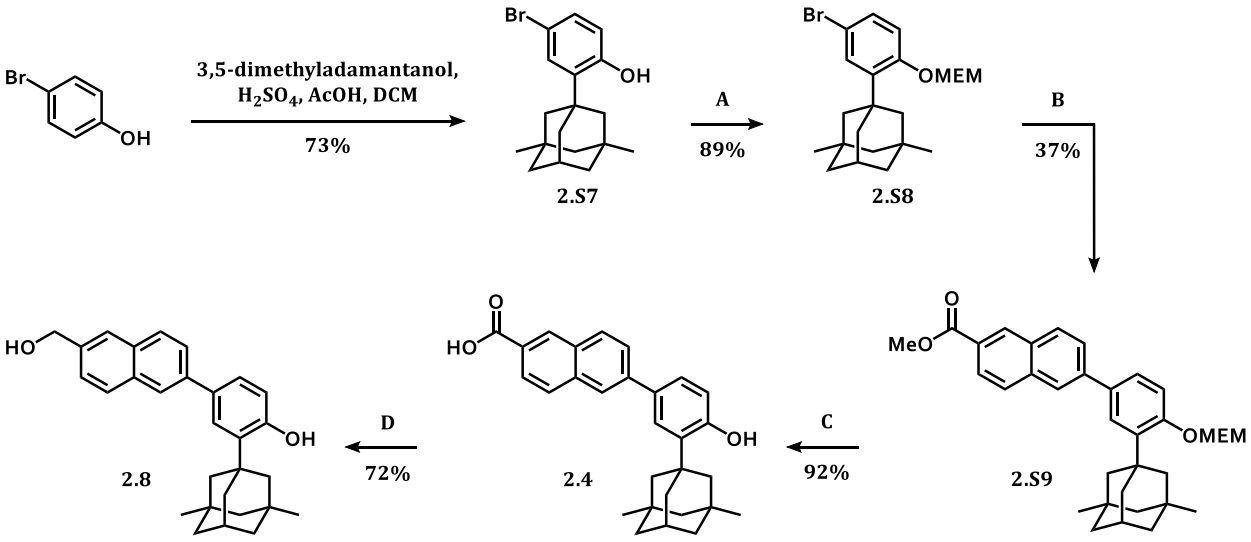

Figure S2. Synthesis of bulk panel (R = dimethyladamantyl).

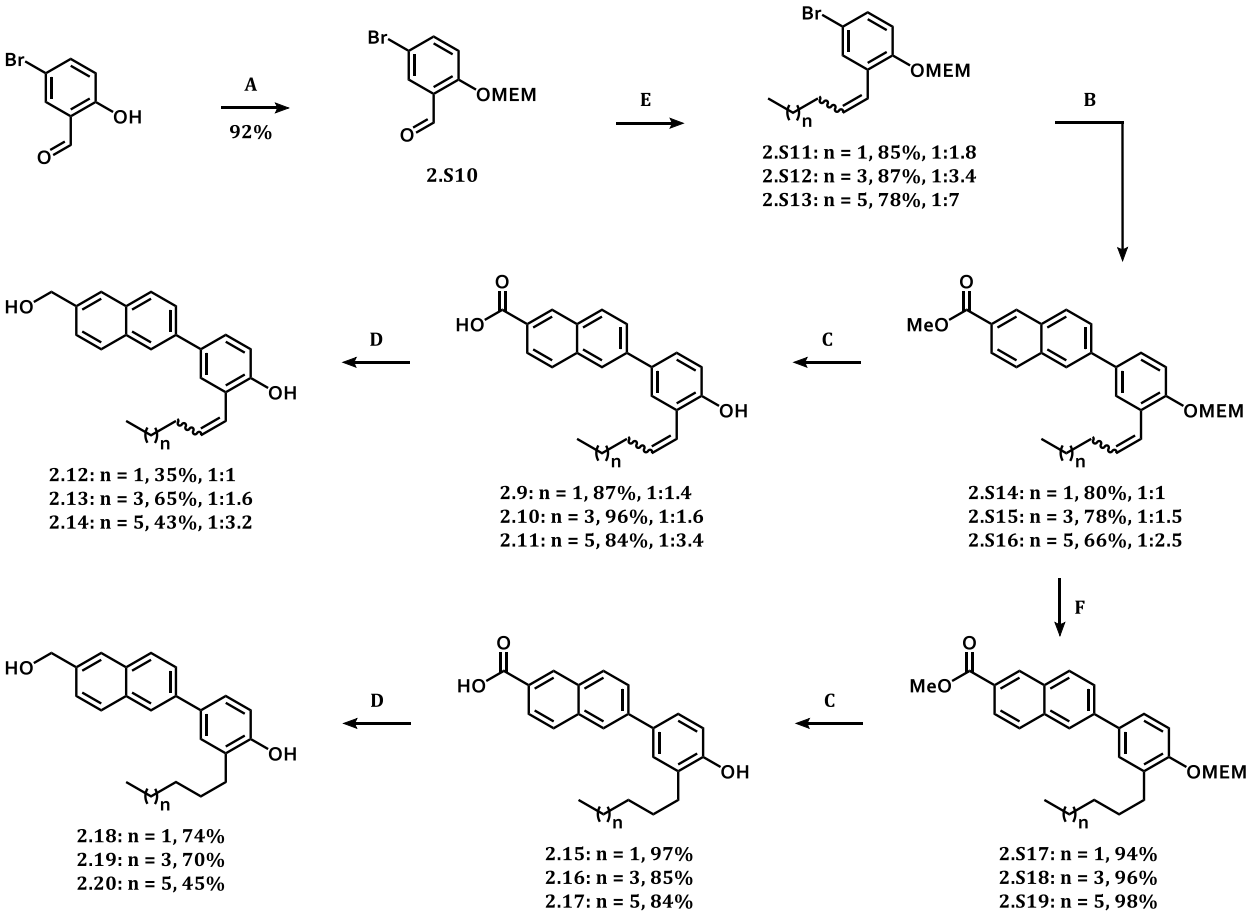

Figure S3. Synthesis of lipid mimics.

Table S1. Calculated LogP and TPSA for final analogs

Analogue	cLogP	TPSA (Å²)	Analogue	cLogP	TPSA (Å²)
2.1	4.32	57.53	**2.11**	8.67	57.53
2.2	5.17	57.53	**2.12**	6.37	40.46
2.3	6.42	57.53	**2.13**	7.38	40.46
2.4	7.75	57.53	**2.14**	8.33	40.46
2.5	3.75	40.46	**2.15**	7.09	57.53
2.6	4.59	40.46	**2.16**	8.09	57.53
2.7	5.85	40.46	**2.17**	8.75	57.53
2.8	7.18	40.46	**2.18**	6.52	40.46
2.9	6.94	57.53	**2.19**	7.53	40.46
2.10	7.95	57.53	**2.20**	8.43	40.46

General procedure A: MEM-protection of phenols. 2-substituted-4-bromophenol (1 eq) was dissolved in THF in a flame-dried flask at 0°C and sodium hydride (60% dispersion, 2.0 eq) was added. The solution was warmed to room temperature. After 30 min, MEMCl (1.5 eq) was added and the reaction was stirred for 2 h. Water was added and the aqueous layer was extracted with EtOAc 3x. The combined organic layers were washed with brine, dried over Na_2SO_4, concentrated, and purified by column chromatography to afford the product.

General procedure B: Miyaura borylation and Suzuki coupling. Bromide (1 eq), sodium carbonate (1.5 eq), and bis(pinacolato)diboron (1.2 eq) were dissolved in toluene and argon was bubbled through for 20 min. $Pd(dppf)Cl_2$ (3%) was added and the solution was degassed further 10 min. The reaction was heated to 110°C and monitored by TLC. Water was added and the aqueous layer was extracted with EtOAc 3x. The combined organic layers were washed with brine, dried over Na_2SO_4, and concentrated. Then, the boronic ester (crude), methyl 6-bromo-2-naphthoate (1 eq), and sodium carbonate (5.0 eq) were dissolved in 4:1 dioxane:water and argon was bubbled through for 20 min. $Pd(PPh_3)_4$ (3%) was added and the solution was degassed further 10 min. The reaction was heated to 100°C and monitored by TLC. Water was added and the aqueous layer was extracted with EtOAc 3x. The combined organic layers were washed with brine, dried over Na_2SO_4, concentrated, and purified by column chromatography to afford the product.

General procedure C: Deprotections. Methyl 6-substituted-4-((2-methoxyethoxy) methoxy)phenyl)-2-naphthoate (1 eq) was dissolved in 4M HCl in dioxane and stirred at room temperature for 1 h. The reaction was quenched with sat. NaHCO3 and the aqueous layer was extracted with EtOAc 3x. The combined organic layers were washed with brine, dried over Na_2SO_4, and concentrated. The resultant solid was then dissolved in 1:1 THF:MeOH with 2 mL 2M NaOH and stirred at room temperature overnight. The solution was acidified to pH = 1 with aqueous HCl, extracted with EtOAc 3x, washed with brine, dried over Na_2SO_4, concentrated, and purified by column chromatography to afford the product.

General procedure D: Reduction of a carboxylic acid to a primary alcohol. Acid (1 eq) was suspended in ether and THF was added until fully dissolved. Lithium aluminium hydride (1.2 eq mmol) was added and the solution was stirred at room temperature and monitored by TLC. The reaction was quenched with aqueous HCl, extracted with EtOAc 3x, washed with brine, dried over Na_2SO_4, concentrated, and purified by column chromatography to afford the product.

General procedure E: Wittig reaction. Alkyltriphenylphosphonium bromide (1.2 eq) dissolved in THF at -20°C was treated with n-BuLi (1.1 eq) and stirred for 1 h. Aldehyde **18** (1 eq) was added and the reaction was warmed to room temperature and monitored by TLC. The reaction was quenched with sat. NH_4Cl and extracted with EtOAc 3x. The combined organic layers were washed with brine, dried over Na_2SO_4, concentrated, and purified by column chromatography to afford the product as a mixture of E and Z alkenes.

General procedure F: Hydrogenation. Alkene (1 eq) was suspended in MeOH and EtOAc was added until dissolved. Argon was bubbled through for 20 min. Pd/C (10%, 135 mg, 0.13

mmol) was added and the mixture was evacuated and backfilled with H_2 3x. The flask was outfitted with a hydrogen balloon and stirred for 20 h. The mixture was filtered through celite and concentrated to afford the product.

Procedures and Characterization

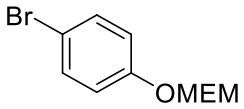

1-bromo-4-((2-methoxyethoxy)methoxy)benzene. 2.S1 was prepared from 4-bromophenol using general procedure A (80% yield). Structure was confirmed by comparison to published data. **^{1}H NMR** (500 MHz, Chloroform-d) δ 7.36 (d, J = 9.0 Hz, 2H), 6.93 (d, J = 9.1 Hz, 2H), 5.23 (d, J = 0.7 Hz, 2H), 3.84 – 3.75 (m, 2H), 3.57 – 3.51 (m, 2H), 3.36 (d, J = 0.8 Hz, 3H). **^{13}C NMR** (126 MHz, Chloroform-d) δ 156.48, 132.43, 118.22, 114.34, 93.66, 71.69, 67.85, 59.16.

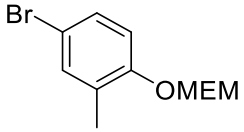

4-bromo-1-((2-methoxyethoxy)methoxy)-2-methylbenzene. 2.S2 was prepared from 4-bromo-2-methylphenol using general procedure A (78% yield). Structure was confirmed by comparison to published data. **^{1}H NMR** (400 MHz, Chloroform-d) δ 7.26 – 7.24 (m, 1H), 7.22 (ddd, J = 8.6, 2.6, 0.6 Hz, 1H), 6.97 (d, J = 8.6 Hz, 1H), 5.26 (s, 2H), 3.84 – 3.77 (m, 2H), 3.59 – 3.51 (m, 2H), 3.37 (s, 3H), 2.19 (s, 3H). **^{13}C NMR** (100 MHz, acetone) δ 154.40, 133.17, 129.37, 116.23, 115.37, 113.64, 93.37, 71.47, 67.59, 58.87, 16.06.

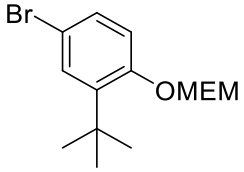

4-bromo-2-(*tert*-butyl)-1-((2-methoxyethoxy)methoxy)benzene. 2.S3 was prepared from 4-bromo-2-(*tert*-butyl)phenol using general procedure A (72% yield). Structure was confirmed by comparison to published data. **^{1}H NMR** (400 MHz, Chloroform-d) δ 7.36 (d, J = 2.5 Hz, 1H), 7.25 (dd, J = 8.7, 2.5 Hz, 1H), 7.06 (d, J = 8.7 Hz, 1H), 5.30 (s, 2H), 3.85 – 3.78 (m, 2H), 3.61 – 3.53 (m, 2H), 3.39 (s, 3H), 1.36 (s, 9H). **^{13}C NMR** (100 MHz, acetone) δ 155.32, 140.72, 129.76, 116.27, 115.26, 114.14, 93.28, 71.60, 67.81, 59.09, 35.13, 29.67.

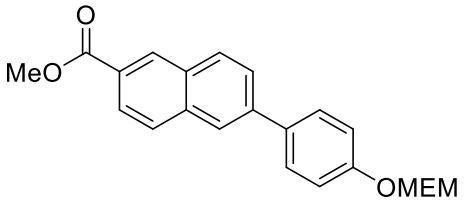

Methyl 6-(4-((2-methoxyethoxy)methoxy)phenyl)-2-naphthoate. 2.S4 was prepared from **2.S1** using general procedure B (48% yield). **^{1}H NMR** (600 MHz, Chloroform-d) δ 8.61 (s, 1H), 8.07 (dd, J = 8.6, 1.7 Hz, 1H), 8.02 (s, 1H), 8.00 (d, J = 8.7 Hz, 1H), 7.91 (d, J = 8.7 Hz, 1H), 7.78 (dd, J = 8.5, 1.8 Hz, 1H), 7.66 (d, J = 8.7 Hz, 2H), 7.19 (d, J = 8.8 Hz, 2H), 5.34 (s, 2H), 3.99 (s, 3H), 3.92 – 3.73 (m, 2H), 3.68 – 3.52 (m, 2H), 3.40 (s, 3H). **^{13}C NMR** (151 MHz, Chloroform-d) δ 167.44, 157.43, 140.65, 136.05, 134.36, 131.55, 130.98, 129.99, 128.70, 128.43, 127.31, 126.40, 125.84, 125.07, 116.88, 93.64, 71.78, 67.90, 59.21, 52.37. **HRMS** Accurate mass (ES+): Found 389.13613, C22H22O5Na (M+Na+) requires 389.13650.

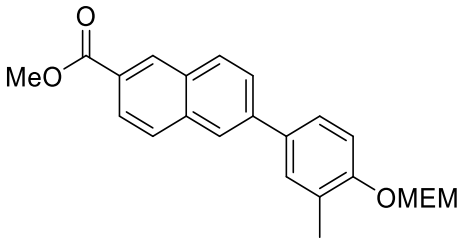

Methyl 6-(4-((2-methoxyethoxy)methoxy)-3-methylphenyl)-2-naphthoate. 2.S5 was prepared from **2.S2** using general procedure B (70% yield). **^{1}H NMR** (400 MHz, Chloroform-d) δ 8.61 (s, 1H), 8.07 (dd, J = 8.6, 1.7 Hz, 1H), 8.01 (s, 1H), 7.99 (d, J = 8.8 Hz, 1H), 7.90 (d, J = 8.9 Hz, 1H), 7.78 (dd, J = 8.5, 1.8 Hz, 1H), 7.54 – 7.49 (m, 2H), 7.23 (d, J = 8.3 Hz, 1H), 5.37 (s, 2H), 3.99 (s, 3H), 3.91 – 3.83 (m, 2H), 3.63 – 3.55 (m, 2H), 3.40 (s, 3H), 2.34 (s, 3H). **^{13}C NMR** (100 MHz, Chloroform-d) δ 167.27, 155.48, 140.64, 135.89, 133.72, 131.32, 130.82, 129.82, 129.75, 128.25, 127.79, 127.00, 126.27, 125.89, 125.61, 124.79, 114.18, 93.46, 71.66, 67.74, 59.07, 52.22, 16.59. **HRMS** Accurate mass (ES+): found 403.15172, C23H24O5Na (M+Na+) requires 403.15215.

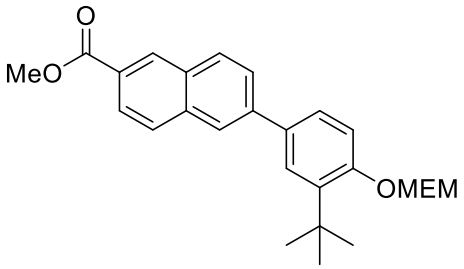

Methyl 6-(3-(tert-butyl)-4-((2-methoxyethoxy)methoxy)phenyl)-2-naphthoate. 2.S6 was prepared from **S3** using general procedure B (62% yield). **^{1}H NMR** (400 MHz, Chloroform-d) δ 8.62 (s, 1H), 8.07 (dd, J = 8.6, 1.7 Hz, 1H), 8.02 – 7.96 (m, 2H), 7.92 (d, J = 8.6 Hz, 1H), 7.78 (dd, J = 8.5, 1.9 Hz, 1H), 7.65 (d, J = 2.4 Hz, 1H), 7.53 (dd, J = 8.5, 2.3 Hz, 1H), 7.31 (d, J = 8.5 Hz, 1H), 5.40 (s, 2H), 3.99 (s, 3H), 3.91 – 3.85 (m, 2H), 3.64 – 3.59 (m, 2H), 3.42 (s, 3H), 1.47 (s, 9H). **^{13}C NMR** (100 MHz, Chloroform-d) δ 167.41, 156.35, 141.32, 138.92, 136.01, 133.61, 131.41, 130.94, 129.87, 128.36, 127.12, 126.57, 126.23, 126.16, 125.72, 125.00, 115.03, 93.29, 71.73, 67.90, 59.21, 52.34, 35.25, 29.99. **HRMS** Accurate mass (ES+): found 445.19880, C26H30O5Na (M+Na+) requires 445.19910.

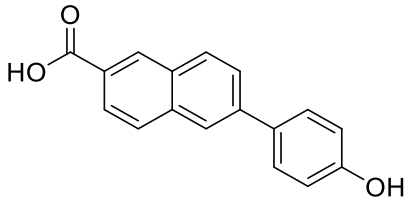

6-(4-hydroxyphenyl)-2-naphthoic acid. 2.1 was prepared from **2.S4** using general procedure C (84% yield). **^{1}H NMR** (600 MHz, Acetone-d6) δ 11.27 (br s, 1H), 8.66 (s, 1H), 8.57 (br s, 1H), 8.19 (s, 1H), 8.13 (d, J = 8.5 Hz, 1H), 8.08 (dd, J = 8.6, 1.6 Hz, 1H), 8.04 (d, J = 8.6 Hz, 1H), 7.90 (dd, J = 8.5, 1.8 Hz, 1H), 7.72 (d, J = 8.7 Hz, 2H), 7.00 (d, J = 8.7 Hz, 2H). **^{13}C NMR** (151 MHz, Acetone) δ 167.77, 158.59, 141.57, 136.99, 132.39, 132.27, 131.54, 130.69, 129.36, 129.16, 128.35, 126.86, 126.59, 125.07, 116.79. **HRMS** Accurate mass (ES-): found 263.07156, C17H11O3 (M-H+) requires 263.07082. **LogP** = 4.32, **TPSA** = 57.53 Å^{2}.

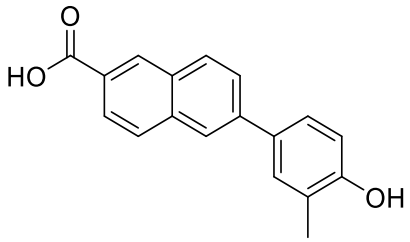

6-(4-hydroxy-3-methylphenyl)-2-naphthoic acid. 2.2 was prepared from **2.S5** using general procedure C (68% yield). **^{1}H NMR** (600 MHz, Acetone-d6) δ 11.19 (br s, 1H), 8.65 (s, 1H), 8.45 (s, 1H), 8.18 (br s, 1H), 8.12 (d, J = 8.6 Hz, 1H), 8.07 (dd, J = 8.6, 1.6 Hz, 1H), 8.03 (d, J = 8.6 Hz, 1H), 7.90 (dd, J = 8.5, 1.8 Hz, 1H), 7.62 (d, J = 1.7 Hz, 1H), 7.52 (dd, J = 8.1, 2.2 Hz, 1H), 6.98 (d, J = 8.3 Hz, 1H), 2.32 (s, 3H). **^{13}C NMR** (151 MHz, Acetone) δ 167.79, 156.62, 141.80, 137.02, 132.36, 132.24, 131.55, 130.65, 130.62, 129.16, 128.27, 126.95, 126.63, 126.57, 125.81, 125.01, 116.12, 16.35. **HRMS** Accurate mass (ES): found 278.09419, C18H14O3 (M) requires 278.09430. **LogP** = 5.17, **TPSA** = 57.53 Å^{2}.

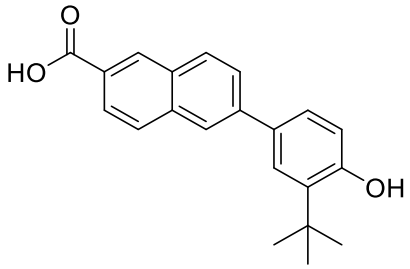

6-(3-(tert-butyl)-4-hydroxyphenyl)-2-naphthoic acid. 2.3 was prepared from **2.S6** using general procedure C (93% yield). **^{1}H NMR** (600 MHz, Acetone-d6) δ 11.31 (br s, 1H), 8.65 (s, 1H), 8.62 (s, 1H), 8.19 (s, 1H), 8.13 (d, J = 8.8 Hz, 1H), 8.07 (dd, J = 8.5, 1.6 Hz, 1H), 8.04 (d, J = 8.8 Hz, 1H), 7.90 (dd, J = 8.5, 1.8 Hz, 1H), 7.71 (d, J = 2.3 Hz, 1H), 7.52 (dd, J = 8.2, 2.3 Hz, 1H), 7.00 (d, J = 8.2 Hz, 1H), 1.50 (s, 9H). **^{13}C NMR** (151 MHz, Acetone) δ 167.75, 157.04, 142.31, 137.24, 137.03, 132.21, 131.55, 130.63, 129.15, 128.22, 127.10, 126.76, 126.74, 126.54, 125.10, 117.80, 35.47, 29.89. **HRMS** Accurate mass (ES+): found 321.14907, C21H21O3 (M+H+) requires 321.14907. **LogP** = 6.42, **TPSA** = 57.53 Å^2.

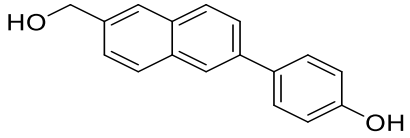

4-(6-(hydroxymethyl)naphthalen-2-yl)phenol. 2.5 was prepared from **2.1** using general procedure D **(**64% yield). **^{1}H NMR** (400 MHz, Acetone-d6) δ 8.51 (s, 1H), 8.07 (d, J = 1.9 Hz, 1H), 7.92 (d, J = 4.9 Hz, 1H), 7.90 (d, J = 4.9 Hz, 1H), 7.85 (s, 1H), 7.77 (dd, J = 8.6, 1.9 Hz, 1H), 7.66 (d, J = 8.6 Hz, 2H), 7.51 (dd, J = 8.5, 1.7 Hz, 1H), 6.98 (d, J = 8.8 Hz, 2H), 4.80 (d, J = 5.9 Hz, 2H), 4.34 (t, J = 5.8 Hz, 1H). **^{13}C NMR** (151 MHz, Acetone) δ 158.15, 140.79, 138.83, 134.13, 133.21, 133.01, 129.09, 128.82, 126.48, 126.07, 125.26, 125.12, 116.70, 64.81. **HRMS** Accurate mass (ES+): found 273.08875, C17H14O2Na (M+Na+) requires 273.08915. **LogP** = 3.75, **TPSA** = 40.46 Å^2.

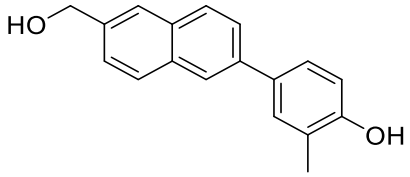

4-(6-(hydroxymethyl)naphthalen-2-yl)-2-methylphenol. 2.6 was prepared from **2.2** using general procedure D (82% yield). **^{1}H NMR** (400 MHz, Acetone-d6) δ 8.40 (s, 1H), 8.06 (d, J = 1.3 Hz, 1H), 7.93 – 7.86 (m, 2H), 7.84 (s, 1H), 7.76 (dd, J = 8.5, 1.9 Hz, 1H), 7.56 (d, J = 2.4 Hz, 1H), 7.51 (dd, J = 8.4, 1.7 Hz, 1H), 7.46 (dd, J = 8.3, 2.4 Hz, 1H), 6.96 (d, J = 8.3 Hz, 1H), 4.80 (d, J = 5.7 Hz, 2H), 4.36 (t, J = 5.8 Hz, 1H), 2.31 (s, 3H). **^{13}C NMR** (151 MHz, Acetone) δ 156.15, 140.71, 139.03, 134.15, 133.18, 133.01, 130.43, 129.01, 128.80, 126.45, 126.35,

126.15, 125.62, 125.27, 125.07, 116.05, 64.83, 16.37. **HRMS** Accurate mass (ES+): found 287.10434, C18H16O2Na (M+Na+) requires 287.10480. **LogP** = 4.59, **TPSA** = 40.46 Å^2.

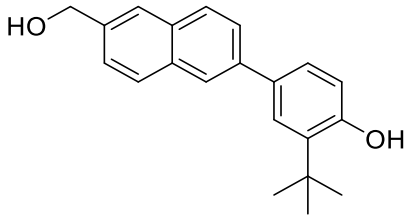

2-(tert-butyl)-4-(6-(hydroxymethyl)naphthalen-2-yl)phenol. 2.7 was prepared from **2.3** using general procedure D (82% yield). **^{1}H NMR** (600 MHz, Acetone-d6) δ 8.52 (s, 1H), 8.06 (d, J = 1.9 Hz, 1H), 7.91 (dd, J = 8.4, 2.4 Hz, 2H), 7.85 (s, 1H), 7.77 (dd, J = 8.5, 1.9 Hz, 1H), 7.67 (d, J = 2.3 Hz, 1H), 7.51 (dd, J = 8.4, 1.6 Hz, 1H), 7.46 (dd, J = 8.2, 2.3 Hz, 1H), 6.97 (d, J = 8.2 Hz, 1H), 4.81 (s, 2H), 4.33 (s, 1H), 1.50 (s, 9H). **^{13}C NMR** (151 MHz, Acetone) δ 156.54, 140.66, 139.54, 137.05, 134.15, 133.15, 132.86, 129.03, 128.80, 126.52, 126.46, 126.44, 126.29, 125.27, 125.14, 117.69, 64.83, 35.43, 29.92. **HRMS** Accurate mass (ES-): found 305.15363, C21H21O2 (M-H+) requires 305.15416. **LogP** = 5.85, **TPSA** = 40.46 Å^2.

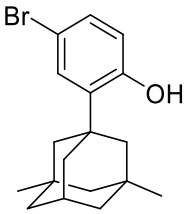

4-bromo-2-((1r,3R,5S,7r)-3,5-dimethyladamantan-1-yl)phenol [2.S7]. 3,5-dimethyladamantanol (200 mg, 1.1 mmol) and 4-bromophenol (1.1 eq, 211 mg, 1.2 mmol) were dissolved in 2 mL DCM with 1.5 mL acetic acid and 0.3 mL sulfuric acid and stirred at room temperature for 2 d. The reaction was quenched with sat. Na_2CO_3 and extracted with EtOAc 3x. The combined organic layers were washed with brine, dried over Na_2SO_4, concentrated, and purified by column chromatography to afford the product as a white solid (269 mg, 73% yield). **^{1}H NMR** (400 MHz, Chloroform-d) δ 7.29 (d, J = 2.4 Hz, 1H), 7.15 (dd, J = 8.4, 2.4 Hz, 1H), 6.53 (d, J = 8.4 Hz, 1H), 4.79 (s, 1H), 2.16 (hept, J = 3.2 Hz, 1H), 1.90 (d, J = 1.9 Hz, 2H), 1.76 – 1.60 (m, 4H), 1.47 – 1.32 (m, 4H), 1.20 (d, J = 1.8 Hz, 2H), 0.87 (s, 6H). **^{13}C NMR** (100 MHz, Chloroform-d) δ 153.61, 138.31, 130.37, 129.48, 118.44, 113.35, 51.09, 46.61, 43.21, 38.86, 38.77, 31.56, 30.99, 30.07. **HRMS** Accurate mass (ES): found 334.09248, C18H23OBr (M) requires 334.09323.

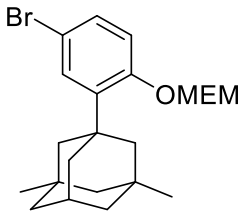

(1r,3R,5S,7r)-1-(5-bromo-2-((2-methoxyethoxy)methoxy)phenyl)-3,5-dimethyladamantane. 2.S8 was prepared from **2.S7** using general procedure A (89% yield). **^{1}H NMR** (400 MHz, Chloroform-d) δ 7.31 (d, J = 2.5 Hz, 1H), 7.23 (dd, J = 8.7, 2.5 Hz, 1H), 7.02 (d, J = 8.7 Hz, 1H), 5.28 (s, 2H), 3.85 – 3.80 (m, 2H), 3.61 – 3.53 (m, 2H), 3.39 (s, 3H), 2.14 (hept, J = 3.1 Hz, 1H), 1.89 (dd, J = 3.0, 1.5 Hz, 2H), 1.75 – 1.58 (m, 4H), 1.45 – 1.32 (m, 4H), 1.24 – 1.14 (m, 2H), 0.86 (s, 6H). **^{13}C NMR** (101 MHz, Chloroform-d) δ 155.58, 140.34, 129.96, 129.59, 116.42, 114.51, 93.43, 71.62, 67.91, 59.14, 51.05, 46.79, 43.16, 39.03, 38.90, 31.49, 31.05, 30.01. **HRMS** Accurate mass (ES+): found 445.13469, C22H31O3BrNa (M+Na+) requires 445.13543.

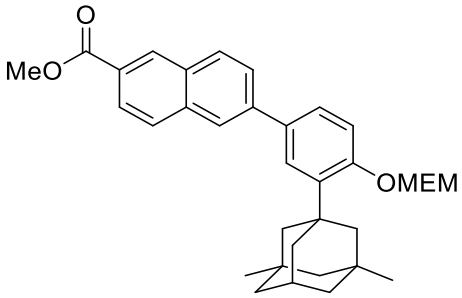

Methyl 6-(3-((1r,3R,5S,7r)-3,5-dimethyladamantan-1-yl)-4-((2-methoxyethoxy) methoxy)phenyl)-2-naphthoate. 2.S9 was prepared from **2.S8** using general procedure B (37% yield). **^{1}H NMR** (400 MHz, Chloroform-d) δ 8.59 (s, 1H), 8.05 (dd, J = 8.6, 1.7 Hz, 1H), 7.99 – 7.95 (m, 2H), 7.91 (d, J = 8.6 Hz, 1H), 7.76 (dd, J = 8.5, 1.8 Hz, 1H), 7.58 (d, J = 2.3 Hz, 1H), 7.48 (dd, J = 8.5, 2.3 Hz, 1H), 7.24 (d, J = 2.3 Hz, 1H), 5.36 (s, 2H), 3.97 (s, 3H), 3.89 – 3.85 (m, 2H), 3.62 – 3.56 (m, 2H), 3.40 (s, 3H), 2.17 (p, J = 3.2 Hz, 1H), 2.00 (s, 2H), 1.85 – 1.70 (m, 4H), 1.47 – 1.35 (m, 4H), 1.21 (s, 2H), 0.87 (s, 6H). **^{13}C NMR** (100 MHz, Chloroform-d) δ 167.43, 156.58, 141.42, 138.56, 136.01, 133.83, 131.41, 130.96, 129.85, 128.38, 127.11, 126.64, 126.23, 126.07, 125.71, 125.02, 115.17, 93.44, 71.75, 68.03, 59.22, 52.34, 51.24, 47.10, 43.36, 39.27, 39.13, 31.62, 31.18, 30.21. **HRMS** Accurate mass (ES+): found 529.29516, C34H41O5 (M+H+) requires 529.29540.

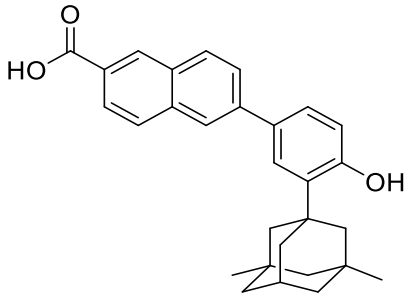

6-(3-((1r,3R,5S,7r)-3,5-dimethyladamantan-1-yl)-4-hydroxyphenyl)-2-naphthoic acid. 2.4 was prepared from **2.S9** using general procedure C (92% yield). **^{1}H NMR** (400 MHz, Acetone-d6) δ 8.65 (s, 1H), 8.18 (s, 1H), 8.13 (d, J = 8.6 Hz, 1H), 8.07 (dd, J = 8.6, 1.6 Hz, 1H), 8.04 (d, J = 8.6 Hz, 1H), 7.90 (dd, J = 8.6, 1.8 Hz, 1H), 7.66 (d, J = 2.3 Hz, 1H), 7.51 (dd, J = 8.2, 2.4 Hz, 1H), 6.97 (d, J = 8.2 Hz, 1H), 2.19 (p, J = 3.2 Hz, 1H), 2.11 (d, J = 2.0 Hz, 2H), 1.96 – 1.83 (m, 4H), 1.53 – 1.38 (m, 4H), 1.24 (s, 2H), 0.89 (s, 6H). **^{13}C NMR** (151 MHz, Acetone-d6) δ 167.84, 157.22, 142.39, 137.01, 132.42, 132.22, 131.55, 130.64, 129.14, 128.32, 127.13, 126.74, 126.58, 126.56, 125.10, 117.99, 51.89, 47.34, 44.01, 39.65, 39.46, 32.10, 31.43, 31.07, 30.59. **HRMS** Accurate mass (ES+): found 427.22715, C29H31O3 (M+H+) requires 427.22732. **LogP** = 7.75, **TPSA** = 57.53 Å^{2}.

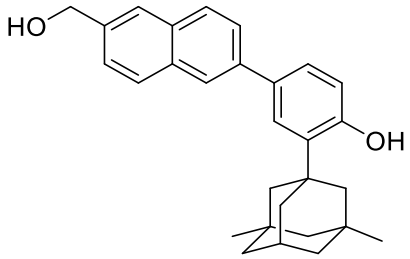

2-((1r,3R,5S,7r)-3,5-dimethyladamantan-1-yl)-4-(6-(hydroxymethyl)naphthalen-2-yl)phenol. 2.8 was prepared from **2.7** using general procedure D (72% yield). **^{1}H NMR** (400 MHz, Acetone-d$_6$) δ 8.51 (s, 1H), 8.05 (s, 1H), 7.90 (dd, J = 8.5, 2.5 Hz, 2H), 7.84 (s, 1H), 7.76 (dd, J = 8.5, 1.8 Hz, 1H), 7.61 (d, J = 2.3 Hz, 1H), 7.51 (dd, J = 8.4, 1.7 Hz, 1H), 7.45 (dd, J = 8.2, 2.3 Hz, 1H), 6.95 (d, J = 8.2 Hz, 1H), 4.81 (d, J = 5.0 Hz, 2H), 4.37 (t, J = 5.8 Hz, 1H), 2.18 (p, J = 3.1 Hz, 1H), 2.10 (d, J = 3.2 Hz, 2H), 1.94 – 1.84 (m, 4H), 1.52 – 1.38 (m, 4H), 1.24 (s, 2H), 0.89 (s, 6H). **^{13}C NMR** (151 MHz, Acetone-d6) δ 156.71, 140.62, 139.63, 136.83, 134.13, 133.13, 133.03, 129.03, 128.78, 126.47, 126.43, 126.32, 126.27, 125.28, 125.13, 117.88, 64.83, 51.89, 47.35, 44.01, 39.66, 39.41, 32.08, 31.44, 31.06. **HRMS** Accurate mass (ES-): found 411.23320, C29H31O2 (M-H+) requires 411.23240. **LogP** = 7.18, **TPSA** = 40.46 Å^{2}.

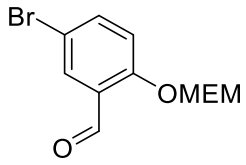

5-bromo-2-((2-methoxyethoxy)methoxy)benzaldehyde. 2.S10 was prepared from 5-bromosalicylaldehyde using general procedure A (92% yield). **^{1}H NMR** (400 MHz, Chloroform-d) δ 10.40 (s, 1H), 7.93 (d, J = 2.6 Hz, 1H), 7.61 (dd, J = 9.0, 2.6 Hz, 1H), 7.19 (d, J = 8.9 Hz, 1H), 5.38 (s, 2H), 3.89 – 3.83 (m, 2H), 3.57 – 3.54 (m, 2H), 3.37 (d, J = 0.4 Hz, 3H). **^{13}C NMR** (151 MHz, Acetone-d6) δ 188.45, 158.73, 138.45, 131.07, 126.86, 117.39, 114.96, 93.97, 71.60, 68.52, 59.19. **HRMS** Accurate mass (ES+): found 289.00740, C11H14O4Br (M+H+) requires 289.00755.

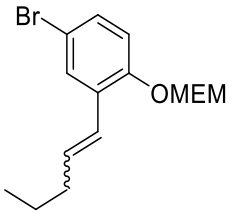

4-bromo-1-((2-methoxyethoxy)methoxy)-2-(pent-1-en-1-yl)benzene. 2.S11 was prepared from **2.S10** using general procedure E (85% yield, mixture of ~1:1.8 E:Z alkenes). **^{1}H NMR** (400 MHz, Chloroform-d) δ E alkene: 7.55 (d, J = 2.5 Hz, 1H), 7.24 (dd, J = 8.8, 2.5 Hz, 1H), 7.01 (d, J = 8.8 Hz, 1H), 6.63 (dt, J = 15.9, 1.5 Hz, 1H), 6.20 (dt, J = 15.9, 7.0 Hz, 1H), 5.27 (s, 2H), 3.85 – 3.79 (m, 2H), 3.57 – 3.53 (m, 2H), 3.38 (s, 3H), 2.26-2.18 (m, 2H), 1.56-1.41 (m, 2H), 0.99-0.90 (m, 3H). Z alkene: 7.35 (d, J = 2.5 Hz, 1H), 7.29 (dd, J = 8.9, 2.6 Hz, 1H), 7.05 (d, J = 8.7 Hz, 1H), 6.44 (dt, J = 11.6, 1.8 Hz, 1H), 5.75 (dt, J = 11.6, 7.3 Hz, 1H), 5.26 (s, 2H), 3.85 – 3.79 (m, 2H), 3.57 – 3.53 (m, 2H), 3.37 (s, 2H), 2.26-2.18 (m, 2H), 1.56-1.41 (m, 2H), 0.99-0.90 (m, 3H). **^{13}C NMR** (151 MHz, CDCl3) δ 153.94, 153.03, 134.22, 133.22, 132.69, 130.61, 130.35, 130.03, 129.66, 128.97, 123.27, 123.23, 116.76, 116.49, 114.71, 113.86, 93.96, 93.88, 71.65, 71.63, 67.90, 67.88, 59.09, 35.51, 30.66, 23.01, 22.60, 13.86, 13.82. **HRMS** Accurate mass (ES-): found 327.06017, C15H22BrO3 (M-H+) requires 327.059581.

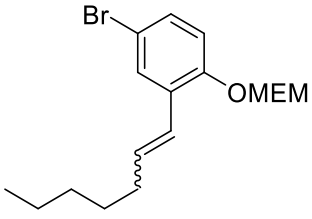

4-bromo-2-(hept-1-en-1-yl)-1-((2-methoxyethoxy)methoxy)benzene. 2.S12 was prepared from **2.S10** using general procedure E (87% yield, mixture of ~1:3.4 E:Z alkenes).

^{1}H NMR (400 MHz, Chloroform-d) δ E alkene: 7.53 (d, J = 2.5 Hz, 1H), 7.22 (dd, J = 8.8, 2.5 Hz, 1H), 7.00 (d, J = 8.8 Hz, 1H), 6.61 (dt, J = 15.9, 1.6 Hz, 1H), 6.19 (dt, J = 15.9, 7.0 Hz, 1H), 5.26 (s, 2H), 3.83 – 3.77 (m, 2H), 3.56 – 3.51 (m, 2H), 3.37 (s, 3H), 2.27 – 2.16 (m, 2H), 1.51 – 1.36 (m, 2H), 1.35 – 1.24 (m, 4H), 0.94 – 0.83 (m, 3H). Z alkene: 7.33 (d, J = 2.5 Hz, 1H), 7.28 (dd, J = 8.7, 2.5 Hz, 1H), 7.04 (d, J = 8.8 Hz, 1H), 6.40 (dt, J = 11.8, 2.0 Hz, 1H), 5.74 (dt, J = 11.6, 7.4 Hz, 1H), 5.24 (s, 2H), 3.83 – 3.77 (m, 2H), 3.56 – 3.51 (m, 2H), 3.36 (s, 3H), 2.27 – 2.16 (m, 2H), 1.51 – 1.36 (m, 2H), 1.35 – 1.24 (m, 4H), 0.94 – 0.83 (m, 3H). **^{13}C NMR** (126 MHz, $CDCl_3$) δ 153.84, 152.93, 134.36, 133.38, 132.58, 130.52, 130.25, 129.93, 129.54, 128.85, 122.99, 116.64, 116.36, 114.62, 113.78, 93.85, 93.77, 71.58, 71.55, 67.82, 67.80, 59.02, 33.38, 31.48, 31.47, 29.45, 29.05, 28.54, 22.58, 22.54, 14.10, 14.08. **HRMS** Accurate mass (ES+): found 379.08836, C17H25O3BrNa (M+Na+) requires 379.08848.

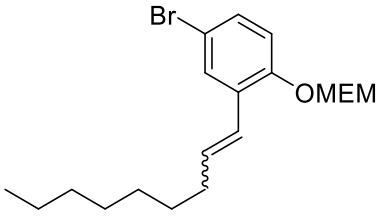

4-bromo-1-((2-methoxyethoxy)methoxy)-2-(non-1-en-1-yl)benzene. 2.S13 was prepared from **2.S10** using general procedure E (78% yield, mixture of ~1:7 E:Z alkenes). **^{1}H NMR** (400 MHz, Chloroform-d) δ E alkene: 7.53 (d, J = 2.5 Hz, 1H), 7.22 (dd, J = 8.7, 2.5 Hz, 1H), 7.00 (d, J = 8.8 Hz, 1H), 6.60 (dt, J = 16.0, 1.6 Hz, 1H), 6.19 (dt, J = 15.9, 7.0 Hz, 1H), 5.26 (s, 2H), 3.83 – 3.78 (m, 2H), 3.56 – 3.52 (m, 2H), 3.37 (s, 3H), 2.27 – 2.16 (m, 2H), 1.48 – 1.36 (m, 2H), 1.33 – 1.21 (m, 8H), 0.92 – 0.83 (m, 3H). Z alkene: 7.33 (d, J = 2.5 Hz, 1H), 7.28 (dd, J = 8.8, 2.5 Hz, 1H), 7.04 (d, J = 8.8 Hz, 1H), 6.40 (dt, J = 11.6, 1.8 Hz, 1H), 5.73 (dt, J = 11.7, 7.4 Hz, 1H), 5.24 (s, 2H), 3.83 – 3.78 (m, 2H), 3.56 – 3.52 (m, 2H), 3.36 (s, 3H), 2.27 – 2.16 (m, 2H), 1.48 – 1.36 (m, 2H), 1.33 – 1.21 (m, 8H), 0.92 – 0.83 (m, 3H). **^{13}C NMR** (151 MHz, $CDCl_3$) δ 153.97, 153.06, 134.53, 133.58, 132.72, 130.64, 130.37, 130.09, 129.69, 129.01, 123.07, 116.79, 116.51, 114.75, 113.91, 94.00, 93.92, 71.70, 71.67, 67.92, 59.15, 33.50, 31.97, 31.94, 29.87, 29.48, 29.34, 29.31, 29.27, 28.67, 22.79, 22.76, 14.21. **HRMS** Accurate mass (ES+): found 407.11965, C19H29O3BrNa (M+Na+) requires 407.11978.

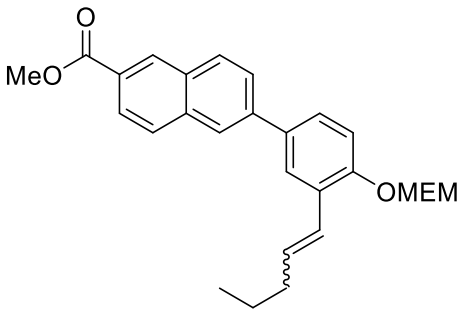

Methyl 6-(4-((2-methoxyethoxy)methoxy)-3-(pent-1-en-1-yl)phenyl)-2-naphthoate. 2.S14 was prepared from **2.S11** using general procedure B (63% yield, mix of ~1:1 E:Z alkenes). **^{1}H NMR** (400 MHz, Chloroform-d, mix of alkenes) δ 8.62 (s, 2H), 8.09 (d, J = 1.7 Hz, 1H), 8.07 (d, J = 1.7 Hz, 1H), 8.04 – 8.00 (m, 3H), 7.99 (d, J = 3.1 Hz, 1H), 7.93 (d, J = 3.2 Hz, 1H), 7.91 (d, J = 3.0 Hz, 1H), 7.82 – 7.76 (m, 3H), 7.61 (d, J = 2.4 Hz, 1H), 7.57 (dd, J = 8.5, 2.4 Hz, 1H), 7.52 (dd, J = 8.5, 2.4 Hz, 1H), 7.29 (d, *J* = 8.5 Hz, 1H), 7.26 (d, *J* = 8.6 Hz, 1H), 6.78 (d, J = 16.0 Hz, 1H), 6.59 (d, J = 11.6 Hz, 1H), 6.34 (dt, J = 15.9, 6.9 Hz, 1H), 5.81 (dt, J = 11.6, 7.3 Hz, 1H), 5.39 – 5.33 (m, 4H), 3.99 (s, 6H), 3.90 – 3.85 (m, 4H), 3.61 – 3.57 (m, 4H), 3.42 – 3.37 (m, 6H), 2.37 – 2.21 (m, 4H), 1.61 – 1.44 (m, 4H), 1.03 – 0.91 (m, 6H). **^{13}C NMR** (100 MHz, Chloroform-d, mix of alkenes) δ 167.40, 167.39, 154.88, 154.05, 140.86, 140.75, 136.00, 135.99, 134.33, 133.70, 133.66, 132.58, 131.50, 131.50, 130.95, 130.94, 129.98, 129.90, 129.29, 128.40, 128.39, 128.33, 128.06, 127.25, 127.23, 127.08, 126.97, 126.47, 126.38, 125.80, 125.77, 125.48, 125.07, 125.04, 124.32, 115.39, 115.15, 93.91, 93.88, 93.84, 93.80, 71.75, 71.72, 67.93, 59.19, 52.37, 52.35, 35.71, 30.96, 23.21, 22.77, 14.02, 13.94. **HRMS** Accurate mass (ES-): found 433.20254, C27H29O5 (M-H+) requires 433.20150.

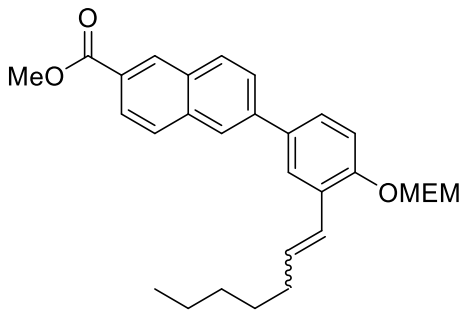

Methyl 6-(3-(hept-1-en-1-yl)-4-((2-methoxyethoxy)methoxy)phenyl)-2-naphthoate. 2.S15 was prepared from **2.S12** using general procedure B (59% yield, mix of ~1:1.5 E:Z alkenes). **^{1}H NMR** (400 MHz, Chloroform-d) δ E alkene: 8.62 (s, 1H), 8.09 (d, J = 1.8 Hz, 1H), 8.03 – 7.98 (m, 2H), 7.90 (d, J = 5.0 Hz, 1H), 7.81 – 7.76 (m, 2H), 7.51 (dd, J = 8.6, 2.4 Hz, 1H), 7.25 (d, J = 8.6 Hz, 1H), 6.77 (d, J = 15.9 Hz, 1H), 6.34 (dt, J = 15.9, 6.9 Hz, 1H), 5.37 (s, 2H), 3.99 (s, 3H), 3.91 – 3.85 (m, 2H), 3.61 – 3.56 (m, 2H), 3.40 (s, 3H), 2.38 – 2.23 (m, 2H), 1.56 – 1.29 (m, 6H), 0.94 – 0.83 (m, 3H). Z alkene: 8.62 (s, 1H), 8.07 (d, J = 1.7 Hz, 1H), 8.03 – 7.98 (m, 2H), 7.92 (d, J = 5.0 Hz, 1H), 7.81 – 7.76 (m, 1H), 7.61 (d, J = 2.4 Hz, 1H), 7.57 (dd, J = 8.5, 2.4 Hz, 1H), 7.29 (d, J = 8.5 Hz, 1H), 6.58 (d, J = 11.6 Hz, 1H), 5.81 (dt, J = 11.6, 7.3 Hz, 1H), 5.36 (s, 2H), 3.99 (s, 3H), 3.91 – 3.85 (m, 2H), 3.61 – 3.56 (m, 2H), 3.40 (s, 3H), 2.38 – 2.23 (m, 2H), 1.56 – 1.29 (m, 6H), 0.94 – 0.83 (m, 3H). **^{13}C NMR** (100 MHz, Chloroform-d, mix of alkenes) δ 167.38, 167.37, 154.87, 154.03, 140.85, 140.73, 135.99, 135.98, 134.31, 133.87, 133.68, 132.84, 131.49, 130.94, 129.95, 129.89, 129.26, 128.37, 128.33, 128.04, 127.23, 127.21, 127.05, 126.94, 126.45, 126.37, 125.79, 125.76, 125.45, 125.06, 125.02, 124.13, 115.38, 115.13, 93.90, 93.86, 93.82, 93.79, 71.74, 71.71, 67.92, 59.17, 52.35, 33.61, 31.75, 31.63, 29.73, 29.28, 28.93, 22.73, 22.70, 14.20. **HRMS** Accurate mass (ES+): found 463.24847, C29H35O5 (M+H+) requires 463.24845.

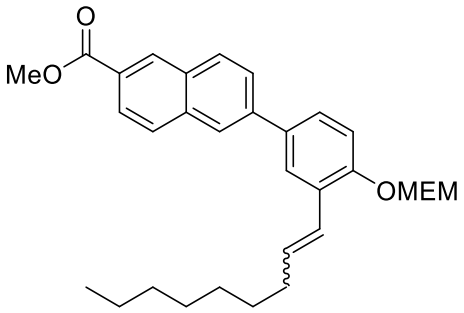

Methyl 6-(4-((2-methoxyethoxy)methoxy)-3-(non-1-en-1-yl)phenyl)-2-naphthoate. 2.S16 was prepared from **2.S13** using general procedure B (50% yield, mix of ~1:2.5 E:Z alkenes). **^{1}H NMR** (400 MHz, Chloroform-d) δ E alkene: 8.62 (s, 1H), 8.09-8.07 (m, 1H), 8.04 – 7.98 (m, 2H), 7.94 – 7.90 (m, 1H), 7.83 – 7.74 (m, 2H), 7.51 (dd, J = 8.5, 2.4 Hz, 1H), 7.25 (d, J = 8.8 Hz, 1H), 6.77 (d, J = 16.0 Hz, 1H), 6.34 (dt, J = 15.9, 6.9 Hz, 1H), 5.37 (s, 2H), 3.99 (s, 3H), 3.90 – 3.85 (m, 2H), 3.61 – 3.57 (m, 2H), 3.40 (s, 3H), 2.37 – 2.23 (m, 2H), 1.54 – 1.22 (m, 10H), 0.93 – 0.80 (m, 3H). Z alkene: 8.62 (s, 1H), 8.09-8.07 (m, 1H), 8.04 – 7.98 (m, 2H), 7.94 – 7.90 (m, 1H), 7.83 – 7.74 (m, 1H), 7.61 (d, J = 2.4 Hz, 1H), 7.57 (dd, J = 8.5, 2.4 Hz, 1H), 7.29 (d, J = 8.5 Hz, 1H), 6.57 (d, J = 11.5 Hz, 1H), 5.81 (dt, J = 11.6, 7.3 Hz, 1H), 5.36 (s, 2H), 3.99 (s, 3H), 3.90 – 3.85 (m, 2H), 3.61 – 3.57 (m, 2H), 3.40 (s, 3H), 2.37 – 2.23 (m, 2H), 1.54 – 1.22 (m, 10H), 0.93 – 0.80 (m, 3H). **^{13}C NMR** (100 MHz, Chloroform-d, mix of alkenes) δ 167.39, 154.89, 154.04, 140.87, 140.75, 136.01, 134.32, 133.89, 133.69, 132.86, 131.50, 130.95, 129.96, 129.90, 129.28, 128.39, 128.05, 127.24, 127.06, 126.95, 126.47, 126.38, 125.79, 125.77, 125.47, 125.07, 125.03, 124.14, 124.11, 115.39, 115.13, 93.92, 93.87, 93.84, 93.83, 71.75, 71.72, 67.93, 59.19, 52.37, 52.35, 33.66, 31.99, 31.97, 30.07, 29.62, 29.53, 29.40, 29.37, 29.35, 28.97, 22.81, 22.76, 14.25, 14.21. **HRMS** Accurate mass (ES+): found 491.27978, C31H39O5 (M+H+) requires 491.27975.

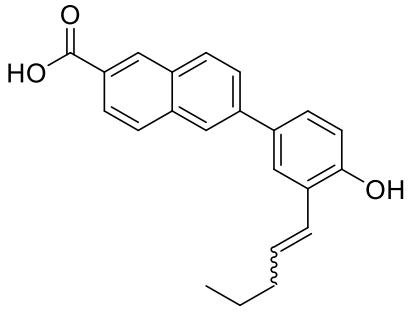

6-(4-hydroxy-3-(pent-1-en-1-yl)phenyl)-2-naphthoic acid. 2.9 was prepared from **2.S14** using general procedure C (87% yield, mix of ~1:1.4 E:Z alkenes). **^{1}H NMR** (600 MHz, Acetone-d_6) δ E alkene: 8.66 (s, 1H), 8.23 (s, 1H), 8.15 – 8.11 (m, 1H), 8.09 – 8.04 (m, 2H), 7.94 – 7.88 (m, 2H), 7.54 (dd, J = 8.3, 2.4 Hz, 1H), 7.02 (d, J = 8.3 Hz, 1H), 6.81 (d, J = 16.0 Hz, 1H), 6.48 (dt, J = 16.0, 7.0 Hz, 1H), 2.25 (qd, J = 7.2, 1.5 Hz, 2H), 1.57 – 1.48 (m, 2H), 0.98 (t, J

= 7.4 Hz, 3H). Z alkene: 8.66 (s, 1H), 8.19 (s, 1H), 8.15 – 8.11 (m, 1H), 8.09 – 8.04 (m, 2H), 7.94 – 7.88 (m, 1H), 7.68 (d, J = 2.4 Hz, 1H), 7.60 (dd, J = 8.3, 2.4 Hz, 1H), 7.05 (d, J = 8.3 Hz, 1H), 6.62 (d, J = 11.6 Hz, 1H), 5.78 (dt, J = 11.6, 7.3 Hz, 1H), 2.36 (qd, J = 7.4, 1.8 Hz, 2H), 1.57 – 1.48 (m, 2H), 0.95 (t, J = 7.4 Hz, 3H). **^{13}C NMR** (151 MHz, Acetone, mix of alkenes) δ 167.79, 155.99, 155.29, 141.71, 141.66, 136.99, 133.66, 132.70, 132.30, 132.08, 132.00, 131.57, 131.56, 130.76, 130.64, 129.72, 129.19, 128.34, 128.31, 127.90, 127.55, 126.99, 126.89, 126.63, 126.57, 126.42, 126.30, 126.10, 125.72, 125.27, 125.20, 125.16, 117.13, 116.87, 36.35, 31.59, 23.73, 23.38, 14.15, 14.05. **HRMS** Accurate mass (ES-): 331.13425, C22H19O3 (M-H+) requires 331.13342. **LogP** = 6.94, **TPSA** = 57.53 Å^2.

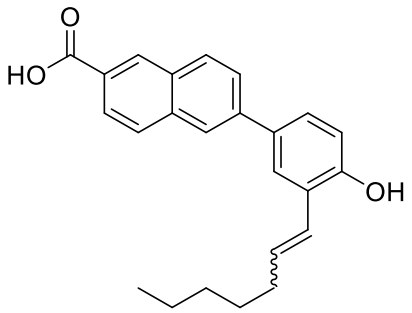

6-(3-(hept-1-en-1-yl)-4-hydroxyphenyl)-2-naphthoic acid. 2.10 was prepared from **2.S15** using general procedure C (96% yield, mix of ~1:1.6 E:Z alkenes). **^{1}H NMR** (600 MHz, Acetone-d6) δ E alkene: 11.26 (br s, 1H), 8.66 (s, 1H), 8.45 (br s, 1H), 8.22 (s, 1H), 8.17 – 8.11 (m, 1H), 8.09 (t, J = 1.9 Hz, 1H), 8.06 – 8.02 (m, 1H), 7.94 – 7.88 (m, 2H), 7.55 (dd, J = 8.3, 2.4 Hz, 1H), 7.02 (d, J = 8.3 Hz, 1H), 6.80 (d, J = 16.0 Hz, 1H), 6.49 (dt, J = 15.9, 7.0 Hz, 1H), 2.27 (qd, J = 7.2, 1.6 Hz, 2H), 1.54 – 1.48 (m, 2H), 1.39 – 1.28 (m, 4H), 0.91 (t, J = 7.1 Hz, 3H). Z alkene: 11.26 (br s, 1H), 8.66 (s, 1H), 8.45 (br s, 1H), 8.18 (s, 1H), 8.17 – 8.11 (m, 1H), 8.07 (t, J = 1.9 Hz, 1H), 8.06 – 8.02 (m, 1H), 7.94 – 7.88 (m, 1H), 7.68 (d, J = 2.6 Hz, 1H), 7.61 (dd, J = 8.3, 2.4 Hz, 1H), 7.05 (d, J = 8.4 Hz, 1H), 6.61 (d, J = 11.6 Hz, 1H), 5.78 (dt, J = 11.6, 7.3 Hz, 1H), 2.38 (qd, J = 7.4, 1.8 Hz, 2H), 1.54 – 1.48 (m, 2H), 1.39 – 1.28 (m, 4H), 0.87 (t, J = 7.1 Hz, 3H). **^{13}C NMR** (151 MHz, Acetone, mix of alkenes) δ 167.76, 167.75, 156.00, 155.29, 141.73, 141.67, 137.00, 133.89, 132.70, 132.31, 132.29, 132.08, 131.58, 131.56, 130.76, 130.65, 129.71, 129.21, 129.18, 128.34, 128.31, 127.89, 127.54, 127.00, 126.91, 126.63, 126.57, 126.45, 126.30, 126.10, 125.51, 125.21, 125.16, 125.11, 117.14, 116.87, 34.26, 32.36, 32.25, 30.59, 30.32, 30.02, 29.52, 23.24, 14.35, 14.33. **HRMS** Accurate mass (ES-): found 359.16569, C24H23O3 (M-H+) requires 359.16472. **LogP** = 7.95, **TPSA** = 57.53 Å^2.

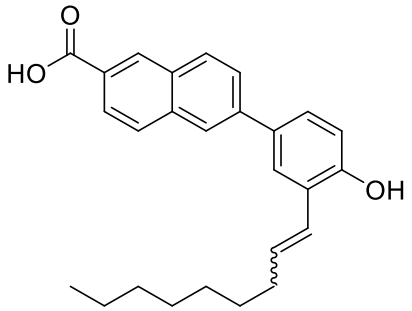

6-(4-hydroxy-3-(non-1-en-1-yl)phenyl)-2-naphthoic acid. 2.11 was prepared from **2.S16** using general procedure C (84% yield, mix of ~1:3.4 E:Z alkenes). **^{1}H NMR** (600 MHz, Acetone-d6) δ E alkene: 8.66 (s, 1H), 8.22 (s, 1H), 8.16 – 8.13 (m, 1H), 8.09 – 8.03 (m, 2H), 7.93 – 7.88 (m, 2H), 7.54 (dd, J = 8.3, 2.3 Hz, 1H), 7.02 (d, J = 8.3 Hz, 1H), 6.81 (d, J = 15.9 Hz, 1H), 6.48 (dt, J = 15.9, 6.9 Hz, 1H), 2.27 (q, J = 8.2 Hz, 2H), 1.54 – 1.47 (m, 2H), 1.38 – 1.23 (m, 8H), 0.92 – 0.78 (m, 3H). Z alkene: 8.66 (s, 1H), 8.18 (s, 1H), 8.16 – 8.13 (m, 1H), 8.09 – 8.03 (m, 2H), 7.93 – 7.88 (m, 1H), 7.68 (d, J = 2.4 Hz, 1H), 7.60 (dd, J = 8.3, 2.4 Hz, 1H), 7.05 (d, J = 8.3 Hz, 1H), 6.61 (d, J = 11.6 Hz, 1H), 5.78 (dt, J = 11.7, 7.4 Hz, 1H), 2.38 (qd, J = 7.4, 1.7 Hz, 2H), 1.54 – 1.47 (m, 2H), 1.38 – 1.23 (m, 8H), 0.92 – 0.78 (m, 3H). **^{13}C NMR** (151 MHz, Acetone) δ 167.73, 155.99, 155.28, 141.73, 141.68, 137.00, 133.89, 132.70, 132.32, 132.30, 132.08, 131.57, 131.56, 130.76, 130.65, 129.72, 129.20, 129.19, 128.36, 128.32, 127.89, 127.54, 127.01, 126.92, 126.62, 126.57, 126.44, 126.30, 126.09, 125.52, 125.21, 125.17, 125.15, 117.11, 116.85, 34.29, 32.61, 32.58, 30.63, 30.34, 29.52, 23.34, 23.29, 14.36, 14.32. **HRMS** Accurate mass (ES-): found 387.19704, C26H27O3 (M-H+) requires 387.19602. **LogP** = 8.67, **TPSA** = 57.53 Å^{2}.

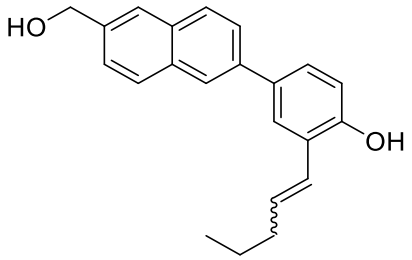

4-(6-(hydroxymethyl)naphthalen-2-yl)-2-(pent-1-en-1-yl)phenol. 2.12 was prepared from **2.9** using general procedure D (35% yield, mix of ~1:1 E:Z alkenes). **^{1}H NMR** (600 MHz, Acetone-d6, mix of alkenes) δ 8.10 (d, J = 1.8 Hz, 1H), 8.06 (d, J = 1.8 Hz, 1H), 7.94 – 7.88 (m, 4H), 7.87 (d, J = 2.4 Hz, 1H), 7.85 (s, 2H), 7.79 (dd, J = 8.5, 1.9 Hz, 1H), 7.76 (dd, J = 8.5, 1.9 Hz, 1H), 7.64 (d, J = 2.3 Hz, 1H), 7.55 (dd, J = 8.3, 2.4 Hz, 1H), 7.53 (s, 1H), 7.51 (s, 1H), 7.49 (dd, J = 8.3, 2.4 Hz, 1H), 7.04 (d, J = 8.3 Hz, 1H), 7.01 (d, J = 8.3 Hz, 1H), 6.83 (dt, J = 16.0, 1.6 Hz, 1H), 6.64 (dt, J = 11.3, 1.8 Hz, 1H), 6.46 (dt, J = 16.0, 7.0 Hz, 1H), 5.77 (dt, J = 11.6, 7.3 Hz, 1H), 4.82 (s, 4H), 4.40 (s, 2H), 2.36 (qd, J = 7.3, 1.8 Hz, 2H), 2.25 (qd, J = 7.1, 1.6 Hz, 2H), 1.58 – 1.47 (m, 4H), 0.98 (t, J = 7.4 Hz, 3H), 0.95 (t, J = 7.4 Hz, 3H). **^{13}C NMR** (151 MHz, Acetone, mix of alkenes) δ 155.47, 154.81, 140.69, 140.64, 138.93, 138.88, 134.09, 133.48, 133.31, 133.20,

132.68, 131.77, 129.48, 129.15, 129.04, 128.83, 128.82, 127.63, 127.34, 126.50, 126.45, 126.25, 126.16, 126.06, 126.04, 125.93, 125.83, 125.37, 125.29, 125.21, 125.17, 117.03, 116.75, 64.84, 64.83, 36.34, 31.58, 23.73, 23.37, 14.16, 14.06. **HRMS** Accurate mass (ES-): found 317.15505, C22H21O2 (M-H+) requires 317.15416. **LogP** = 6.37, **TPSA** = 40.46 Å^2.

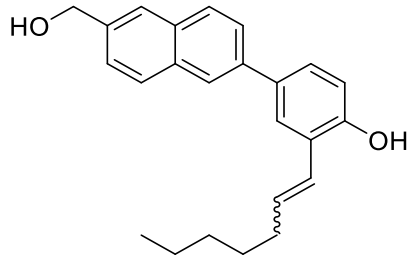

2-(hept-1-en-1-yl)-4-(6-(hydroxymethyl)naphthalen-2-yl)phenol. 2.13 was prepared from **2.10** using general procedure D (65% yield, mix of ~1:1.6 E:Z alkenes). **^{1}H NMR** (600 MHz, Acetone-d6) δ E alkene: 8.41 (br s, 1H), 8.09 (d, J = 1.8 Hz, 1H), 7.94 – 7.84 (m, 4H), 7.79 (dd, J = 8.5, 1.8 Hz, 1H), 7.55 – 7.50 (m, 1H), 7.49 (dd, J = 8.3, 2.3 Hz, 1H), 7.01 (d, J = 8.3 Hz, 1H), 6.82 (d, J = 16.0 Hz, 1H), 6.47 (dt, J = 15.9, 6.9 Hz, 1H), 4.82 (s, 2H), 4.38 (s, 1H), 2.26 (qd, J = 7.0, 1.5 Hz, 2H), 1.56 – 1.46 (m, 2H), 1.40 – 1.28 (m, 4H), 0.91 (t, J = 7.1 Hz, 3H). Z alkene: 8.41 (br s, 1H), 8.06 (d, J = 1.8 Hz, 1H), 7.94 – 7.84 (m, 3H), 7.76 (dd, J = 8.5, 1.9 Hz, 1H), 7.64 (d, J = 2.4 Hz, 1H), 7.55 (dd, J = 8.3, 2.4 Hz, 1H), 7.55 – 7.50 (m, 1H), 7.03 (d, J = 8.4 Hz, 1H), 6.63 (d, J = 11.6 Hz, 1H), 5.78 (dt, J = 11.6, 7.4 Hz, 1H), 4.82 (s, 2H), 4.38 (s, 1H), 2.37 (qd, J = 7.5, 1.7 Hz, 2H), 1.56 – 1.46 (m, 2H), 1.40 – 1.28 (m, 4H), 0.87 (t, J = 7.1 Hz, 3H). **^{13}C NMR** (151 MHz, Acetone, mix of alkenes) δ 155.48, 154.80, 140.71, 140.66, 138.93, 138.88, 134.09, 133.70, 133.31, 133.20, 132.68, 132.03, 129.46, 129.13, 129.03, 128.82, 128.79, 127.61, 127.31, 126.50, 126.44, 126.27, 126.16, 126.07, 126.03, 125.93, 125.63, 125.30, 125.21, 125.16, 117.03, 116.75, 64.82, 34.24, 32.35, 32.23, 30.59, 30.32, 30.01, 29.51, 23.23, 14.35. **HRMS** Accurate mass (ES-): found 345.18621, C24H25O2 (M-H+) requires 345.18546. **LogP** = 7.38, **TPSA** = 40.46 Å^2.

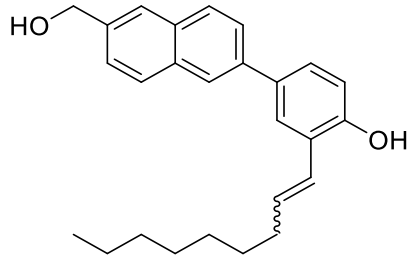

4-(6-(hydroxymethyl)naphthalen-2-yl)-2-(non-1-en-1-yl)phenol. 2.14 was prepared from **2.11** using general procedure D (43% yield, mix of ~1:3.2 E:Z alkenes). **^{1}H NMR** (600 MHz, Acetone-d6) δ E alkene: 8.55 (br s, 1H), 8.09 (d, J = 1.9 Hz, 1H), 7.93 – 7.85 (m, 4H), 7.79 (dd, J = 8.5, 1.9 Hz, 1H), 7.53 – 7.51 (m, 1H), 7.49 (dd, J = 8.3, 2.4 Hz, 1H), 7.00 (d, J = 8.3 Hz,

1H), 6.81 (d, J = 15.9 Hz, 1H), 6.46 (dt, J = 16.0, 7.0 Hz, 1H), 4.82 – 4.81 (m, 2H), 4.34 (s, 1H), 2.27 (qd, J = 7.1, 1.6 Hz, 2H), 1.54 – 1.46 (m, 2H), 1.40 – 1.23 (m, 8H), 0.88 (t, J = 6.9 Hz, 3H). Z alkene: 8.35 (br s, 1H), 8.06 (d, J = 1.3 Hz, 1H), 7.93 – 7.85 (m, 3H), 7.76 (dd, J = 8.5, 1.9 Hz, 1H), 7.64 (d, J = 2.3 Hz, 1H), 7.55 (dd, J = 8.4, 2.4 Hz, 1H), 7.53 – 7.51 (m, 1H), 7.02 (d, J = 8.3 Hz, 1H), 6.61 (d, J = 11.6 Hz, 1H), 5.77 (dt, J = 11.6, 7.4 Hz, 1H), 4.82 – 4.81 (m, 2H), 4.34 (s, 1H), 2.38 (qd, J = 7.5, 1.8 Hz, 2H), 1.54 – 1.46 (m, 2H), 1.40 – 1.23 (m, 8H), 0.83 (t, J = 6.9 Hz, 3H). **^{13}C NMR** (151 MHz, Acetone, mix of alkenes) δ 155.51, 154.82, 140.79, 140.74, 138.95, 138.89, 134.12, 133.70, 133.33, 133.23, 132.70, 132.05, 129.48, 129.14, 129.04, 128.83, 128.80, 127.63, 127.32, 126.49, 126.45, 126.29, 126.17, 126.08, 126.04, 125.94, 125.64, 125.27, 125.26, 125.23, 125.19, 117.03, 116.75, 64.83, 64.81, 34.29, 32.59, 32.58, 30.65, 30.34, 29.95, 29.53, 23.33, 23.29, 14.36, 14.34. **HRMS** Accurate mass (ES-): found 373.21754, C26H29O2 (M-H+) requires 373.21676. **LogP** = 8.33, **TPSA** = 40.46 Å^2.

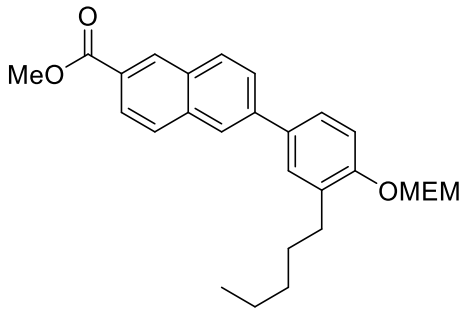

Methyl 6-(4-((2-methoxyethoxy)methoxy)-3-pentylphenyl)-2-naphthoate. 2.S17 was prepared from **2.S14** using general procedure F (94% yield). **^{1}H NMR** (400 MHz, Chloroform-d) δ 8.61 (s, 1H), 8.08 (dd, J = 8.6, 1.7 Hz, 1H), 8.02 (s, 1H), 7.99 (d, J = 8.7 Hz, 1H), 7.91 (d, J = 8.6 Hz, 1H), 7.79 (dd, J = 8.5, 1.8 Hz, 1H), 7.54 – 7.49 (m, 2H), 7.25 (d, J = 7.7 Hz, 1H), 5.37 (s, 2H), 3.99 (s, 3H), 3.89 – 3.86 (m, 2H), 3.62 – 3.59 (m, 2H), 3.41 (s, 3H), 2.75 – 2.68 (m, 2H), 1.72 – 1.62 (m, 2H), 1.42 – 1.37 (m, 4H), 0.93 (t, J = 7.1 Hz, 3H). **^{13}C NMR** (100 MHz, Chloroform-d) δ 167.36, 155.27, 140.88, 135.98, 133.82, 132.55, 131.40, 130.90, 129.82, 129.12, 128.33, 127.09, 126.43, 125.96, 125.69, 124.91, 114.37, 93.52, 71.73, 67.79, 59.16, 52.30, 31.93, 30.60, 29.96, 22.70, 14.19. **HRMS** Accurate mass (ES+): found 437.23271, C27H33O5 (M+H+) requires 437.23280.

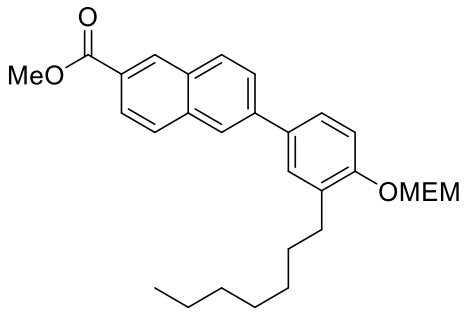

Methyl 6-(3-heptyl-4-((2-methoxyethoxy)methoxy)phenyl)-2-naphthoate. 2.S18 was prepared from **2.S15** using general procedure F (96% yield). **^{1}H NMR** (400 MHz, Chloroform-d) δ 8.61 (s, 1H), 8.07 (dd, J = 8.6, 1.7 Hz, 1H), 8.01 (s, 1H), 7.98 (d, J = 8.6 Hz, 1H), 7.90 (d, J = 8.6 Hz, 1H), 7.78 (dd, J = 8.5, 1.8 Hz, 1H), 7.55 – 7.47 (m, 2H), 7.24 (d, J = 8.6 Hz, 1H), 5.36 (s, 2H), 3.98 (s, 3H), 3.90 – 3.85 (m, 2H), 3.62 – 3.57 (m, 2H), 3.41 (s, 3H), 2.75 – 2.68 (m, 2H), 1.70 – 1.62 (m, 2H), 1.42 – 1.28 (m, 8H), 0.90 (t, J = 6.8 Hz, 3H). **^{13}C NMR** (100 MHz, Chloroform-d) δ 167.31, 155.23, 140.84, 135.95, 133.78, 132.52, 131.36, 130.86, 129.78, 129.07, 128.29, 127.05, 126.39, 125.92, 125.65, 124.86, 114.33, 93.48, 71.70, 67.76, 59.11, 52.25, 31.94, 30.61, 30.26, 29.69, 29.32, 22.78, 14.22. **HRMS** Accurate mass (ES+): found 465.26403, C29H37O5 (M+H+) requires 465.26410.

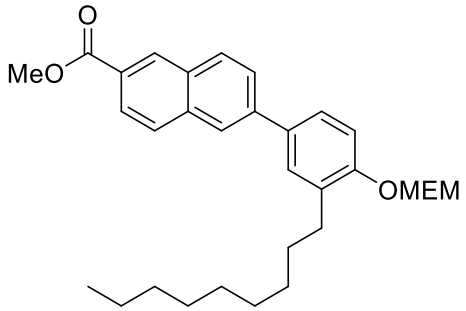

Methyl 6-(4-((2-methoxyethoxy)methoxy)-3-nonylphenyl)-2-naphthoate. 2.S19 was prepared from **2.S16** using general procedure F (98% yield). **^{1}H NMR** (399 MHz, Chloroform-d) δ 8.61 (s, 1H), 8.07 (dd, J = 8.6, 1.7 Hz, 1H), 8.01 (s, 1H), 7.99 (d, J = 8.6 Hz, 1H), 7.91 (d, J = 8.6 Hz, 1H), 7.79 (dd, J = 8.5, 1.8 Hz, 1H), 7.53 – 7.49 (m, 2H), 7.24 (d, J = 9.2 Hz, 1H), 5.36 (s, 2H), 3.99 (s, 3H), 3.89 – 3.85 (m, 2H), 3.62 – 3.58 (m, 2H), 3.41 (s, 3H), 2.73 – 2.68 (m, 2H), 1.69 – 1.60 (m, 2H), 1.43 – 1.24 (m, 12H), 0.89 (t, J = 6.7 Hz, 3H). **^{13}C NMR** (100 MHz, Chloroform-d) δ 167.43, 155.31, 140.95, 136.03, 133.89, 132.62, 131.45, 130.95, 129.87, 129.17, 128.37, 127.14, 126.49, 125.99, 125.74, 124.96, 114.42, 93.57, 71.78, 67.83, 59.21, 52.36, 32.06, 30.67, 30.32, 29.79, 29.74, 29.71, 29.51, 22.83, 14.27. **HRMS** Accurate mass (ES+): found 493.29547, C31H41O5 (M+H+) requires 493.29540.

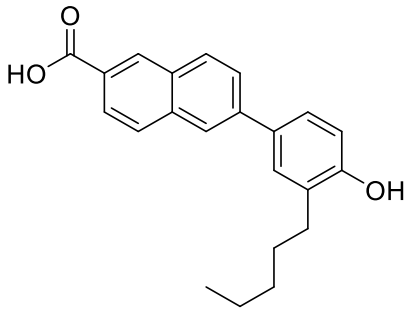

6-(4-hydroxy-3-pentylphenyl)-2-naphthoic acid. 2.15 was prepared from **2.S17** using general procedure C (97% yield). **^{1}H NMR** (400 MHz, Acetone-d6) δ 11.33 (br s, 1H), 8.65 (s, 1H), 8.46 (br s, 1H), 8.20 (s, 1H), 8.13 (d, J = 8.6 Hz, 1H), 8.07 (dd, J = 8.6, 1.6 Hz, 1H), 8.04 (d, J = 8.4 Hz, 1H), 7.91 (dd, J = 8.6, 1.9 Hz, 1H), 7.63 (d, J = 2.3 Hz, 1H), 7.53 (dd, J = 8.3, 2.4 Hz, 1H), 6.98 (d, J = 8.3 Hz, 1H), 2.73 (dd, J = 8.6, 7.0 Hz, 2H), 1.70 (qd, J = 8.4, 7.4, 4.7 Hz, 2H), 1.43 – 1.35 (m, 4H), 0.91 (t, J = 7.1 Hz, 3H). **^{13}C NMR** (151 MHz, Acetone) δ 167.74, 156.29, 141.90, 137.03, 132.39, 132.24, 131.56, 130.63, 129.97, 129.16, 128.22, 126.99, 126.62, 126.55, 125.02, 116.43, 32.58, 31.01, 30.50, 23.28, 14.37. **HRMS** Accurate mass (ES-): found 333.14998, C22H21O3 (M-H+) requires 333.14907. **LogP** = 7.09, **TPSA** = 57.53 Å^2.

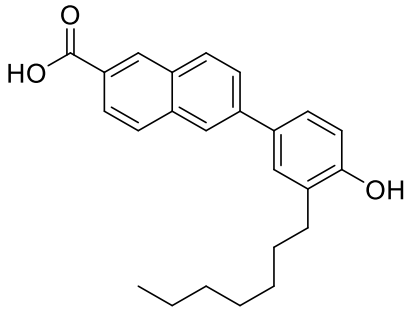

6-(3-heptyl-4-hydroxyphenyl)-2-naphthoic acid. 2.16 was prepared from **2.S18** using general procedure C (85% yield). **^{1}H NMR** (400 MHz, Acetone-d6) δ 8.65 (s, 1H), 8.19 (s, 1H), 8.13 (d, J = 8.8 Hz, 1H), 8.07 (dd, J = 8.6, 1.6 Hz, 1H), 8.03 (d, J = 8.6 Hz, 1H), 7.91 (dd, J = 8.6, 1.8 Hz, 1H), 7.63 (d, J = 2.4 Hz, 1H), 7.53 (dd, J = 8.3, 2.4 Hz, 1H), 6.99 (d, J = 8.3 Hz, 1H), 2.76 – 2.71 (m, 2H), 1.70 (p, J = 7.4 Hz, 2H), 1.47 – 1.28 (m, 8H), 0.88 (t, J = 6.9 Hz, 3H). **^{13}C NMR** (151 MHz, Acetone) δ 167.78, 156.29, 141.89, 137.03, 132.38, 132.24, 131.56, 130.64, 130.63, 129.97, 129.16, 128.26, 126.99, 126.62, 126.57, 125.02, 116.43, 32.65, 31.04, 30.82, 30.34, 30.00, 23.36, 14.37. **HRMS** Accurate mass (ES-): found 361.18001, C24H25O3 (M-H+) requires 361.18037. **LogP** = 8.09, **TPSA** = 57.53 Å^2.

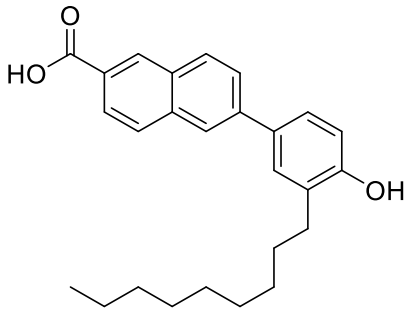

6-(4-hydroxy-3-nonylphenyl)-2-naphthoic acid. 2.17 was prepared from **2.S19** using general procedure C (84% yield). **^{1}H NMR** (400 MHz, Acetone-d6) δ 8.65 (s, 1H), 8.19 (s, 1H), 8.13 (d, J = 8.6 Hz, 1H), 8.07 (dd, J = 8.6, 1.6 Hz, 1H), 8.03 (d, J = 8.6 Hz, 1H), 7.91 (dd, J = 8.6,

1.9 Hz, 1H), 7.63 (d, J = 2.4 Hz, 1H), 7.53 (dd, J = 8.3, 2.4 Hz, 1H), 6.98 (d, J = 8.3 Hz, 1H), 2.77 – 2.70 (m, 2H), 1.75 – 1.65 (m, 2H), 1.46 – 1.24 (m, 12H), 0.87 (t, J = 6.7 Hz, 3H). **^{13}C NMR** (151 MHz, Acetone) δ 167.80, 156.28, 141.89, 137.03, 132.39, 132.24, 131.55, 130.63, 129.98, 129.15, 128.28, 126.99, 126.61, 126.57, 125.02, 116.42, 32.64, 31.03, 30.79, 30.59, 30.37, 30.35, 30.32, 23.33, 14.35. **HRMS** Accurate mass (ES-): found 389.21212, C26H29O3 (M-H+) requires 389.21167. **LogP** = 8.75, **TPSA** = 57.53 Å^2.

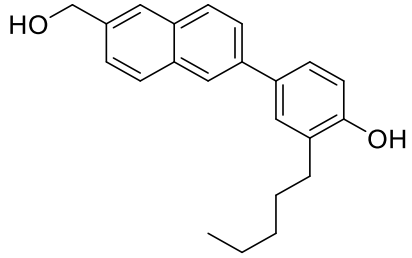

4-(6-(hydroxymethyl)naphthalen-2-yl)-2-pentylphenol. 2.18 was prepared from **2.15** using general procedure E (74% yield). **^{1}H NMR** (400 MHz, Acetone-d6) δ 8.37 (s, 1H), 8.07 (d, J = 1.2 Hz, 1H), 7.90 (d, J = 8.4 Hz, 2H), 7.84 (d, J = 1.0 Hz, 1H), 7.77 (dd, J = 8.5, 1.8 Hz, 1H), 7.57 (d, J = 2.4 Hz, 1H), 7.51 (dd, J = 8.5, 1.7 Hz, 1H), 7.46 (dd, J = 8.3, 2.4 Hz, 1H), 6.97 (d, J = 8.3 Hz, 1H), 4.81 (s, 2H), 4.40 (s, 1H), 2.76 – 2.71 (m, 2H), 1.70 (dt, J = 14.9, 7.4 Hz, 2H), 1.43 – 1.36 (m, 4H), 0.92 (t, J = 7.0 Hz, 3H). **^{13}C NMR** (151 MHz, Acetone) δ 155.78, 140.59, 139.11, 134.13, 133.14, 133.02, 130.45, 129.72, 129.01, 128.79, 126.43, 126.32, 126.17, 125.29, 125.05, 116.35, 64.85, 32.57, 31.02, 30.52, 23.27, 14.38. **HRMS** Accurate mass (ES-): found 319.17025, C22H23O2 (M-H+) requires 319.16981. **LogP** = 6.52, **TPSA** = 40.46 Å^2.

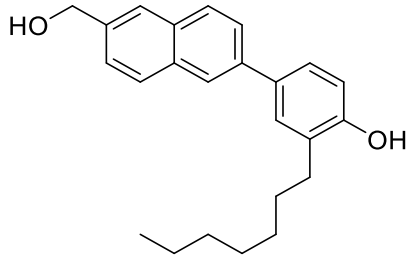

2-heptyl-4-(6-(hydroxymethyl)naphthalen-2-yl)phenol. 2.19 was prepared from **2.16** using general procedure D (70% yield). **^{1}H NMR** (400 MHz, Acetone-d6) δ 8.37 (s, 1H), 8.07 (d, J = 1.5 Hz, 1H), 7.90 (d, J = 8.3 Hz, 2H), 7.84 (s, 1H), 7.77 (dd, J = 8.5, 1.9 Hz, 1H), 7.57 (d, J = 2.4 Hz, 1H), 7.51 (dd, J = 8.4, 1.7 Hz, 1H), 7.46 (dd, J = 8.3, 2.4 Hz, 1H), 6.97 (d, J = 8.3 Hz, 1H), 4.81 (s, 2H), 4.38 (s, 1H), 2.76 – 2.70 (m, 2H), 1.75 – 1.66 (m, 2H), 1.44 – 1.28 (m, 8H), 0.89 (t, J = 6.9 Hz, 3H). **^{13}C NMR** (151 MHz, Acetone) δ 155.79, 140.61, 139.12, 134.13, 133.15, 133.01, 130.45, 129.72, 129.01, 128.79, 126.43, 126.32, 126.17, 125.29, 125.05, 116.35, 64.84, 32.64, 31.06, 30.84, 30.33, 30.00, 23.34, 14.38. **HRMS** Accurate mass (ES-): found 347.20183, C24H27O2 (M-H+) requires 347.20111. **LogP** = 7.53, **TPSA** = 40.46 Å^2.

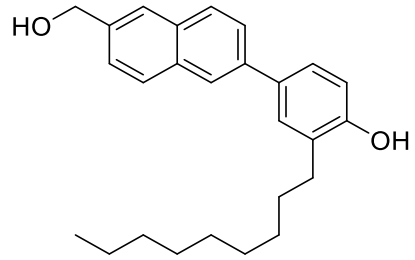

4-(6-(hydroxymethyl)naphthalen-2-yl)-2-nonylphenol. 2.20 was prepared from **2.17** using general procedure D (45% yield). **^{1}H NMR** (400 MHz, Acetone-d6) δ 8.35 (s, 1H), 8.06 (s, 1H), 7.90 (dd, J = 8.5, 2.4 Hz, 2H), 7.84 (s, 1H), 7.77 (dd, J = 8.5, 1.9 Hz, 1H), 7.57 (d, J = 2.4 Hz, 1H), 7.51 (dd, J = 8.5, 1.7 Hz, 1H), 7.46 (dd, J = 8.3, 2.4 Hz, 1H), 6.96 (d, J = 8.3 Hz, 1H), 4.80 (d, J = 5.9 Hz, 2H), 4.35 (t, J = 5.8 Hz, 1H), 2.76 – 2.70 (m, 2H), 1.74 – 1.65 (m, 2H), 1.46 – 1.25 (m, 12H), 0.88 (t, J = 6.8 Hz, 3H). **^{13}C NMR** (151 MHz, Acetone) δ 155.81, 140.67, 139.13, 134.15, 133.17, 133.03, 130.46, 129.75, 129.01, 128.79, 126.44, 126.33, 126.18, 125.28, 125.06, 116.36, 64.84, 32.64, 31.05, 30.83, 30.37, 30.35, 30.32, 23.33, 14.36. **HRMS** Accurate mass (ES-): found 375.23316, C26H31O2 (M-H+) requires 375.23240. **LogP** = 8.43, **TPSA** = 40.46 Å^{2}.

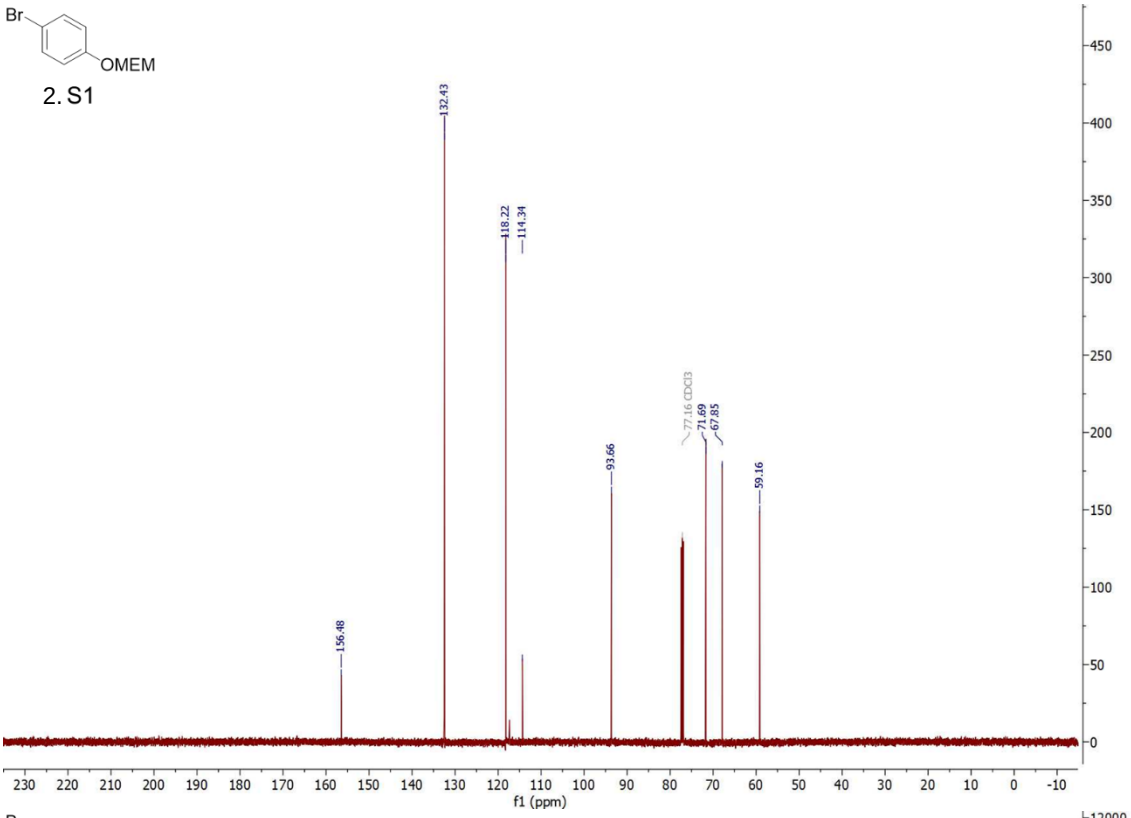
Br
OMEM
2. S1
132.43
118.22
114.34
93.66
77.16 CDCl3
71.69
67.85
59.16
156.48
f1 (ppm)

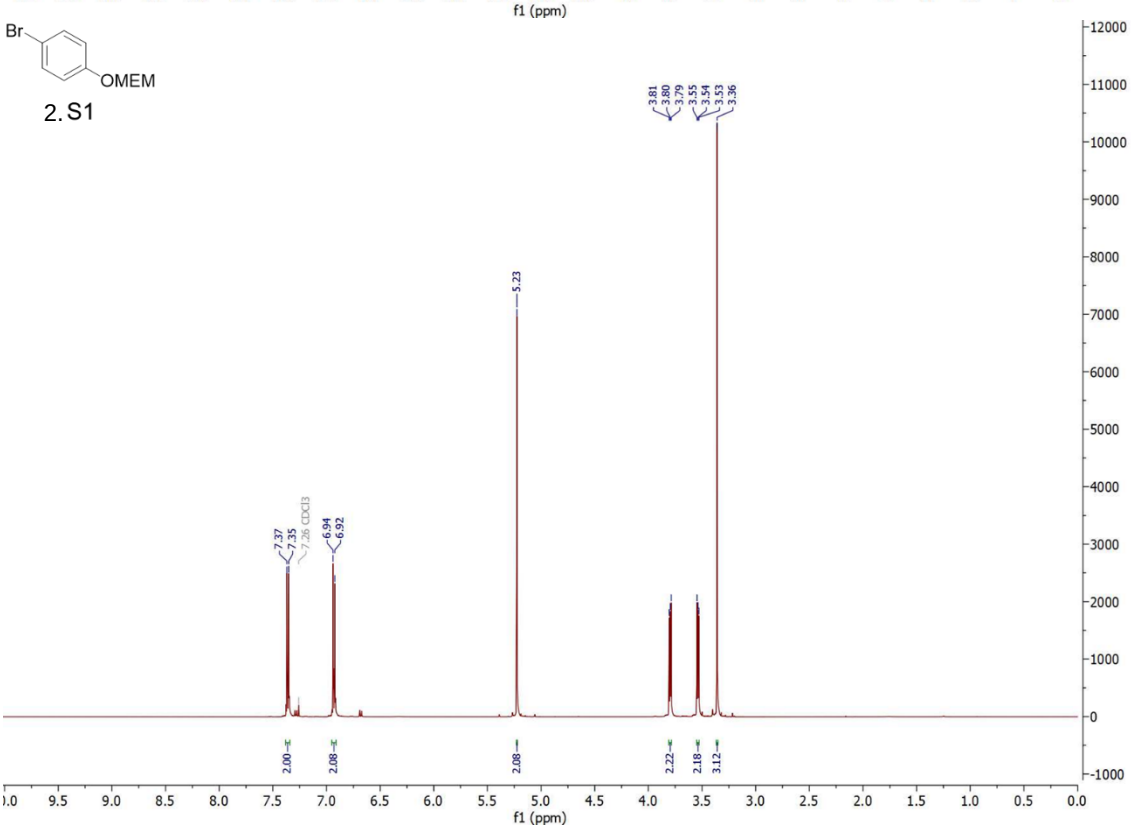
Br
OMEM
2. S1
3.81
3.80
3.79
3.55
3.54
3.53
3.36
5.23
7.37
7.35
7.26 CDCl3
6.94
6.92
2.00
2.08
2.08
2.22
2.18
3.12
f1 (ppm)

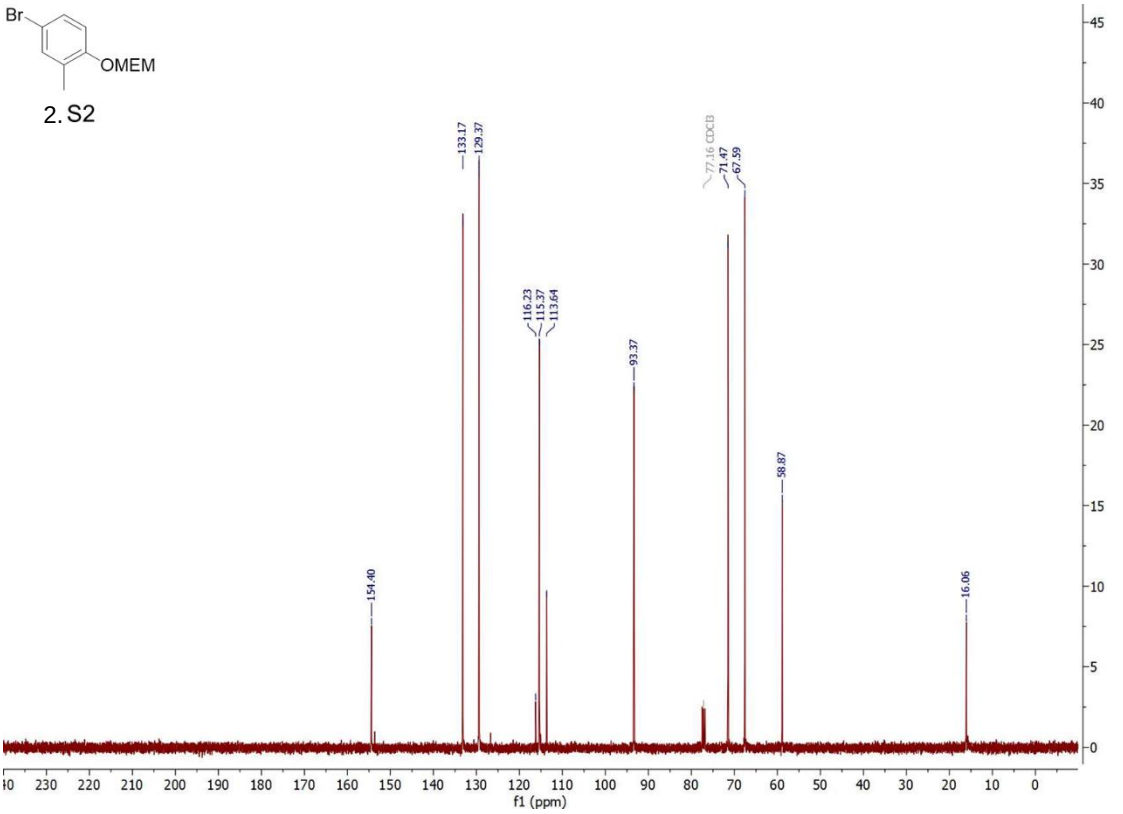
Br
OMEM
2. S2
154.40
133.17
129.37
116.23
115.37
113.64
93.37
77.16 CDCB
71.47
67.59
58.87
16.06
f1 (ppm)

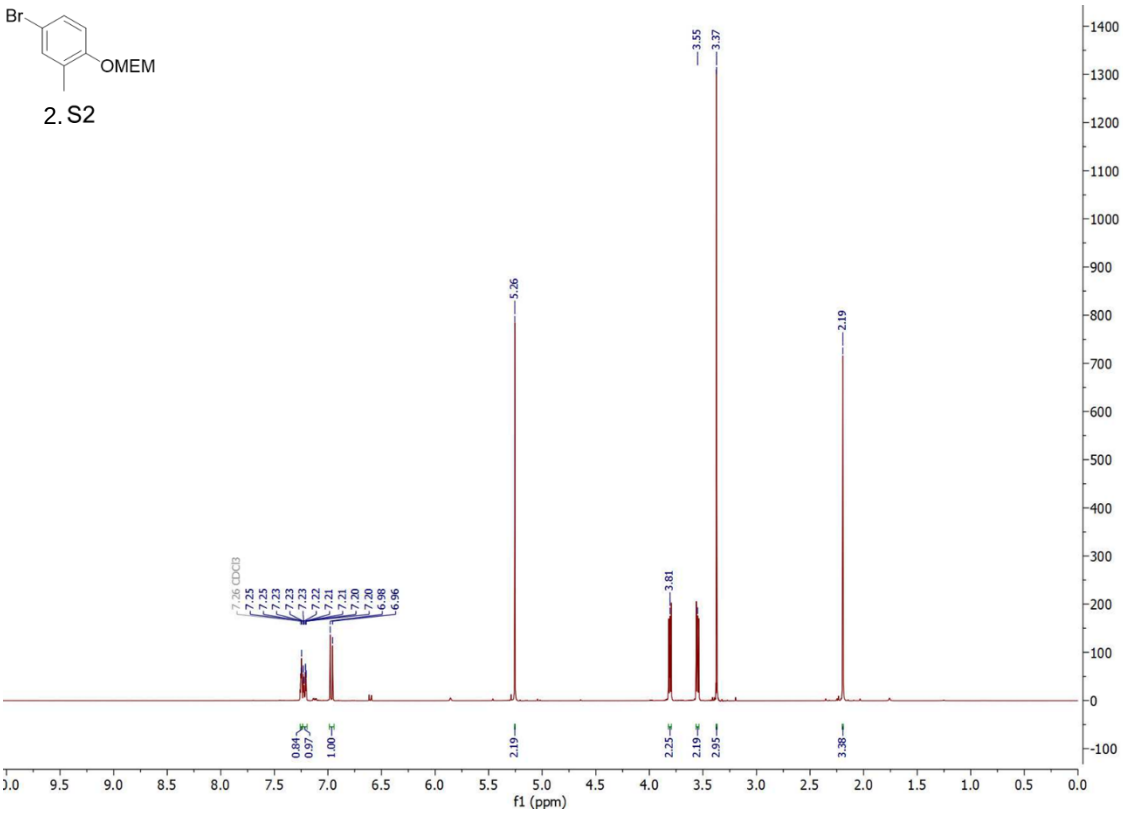
Br
OMEM
2. S2
7.26 CDCB
7.25
7.25
7.23
7.23
7.23
7.22
7.21
7.21
7.20
7.20
6.98
6.96
5.26
3.81
3.55
3.37
2.19
0.84
0.97
1.00
2.19
2.25
2.19
2.95
3.38
f1 (ppm)

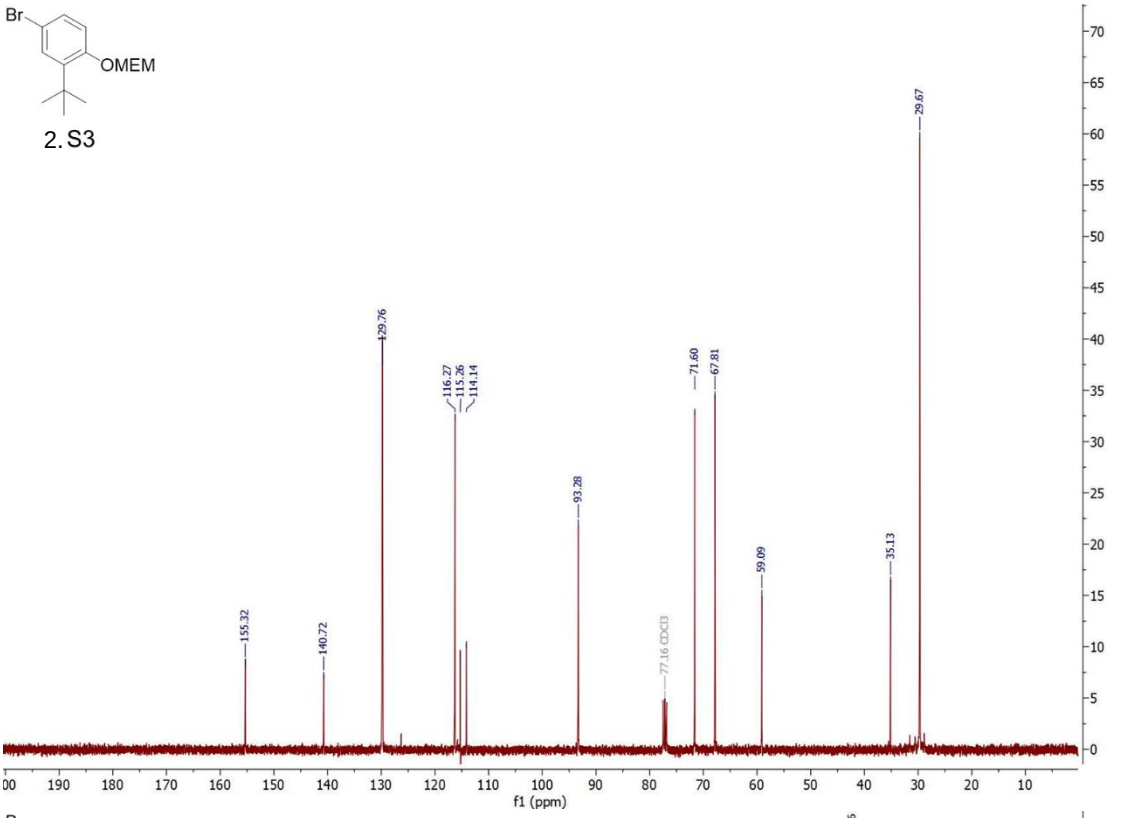
Br
OMEM
2. S3
155.32
140.72
129.76
116.27
115.26
114.14
93.28
77.16 CDCl3
71.60
67.81
59.09
35.13
29.67
f1 (ppm)

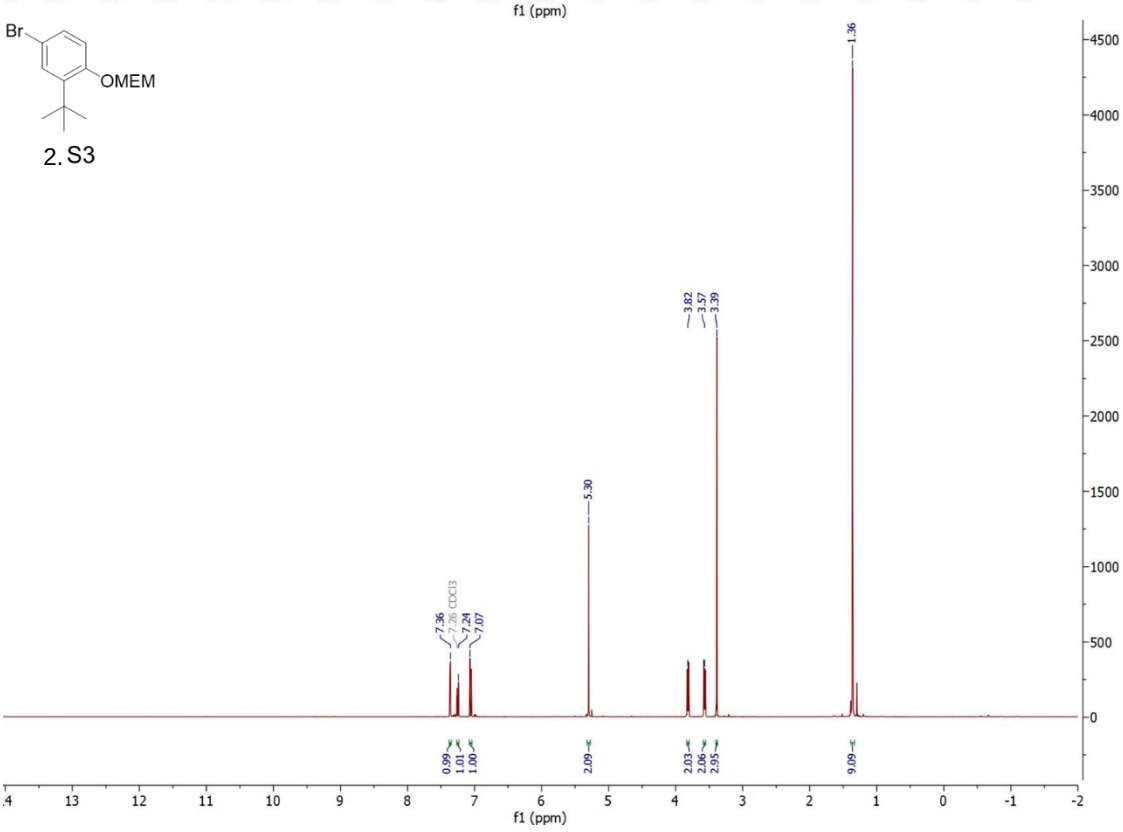
Br
OMEM
2. S3
7.36
7.26 CDCl3
7.24
7.07
5.30
3.82
3.57
3.39
1.36
0.99
1.01
1.00
2.09
2.03
2.06
2.95
9.09
f1 (ppm)

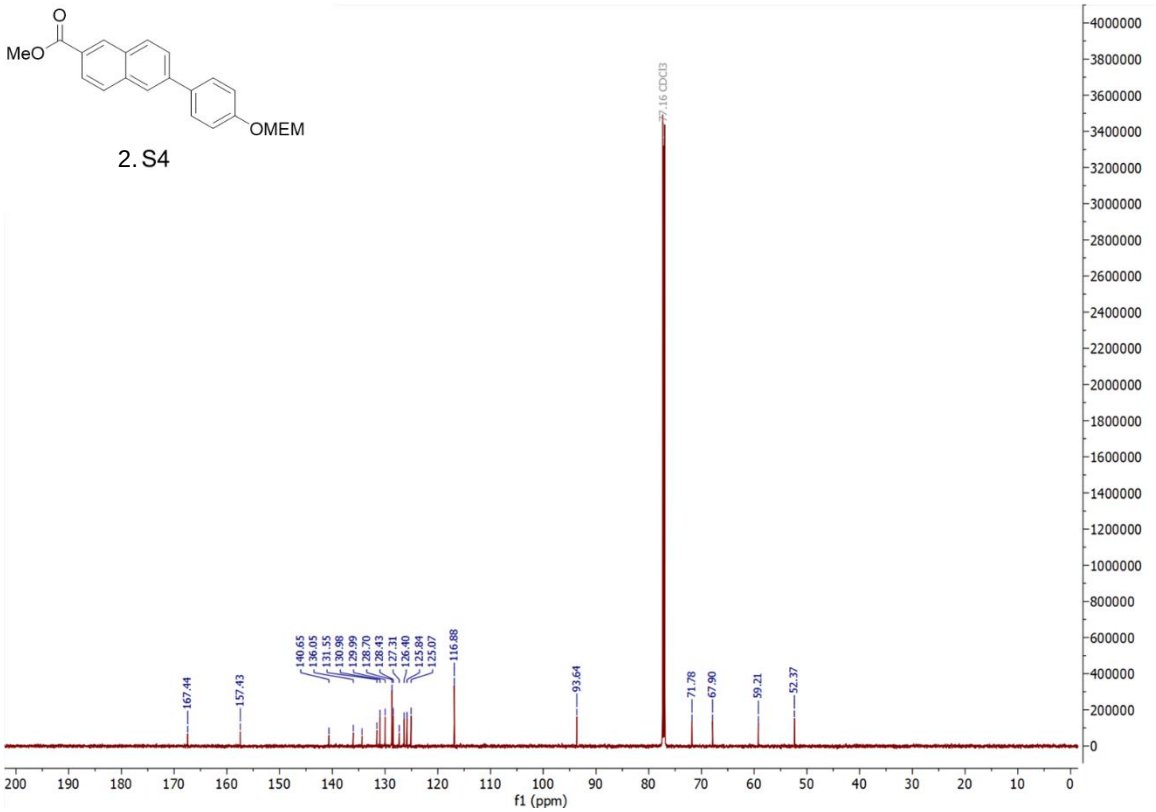
MeO
OMEM
2.S4
167.44
157.43
140.65
136.05
131.55
130.98
129.99
128.70
128.43
127.31
126.40
125.84
125.07
116.88
93.64
77.16 CDCl3
71.78
67.90
59.21
52.37
f1 (ppm)

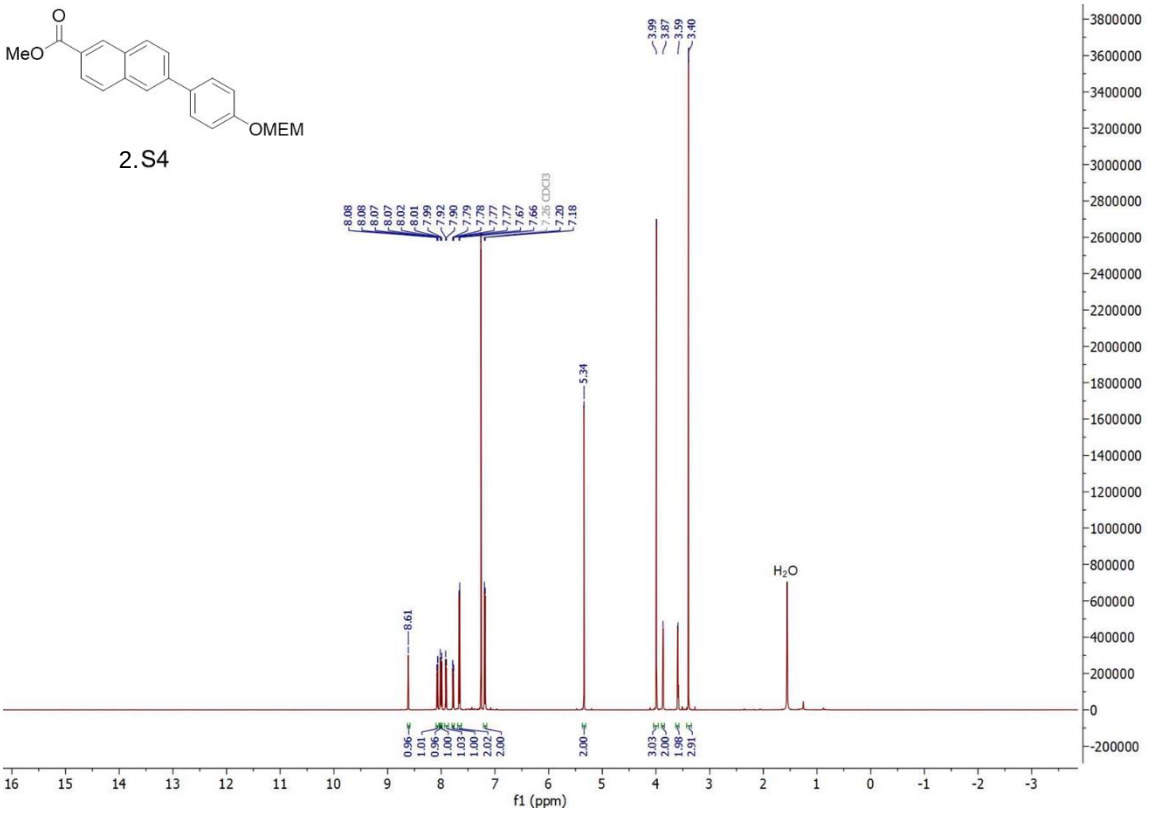
MeO
OMEM
2.S4
8.08
8.08
8.07
8.07
8.02
8.01
7.99
7.92
7.90
7.79
7.78
7.77
7.77
7.67
7.66
7.26 CDCl3
7.20
7.18
3.99
3.97
3.59
3.40
5.34
8.61
H2O
0.96
1.01
0.96
1.00
1.03
1.00
2.02
2.00
2.00
3.03
2.00
1.00
2.91
f1 (ppm)

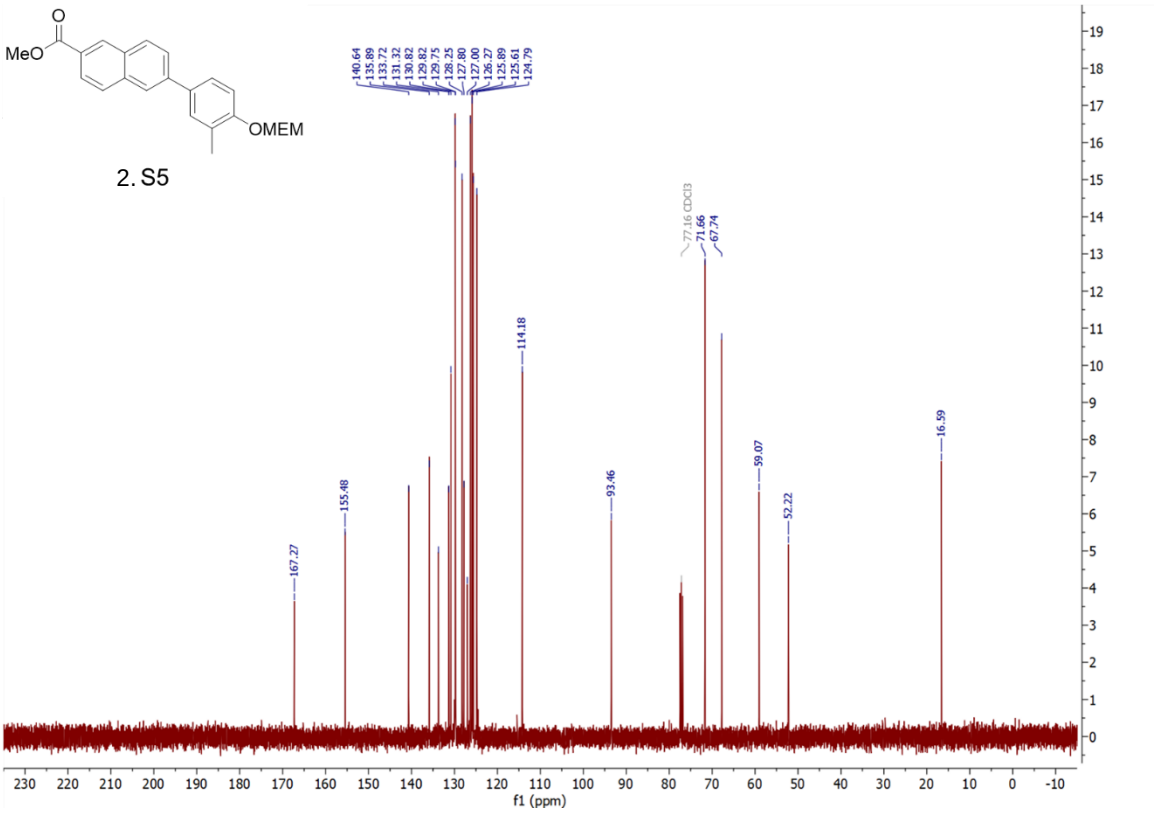
MeO
O
OMEM
2. S5
140.64
135.89
133.72
131.32
130.82
129.82
129.75
128.25
127.80
127.00
126.27
125.89
125.61
124.79
77.16 CDCl3
71.66
67.74
114.18
93.46
59.07
52.22
16.59
167.27
155.48
f1 (ppm)

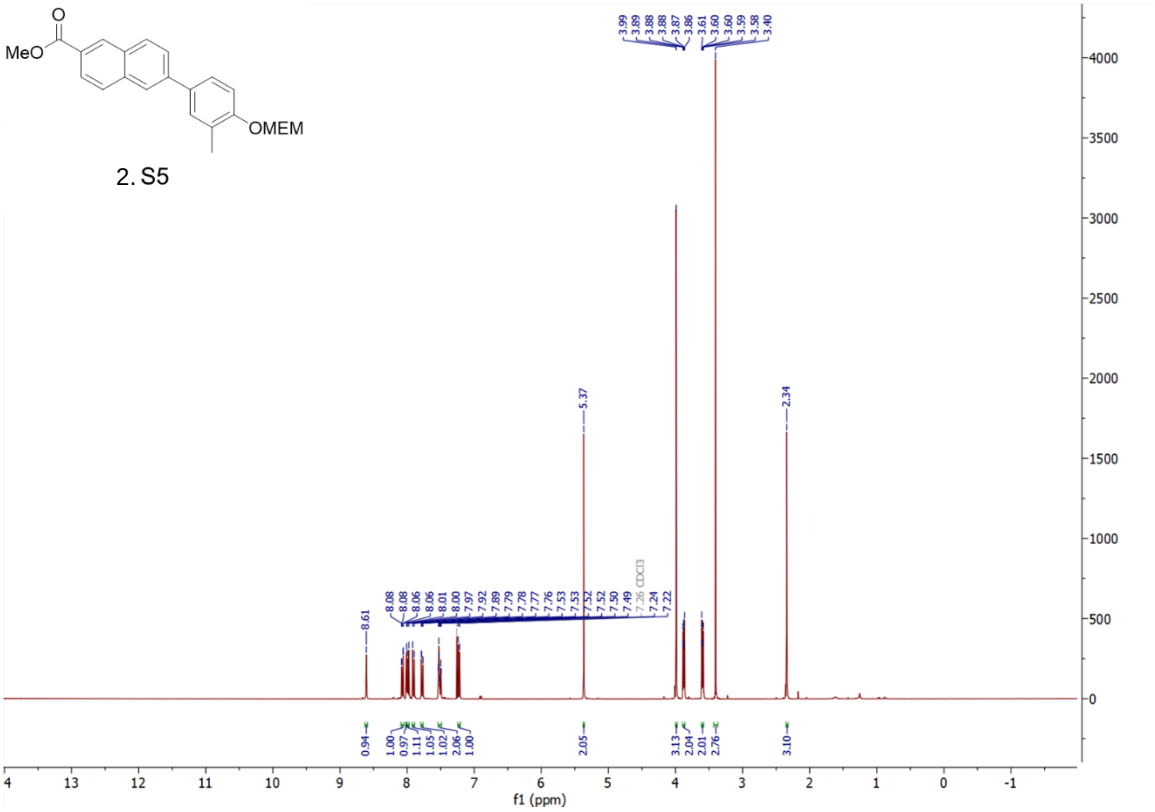
MeO
O
OMEM
2. S5
3.99
3.89
3.88
3.88
3.87
3.86
3.61
3.60
3.60
3.59
3.58
3.40
5.37
2.34
8.61
8.08
8.08
8.06
8.06
8.01
8.00
7.97
7.92
7.89
7.79
7.78
7.77
7.76
7.53
7.53
7.52
7.52
7.50
7.49
7.26 CDCl3
7.24
7.22
0.94
1.00
0.97
1.11
1.05
1.02
2.06
1.00
2.05
3.13
2.04
2.01
2.76
3.10
f1 (ppm)

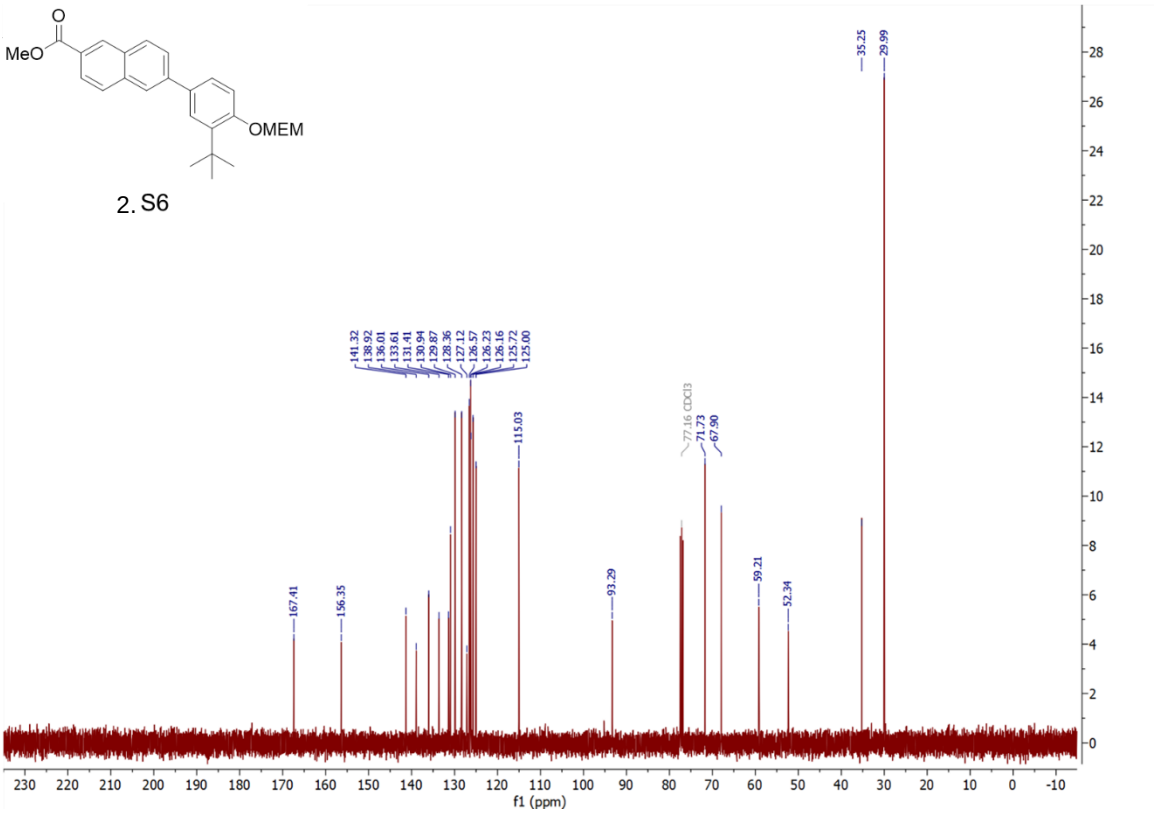
MeO
O
OMEM
2. S6
35.25
29.99
141.32
138.92
136.01
133.61
131.41
130.94
129.87
128.36
127.12
126.57
126.23
126.16
125.72
125.00
115.03
77.16 CDCl3
71.73
67.90
167.41
156.35
93.29
59.21
52.34
f1 (ppm)

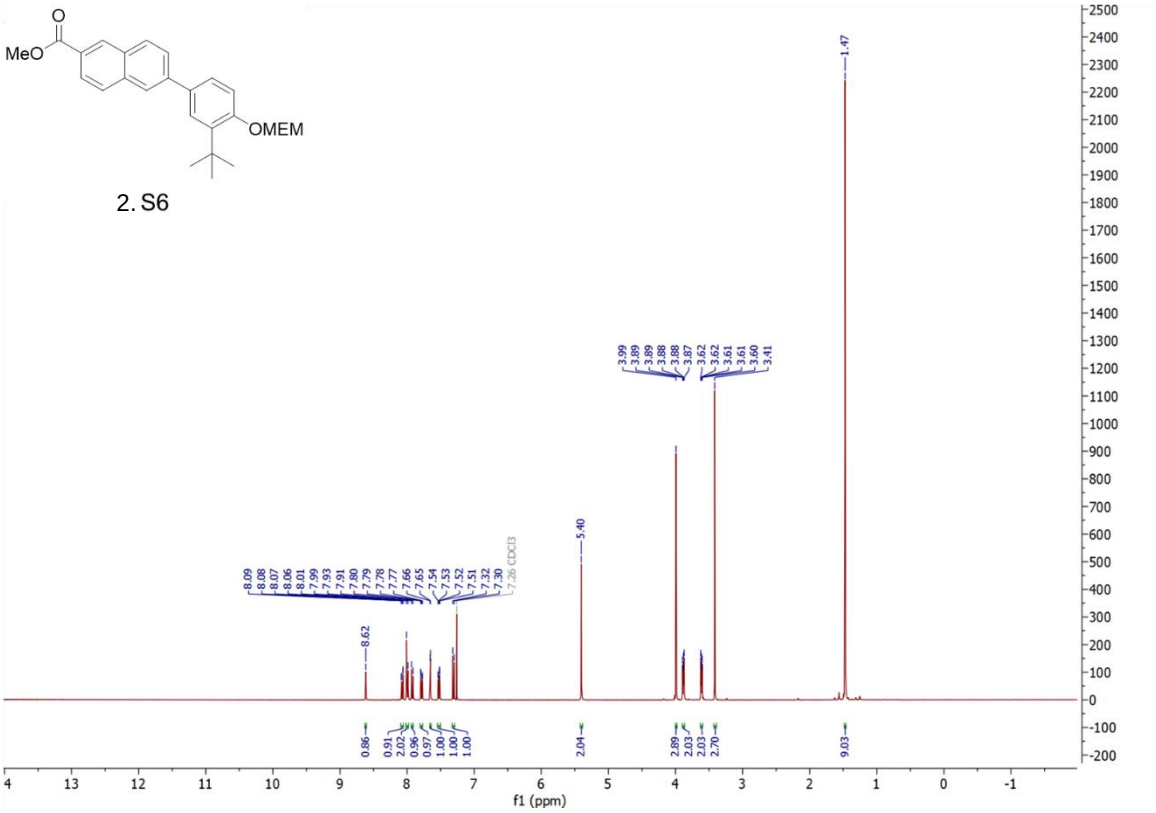
MeO
O
OMEM
2. S6
1.47
5.40
8.62
7.26 CDCl3
f1 (ppm)

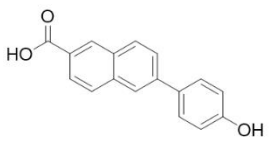
HO
O
OH

2.1

d6-acetone
d6-acetone
141.57
136.99
132.39
132.27
131.54
130.69
129.37
129.17
128.36
126.67
126.60
125.08
167.77
158.60
116.80
f1 (ppm)

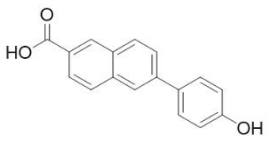
HO
O
OH

2.1

2.05 (CD3)2CO
8.66
8.57
8.19
8.14
8.08
8.05
7.91
7.72
7.01
11.27
1.16
0.98
0.76
0.96
0.97
0.97
0.99
1.00
1.91
1.93
f1 (ppm)

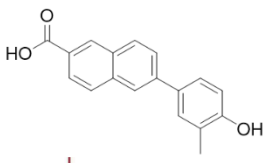
HO
O
OH

2.2

d6-acetone
d6-acetone
141.78
137.01
132.35
132.23
131.54
130.64
130.61
129.15
128.26
126.94
126.63
126.56
125.80
125.00
167.77
156.61
116.11
16.35
f1 (ppm)

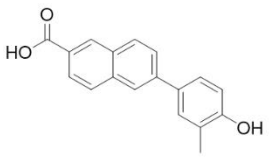
HO
O
OH

2.2

8.65
8.45
8.18
8.11
8.06
8.03
7.89
7.62
7.52
6.97
11.19
2.32
0.53
0.99
0.53
0.97
1.00
1.02
1.07
1.01
1.07
1.02
1.00
2.97
f1 (ppm)

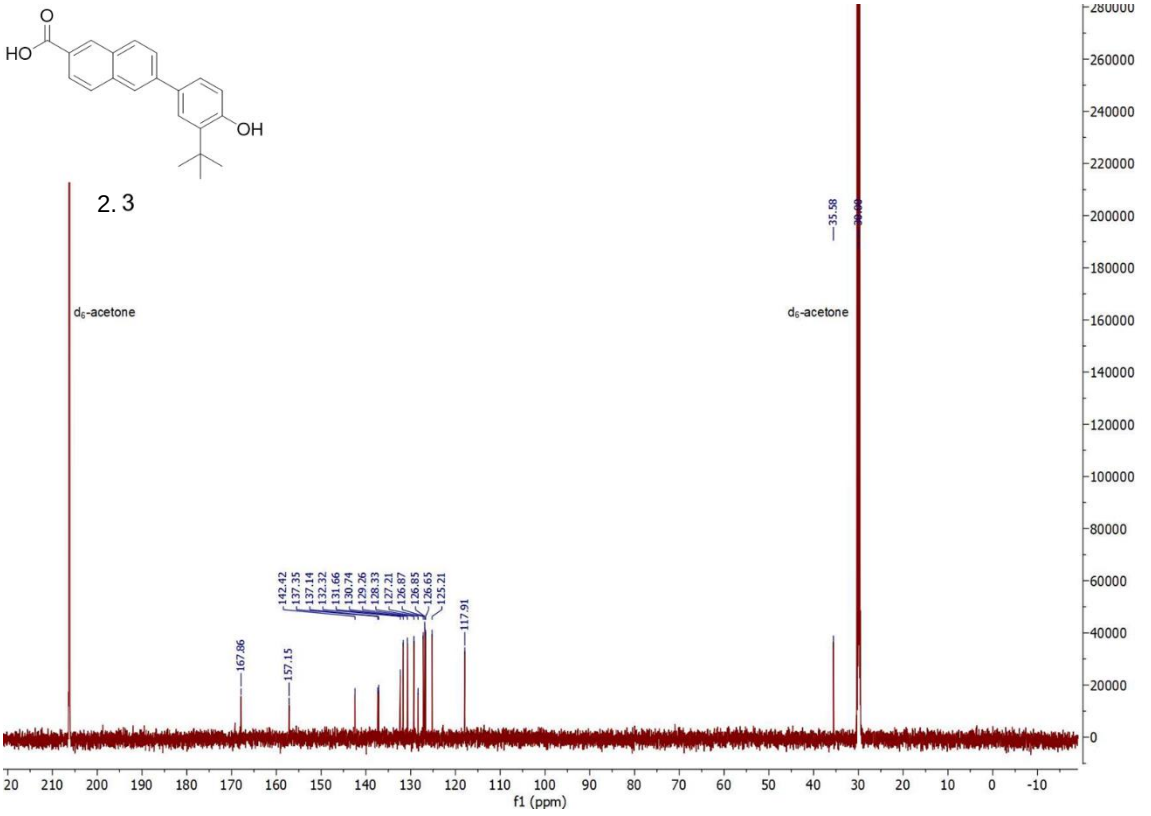
HO
O
OH
2.3
d6-acetone
d6-acetone
142.42
137.35
137.14
132.32
131.66
130.74
129.26
128.33
127.21
126.87
126.85
126.65
125.21
117.91
167.86
157.15
35.58
f1 (ppm)

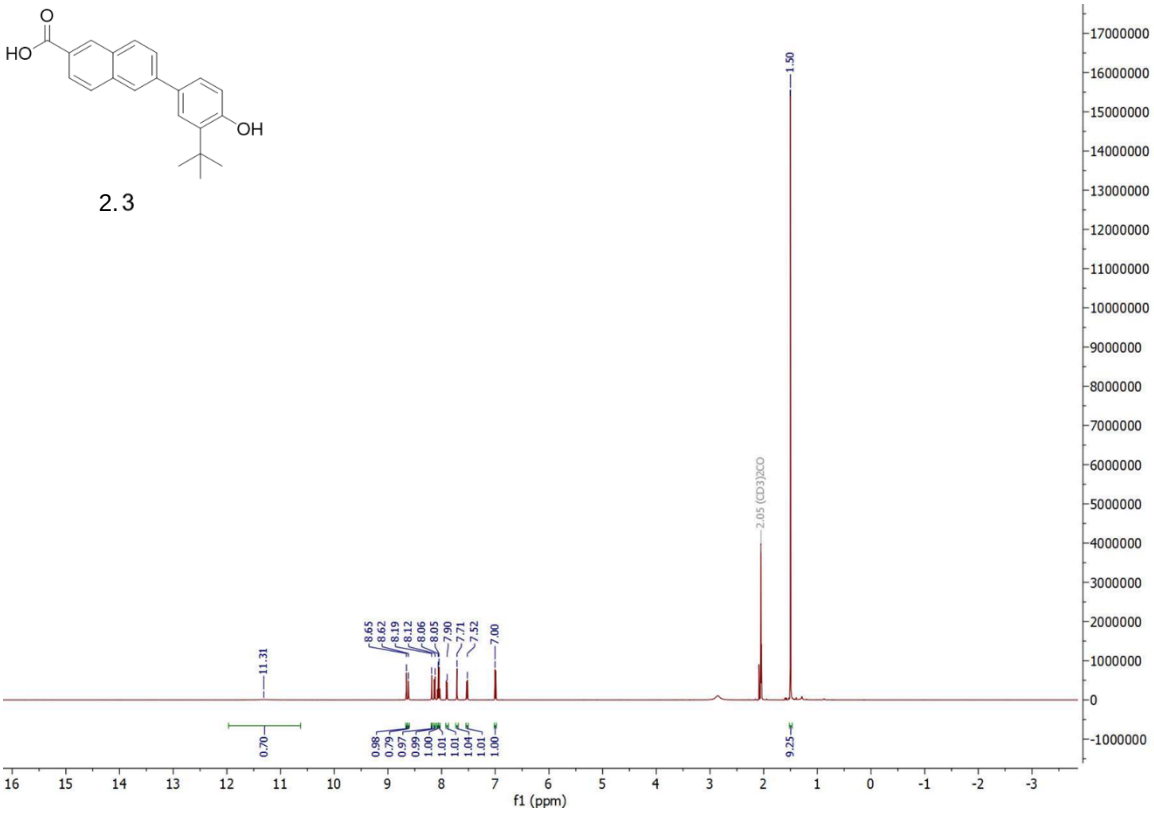
HO
O
OH
2.3
11.31
8.65
8.62
8.19
8.12
8.06
8.05
7.90
7.71
7.52
7.00
2.05 (CD3)2CO
1.50
0.70
0.98
0.79
0.97
0.99
1.00
1.01
1.01
1.04
1.01
1.00
9.25
f1 (ppm)

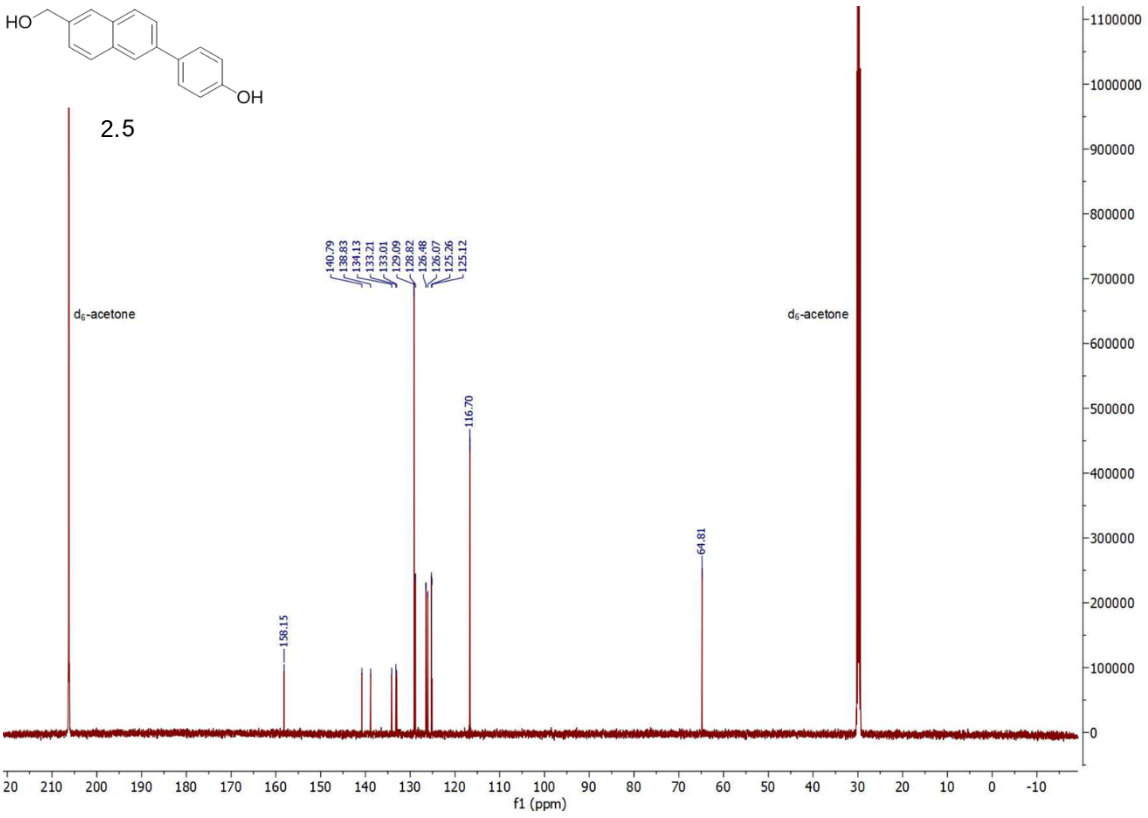
HO
OH
2.5
d6-acetone
d6-acetone
140.79
138.83
134.13
133.21
133.01
129.09
128.82
126.48
126.07
125.26
125.12
116.70
64.81
158.15
f1 (ppm)

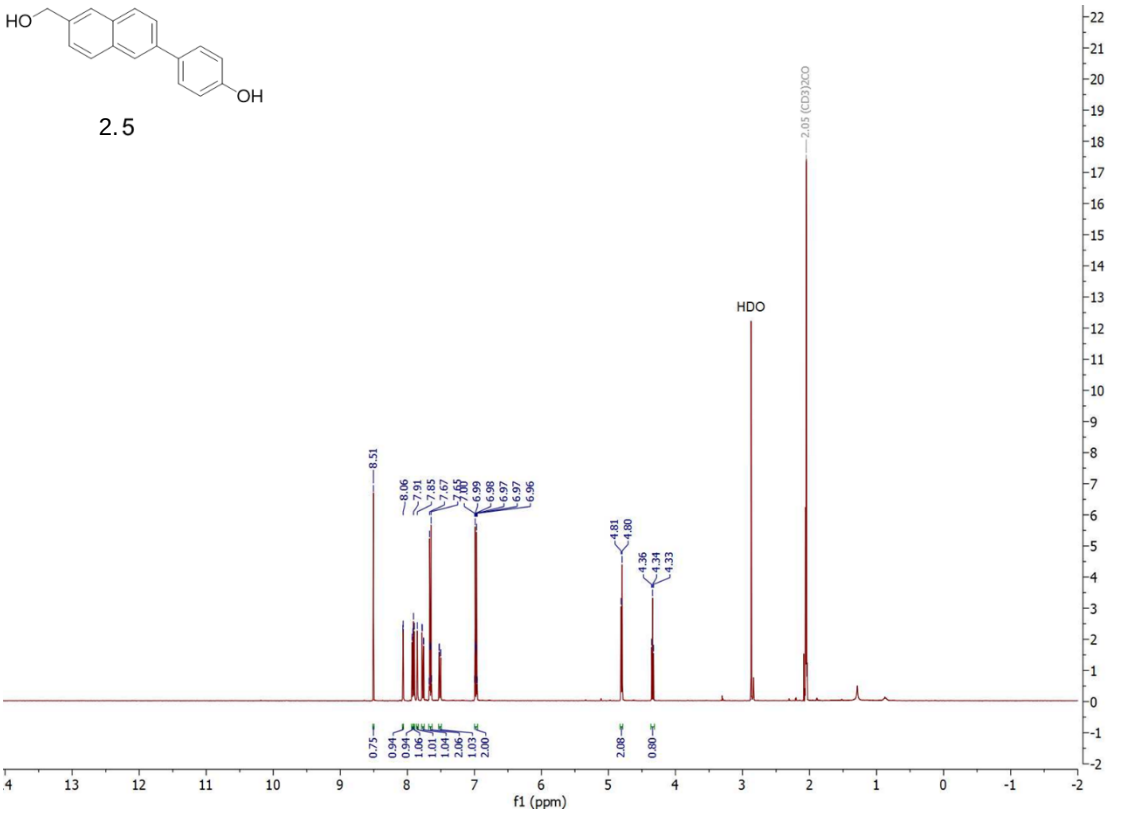
HO
OH
2.5
HDO
2.05 (CD3)2CO
8.51
8.06
7.91
7.85
7.67
7.65
7.03
6.99
6.98
6.97
6.97
6.96
4.81
4.80
4.36
4.34
4.33
0.75
0.94
0.94
1.06
1.01
1.04
2.06
1.03
2.00
2.08
0.80
f1 (ppm)

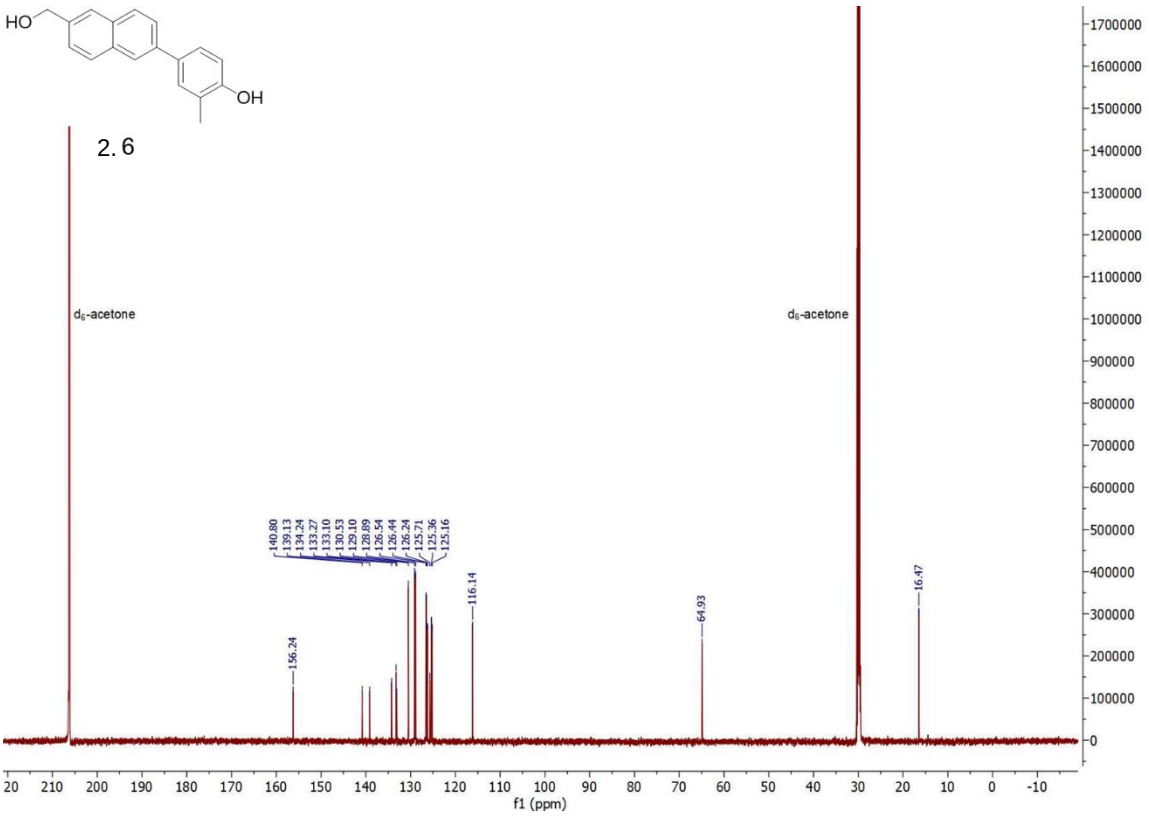
HO
OH
2.6
d6-acetone
d6-acetone
140.80
139.13
134.24
133.27
133.10
130.53
129.10
128.89
126.54
126.44
126.24
125.71
125.36
125.16
116.14
156.24
64.93
16.47
f1 (ppm)

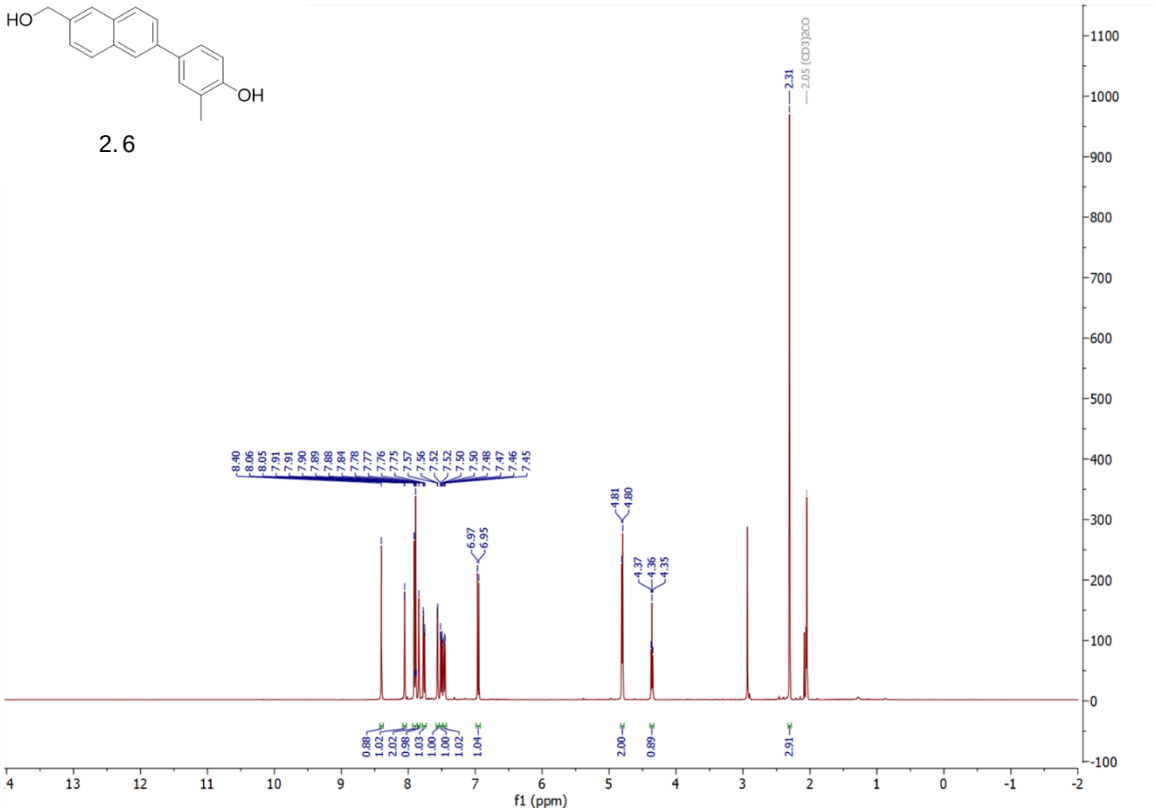
HO
OH
2.6
2.31
2.05 (CD3)2CO
8.40
8.06
8.05
7.91
7.91
7.90
7.89
7.88
7.84
7.78
7.77
7.76
7.75
7.57
7.56
7.52
7.52
7.50
7.50
7.48
7.47
7.46
7.45
6.97
6.95
4.81
4.80
4.37
4.36
4.35
0.88
1.02
2.02
0.98
1.03
1.00
1.00
1.02
1.04
2.00
0.89
2.91
f1 (ppm)

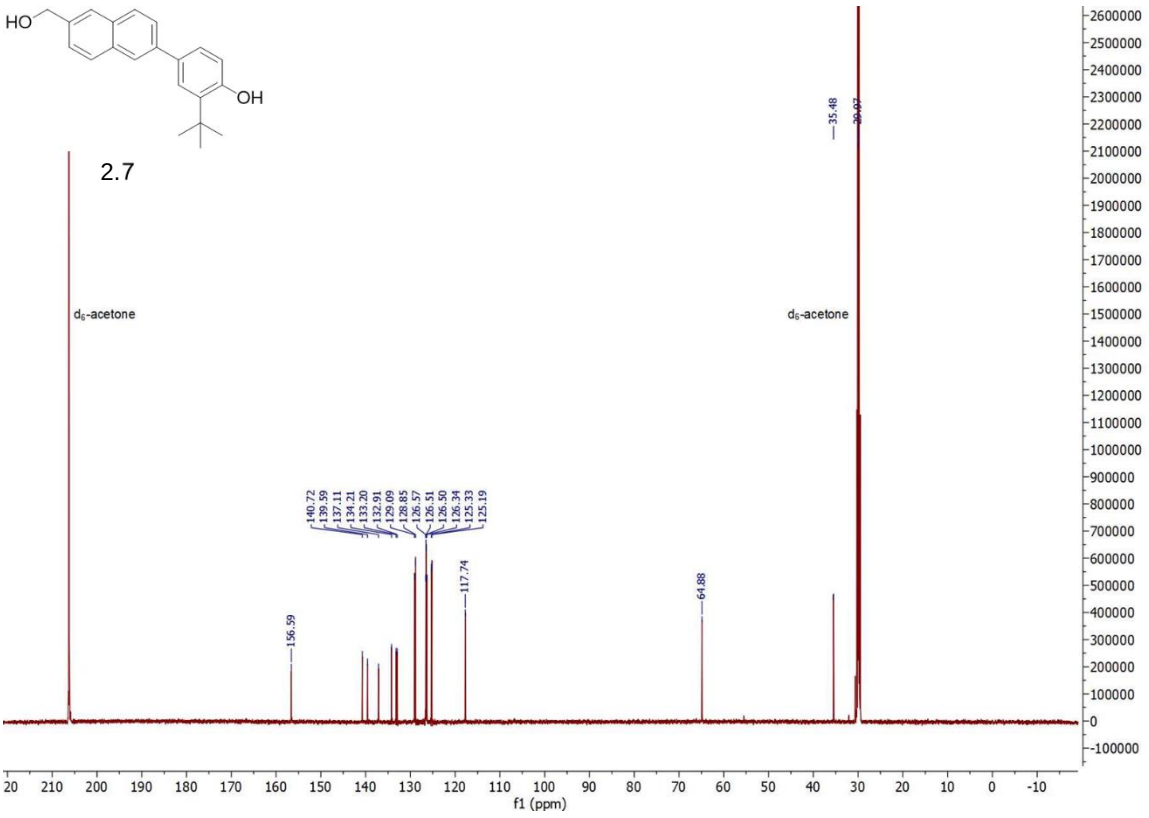
HO
OH
2.7
d6-acetone
d6-acetone
140.72
139.59
137.11
134.21
133.20
132.91
129.09
128.85
126.57
126.51
126.50
126.34
125.33
125.19
117.74
156.59
64.88
35.48
30.67
f1 (ppm)

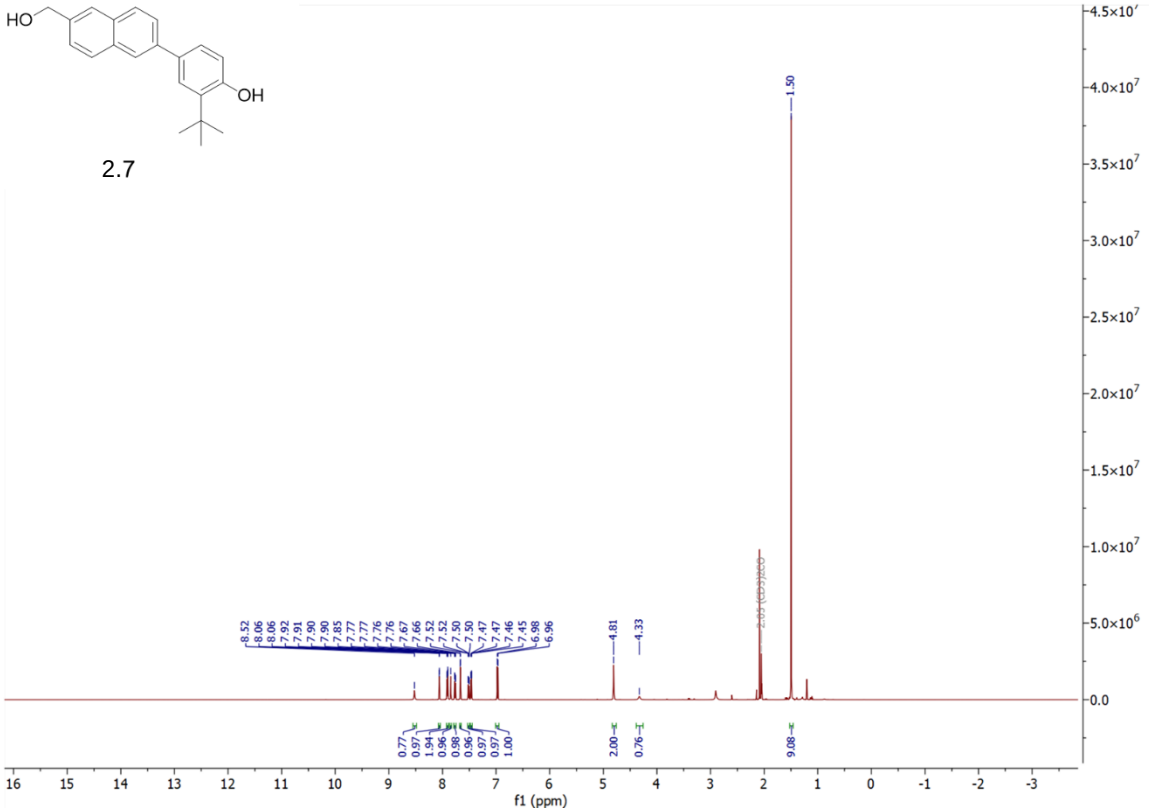
HO
OH
2.7
1.50
8.52
8.06
8.06
7.92
7.91
7.90
7.90
7.85
7.77
7.77
7.76
7.76
7.67
7.66
7.52
7.52
7.50
7.50
7.47
7.47
7.46
7.45
6.98
6.96
4.81
4.33
0.77
0.97
1.94
0.96
0.98
0.96
0.97
1.00
2.00
0.76
9.08
f1 (ppm)

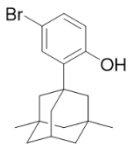
Br
OH

2.S7

51.09
46.61
43.21
38.86
38.77
31.56
30.99
30.07
130.37
129.48
77.16 CDCl3
118.44
113.35
153.61
138.31
f1 (ppm)

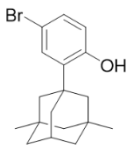
Br
OH

2.S7

2.18
2.18
2.17
2.16
2.15
2.14
2.14
1.90
1.90
1.74
1.71
1.66
1.62
1.44
1.41
1.38
1.35
1.20
1.19
0.87
7.30
7.29
7.28 CDCl3
7.16
7.16
7.14
7.13
6.54
6.52
4.79
1.00
0.74
0.93
0.85
0.97
2.05
4.20
4.17
2.03
6.13
f1 (ppm)

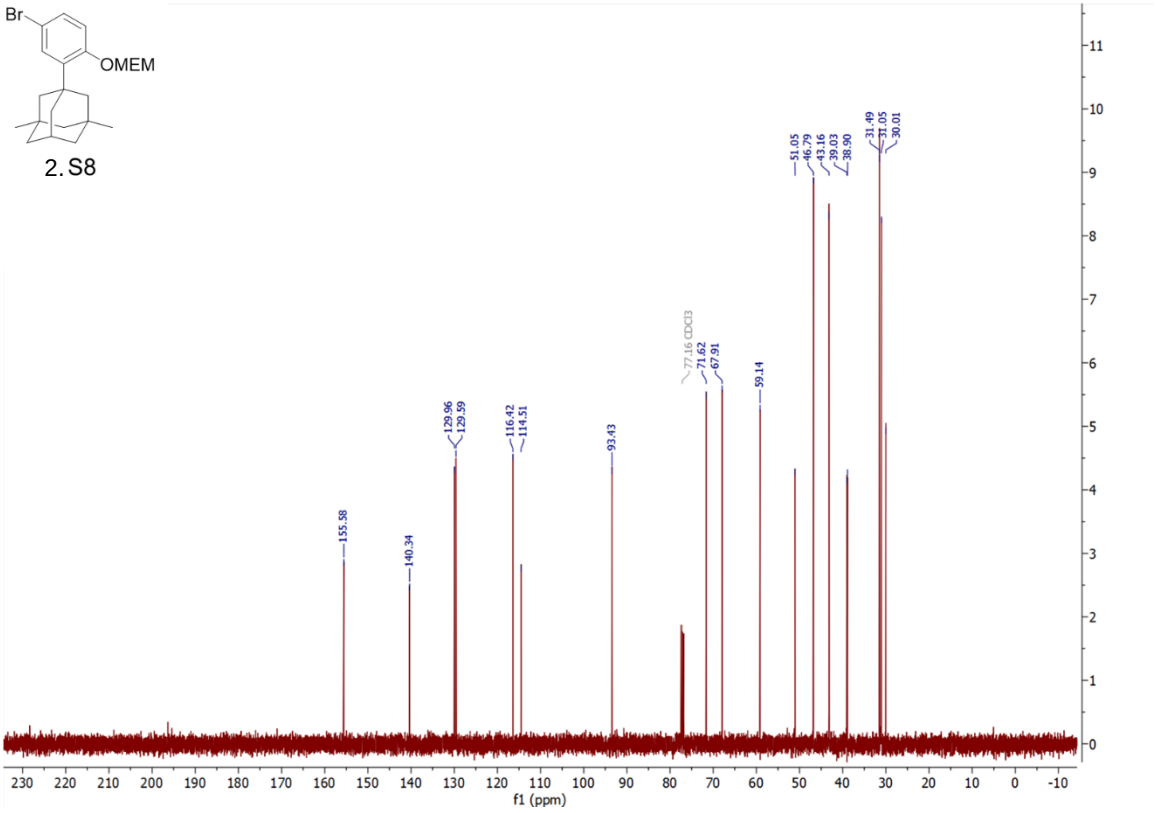
Br
OMEM
2. S8
155.58
140.34
129.96
129.59
116.42
114.51
93.43
77.16 CDCl3
71.62
67.91
59.14
51.05
46.79
43.16
39.03
38.90
31.49
31.05
30.01
f1 (ppm)

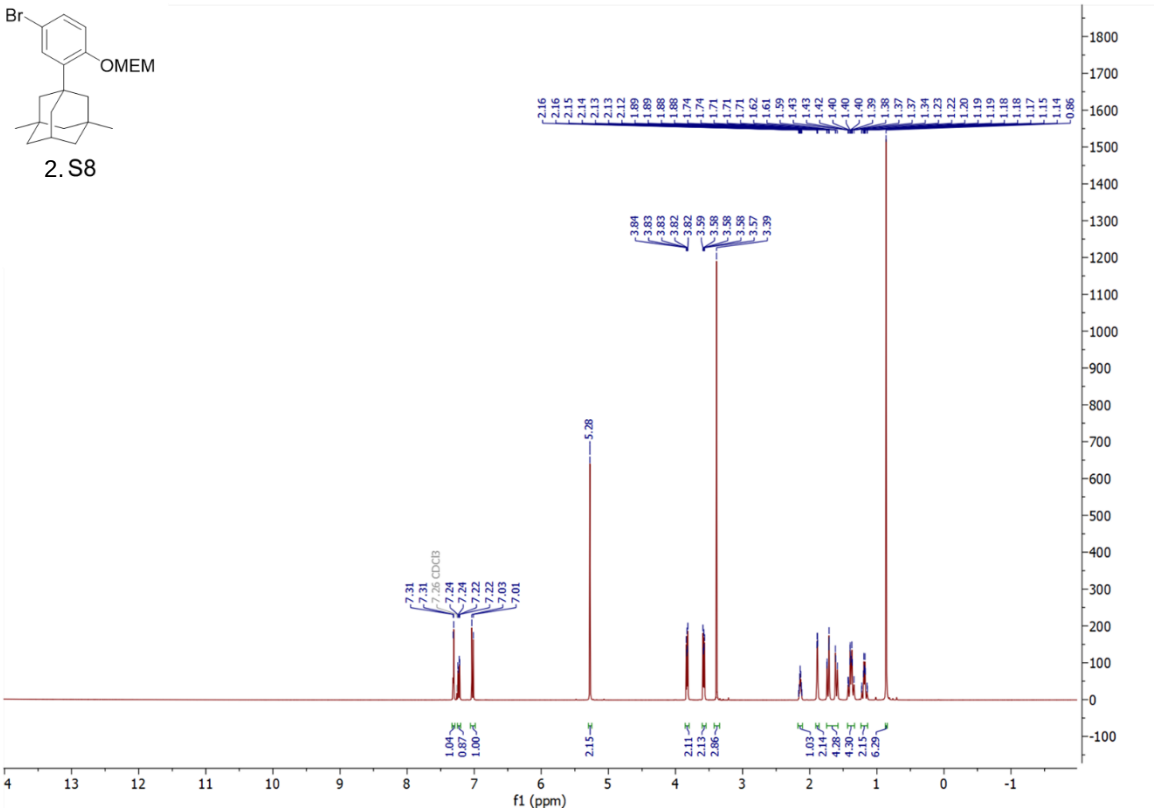
Br
OMEM
2. S8
7.31
7.26 CDCl3
7.24
7.22
7.03
7.01
5.28
3.84
3.83
3.82
3.59
3.58
3.57
3.39
2.16
1.89
1.88
1.74
1.71
1.62
1.61
1.43
1.42
1.40
1.39
1.38
1.37
1.34
1.23
1.22
1.20
1.19
1.18
1.17
1.15
1.14
0.86
1.04
0.87
1.00
2.15
2.11
2.13
2.86
1.03
2.14
4.28
4.30
2.15
6.29
f1 (ppm)

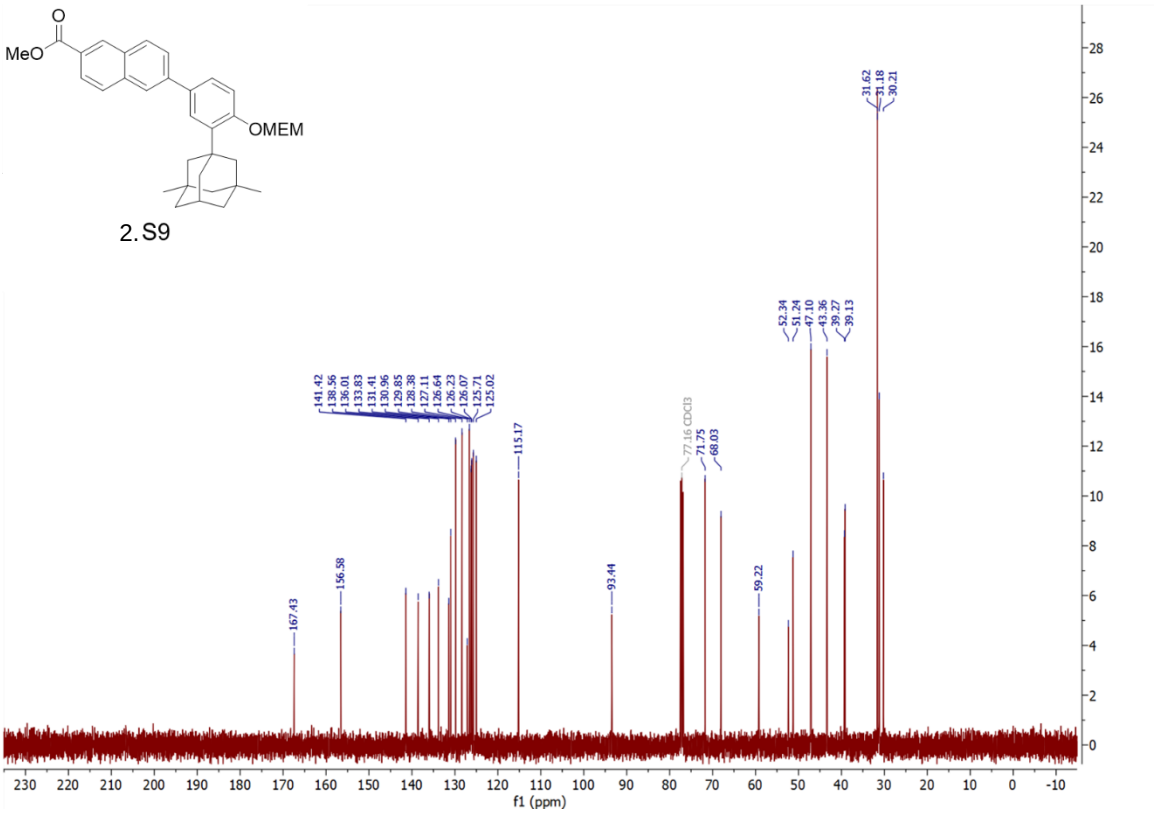
MeO
O
OMEM
2. S9
f1 (ppm)

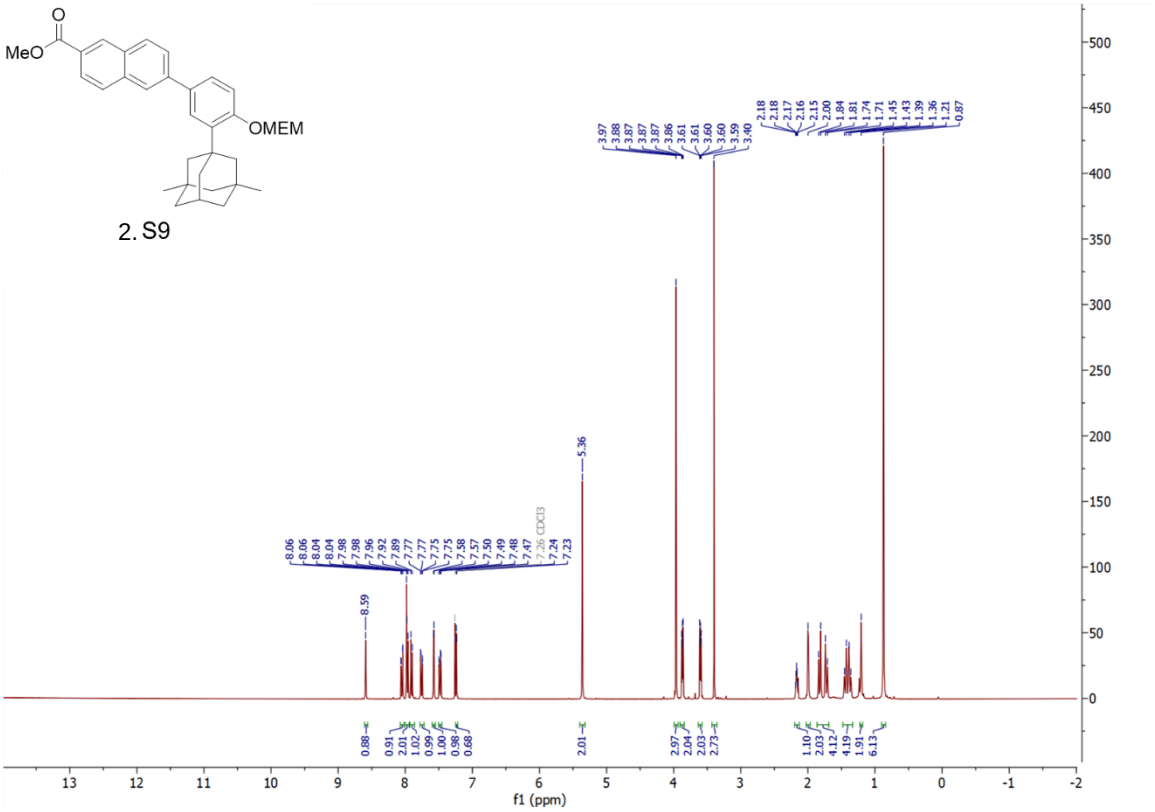
MeO
O
OMEM
2. S9
f1 (ppm)

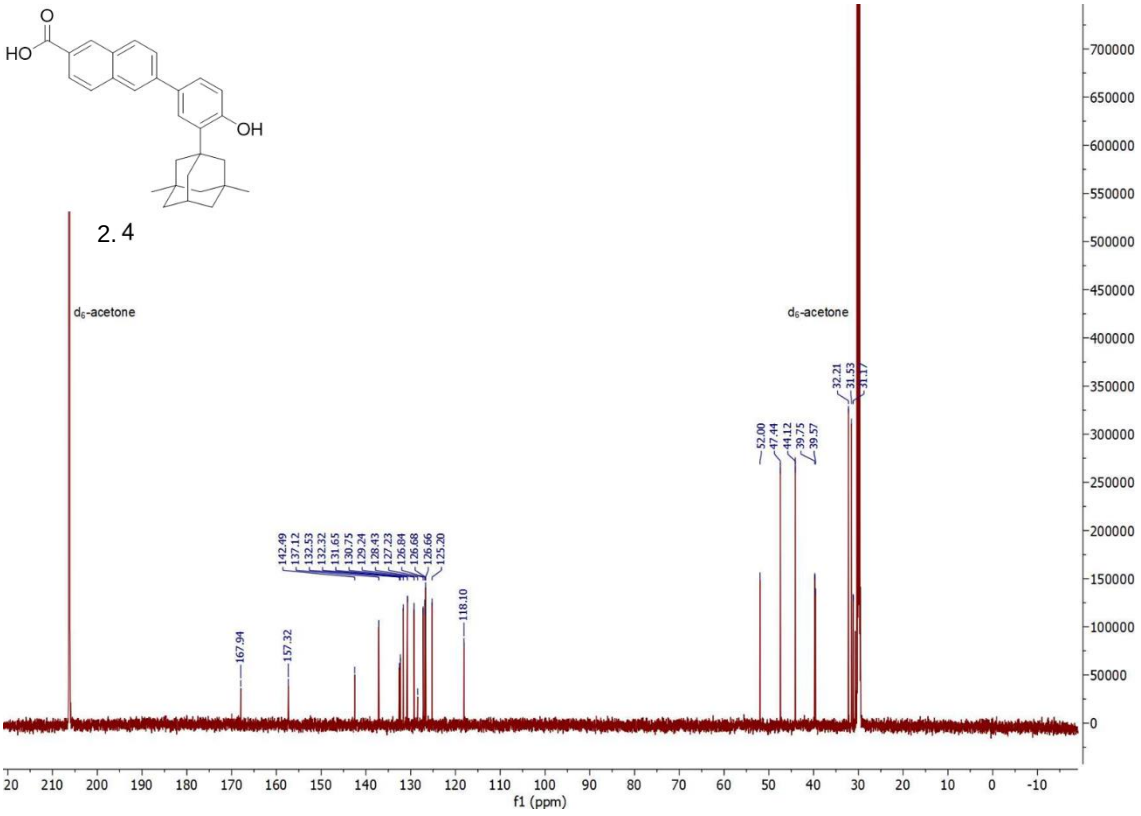
HO
O
OH
2.4
d6-acetone
d6-acetone
167.94
157.32
142.49
137.12
132.53
132.32
131.65
130.75
129.24
128.43
127.23
126.84
126.68
126.66
125.20
118.10
52.00
47.44
44.12
39.75
39.57
32.21
31.53
31.17
f1 (ppm)

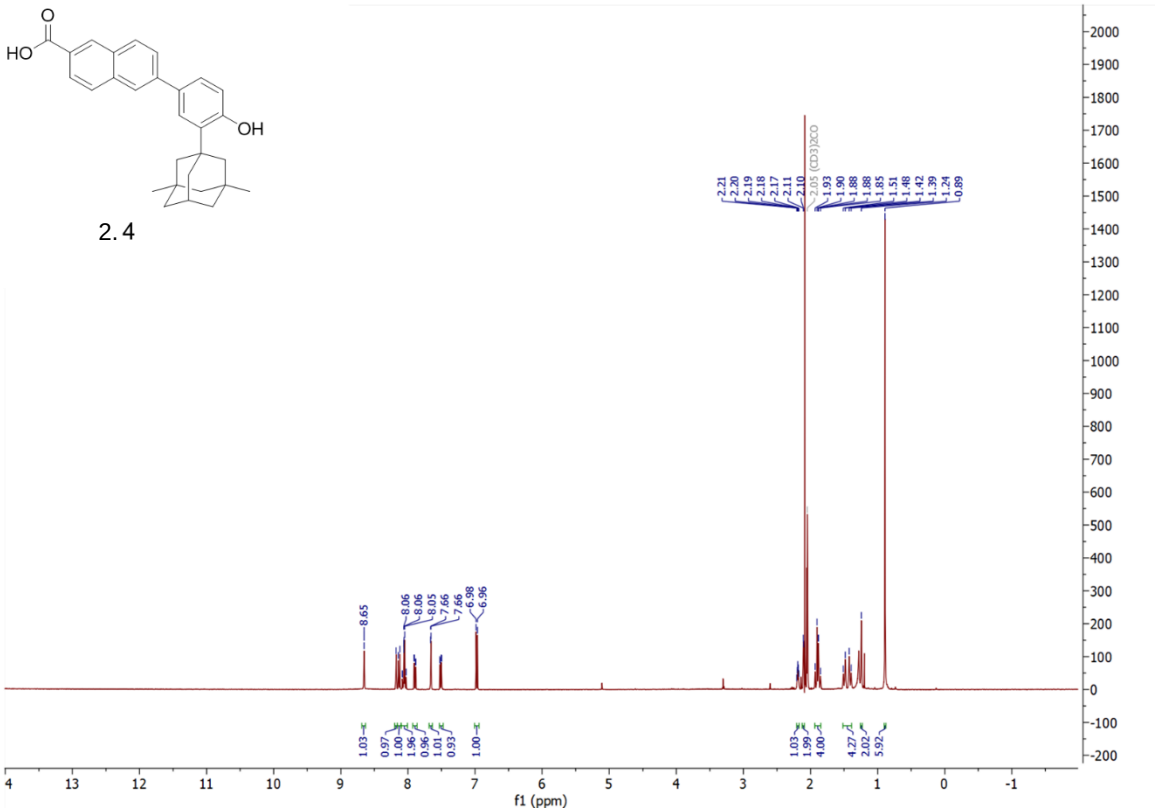
HO
O
OH
2.4
8.65
8.06
8.06
8.05
7.66
7.66
6.98
6.96
2.21
2.20
2.19
2.18
2.17
2.11
2.10
2.05 (CD3)2CO
1.93
1.90
1.88
1.88
1.85
1.51
1.48
1.42
1.39
1.24
0.89
f1 (ppm)

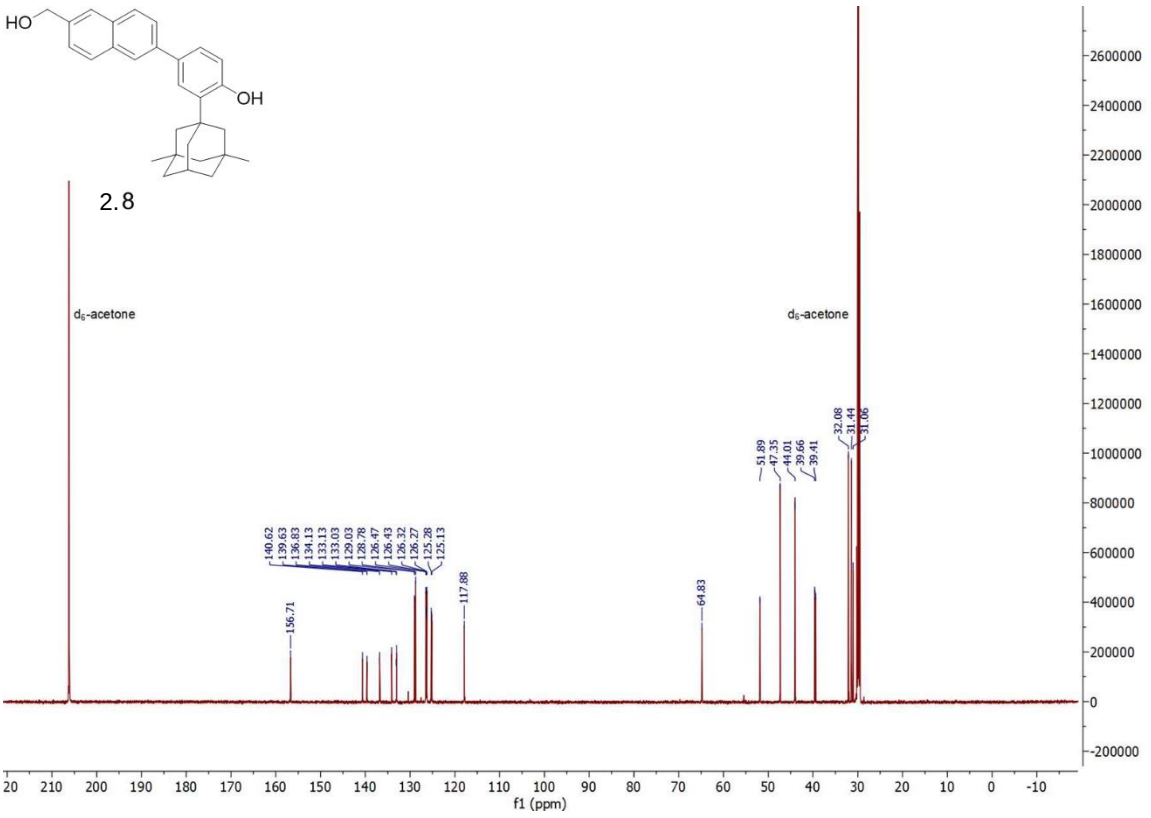
HO
OH
2.8
d6-acetone
d6-acetone
140.62
139.63
136.83
134.13
133.13
133.03
129.03
128.78
126.47
126.43
126.32
126.27
125.28
125.13
117.88
156.71
64.83
51.89
47.35
44.01
39.66
39.41
32.08
31.44
31.06
f1 (ppm)

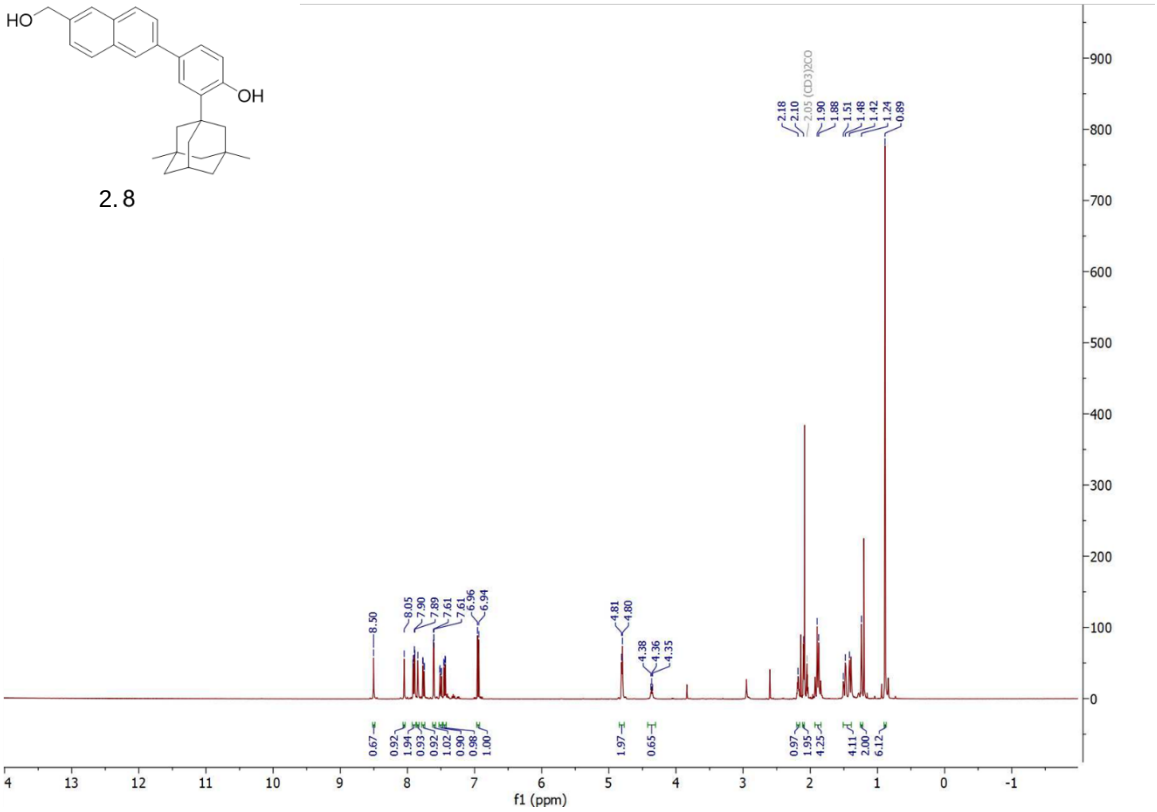
HO
OH
2.8
2.18
2.10
2.09 (CD3)2CO
1.90
1.88
1.51
1.48
1.42
1.24
0.89
8.50
8.05
7.90
7.89
7.61
7.61
6.96
6.94
4.81
4.80
4.38
4.36
4.35
0.67
0.92
1.94
0.93
0.92
1.02
0.90
0.98
1.00
1.97
0.65
0.97
1.95
4.25
4.11
2.00
6.12
f1 (ppm)

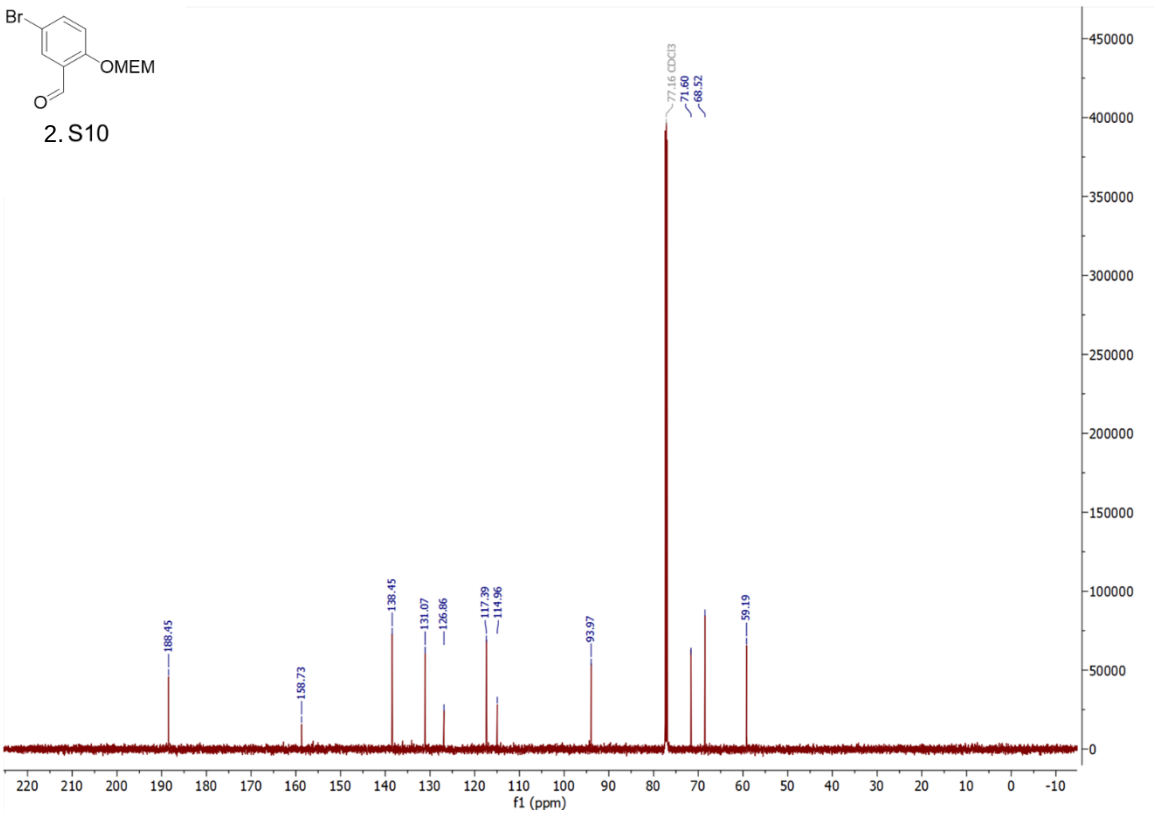
Br
OMEM
O
2. S10
77.16 CDCl3
71.60
68.52
188.45
158.73
138.45
131.07
126.86
117.39
114.96
93.97
59.19
f1 (ppm)

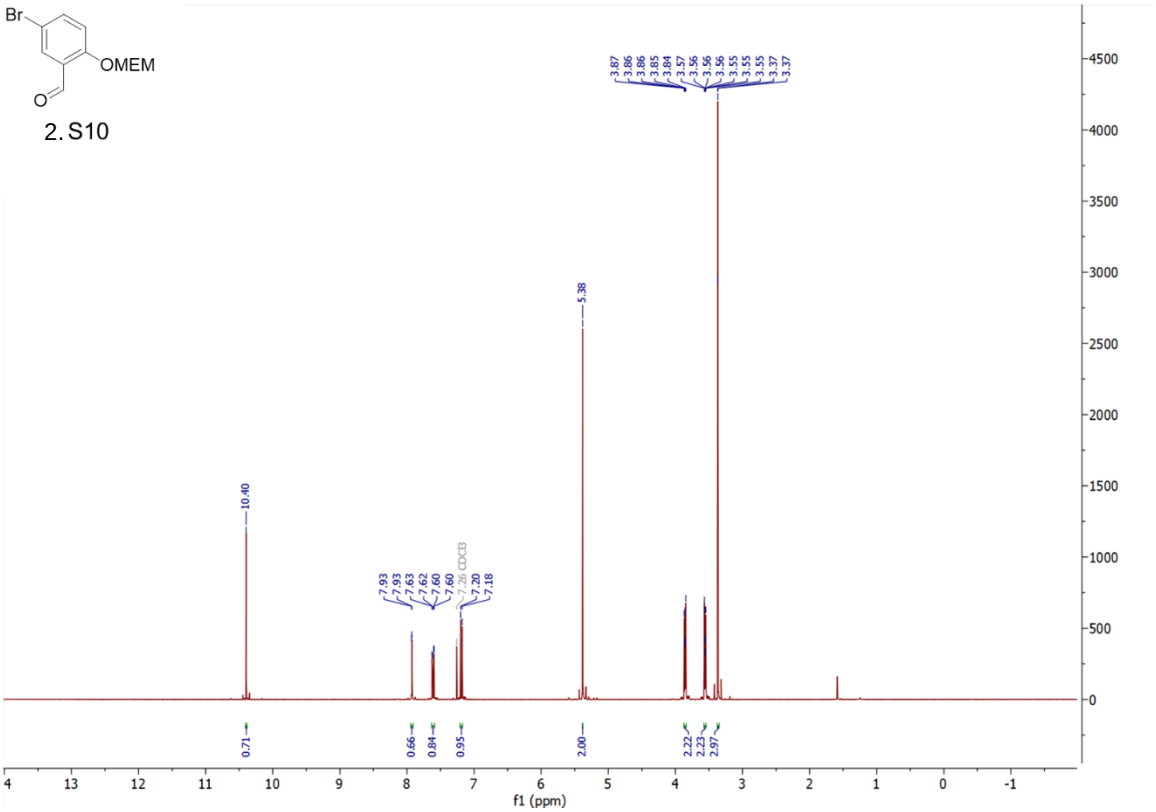
Br
OMEM
O
2. S10
3.87
3.86
3.86
3.85
3.84
3.57
3.56
3.56
3.56
3.55
3.55
3.55
3.37
3.37
5.38
10.40
7.93
7.93
7.63
7.62
7.60
7.60
7.26 CDCl3
7.20
7.18
0.71
0.66
0.84
0.95
2.00
2.22
2.23
2.97
f1 (ppm)

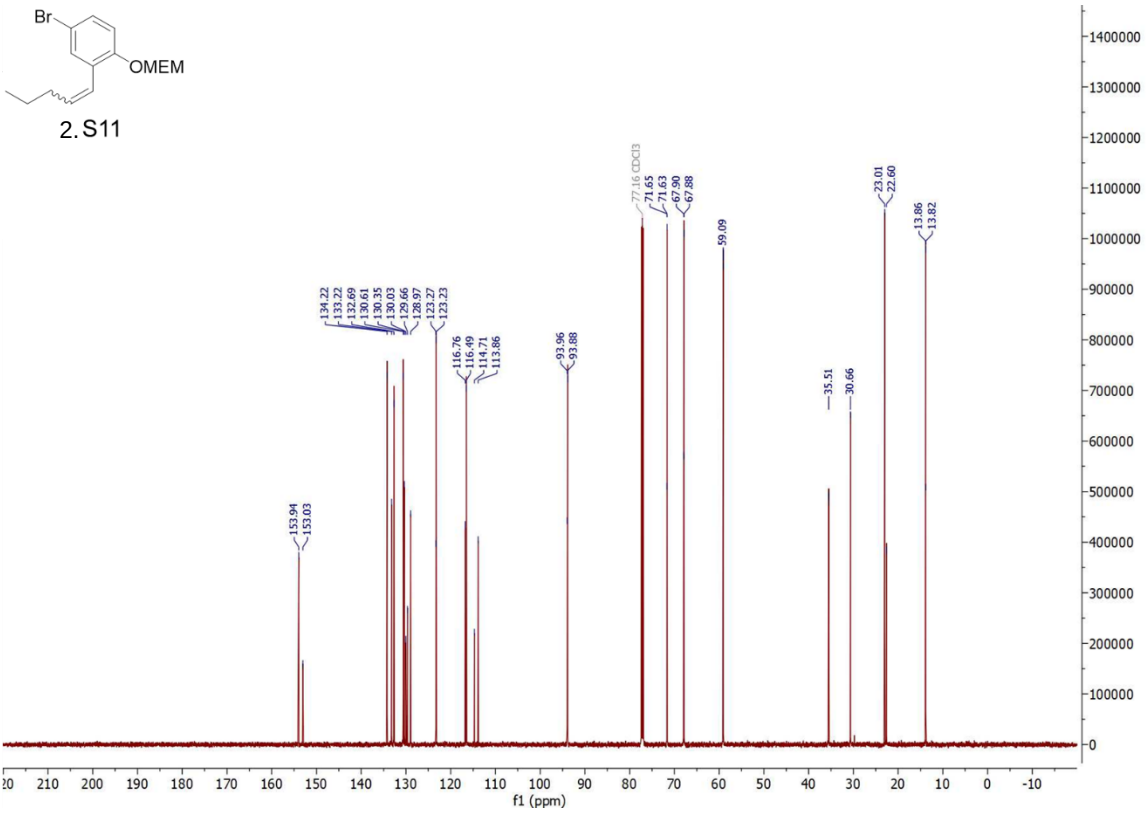
Br
OMEM
2.S11
153.94
153.03
134.22
133.22
132.69
130.61
130.35
130.03
129.66
128.97
123.27
123.23
116.76
116.49
114.71
113.86
93.96
93.88
77.16 CDCl3
71.65
71.63
67.90
67.88
59.09
35.51
30.66
23.01
22.60
13.86
13.82
f1 (ppm)

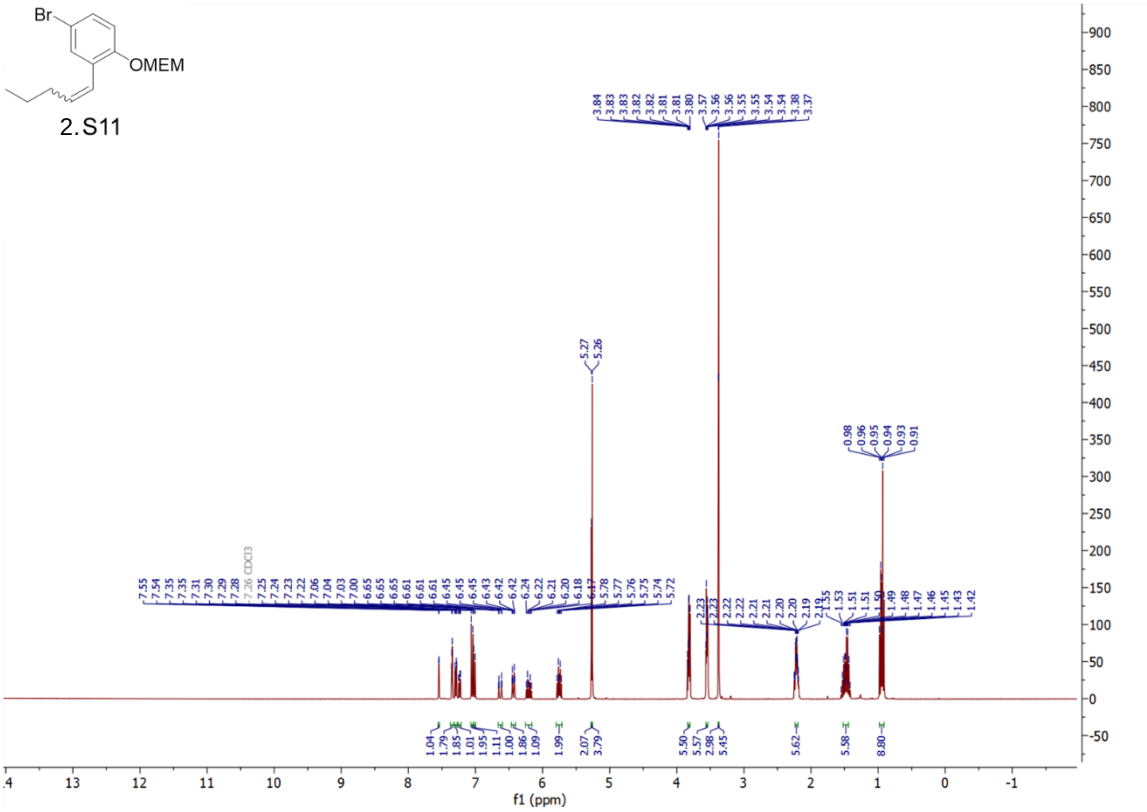
Br
OMEM
2.S11
7.26 CDCl3
5.27
5.26
f1 (ppm)

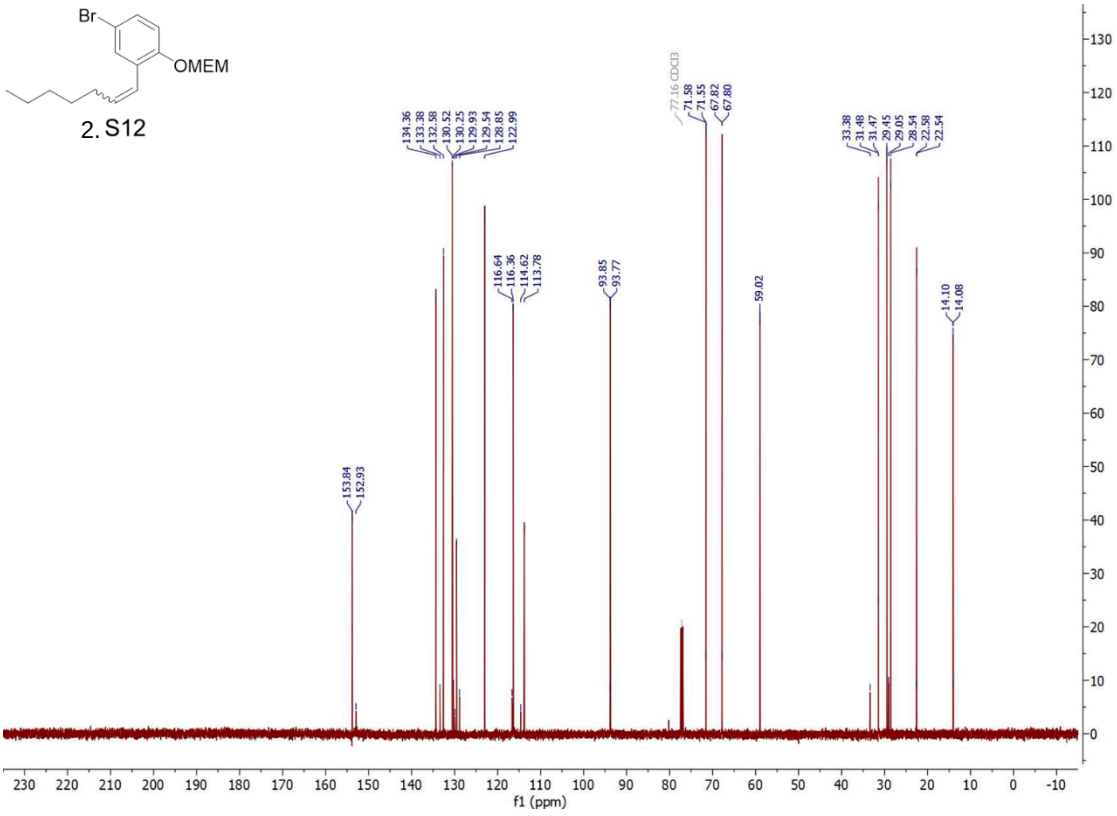
Br
OMEM
2. S12
134.36
133.38
132.58
130.52
130.25
129.93
129.54
128.85
122.99
77.16 CDCl3
71.58
71.55
67.82
67.80
33.38
31.48
31.47
29.45
29.05
28.54
22.58
22.54
116.64
116.56
114.62
113.78
93.85
93.77
59.02
14.10
14.08
153.84
152.93
f1 (ppm)

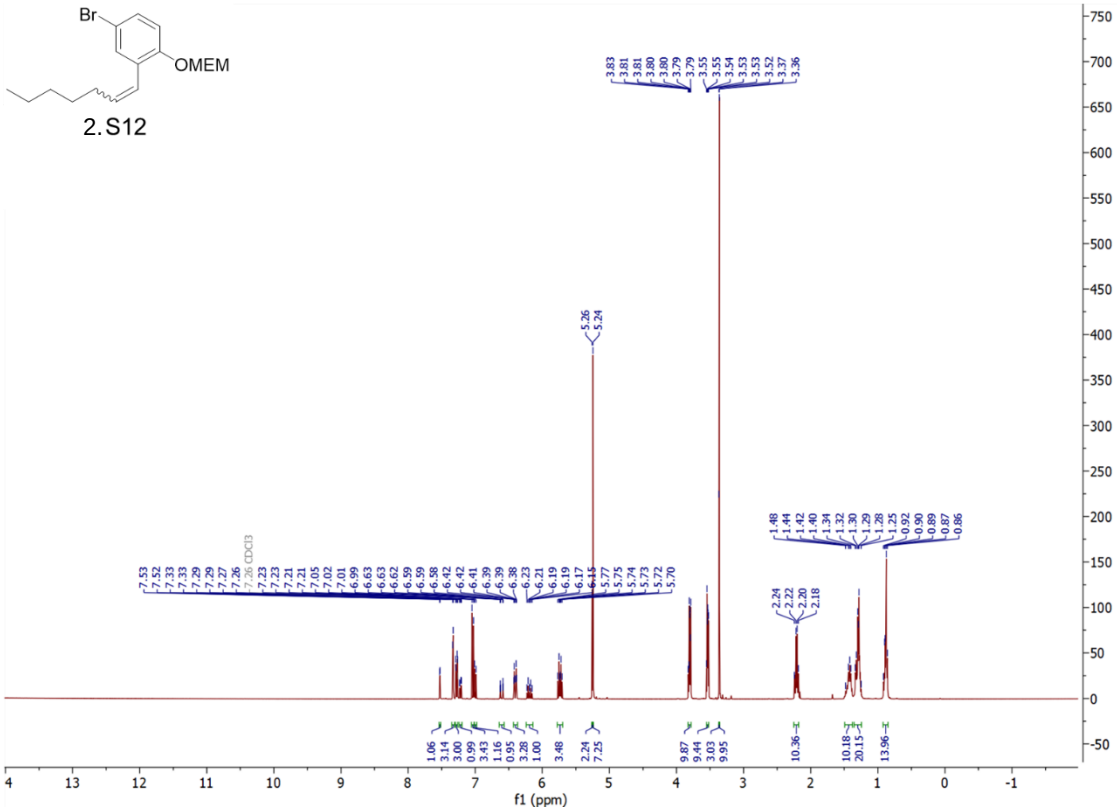
Br
OMEM
2. S12
3.83
3.81
3.81
3.81
3.80
3.80
3.79
3.79
3.55
3.55
3.54
3.53
3.53
3.52
3.37
3.36
5.26
5.24
7.53
7.52
7.33
7.33
7.29
7.29
7.27
7.26
7.26 CDCl3
7.23
7.23
7.21
7.21
7.05
7.02
7.01
6.99
6.63
6.63
6.62
6.59
6.59
6.58
6.42
6.42
6.41
6.39
6.39
6.38
6.23
6.21
6.19
6.17
6.15
5.77
5.75
5.74
5.73
5.72
5.70
1.48
1.44
1.42
1.40
1.34
1.32
1.30
1.29
1.28
1.25
0.92
0.90
0.89
0.87
0.86
2.24
2.22
2.20
2.18
1.06
3.14
3.00
0.99
3.43
1.16
0.95
3.28
1.00
3.48
2.24
7.25
9.87
9.44
3.03
9.95
10.36
10.18
20.15
13.96
f1 (ppm)

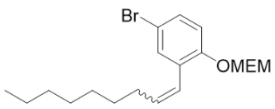
Br
OMEM

2. S13

77.16 CDCl3
71.70
71.67
67.92
134.53
133.58
132.72
130.64
130.37
130.09
129.69
129.01
123.07
116.79
116.51
114.75
113.91
153.97
153.06
94.00
93.92
59.15
31.94
29.87
29.48
29.34
29.31
29.27
28.67
22.79
22.76
14.21
f1 (ppm)

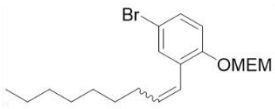
Br
OMEM

2. S13

3.83
3.81
3.80
3.79
3.55
3.54
3.53
3.52
3.37
3.36
5.26
5.24
7.53
7.52
7.33
7.29
7.27
7.26 CDCl3
7.23
7.21
7.05
7.02
7.01
6.99
6.63
6.62
6.59
6.58
6.42
6.41
6.39
6.38
6.23
6.21
6.19
6.17
6.15
5.77
5.75
5.74
5.73
5.72
5.70
1.45
1.43
1.41
1.40
1.38
1.33
1.32
1.31
1.30
1.29
1.28
1.27
1.26
1.25
0.89
0.88
0.87
0.86
0.85
2.24
2.23
2.22
2.21
2.20
2.19
2.18
1.12
6.35
5.99
1.11
6.77
1.29
1.03
6.55
1.00
7.02
2.41
14.02
17.00
16.54
3.13
18.94
18.43
18.29
68.39
24.62
f1 (ppm)

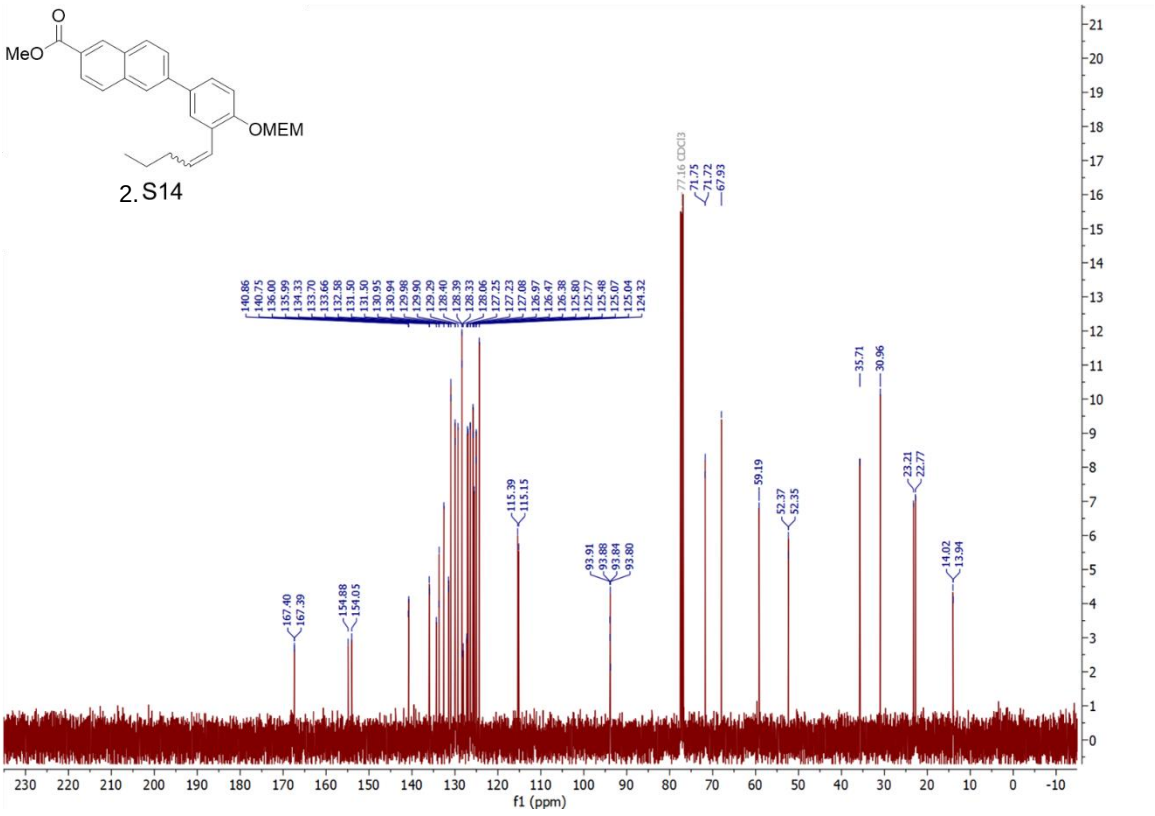
MeO
O
OMEM
2.S14
f1 (ppm)

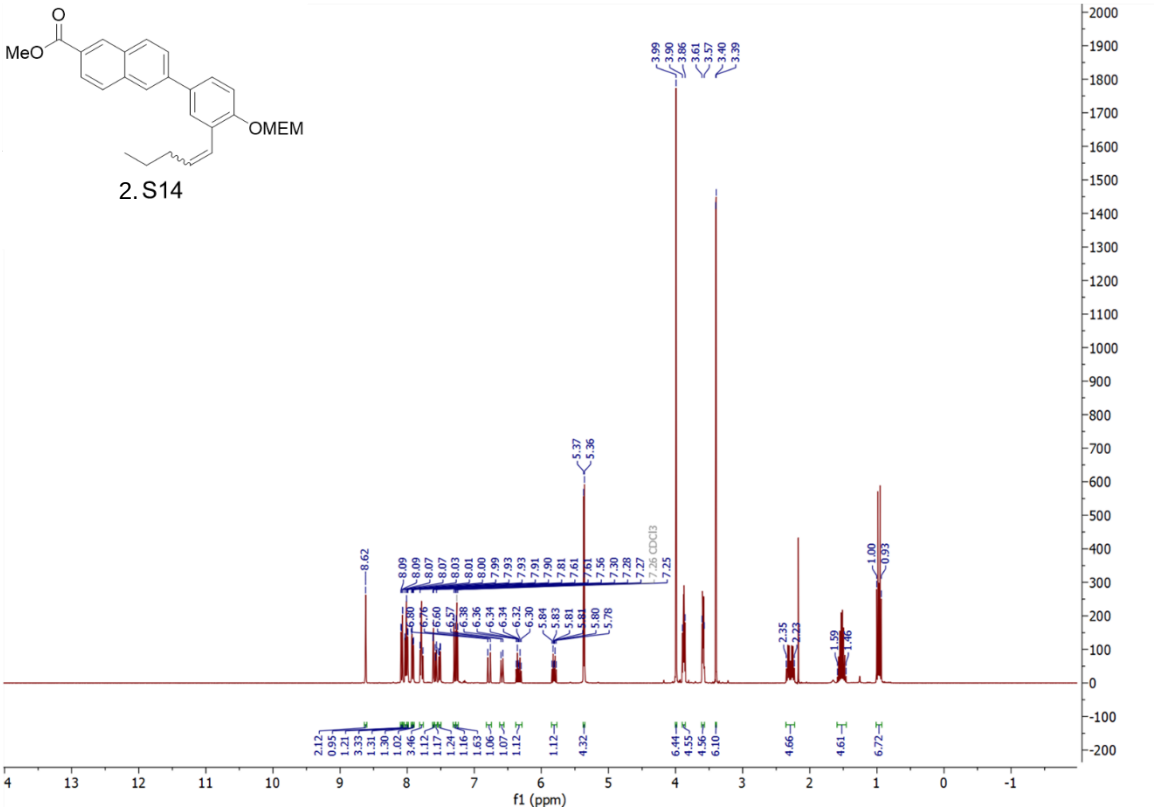
MeO
O
OMEM
2.S14
f1 (ppm)

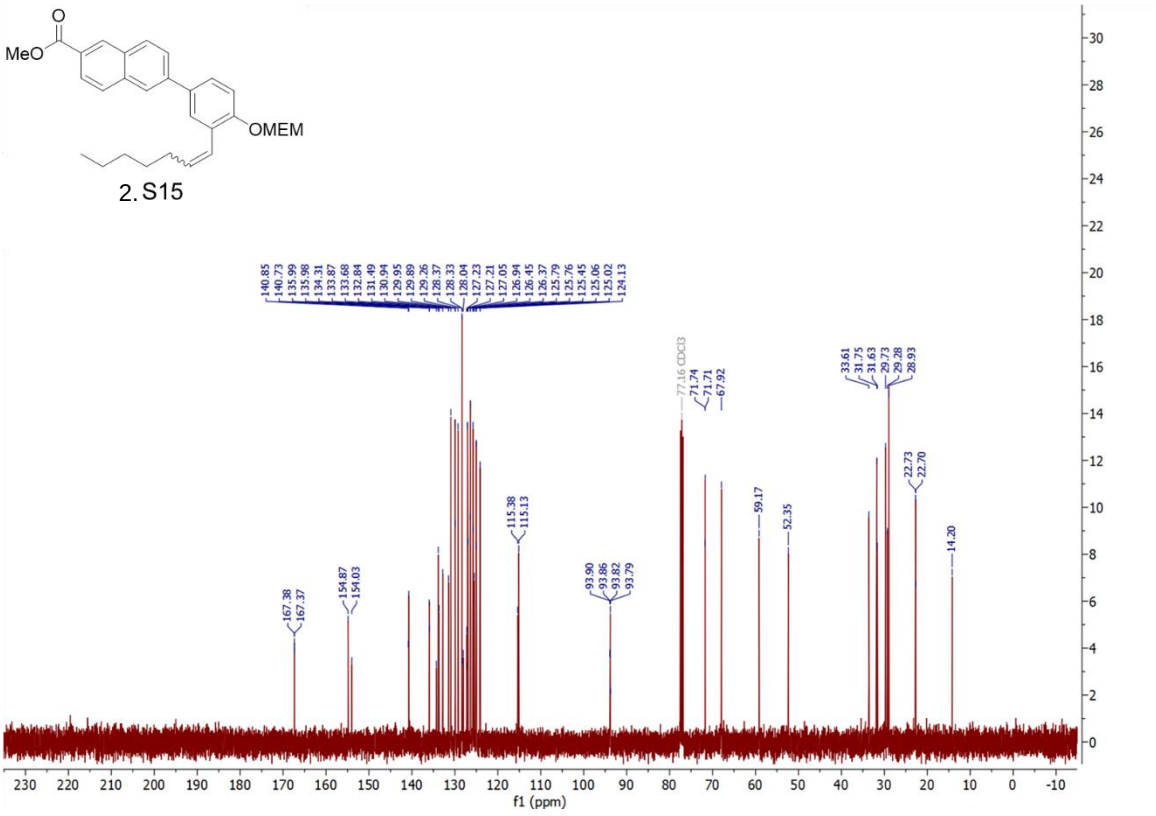
MeO
O
OMEM
2.S15
f1 (ppm)

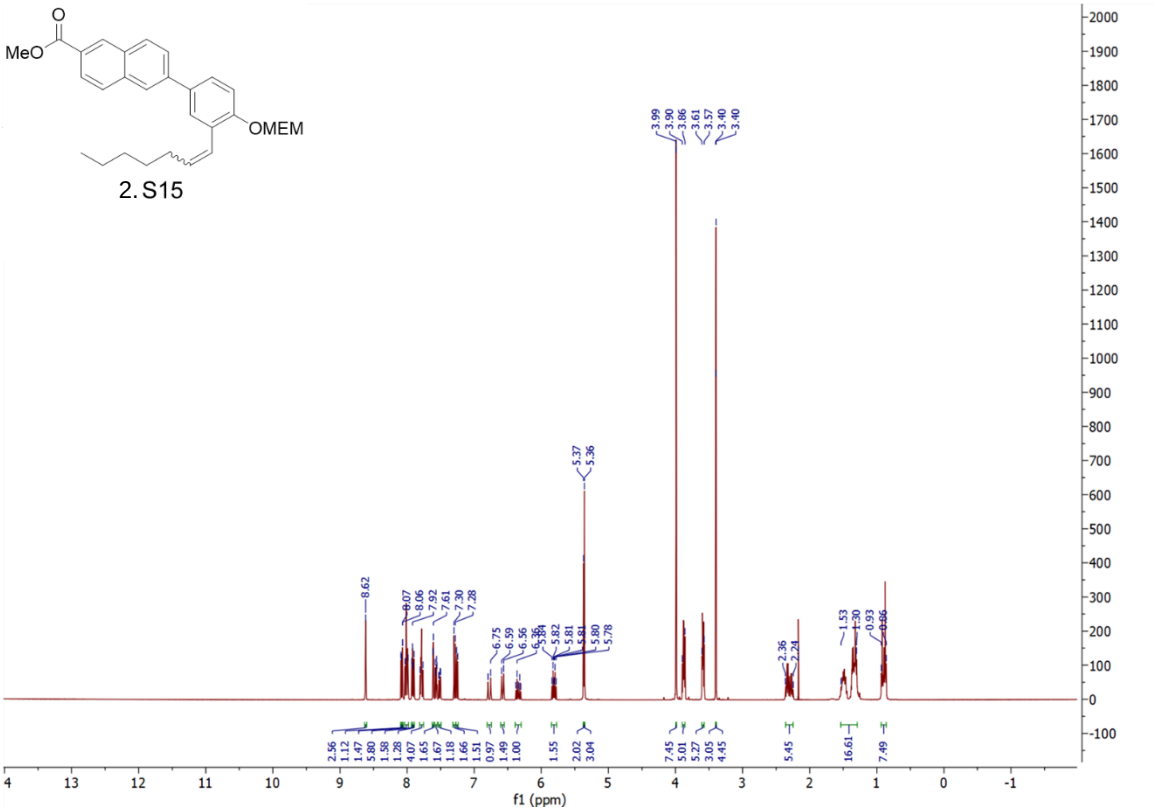
MeO
O
OMEM
2.S15
f1 (ppm)

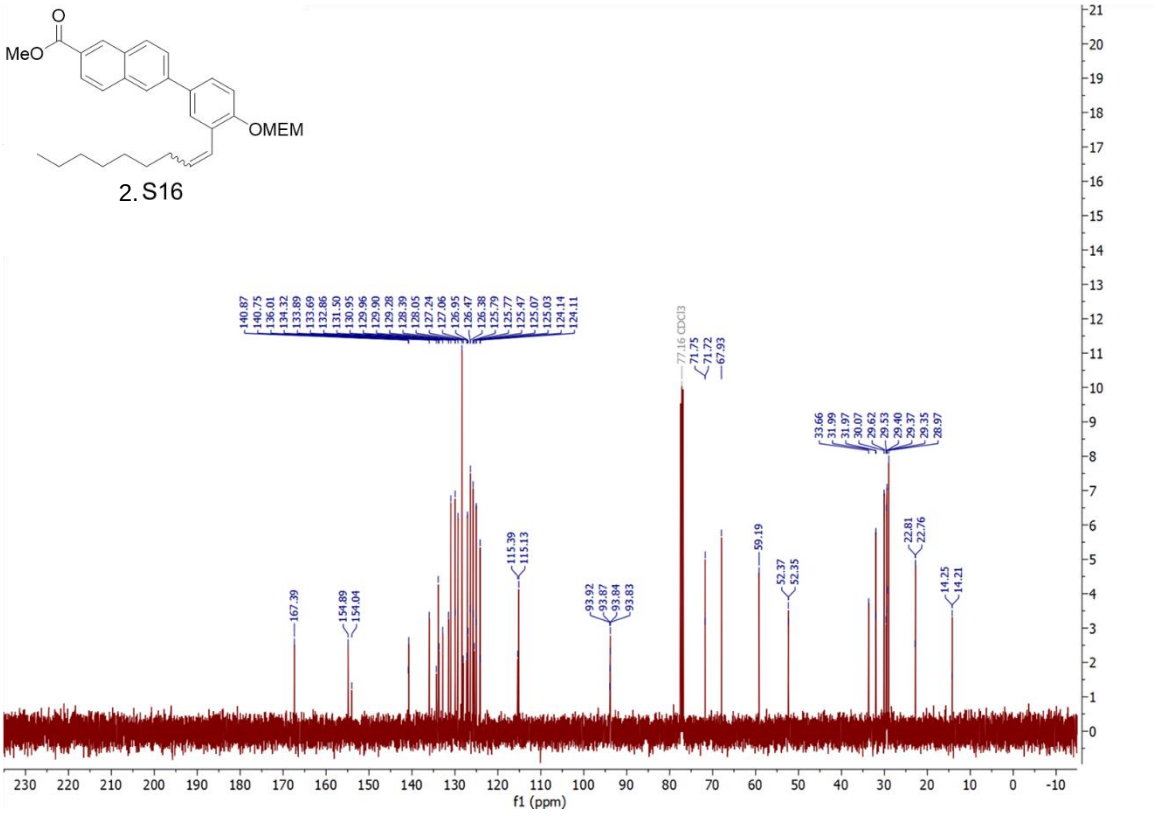
MeO
O
OMEM
2. S16
f1 (ppm)

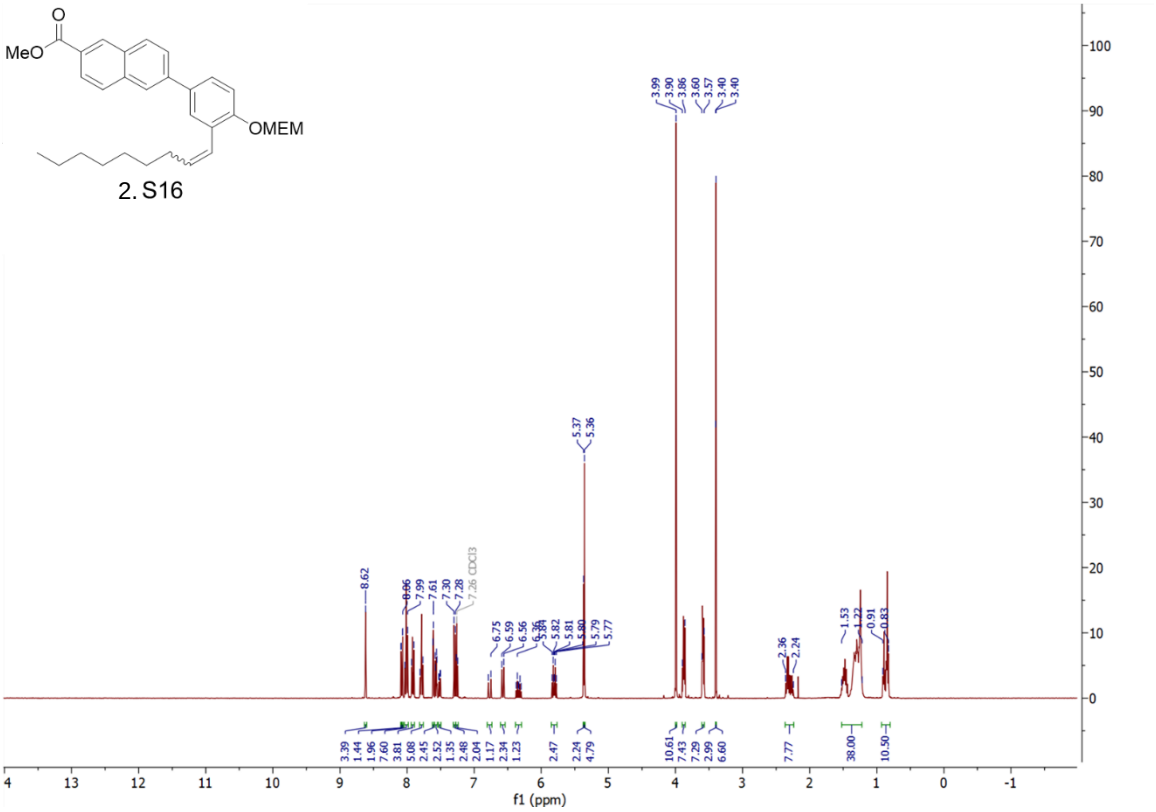
MeO
O
OMEM
2. S16
f1 (ppm)

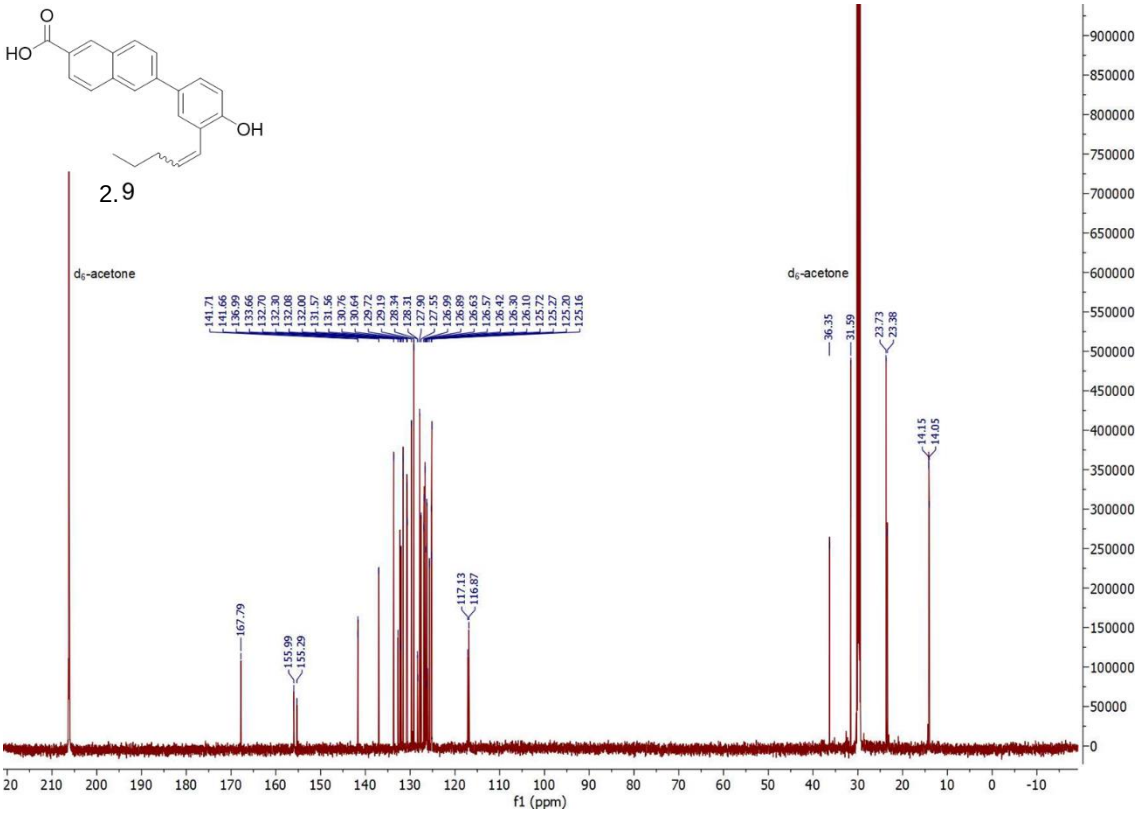
HO
O
OH
2.9
d6-acetone
d6-acetone
141.71
141.66
136.99
133.66
132.70
132.30
132.08
132.00
131.77
131.56
130.76
130.64
129.72
129.19
128.34
128.31
127.90
127.55
126.99
126.89
126.63
126.57
126.42
126.30
126.10
125.72
125.57
125.20
125.16
167.79
155.99
155.29
117.13
116.87
36.35
31.59
23.73
23.38
14.15
14.05
f1 (ppm)

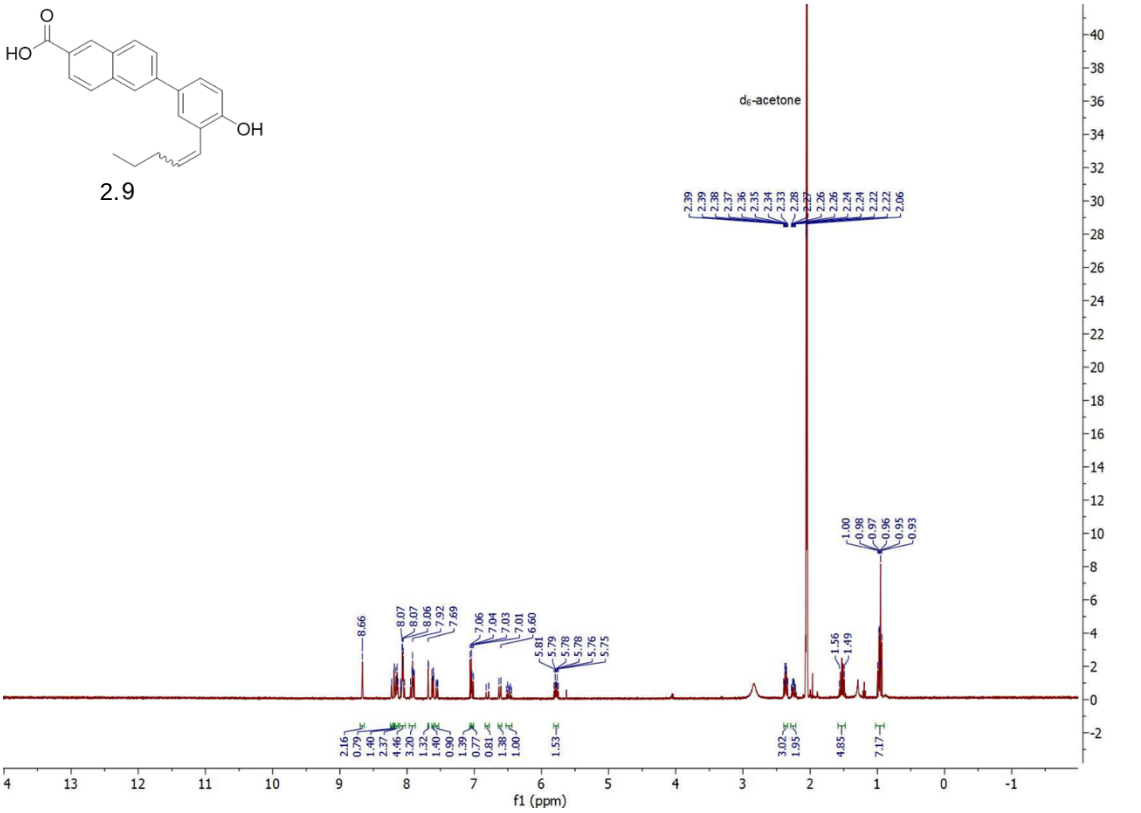
HO
O
OH
2.9
d6-acetone
8.66
8.07
8.07
8.06
7.92
7.69
7.06
7.04
7.03
7.01
6.60
5.81
5.79
5.78
5.76
5.75
2.39
2.39
2.38
2.37
2.36
2.35
2.34
2.33
2.28
2.26
2.26
2.24
2.24
2.22
2.22
2.06
1.56
1.49
1.00
0.98
0.97
0.96
0.95
0.93
2.16
0.79
1.49
2.37
4.46
3.20
1.32
1.40
0.90
1.39
0.77
0.81
1.38
1.00
1.53
3.02
1.95
4.85
7.17
f1 (ppm)

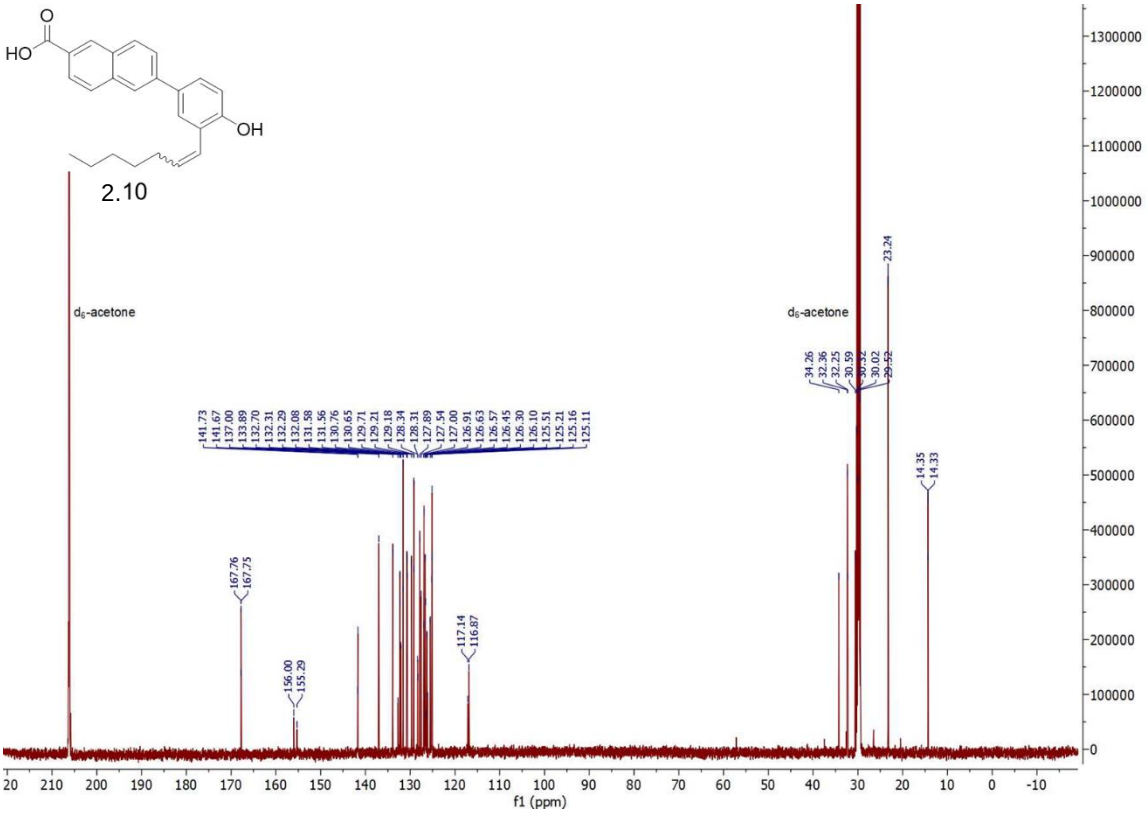
HO
O
OH
2.10
d6-acetone
d6-acetone
141.73
141.67
137.00
133.89
132.70
132.31
132.29
132.08
131.58
131.56
130.76
130.65
129.71
129.21
129.18
128.34
128.31
127.89
127.54
127.06
126.91
126.63
126.57
126.45
126.30
126.10
125.51
125.21
125.16
125.11
167.76
167.75
156.00
155.29
117.14
116.87
34.26
32.36
32.25
30.59
30.52
30.02
29.92
23.24
14.35
14.33
f1 (ppm)

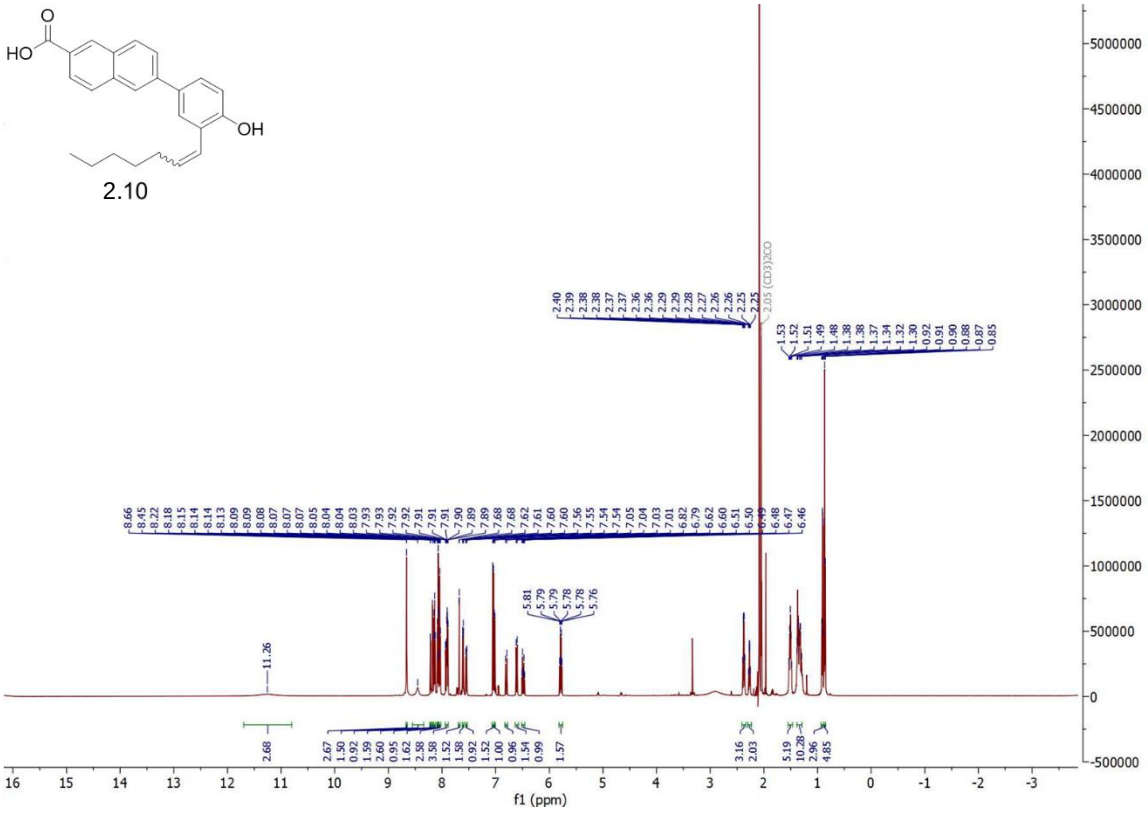
HO
O
OH
2.10
2.05 (CD3)2CO
11.26
f1 (ppm)

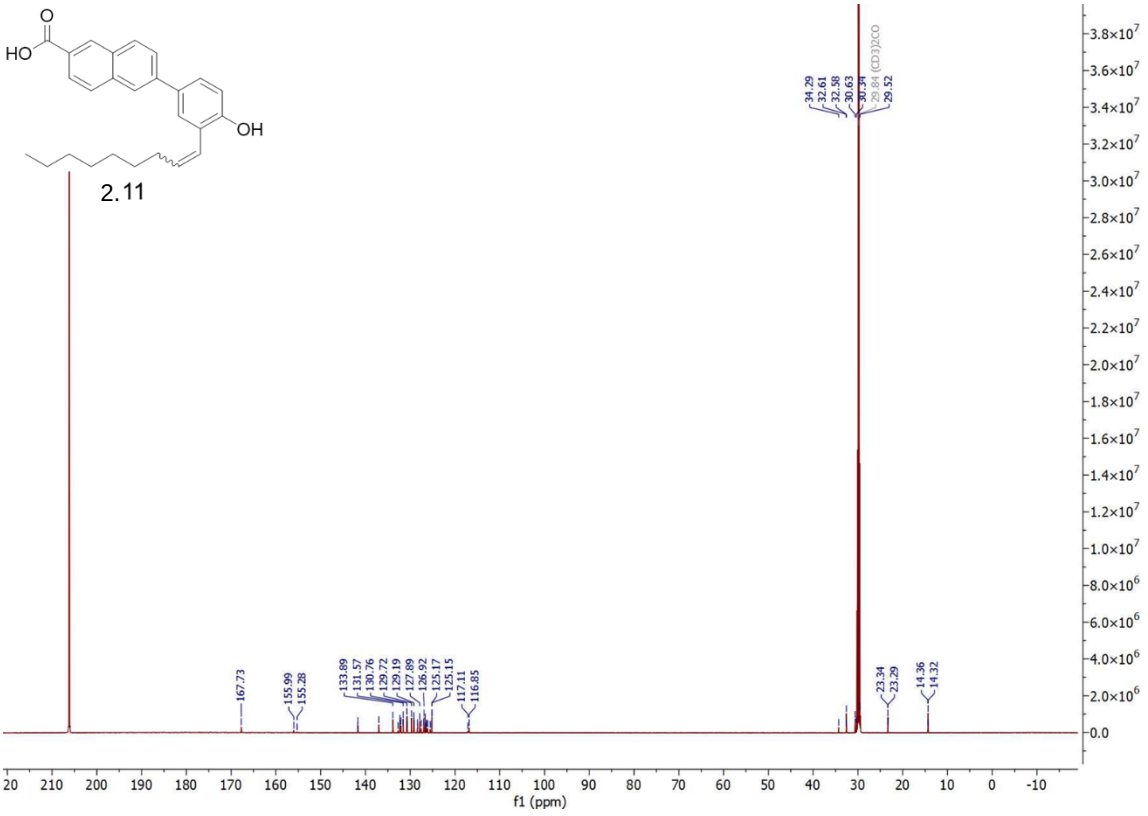
HO
O
OH
2.11
167.73
155.99
155.28
133.89
131.57
130.76
129.72
129.19
127.89
126.92
125.17
125.15
117.11
116.85
34.29
32.61
32.58
30.63
30.34
29.69
29.52
23.34
23.29
14.36
14.32
(CD3)2CO
f1 (ppm)

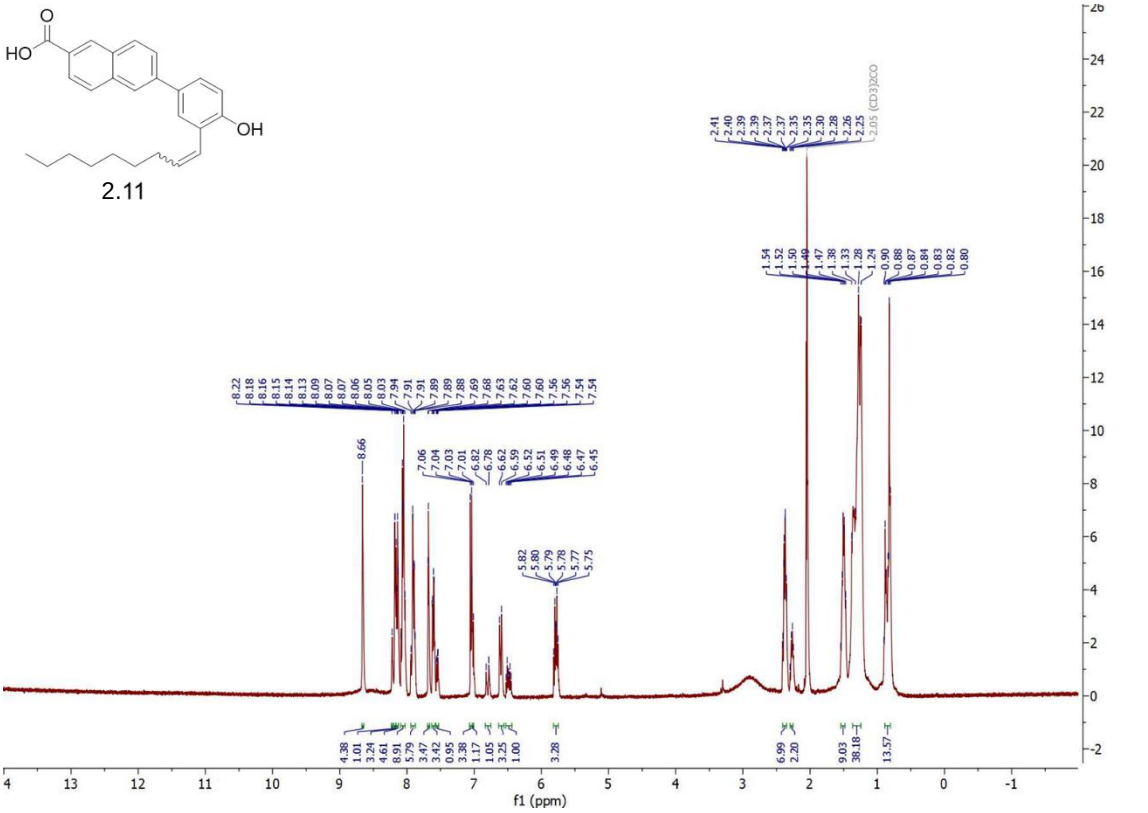
HO
O
OH
2.11
8.66
8.22
8.18
8.16
8.15
8.14
8.13
8.09
8.07
8.07
8.06
8.05
8.03
7.94
7.91
7.91
7.89
7.89
7.88
7.69
7.68
7.63
7.62
7.60
7.60
7.56
7.55
7.54
7.54
7.06
7.04
7.03
7.01
6.82
6.78
6.62
6.59
6.52
6.51
6.49
6.48
6.47
6.47
6.45
5.82
5.80
5.79
5.78
5.77
5.75
2.41
2.40
2.39
2.39
2.37
2.37
2.35
2.35
2.30
2.28
2.26
2.25
2.05
(CD3)2CO
1.54
1.52
1.50
1.49
1.47
1.38
1.33
1.28
1.24
0.90
0.88
0.87
0.84
0.83
0.82
0.80
4.38
1.01
3.24
4.61
8.91
5.79
3.47
3.42
0.95
3.38
1.17
1.05
3.25
1.00
3.28
6.99
2.20
9.03
38.18
13.57
f1 (ppm)

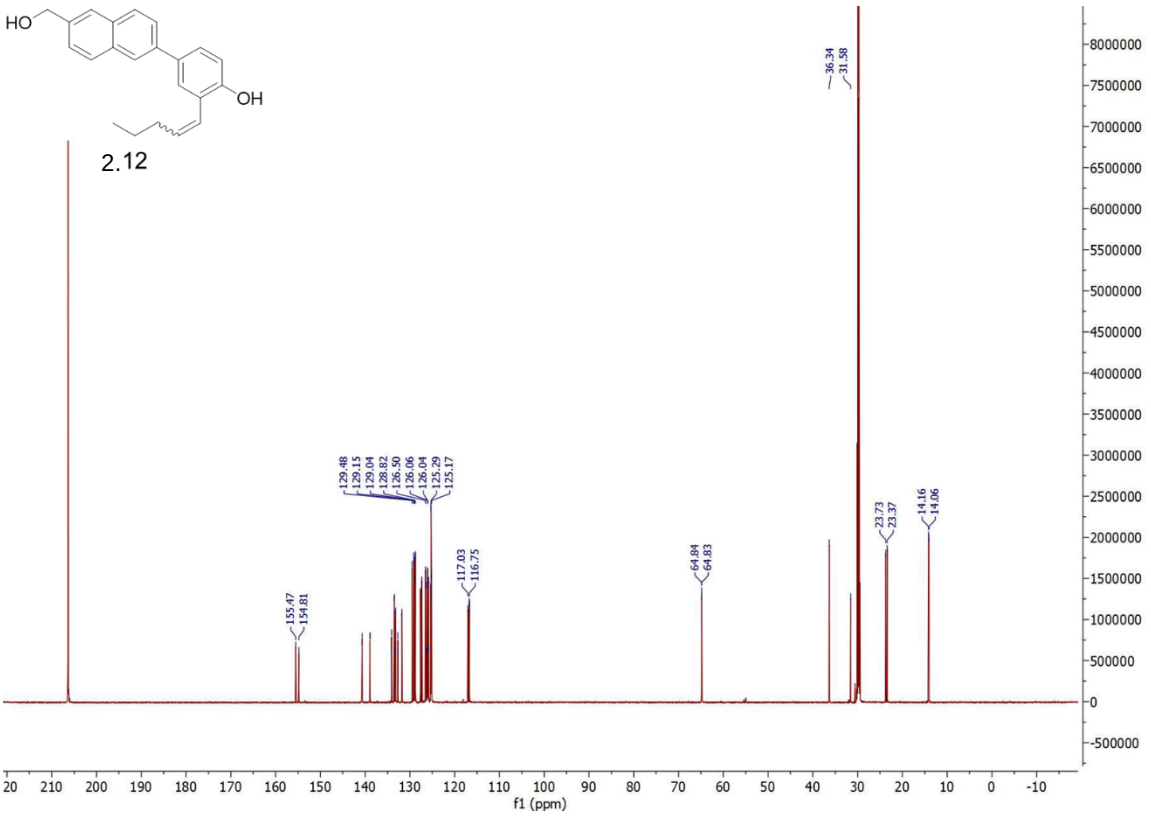
HO
OH
2.12
f1 (ppm)

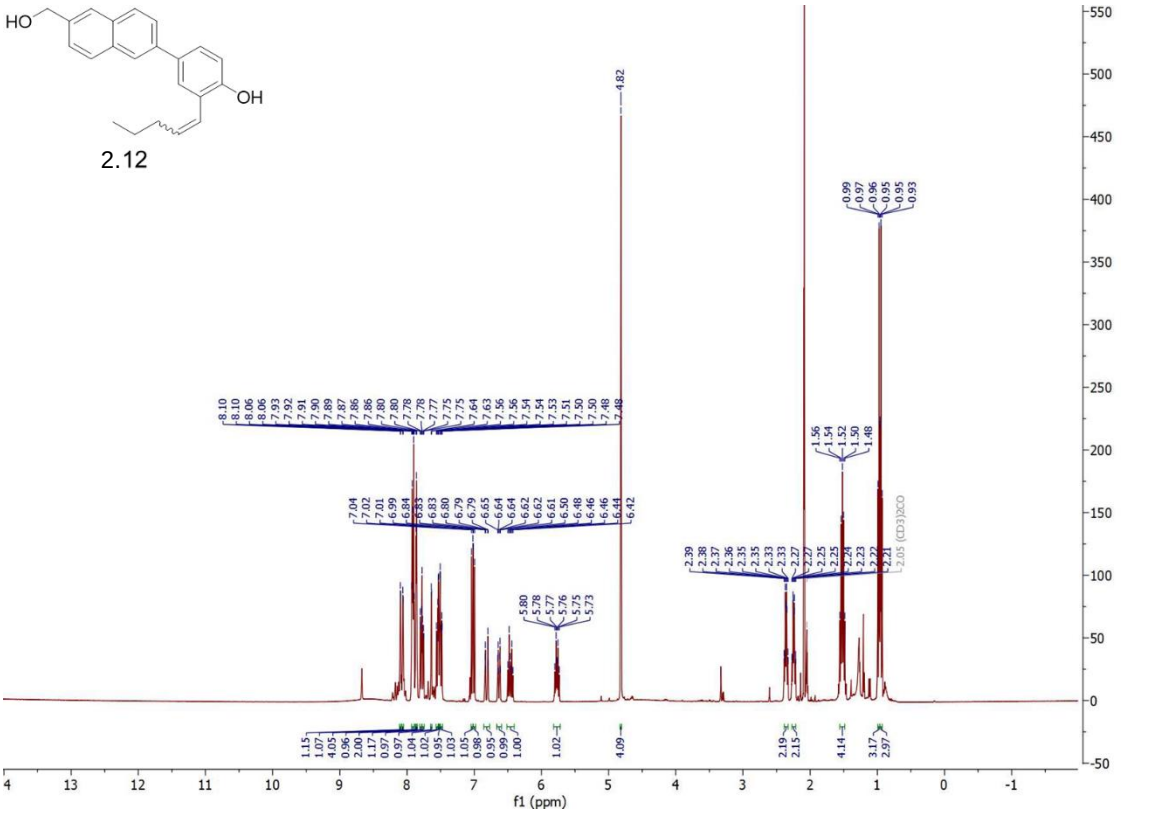
HO
OH
2.12
f1 (ppm)

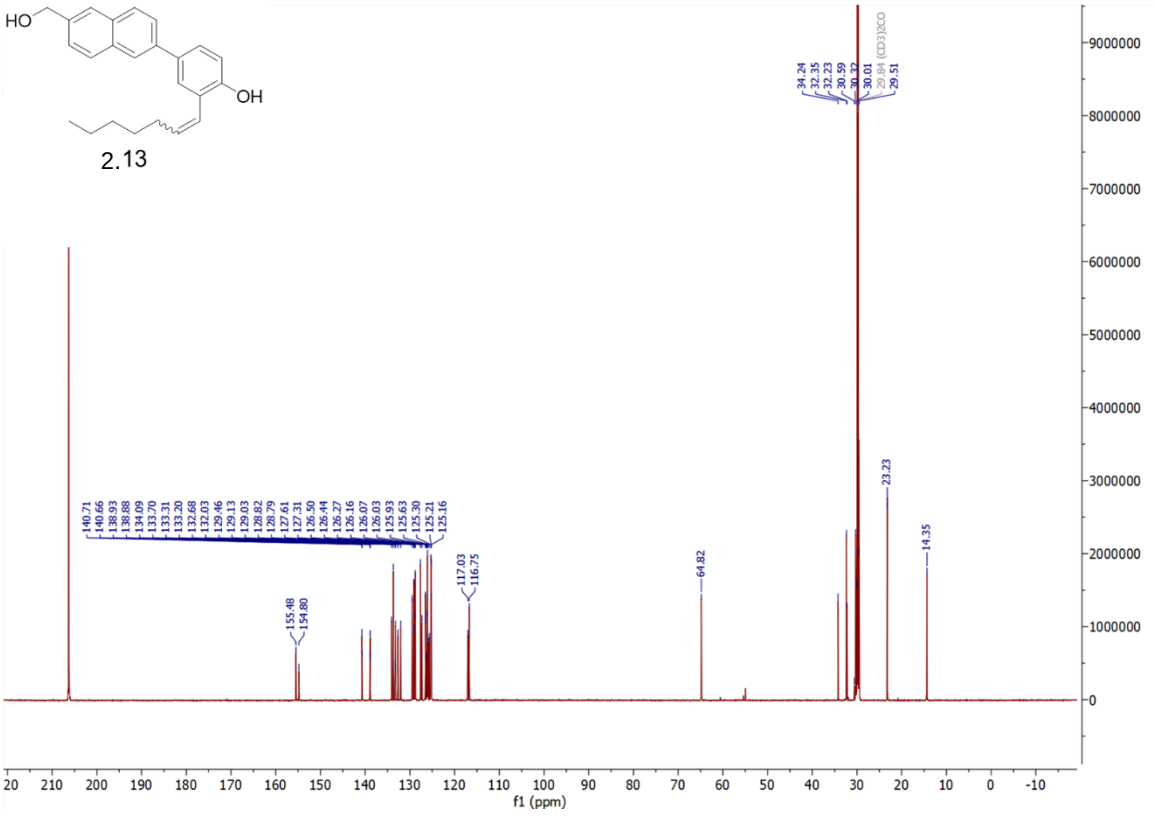
HO
OH
2.13
f1 (ppm)

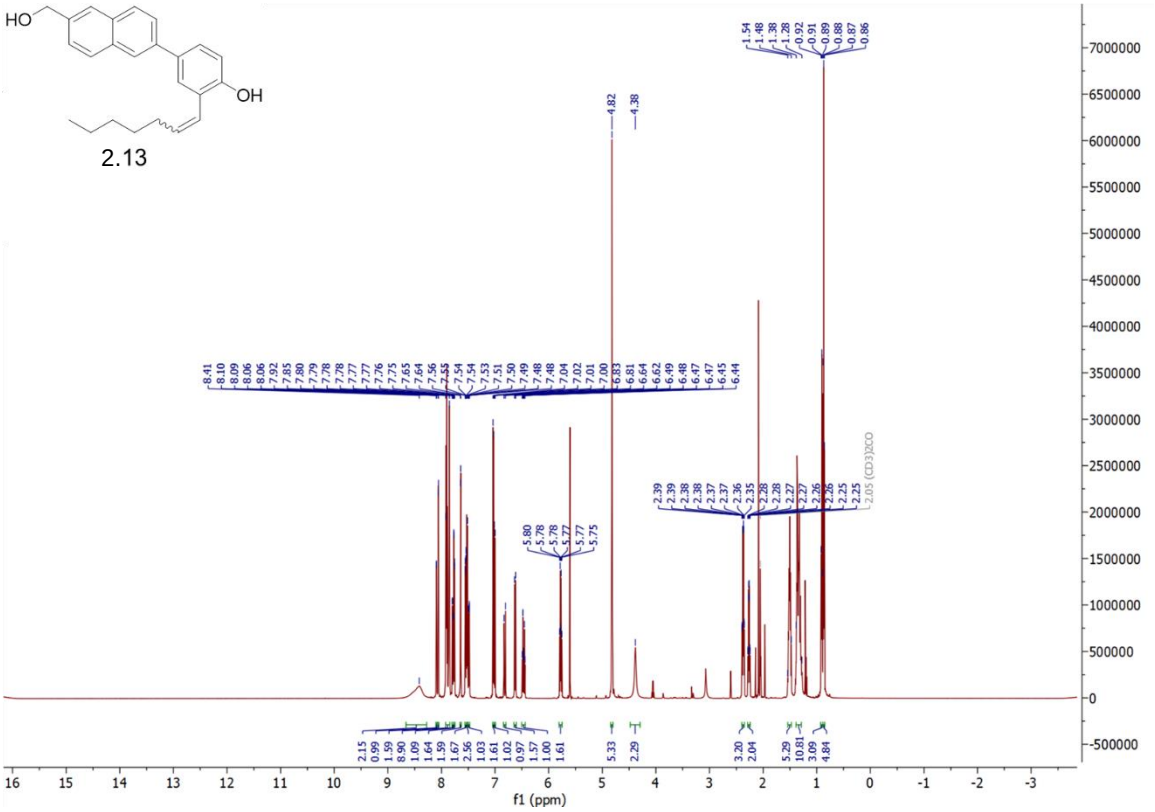
HO
OH
2.13
f1 (ppm)

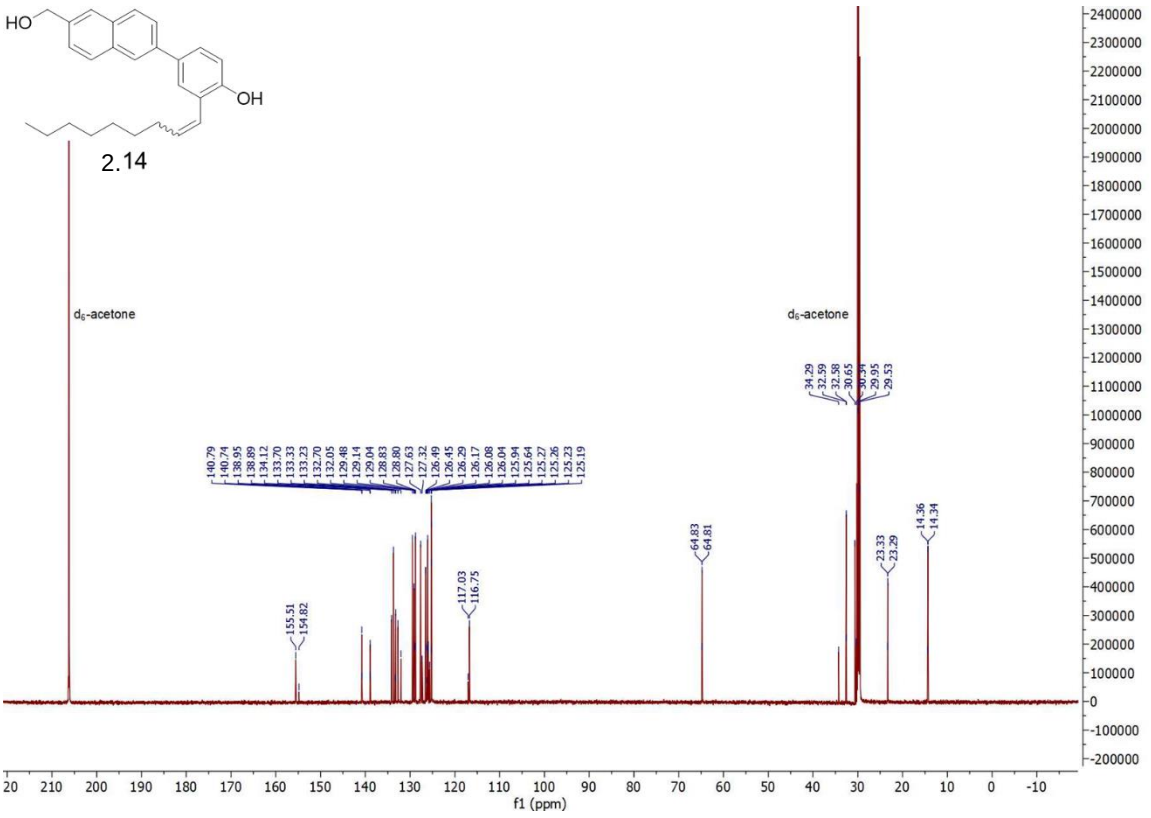
HO
OH
2.14
d6-acetone
d6-acetone
140.79
140.74
138.95
138.89
134.12
133.70
133.33
133.23
132.70
132.05
129.48
129.14
129.04
128.83
128.80
127.63
127.32
126.49
126.45
126.29
126.17
126.08
126.04
125.94
125.64
125.27
125.26
125.23
125.19
155.51
154.82
117.03
116.75
64.83
64.81
34.29
32.59
32.58
30.65
30.04
29.55
29.53
23.33
23.29
14.36
14.34
f1 (ppm)

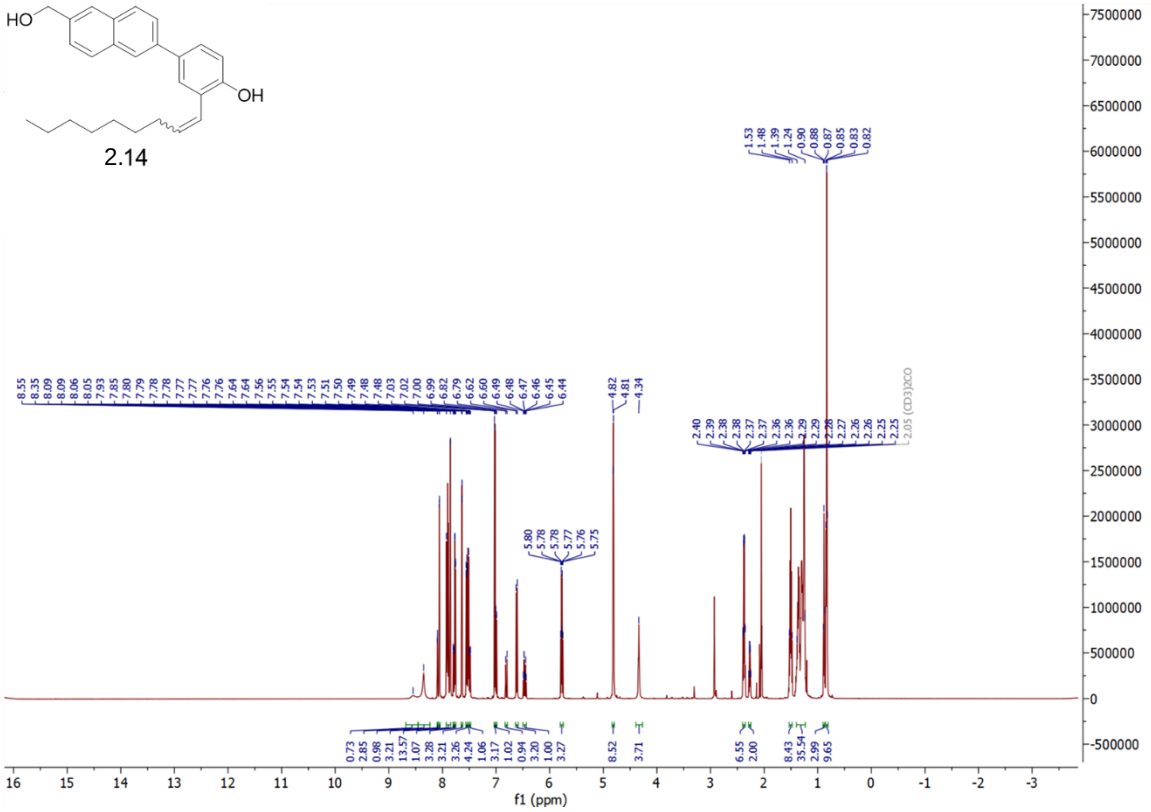
HO
OH
2.14
1.53
1.48
1.39
1.24
0.90
0.88
0.87
0.85
0.83
0.82
8.55
8.35
8.09
8.09
8.06
8.05
7.93
7.85
7.80
7.79
7.78
7.78
7.77
7.77
7.76
7.76
7.64
7.64
7.56
7.55
7.54
7.54
7.53
7.51
7.50
7.49
7.48
7.48
7.03
7.02
7.00
6.99
6.82
6.79
6.62
6.60
6.48
6.47
6.46
6.45
6.44
4.82
4.81
4.34
2.40
2.39
2.38
2.38
2.37
2.37
2.36
2.36
2.29
2.29
2.28
2.27
2.26
2.26
2.25
2.25
2.05 (CD3)2CO
5.80
5.78
5.78
5.77
5.76
5.75
0.73
2.85
0.98
3.21
13.57
1.07
3.28
3.21
3.26
4.24
1.06
3.17
1.02
0.94
3.20
1.00
3.27
8.52
3.71
6.55
2.00
8.43
35.54
2.99
9.65
f1 (ppm)

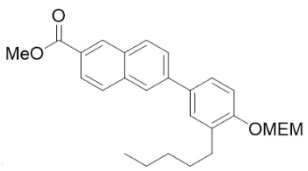
MeO
O
OMEM

2. S17

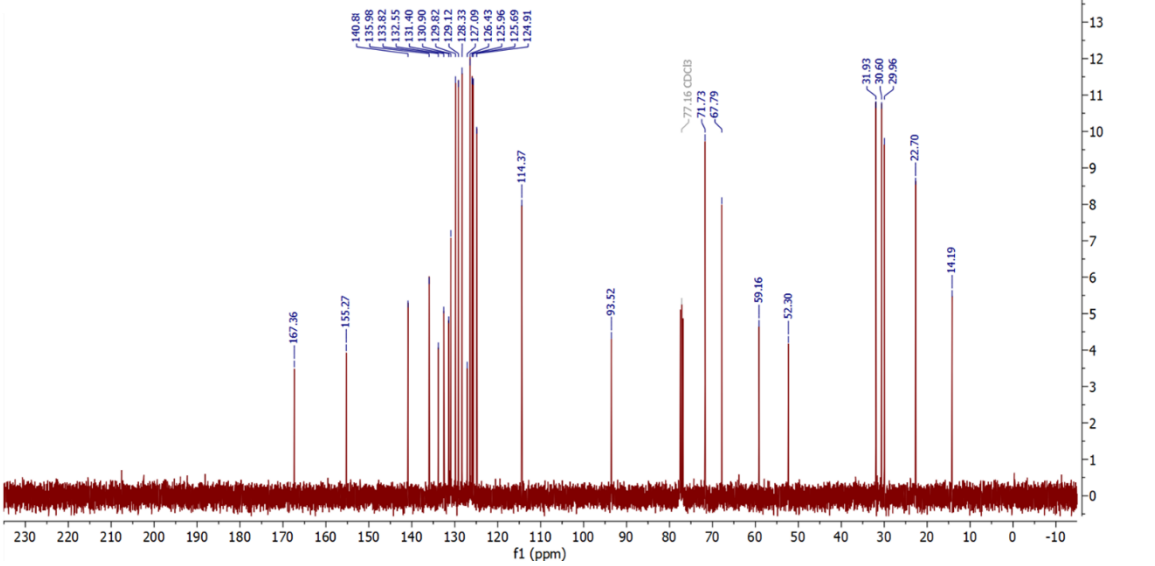
140.81
135.98
133.82
132.55
131.40
130.90
129.82
129.12
128.33
127.09
126.43
125.96
125.69
124.91
114.37
77.16 CDCl3
71.73
67.79
31.93
30.60
29.96
22.70
14.19
167.36
155.27
93.52
59.16
52.30
f1 (ppm)

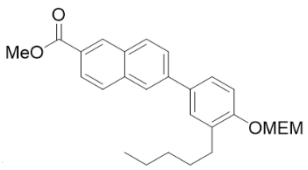
MeO
O
OMEM

2. S17

3.99
3.89
3.86
3.61
3.59
3.41
8.09
8.08
8.07
8.06
8.02
8.00
7.98
7.92
7.90
7.80
7.80
7.78
7.78
7.53
7.50
7.26 CDCl3
7.26
7.24
5.37
8.61
2.74
2.70
1.71
1.63
1.42
1.38
0.95
0.93
0.91
0.97
1.01
1.05
1.10
1.06
1.10
2.13
1.12
1.98
3.20
2.21
2.19
2.96
1.99
2.12
3.96
2.99
f1 (ppm)

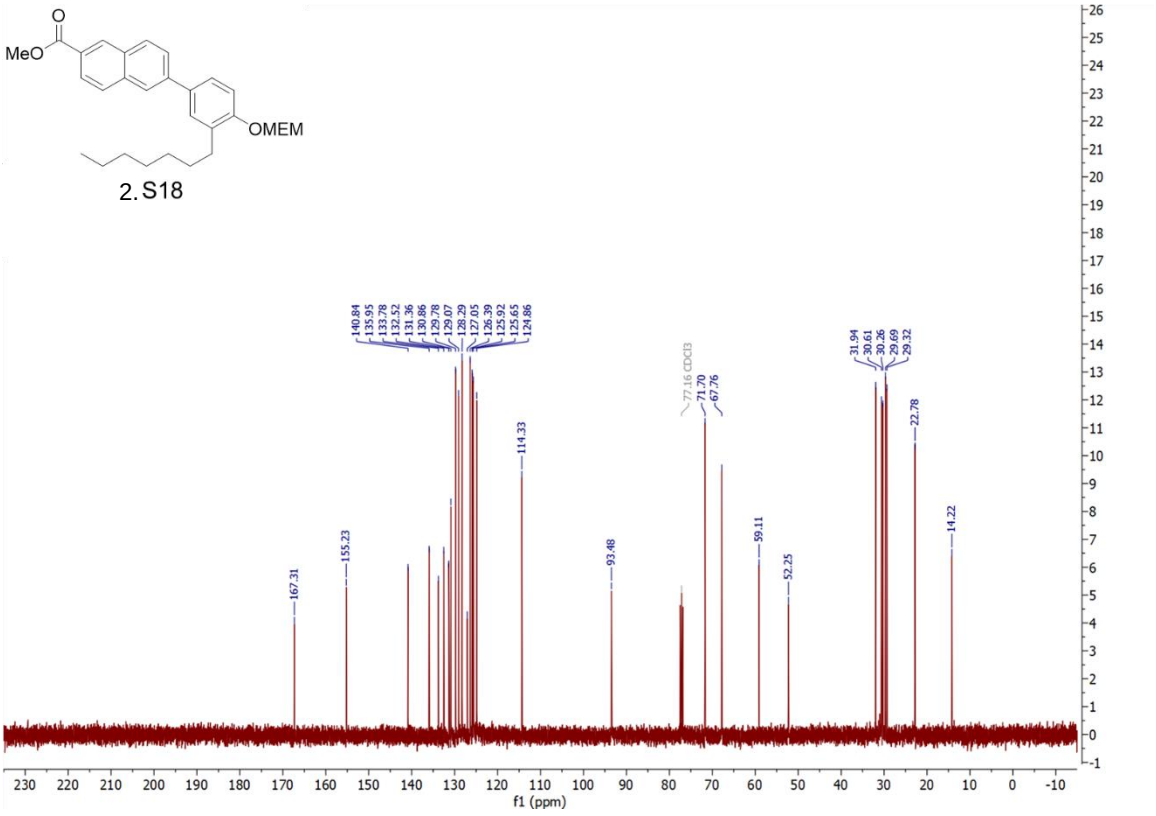
MeO
O
OMEM
2.S18
140.84
135.95
133.78
132.52
131.36
130.86
129.78
129.07
128.29
127.05
126.39
125.92
125.65
124.86
114.33
93.48
77.16 CDCl3
71.70
67.76
59.11
52.25
31.94
30.61
30.26
29.69
29.32
22.78
14.22
167.31
155.23
f1 (ppm)

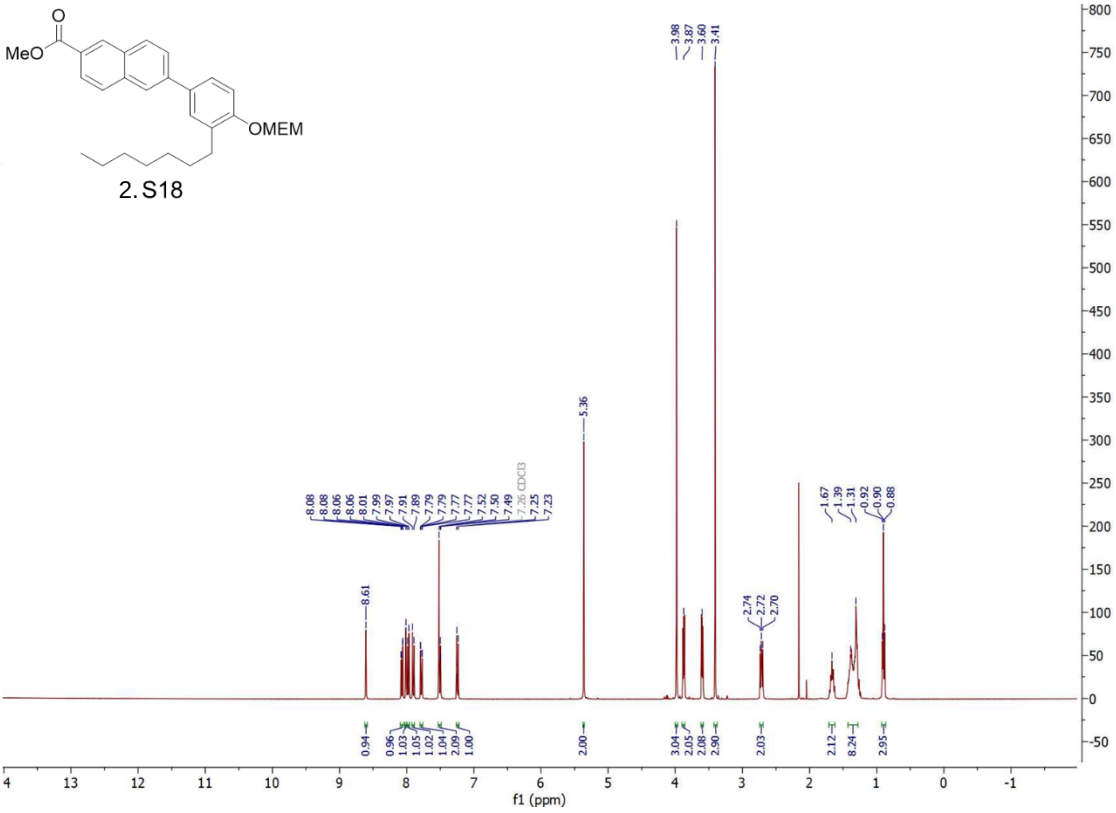
MeO
O
OMEM
2.S18
3.98
3.87
3.60
3.41
5.36
8.06
8.08
8.06
8.06
8.01
7.99
7.97
7.91
7.89
7.79
7.79
7.77
7.77
7.52
7.50
7.49
7.26 CDCl3
7.25
7.23
8.61
2.74
2.72
2.70
1.67
1.39
1.31
0.92
0.90
0.88
0.94
0.96
1.03
1.05
1.02
1.04
2.09
1.00
2.00
3.04
2.05
2.08
2.90
2.03
2.12
8.24
2.95
f1 (ppm)

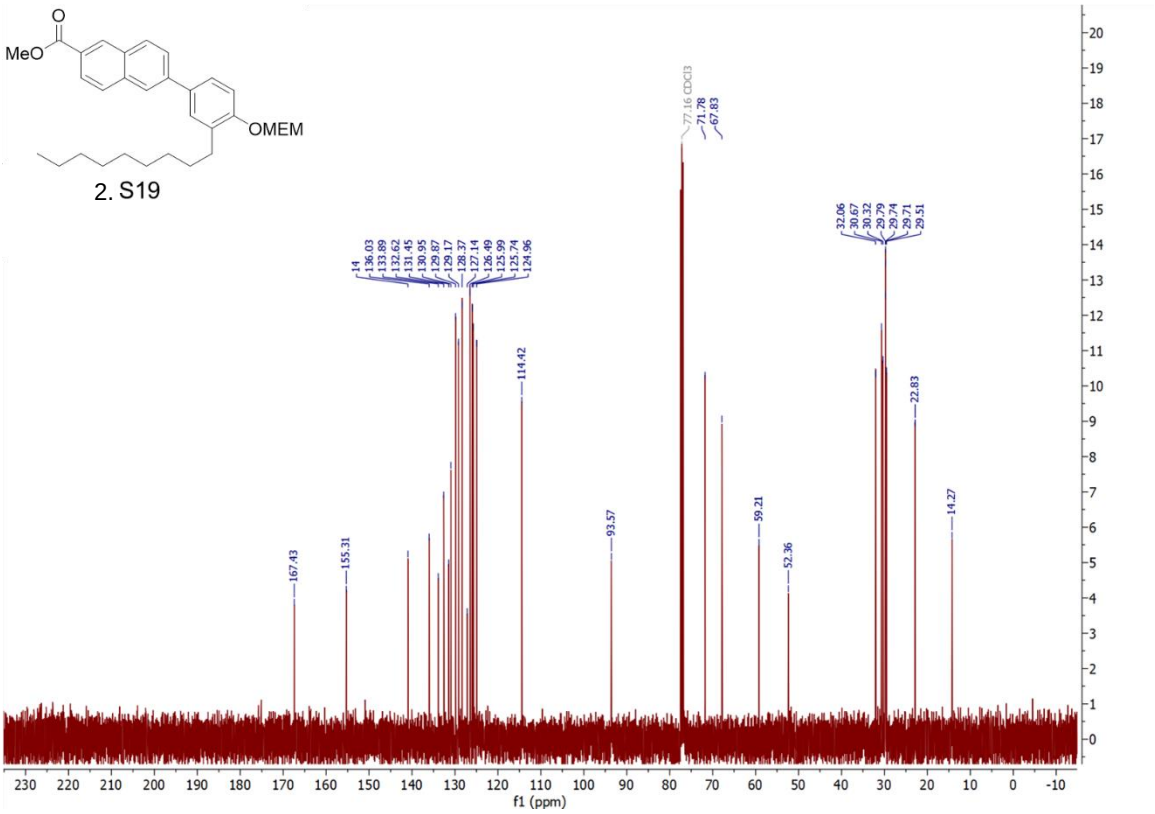
MeO
O
OMEM
2. S19
f1 (ppm)

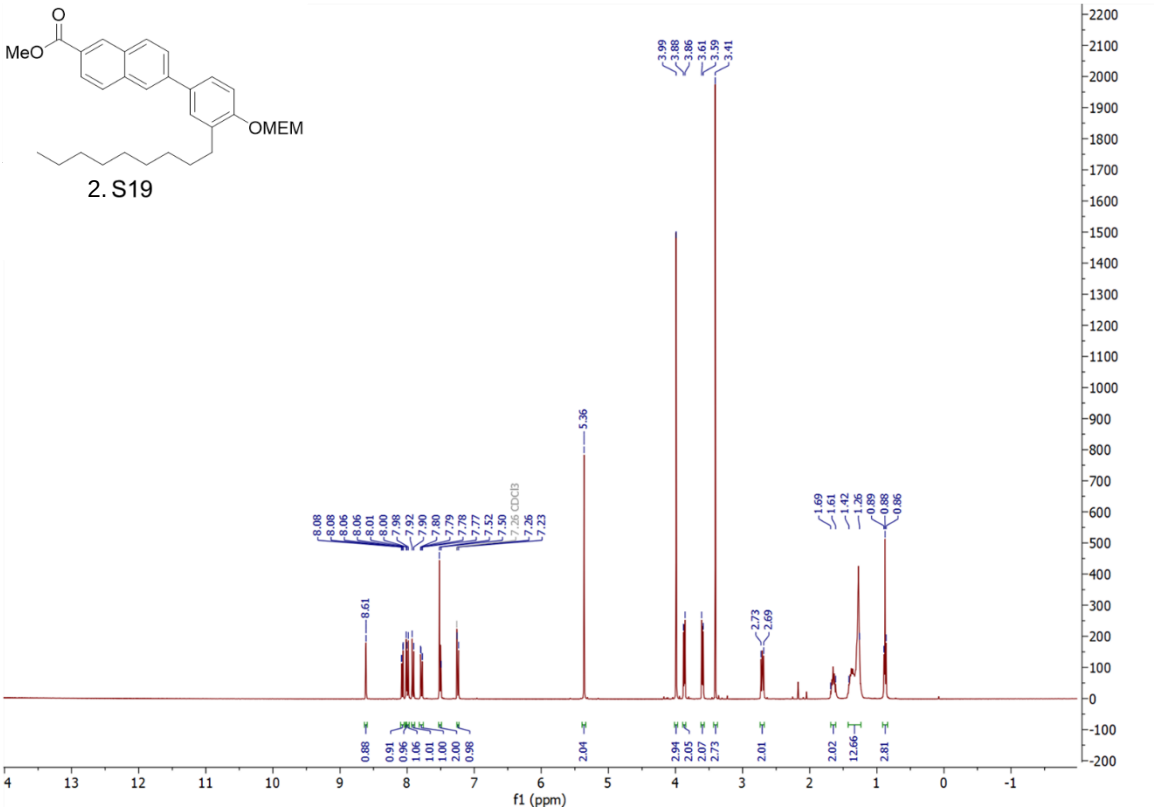
MeO
O
OMEM
2. S19
f1 (ppm)

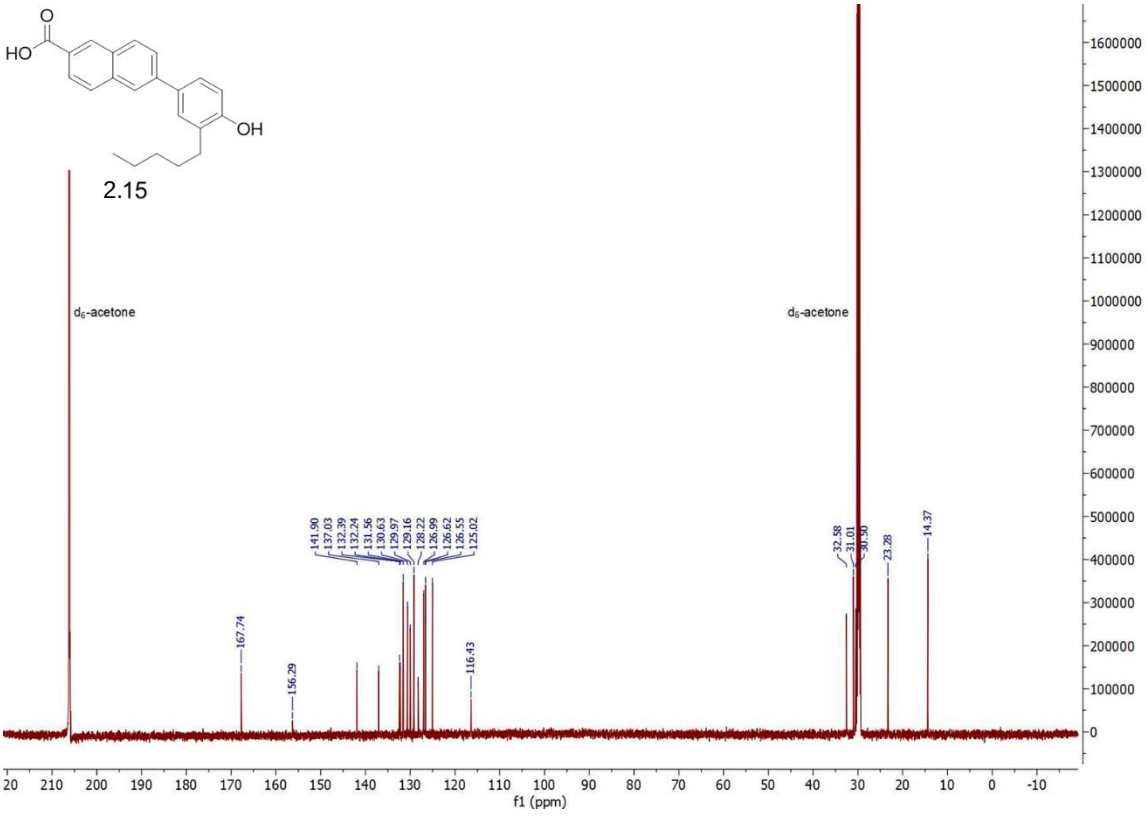
HO
O
OH
2.15
d6-acetone
d6-acetone
141.90
137.03
132.39
132.24
131.56
130.63
129.97
129.16
128.22
126.99
126.62
126.55
125.02
167.74
156.29
116.43
32.58
31.01
30.90
23.28
14.37
f1 (ppm)

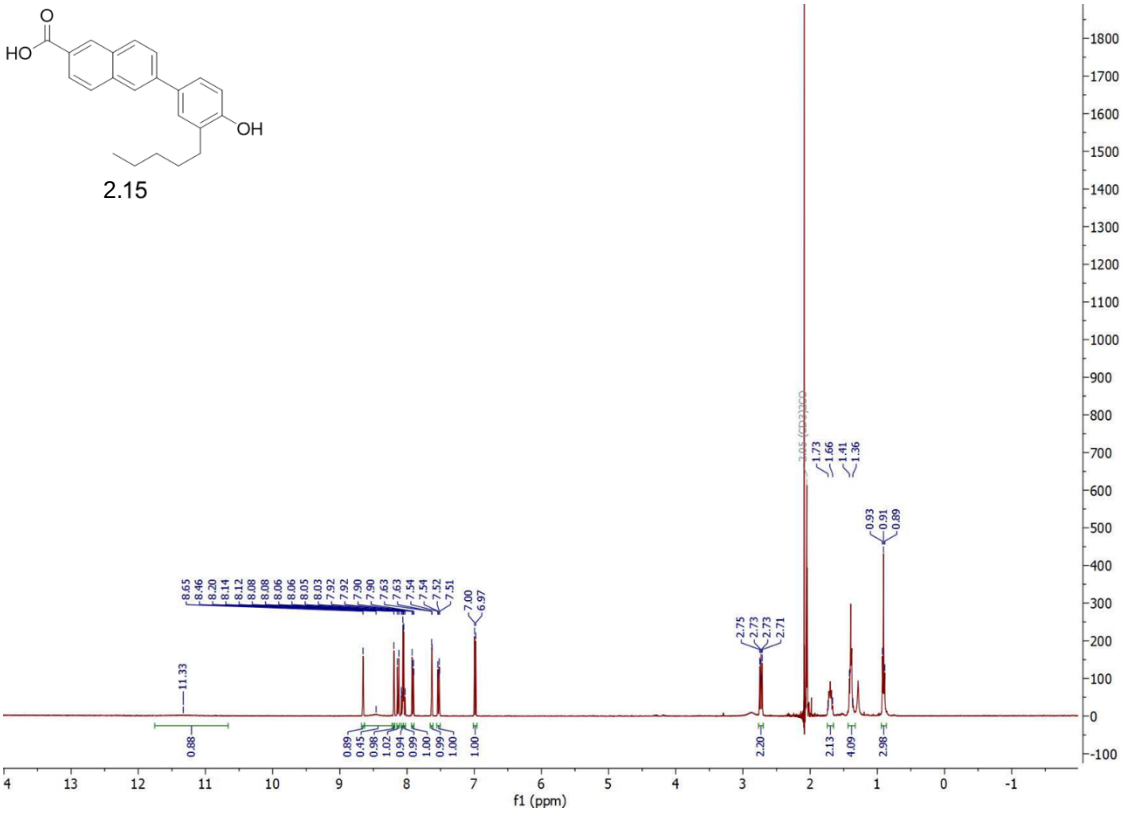
HO
O
OH
2.15
8.65
8.46
8.20
8.14
8.12
8.08
8.08
8.06
8.06
8.05
8.03
7.92
7.92
7.90
7.90
7.63
7.63
7.54
7.54
7.52
7.51
7.00
6.97
11.33
2.75
2.73
2.73
2.71
1.73
1.66
1.41
1.36
0.93
0.91
0.89
0.88
0.89
0.45
0.98
1.02
0.94
0.97
1.00
0.99
1.00
1.00
2.20
2.13
4.09
2.98
f1 (ppm)

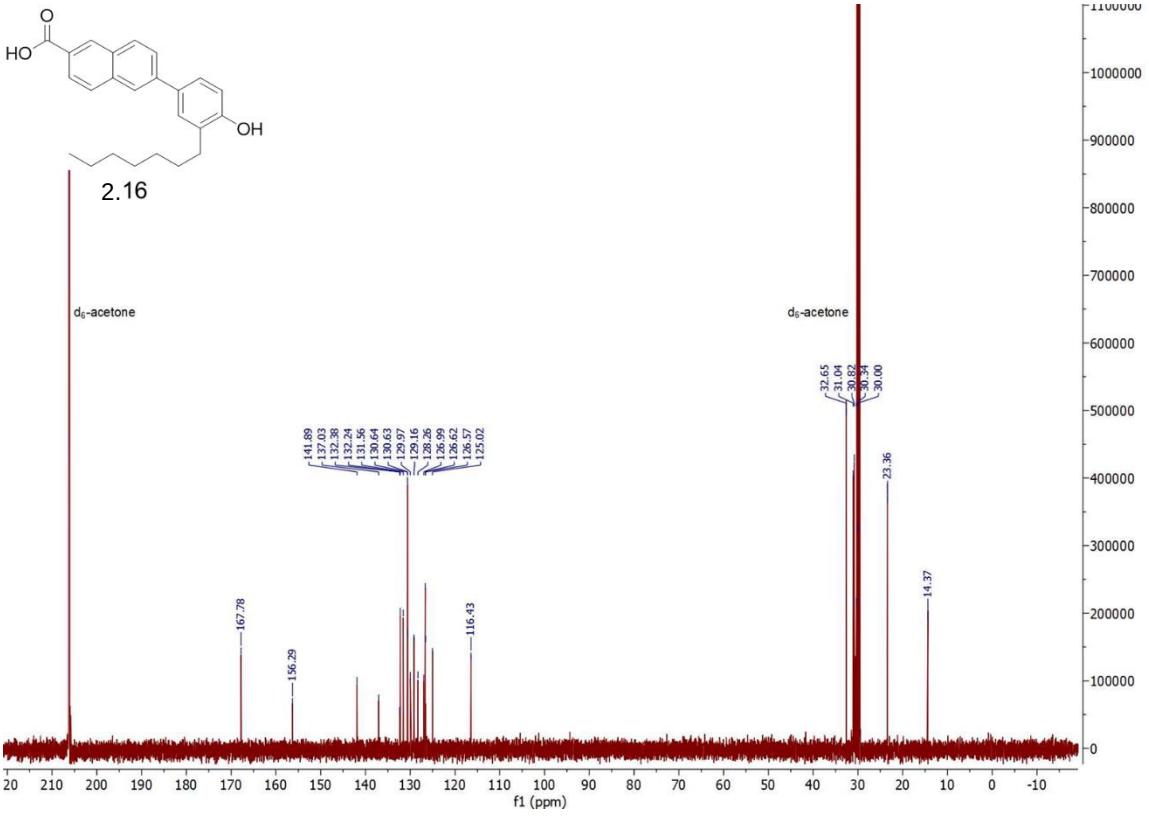
HO
O
OH
2.16
d6-acetone
d6-acetone
167.78
156.29
141.89
137.03
132.38
132.24
131.56
130.64
130.63
129.97
129.16
128.26
126.99
126.62
126.57
125.02
116.43
32.65
31.04
30.82
30.34
30.00
23.36
14.37
f1 (ppm)

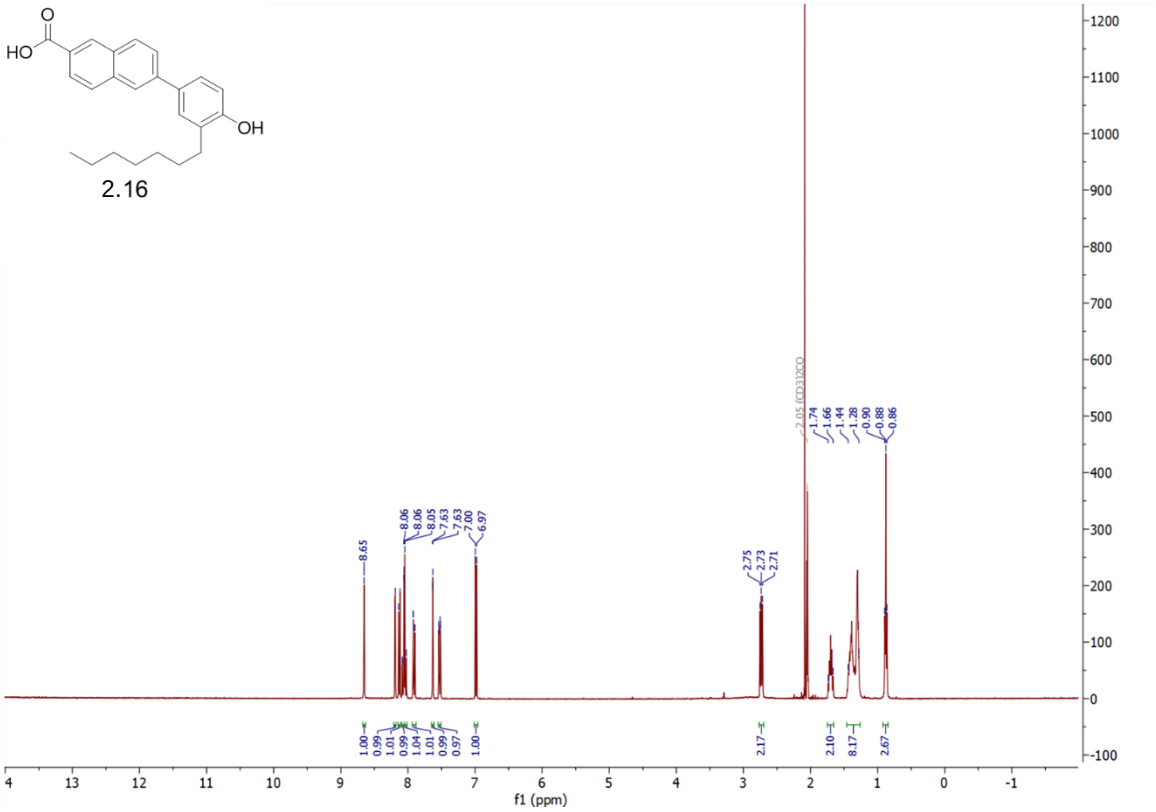
HO
O
OH
2.16
8.65
8.06
8.06
8.05
7.63
7.63
7.00
6.97
2.75
2.73
2.71
2.05 (CD3)2CO
1.74
1.66
1.44
1.28
0.90
0.88
0.86
1.00
0.99
1.01
0.99
1.04
1.01
0.99
0.97
1.00
2.17
2.10
8.17
2.67
f1 (ppm)

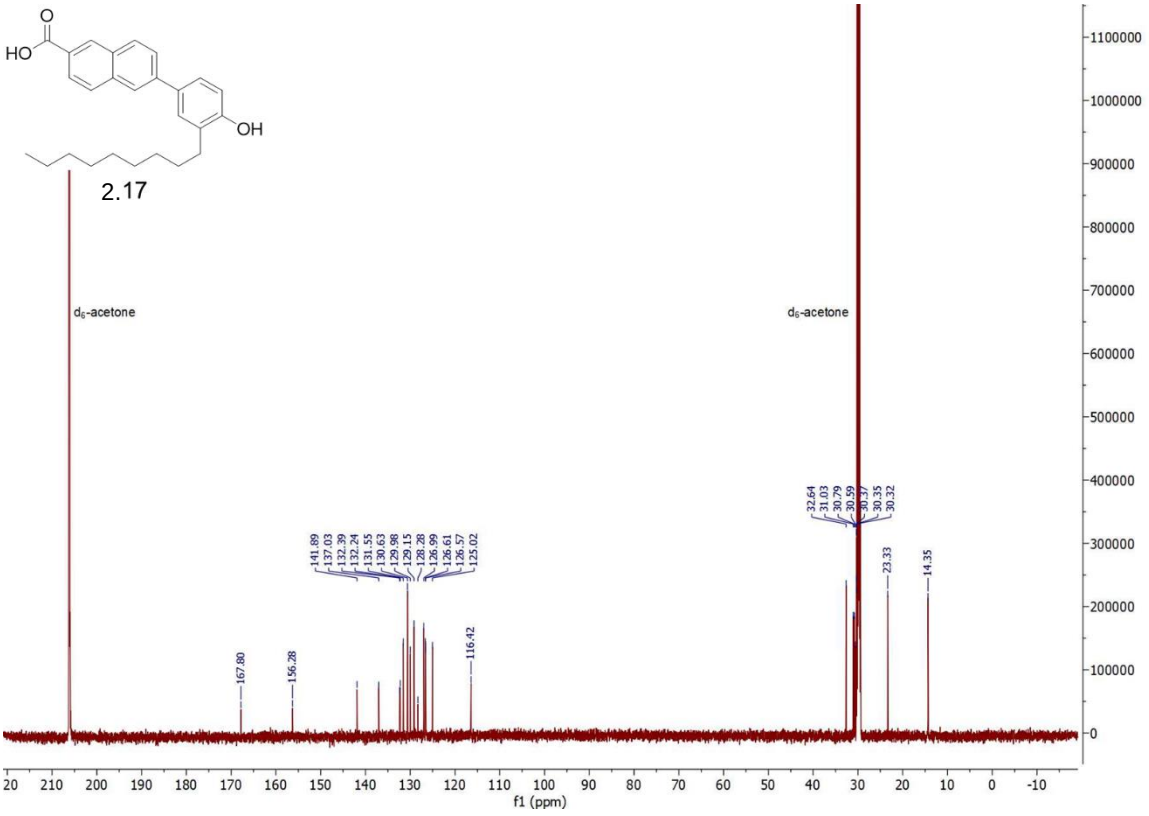
HO
O
OH
2.17
d6-acetone
d6-acetone
167.80
156.28
141.89
137.03
132.39
132.24
131.55
130.63
129.98
129.15
128.28
126.99
126.61
126.57
125.02
116.42
32.64
31.03
30.79
30.59
30.37
30.35
30.32
23.33
14.35
f1 (ppm)

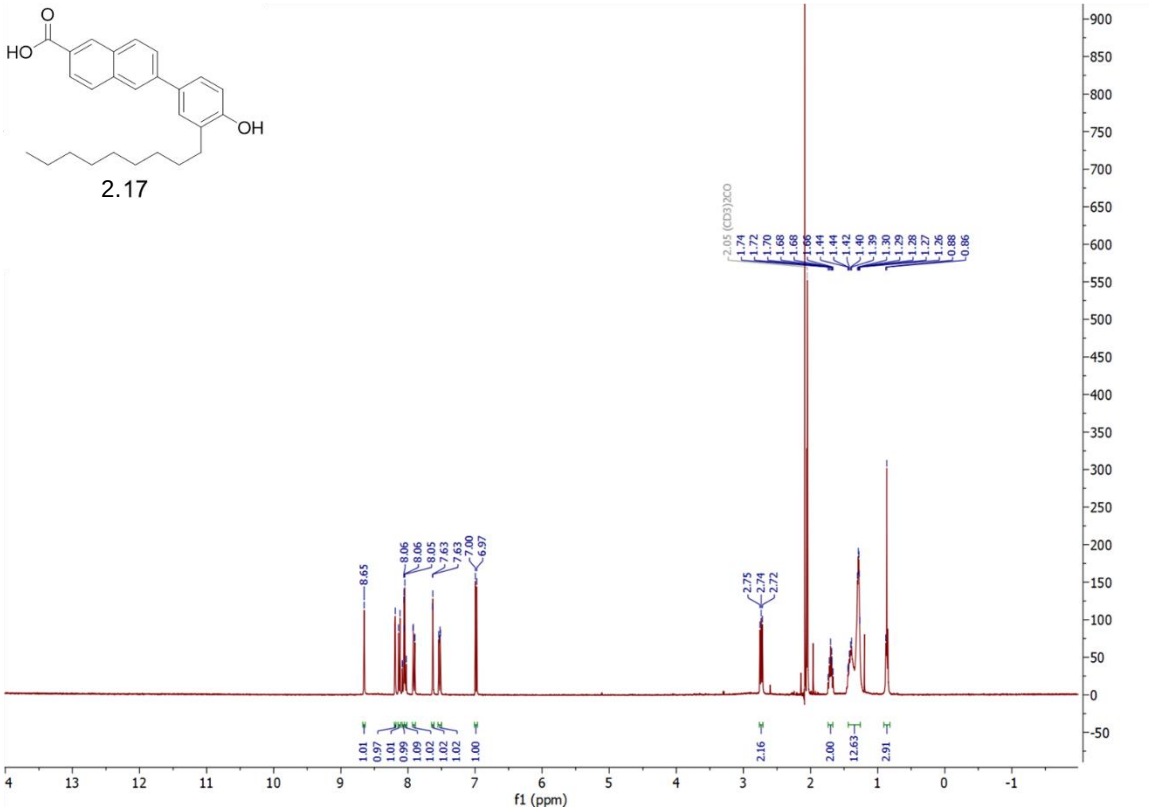
HO
O
OH
2.17
2.05 (CD3)2CO
1.74
1.72
1.70
1.68
1.66
1.44
1.42
1.40
1.39
1.30
1.29
1.28
1.27
1.26
0.88
0.86
8.65
8.06
8.06
8.05
7.63
7.63
7.00
6.97
2.75
2.74
2.72
1.01
0.97
1.01
0.99
1.09
1.02
1.02
1.02
1.00
2.16
2.00
12.63
2.91
f1 (ppm)

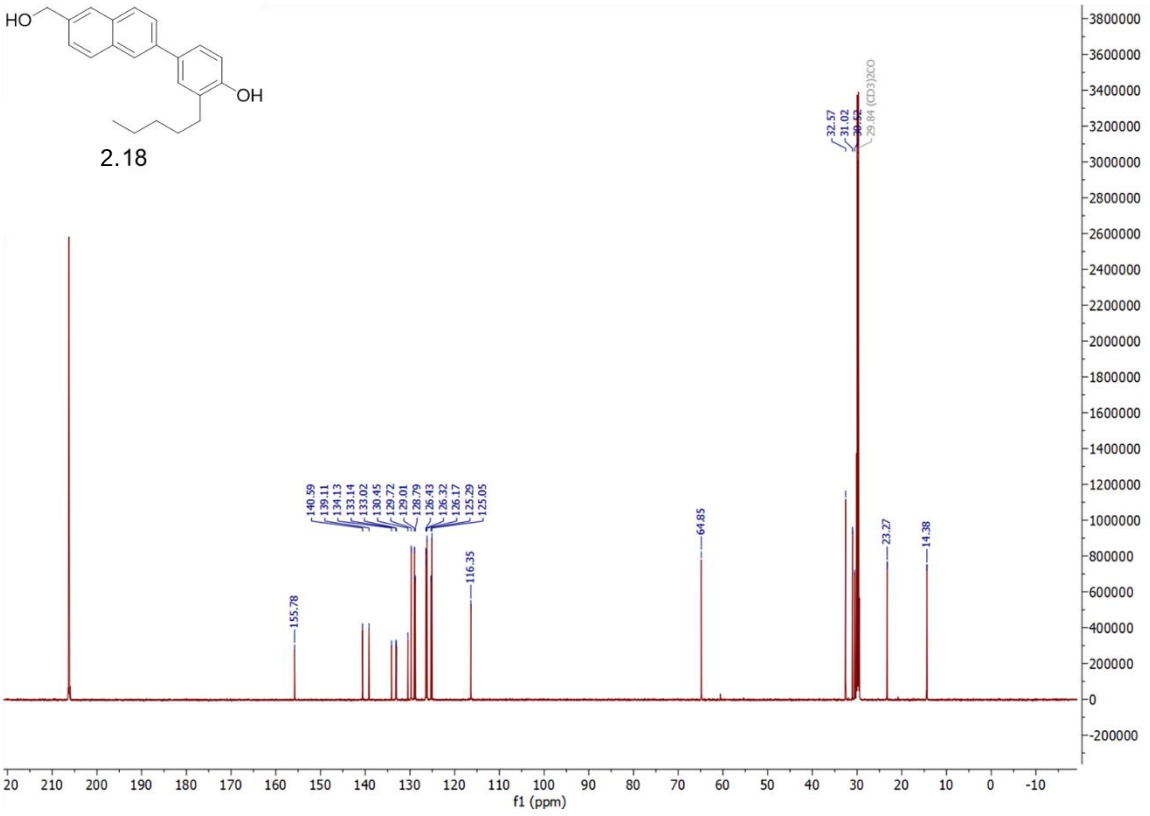
HO
OH
2.18
140.59
139.11
134.13
133.14
133.02
130.45
129.72
129.01
128.79
126.43
126.32
126.17
125.29
125.05
155.78
116.35
64.85
32.57
31.02
30.62
29.84 (CD3)2CO
23.27
14.38
f1 (ppm)

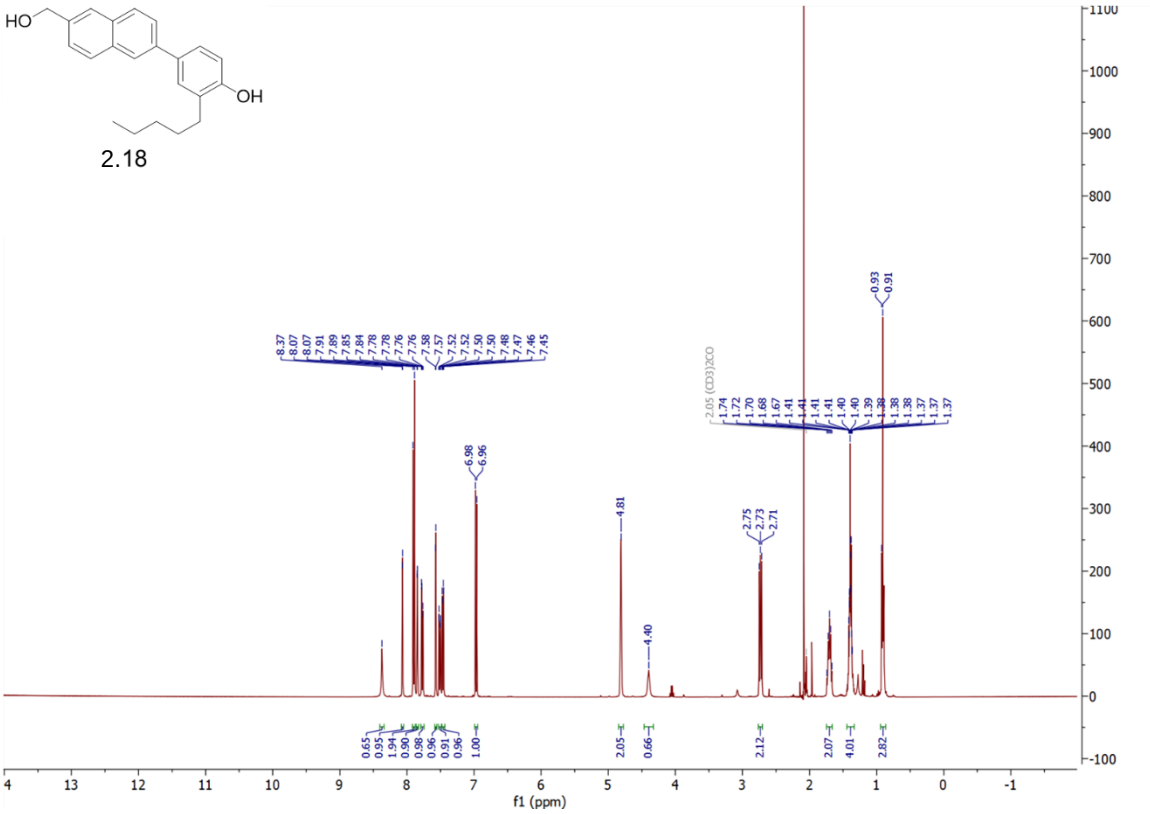
HO
OH
2.18
8.37
8.07
8.07
7.91
7.89
7.85
7.84
7.78
7.78
7.76
7.76
7.58
7.57
7.52
7.52
7.50
7.50
7.48
7.47
7.46
7.45
6.98
6.96
4.81
4.40
2.75
2.73
2.71
2.05 (CD3)2CO
1.74
1.72
1.70
1.68
1.67
1.41
1.41
1.41
1.41
1.40
1.40
1.39
1.38
1.38
1.38
1.37
1.37
1.37
0.93
0.91
0.65
0.95
1.94
0.90
0.98
0.96
0.91
0.96
1.00
2.05
0.66
2.12
2.07
4.01
2.82
f1 (ppm)

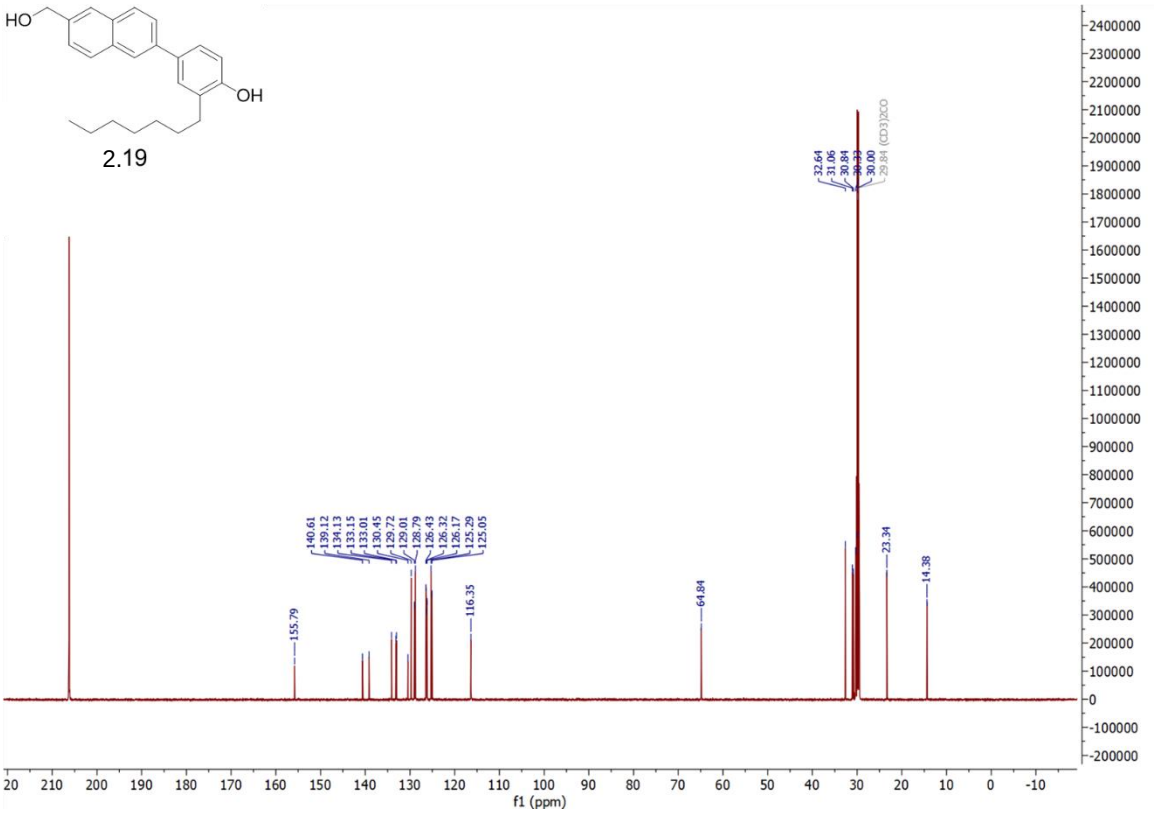
HO
OH
2.19
f1 (ppm)

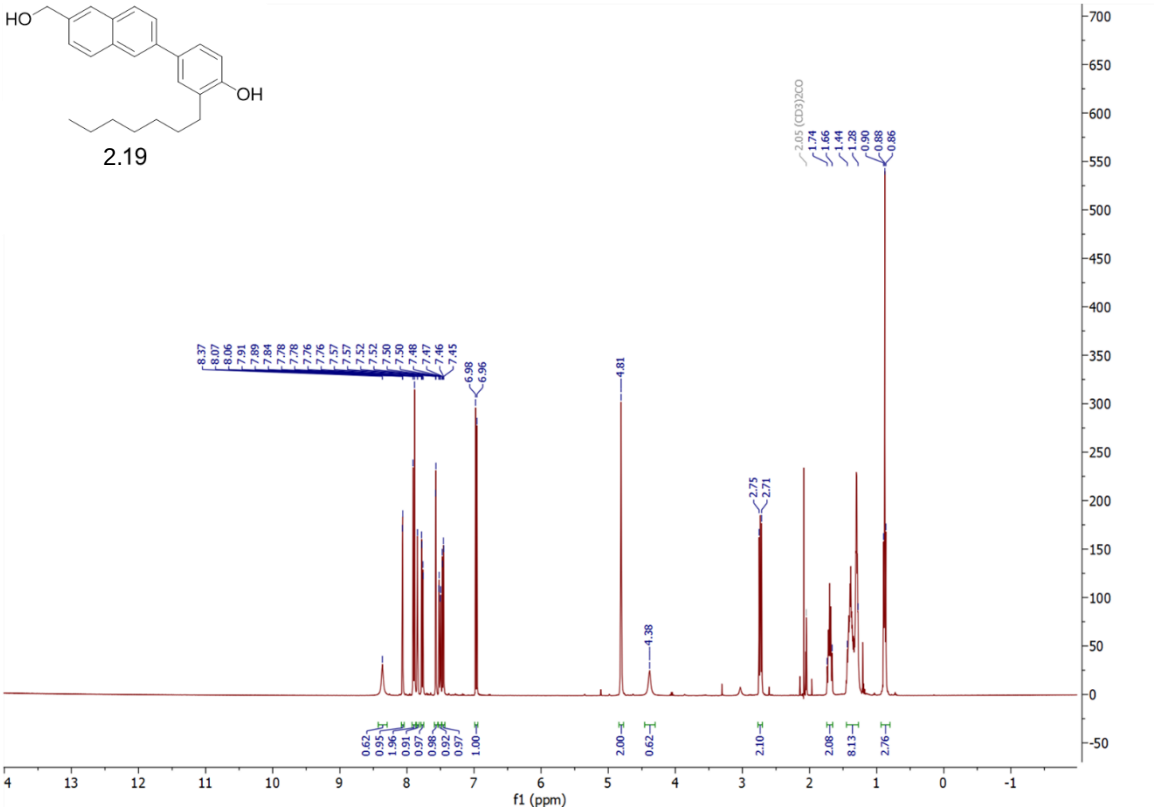
HO
OH
2.19
f1 (ppm)

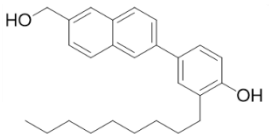
HO
OH

2.20

32.64
31.05
30.83
30.37
30.35
30.32
29.84 (CD3)2CO
133.17
129.75
129.01
128.79
128.44
126.33
126.18
125.28
125.06
116.36
155.81
64.84
23.33
14.36
f1 (ppm)

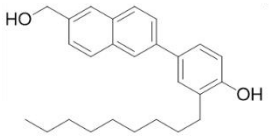
HO
OH

2.20

2.05 (CD3)2CO
1.74
1.66
1.45
1.26
0.88
0.87
0.85
8.35
8.06
7.91
7.91
7.89
7.89
7.84
7.78
7.78
7.76
7.76
7.57
7.56
7.52
7.52
7.50
7.50
7.48
7.47
7.46
7.45
6.97
6.95
4.81
4.80
4.36
4.35
4.33
2.75
2.73
2.71
0.74
0.98
2.01
0.91
1.00
1.02
0.93
0.99
1.00
2.07
0.62
2.18
2.18
12.38
2.67
f1 (ppm)

Chapter 3 Supporting Information

Biology

Biology completed by Wooseong Kim and Iliana E. Escobar.

Minimum Inhibitory Concentration assays were carried out as described by the Clinical and Laboratory Standard Institute. In brief, bacterial strains grown overnight in appropriate media for 20-23 hours were diluted to 10X105 CFU/mL in MHB (Gibco). In a 96-well plate 50µl of diluted culture were added to 50µl of serial two-fold diluted drug in MHB to a final concentration of 5X105 CFU/mL. All assays were performed in triplicate. Experimental plates were incubated for 20-22 hours at 37°C. Optical density (OD) at 600nm was measured using a spectrophotometer (SpectraMax M2, Molecular Devices) as a measure of bacterial growth. MIC was defined as OD600 £ 0.1 after background subtraction.

Chemistry

*Chemistry in Chapter 3 completed by Ana V. Cheng and Cassandra L. Schrank. Synthetic procedures provided only for chemistry completed by Ana V. Cheng (note: Schrank and Cheng shared intermediates and performed each reaction in preparation of analogues **3.3** and **3.4**.)*

General Methods: NMR spectra were recorded using the following spectrometers: Varian INOVA400, Varian INOVA500, VNMR400, and Bruker Ascend 600. Chemical shifts are quoted in ppm relative to the indicated solvents. The following abbreviations are used to describe splitting: s (singlet), d (doublet), t (triplet), q (quartet), m (multiplet), and dd (doublet of doublets). Accurate mass spectra were recorded using a Thermo LTQ-FTMS. Non-aqueous reactions were performed using flame-dried glassware under an atmosphere of Argon with HPLC-grade solvents purified on a Pure Process Technology solvent purification system. Brine refers to a saturated solution of sodium chloride, sat. Na2CO3 to a saturated aqueous solution of sodium carbonate, sat. NaHCO3 to a saturated solution of sodium bicarbonate, and Na2SO4 to magnesium sulfate. Column chromatography was performed using a Biotage® flash chromatography purification system. Chemicals were used as received from Oakwood, Sigma-Aldrich, Alfa Aesar, or AK Scientific. All final compounds were assessed for >95% purity using an Agilent Technologies 1100 Series HPLC with the following parameters: 5µm 9.4 x 250mm FLOW column, a mobile phase gradient of water-acetonitrile dosed with 0.1% formic acid, and a MWD UV/Vis Detector.

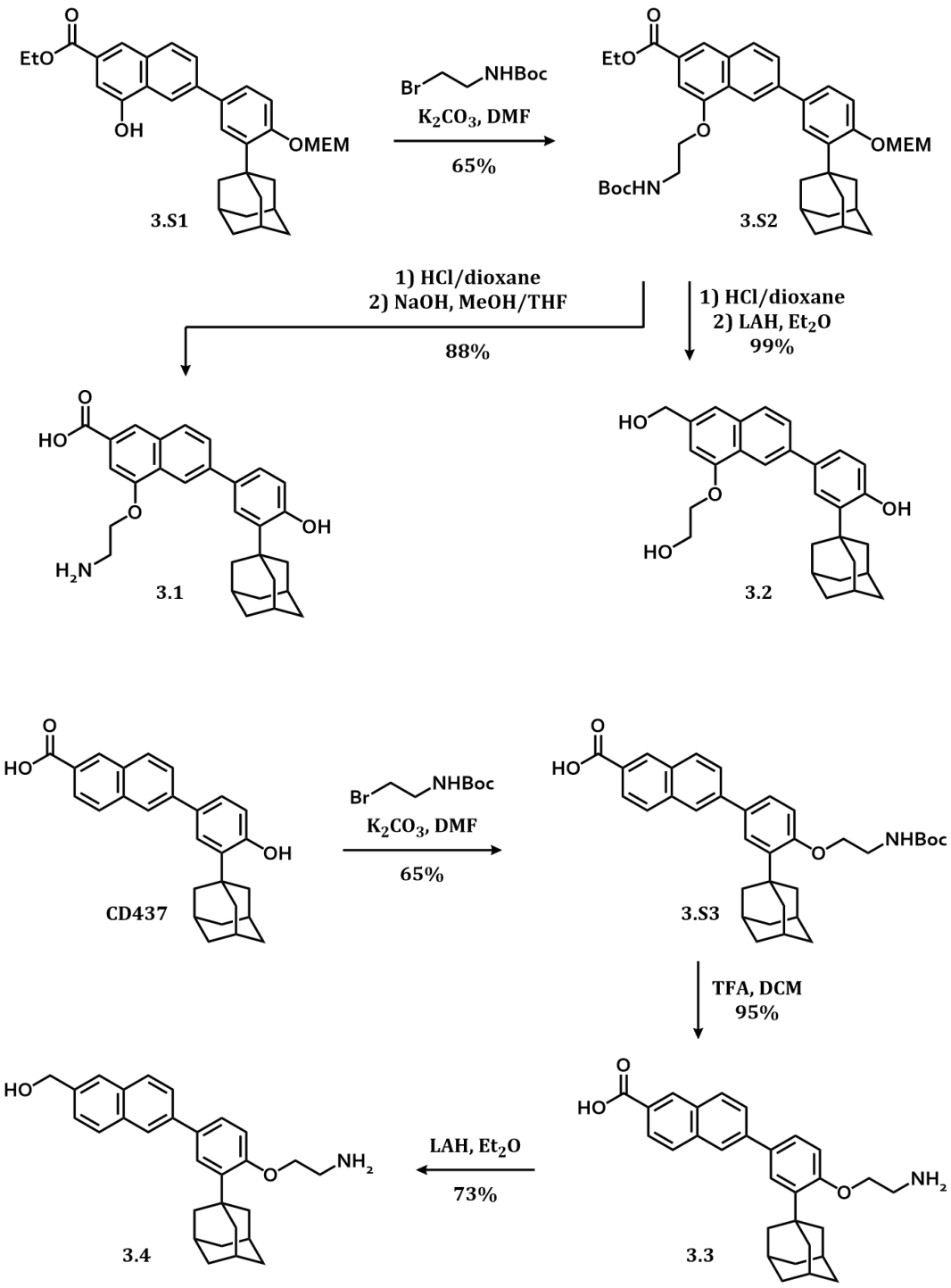

Figure S4. Synthesis of analogues **3.1-3.4.**

Ethyl 6-(3-((3r,5r,7r)-adamantan-1-yl)-4-((2-methoxyethoxy)methoxy)phenyl)-4-(2-((tertbutoxycarbonyl)amino)ethoxy)-2-naphthoate [3.S2]. 3.S1[93] (1.0 eq, 263 mg, 0.495 mmol) and K2CO3 (8.0 eq, 547 mg, 3.96 mmol) were dissolved in DMF (5 mL) and stirred at 50 °C. After 1 h, *N*-Boc-2-bromoethylamine (5.0 eq, 554 mg, 2.48 mmol) was added and the reaction was stirred for 3 d. Once complete, water was added and the reaction solution was extracted with ethyl acetate 4x. The organic layers were combined, washed with brine, dried with sodium sulfate, concentrated, and purified via flash column chromatography in a gradient of hexanes and ethyl acetate to yield the product as a yellow solid (216 mg, 65% yield). **1H NMR** (400 MHz, Acetoned6) δ 8.56 (s, 1H), 8.23 (s, 1H), 8.08 (d, J = 8.4 Hz, 1H), 7.90 (dd, J = 8.6, 1.9 Hz, 1H), 7.66 (d, J = 2.4 Hz, 1H), 7.60 (dd, J = 8.4, 2.3 Hz, 1H), 7.43 (d, J = 1.4 Hz, 1H), 7.28 (d, J = 8.5 Hz, 1H), 6.42 (t, J = 6.2 Hz, 1H), 5.42 (s, 2H), 4.40 (q, J = 7.1 Hz, 2H), 4.32 (t, J = 5.3 Hz, 2H), 3.92 – 3.85 (m, 2H), 3.70 (q, J = 5.5 Hz, 2H), 3.62 – 3.55 (m, 2H), 3.32 (s, 3H), 2.25 (d, J = 2.9 Hz, 6H), 2.10 (s, 3H), 1.83 (s, 6H), 1.41 (t, J = 7.1 Hz, 3H), 1.35 (s, 9H). **13C NMR** (126 MHz, Acetone-d6) δ 166.92, 157.50, 156.83, 155.79, 141.47, 139.57, 134.44, 133.20, 130.41, 128.97, 128.65, 127.59, 126.77, 126.70, 123.80, 120.07, 116.07, 104.59, 94.25, 78.74, 72.40, 68.96, 68.74, 61.59, 58.84, 41.39, 40.73, 37.97, 37.75, 30.02, 28.61, 14.69.

6-(3-((3r,5r,7r)-Adamantan-1-yl)-4-hydroxyphenyl)-4-(2-aminoethoxy)-2-naphthoic acid [3.1]. 3.S2 (1.0 eq, 84 mg, 0.13 mmol) was dissolved in 4.0 M HCl in dioxane (3 mL) and stirred at room temperature for 1 h. The solution was quenched with saturated aqueous Na2CO3 solution and extracted with ethyl acetate 3x. The organic layers were combined, washed with brine, dried with sodium sulfate, and concentrated. The resultant intermediate was dissolved in 5 mL 2:1 methanol:THF and 1 mL 1 M aqueous NaOH and stirred for 3 h. The solution was heated to 50 °C for a further 2 h to drive the reaction to completion, then quenched with 1 M aqueous HCl and extracted with ethyl acetate 3x. The organic layer were combined, washed with brine, dried with sodium sulfate, concentrated, and purified via preparative TLC utilizing a mobile phase of 5% methanol in dichloromethane and 1% acetic acid to yield the product as a light tan solid (50 mg, 88% yield). **1H NMR** (400 MHz, Methanol-d4) δ 8.42 (d, J = 1.8 Hz, 1H), 7.85 (d, J = 8.5 Hz, 1H), 7.72 (dd, J = 8.5, 1.9 Hz, 1H), 7.50 – 7.44 (m, 2H), 7.42 (dd, J = 8.2, 2.3 Hz, 1H), 7.00 (d, J = 1.3 Hz, 1H), 6.84 (d, J = 8.2 Hz, 1H), 4.76 (s, 2H), 4.47 (t, J = 5.0 Hz, 2H), 3.55 (t, J = 5.0 Hz, 2H), 2.25 (d, J = 2.9 Hz, 6H), 2.09 (s, 3H), 1.84 (s, 6H). **13C NMR** (151 MHz, d6-DMSO) δ 156.08, 153.85, 140.28, 137.44, 135.78, 132.46, 130.81, 127.84, 125.69, 125.24, 124.95, 124.49, 118.05, 117.03, 116.48, 104.66, 63.22, 40.43, 40.06, 36.66, 36.31, 28.43, 22.24. **HRMS** Accurate mass (ES+): found 458.23153, C29H32O4N (M+H+) requires 458.56868.

2-((3r,5r,7r)-Adamantan-1-yl)-4-(8-(2-aminoethoxy)-6-(hydroxymethyl)naphthalen-2-yl)phenol [3.2]. 3.S2 (1.0 eq, 102 mg, 0.15 mmol) was dissolved in 4.0 M HCl in dioxane (3 mL) and stirred at room temperature for 1 h. The solution was quenched with saturated aqueous Na2CO3 solution and extracted with ethyl acetate 3x. The organic layers were combined, washed with brine, dried with sodium sulfate, and concentrated. The resultant intermediate was suspended in 2 mL diethyl ether and THF was added until fully dissolved. Lithium aluminum hydride (1.2 eq, 7 mg, 0.18 mmol) dissolved in ether was added and the solution was stirred at room temperature for 3 h. The solution was quenched with 1 M aqueous HCl and extracted with ethyl acetate 3x. The organic layers were combined, washed

with brine, dried with sodium sulfate, concentrated, and purified via flash column chromatography in a gradient of dichloromethane with 1% acetic acid and methanol to yield the product as a tan solid (67 mg, 99% yield). **1H NMR** (600 MHz, DMSO-d6) δ 9.73 (s, 1H), 8.44 (s, 1H), 8.11 (s, 1H), 7.95 (d, J = 8.4 Hz, 1H), 7.75 (d, J = 8.0 Hz, 1H), 7.49 (d, J = 8.2 Hz, 1H), 7.45 – 7.33 (m, 2H), 6.97 (d, J = 8.2 Hz, 1H), 4.40 (s, 2H), 3.33 (s, 2H), 2.13 (s, 6H), 2.02 (s, 3H), 1.71 (s, 6H). **13C NMR** (151 MHz, DMSO) δ 169.31, 156.44, 153.31, 139.48, 135.82, 132.10, 131.86, 130.52, 129.24, 126.61, 126.03, 125.68, 125.25, 122.41, 118.38, 117.10, 105.24, 64.96, 40.43, 38.46, 36.69, 36.35, 28.45. **HRMS** Accurate mass (ES+): found 444.25257, C29H34O3N (M+H+) requires 444.58516.

6-(3-((3r,5r,7r)-Adamantan-1-yl)-4-(2-((tert-butoxycarbonyl)amino)ethoxy)phenyl) -2-naphthoic acid [3.S3]. CD437 (1.0 eq, 32 mg, 0.080 mmol) and potassium carbonate (10.0 eq, 111 mg, 0.80 mmol) were dissolved in 1 mL DMF at 60 °C and stirred for 15 mins. *tert*-butyl (2-bromoethyl)carbamate (8.0 eq, 143 mg, 0.6424 mmol) then added at temperature and stirred for 2-3 d. The reaction was quenched with sat. Na_2CO_3 and extracted with EtOAc (3x). The combined organic layers were dried over MgSO4, concentrated, and purified by flash column chromatography in a gradient of hexanes and ethyl acetate to afford the product as a white solid (28 mg, 65% yield). **1H NMR** (500 MHz, CDCl3) δ 8.61 (s, 1H), 8.06 (dd, *J* = 8.6, 1.7 Hz, 1H), 8.02 – 7.96 (m, 2H), 7.91 (d, *J* = 8.6 Hz, 1H), 7.78 (dd, *J* = 8.5, 1.8 Hz, 1H), 7.59 (d, *J* = 2.3 Hz, 1H), 7.43 (dd, *J* = 8.1, 2.2 Hz, 1H), 6.79 (d, *J* = 8.1 Hz, 1H), 4.91 (s, 1H), 4.45 (t, *J* = 5.2 Hz, 2H), 3.64 – 3.56 (m, 2H), 2.21 (s, 7H), 2.13 (s, 4H), 1.82 (s, 7H), 1.46 (s, 9H). **13C NMR** (126 MHz, CDCl3) δ 154.81, 141.59, 137.09, 136.19, 133.10, 131.37, 131.15, 129.88, 128.42, 126.65, 125.89, 125.74, 124.86, 117.53, 110.17, 40.74, 37.21, 37.09, 29.20, 28.54.

6-(3-((3r,5r,7r)-Adamantan-1-yl)-4-(2-aminoethoxy)phenyl)-2-naphthoic acid [3.3]. 3.S3 (1.0 eq, 97 mg, 0.17 mmol) was dissolved in 0.5 mL DCM with 0.5 mL trifluoroacetic acid (10 eq, 1.7 mmol). This reaction stirred at room temperature for 18 h. It was then quenched with sat. NaHCO3, extracted with DCM (3x), and dried over $MgSO_4$, concentrated, and purified by flash column chromatography in a gradient of hexanes and ethyl acetate to yield a white solid (74 mg, 95% yield). **1H NMR** (500 MHz, DMSO-d6) δ 13.03 (s, 1H), 8.60 (d, *J* = 1.7 Hz, 1H), 8.22 (s, 1H), 8.11 (dd, *J* = 38.9, 8.6 Hz, 2H), 7.93 (ddd, *J* = 42.1, 8.5, 1.8 Hz, 2H), 7.63 (dd, *J* = 8.4, 2.3 Hz, 1H), 7.58 (d, *J* = 2.4 Hz, 1H), 7.09 (d, *J* = 8.6 Hz, 1H), 6.98 (t, *J* = 5.5 Hz, 1H), 4.07 (t, *J* = 5.7 Hz, 2H), 3.44 (q, *J* = 5.7 Hz, 2H), 2.15 (s, 7H), 2.06 (s, 4H), 1.84 – 1.68 (m, 7H). **13C NMR** (126 MHz, DMSO-d6) δ 167.45, 157.60, 155.57, 140.17, 138.09, 135.46, 131.51, 130.90, 130.22, 129.82, 128.34, 127.63, 125.91, 125.67, 125.47, 125.16, 124.06, 113.07, 77.67, 66.19, 36.68, 36.53, 28.49, 28.21. **HRMS (ES+):** Found 442.2378 (0.82 ppm) $C_{29}H_{32}O_3N$ (M+H+) requires 442.2377.

(6-(3-((3r,5r,7r)-Adamantan-1-yl)-4-(2-aminoethoxy)phenyl)naphthalen-2-yl)methanol [3.4]. Lithium aluminum hydride (1.1 eq, 2.0 mg, 0.05 mmol) was dissolved in 0.4 mL Et2O. To this, **3.3** (1.0 eq, 20 mg, 0.045mmol) was added at 0 °C. The reaction mixture stirred, warming to room temperature, for 2 h. It was then cooled to 0 °C and quenched with 0.4 mL of water and 0.4 mL of 1M aqueous NaOH. The slurry was filtered over celite and washed with EtOAc. The collected filtrate was then extracted with EtOAc (3x). The combined organic layers were washed with brine, dried over MgSO4, filtered, concentrated, and

purified by flash column chromatography in a gradient of hexanes and ethyl acetate to yield a yellow oil (14 mg, 73% yield). **1H NMR** (600 MHz, Acetone-d) δ 8.10 (dd, *J* = 1.9, 0.8 Hz, 1H), 7.93 (d, *J* = 8.4 Hz, 2H), 7.87 – 7.85 (m, 1H), 7.79 (dd, *J* = 8.5, 1.8 Hz, 1H), 7.64 (d, *J* = 2.4 Hz, 1H), 7.59 (dd, *J* = 8.4, 2.4 Hz, 1H), 7.52 (dd, *J* = 8.4, 1.7 Hz, 1H), 7.11 (d, *J* = 8.4 Hz, 1H), 6.16 (s, 1H), 4.80 (s, 2H), 4.18 (t, *J* = 5.8 Hz, 2H), 3.62 (q, *J* = 5.8 Hz, 3H), 2.24 (s, 6H), 2.10 (s, 3H), 1.90 – 1.77 (m, 7H). **13C NMR** (151 MHz, Acetoned) δ 317.23, 315.77, 315.62, 310.51, 310.29, 305.51, 302.74, 302.71, 301.74, 290.23, 255.22, 243.84, 241.17, 217.82, 217.43, 214.19, 209.04, 205.01, 199.74, 193.37, 190.77. **HRMS (ES+):** Found 428.2581 (-0.68 ppm) $C_{29}H_{34}O_2N$ (M+H+) requires 428.2584.

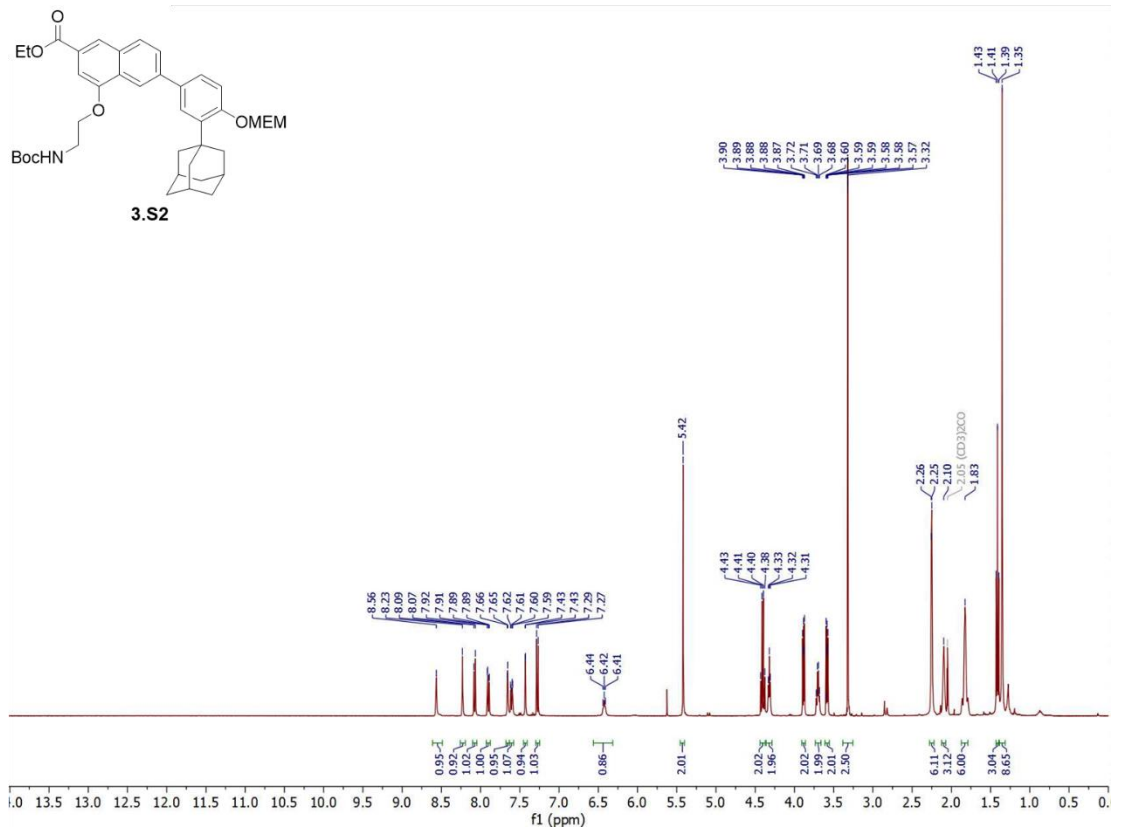
EtO
O
O
OMEM
BocHN
3.S2
f1 (ppm)

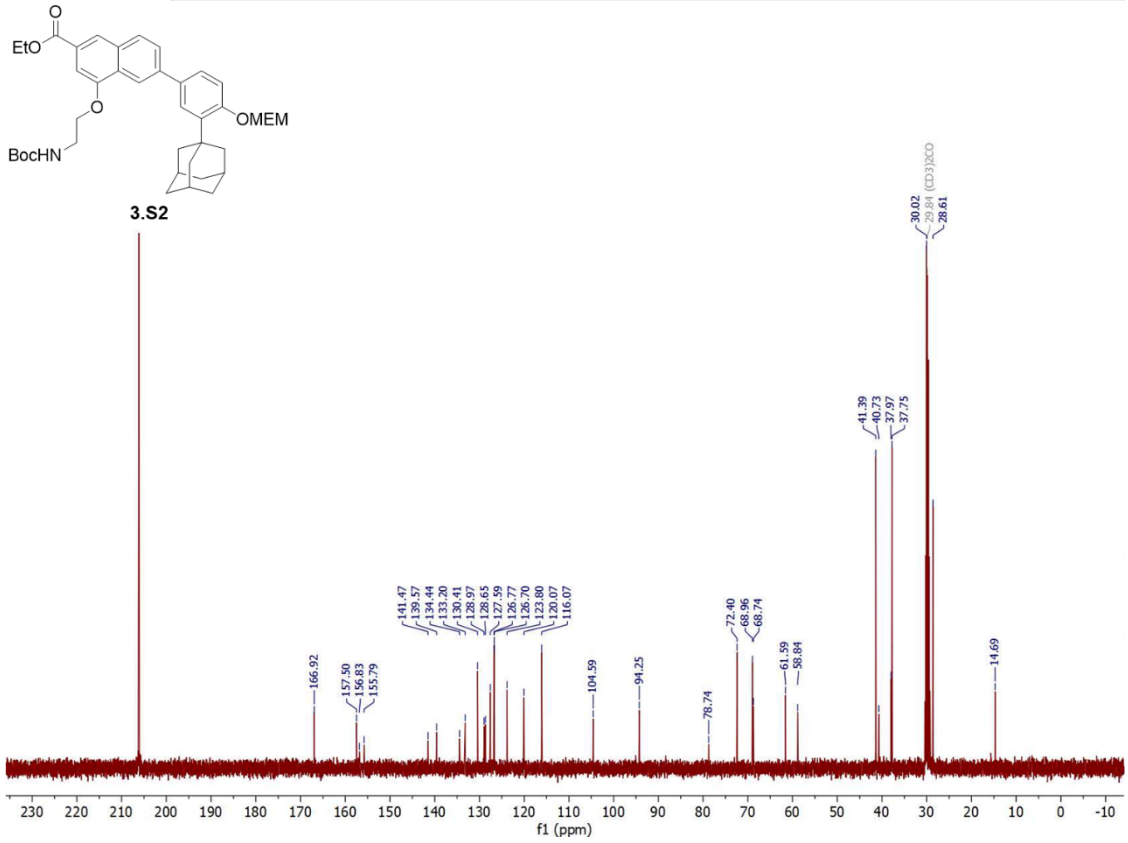
EtO
O
O
OMEM
BocHN
3.S2
f1 (ppm)

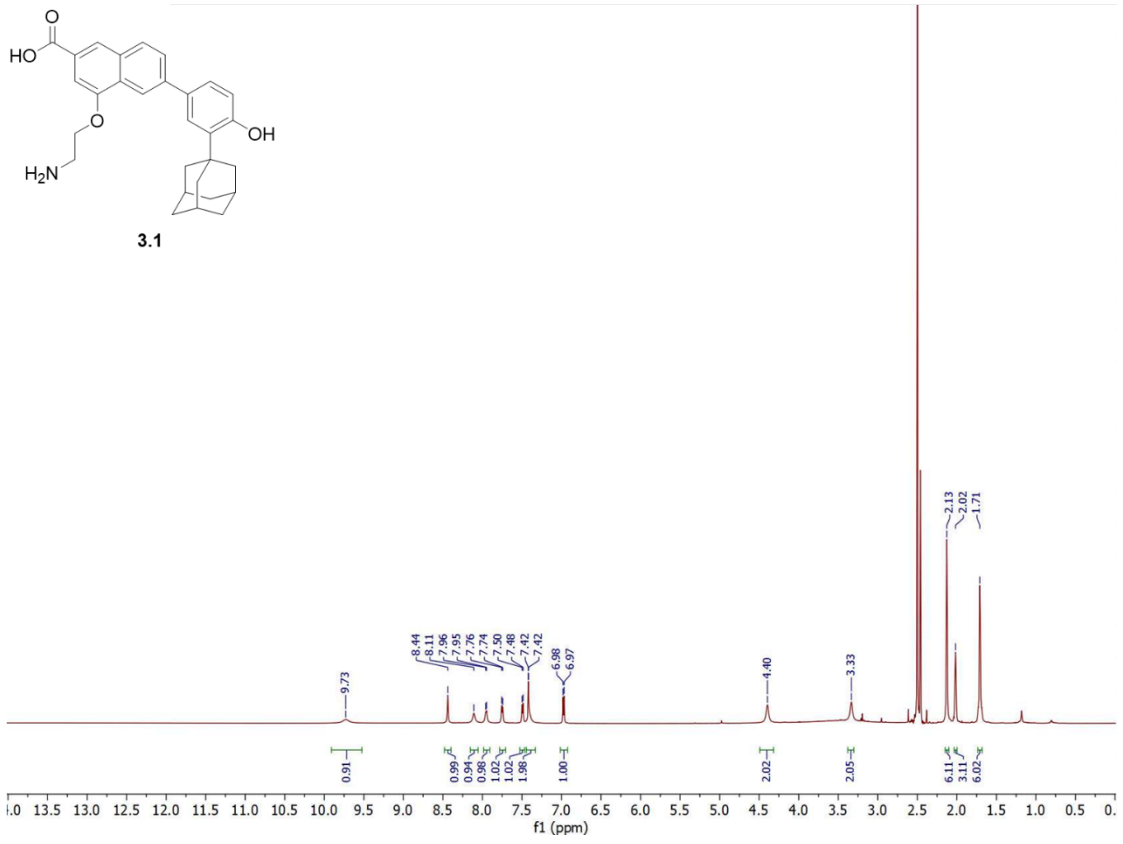
HO
O
O
OH
H2N
3.1
9.73
8.44
8.11
7.96
7.95
7.76
7.74
7.50
7.48
7.42
7.42
6.98
6.97
4.40
3.33
2.13
2.02
1.71
0.91
0.99
0.94
0.98
1.02
1.02
1.98
1.00
2.02
2.05
6.11
3.11
6.02
f1 (ppm)

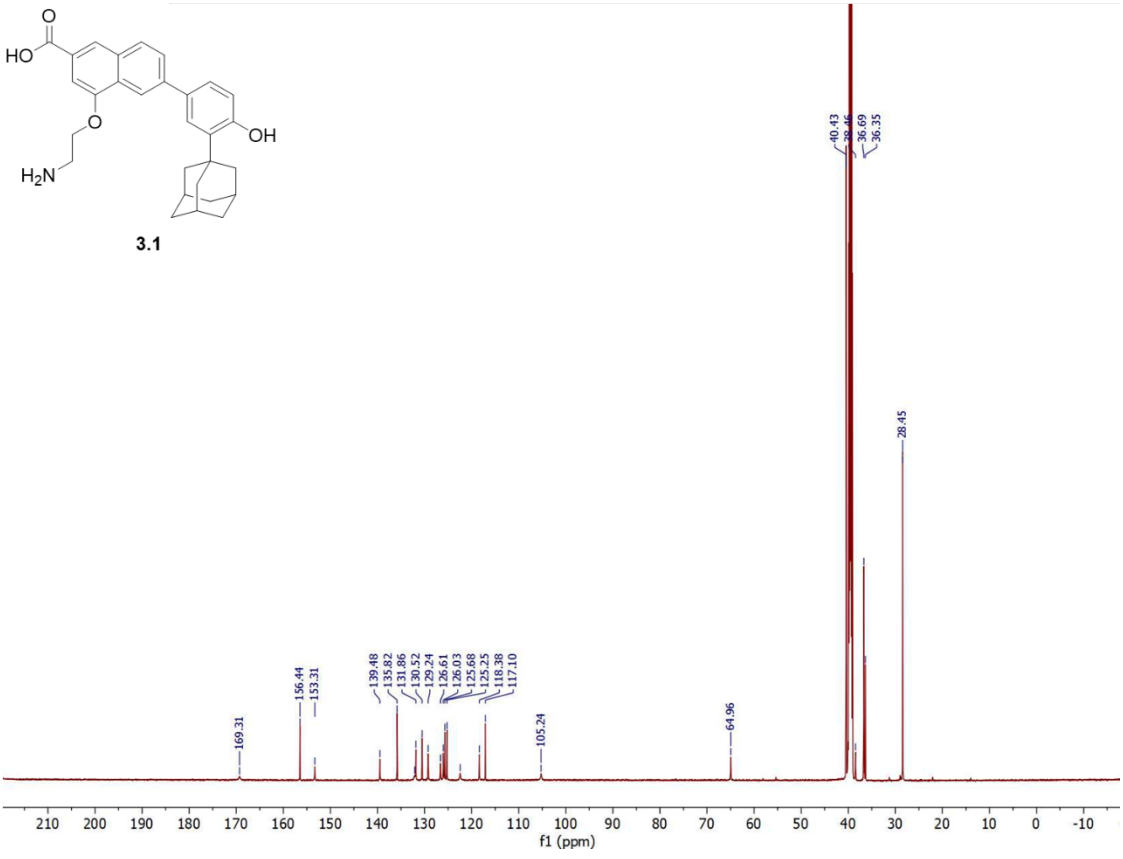
HO
O
O
OH
H2N
3.1
40.43
36.69
36.35
28.45
169.31
156.44
153.31
139.48
135.82
131.86
130.52
129.24
126.61
126.03
125.68
125.25
118.38
117.10
105.24
64.96
f1 (ppm)

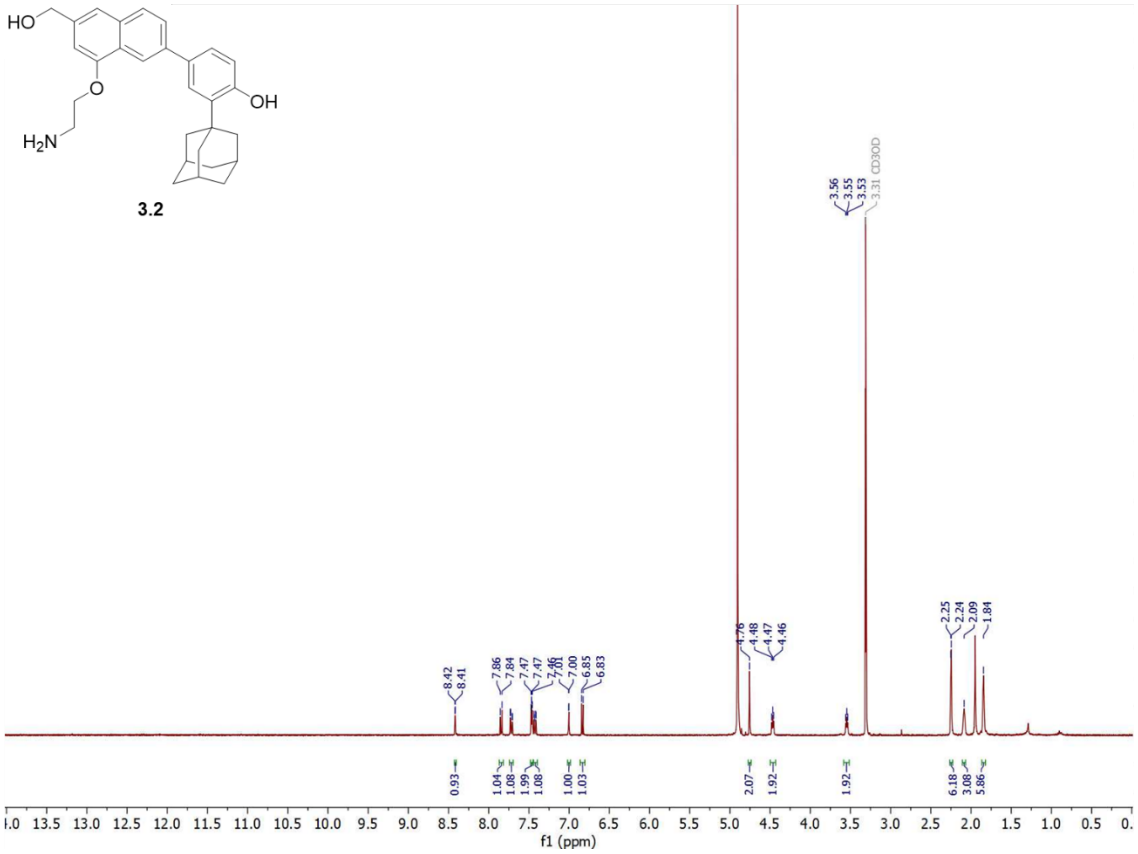
HO
O
OH
H_2N
3.2
8.42
8.41
7.86
7.84
7.47
7.47
7.46
7.46
7.00
6.85
6.83
4.76
4.48
4.47
4.46
3.56
3.55
3.53
3.31 CD3OD
2.25
2.24
2.09
1.84
0.93
1.04
1.08
1.99
1.08
1.00
1.03
2.07
1.92
1.92
6.18
3.08
5.86
f1 (ppm)

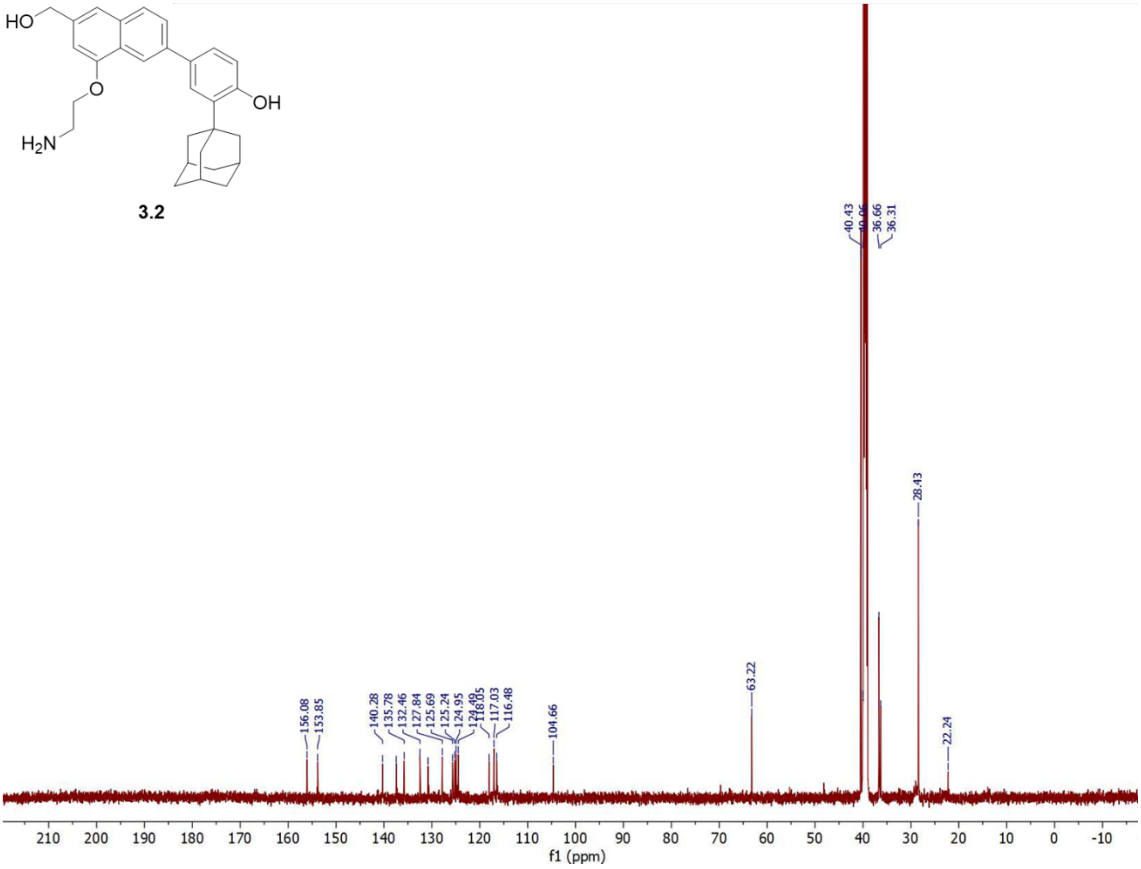
HO
O
OH
H_2N
3.2
40.43
36.66
36.31
28.43
63.22
156.08
153.85
140.28
135.78
132.46
127.84
125.69
125.24
124.95
117.03
116.48
104.66
22.24
f1 (ppm)

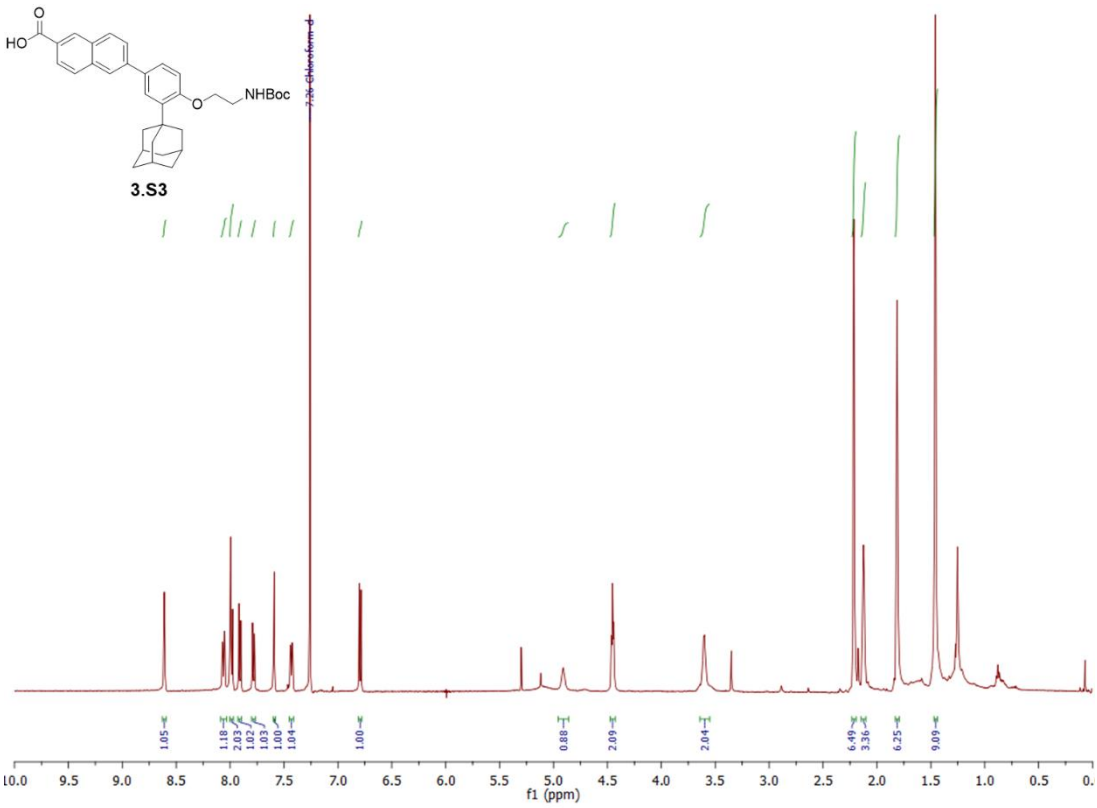
HO
O
NHBoc
3.S3
7.26 Chloroform-d
1.05
1.18
2.03
1.02
1.03
1.00
1.04
1.00
0.88
2.09
2.04
6.49
3.36
6.25
9.09
f1 (ppm)

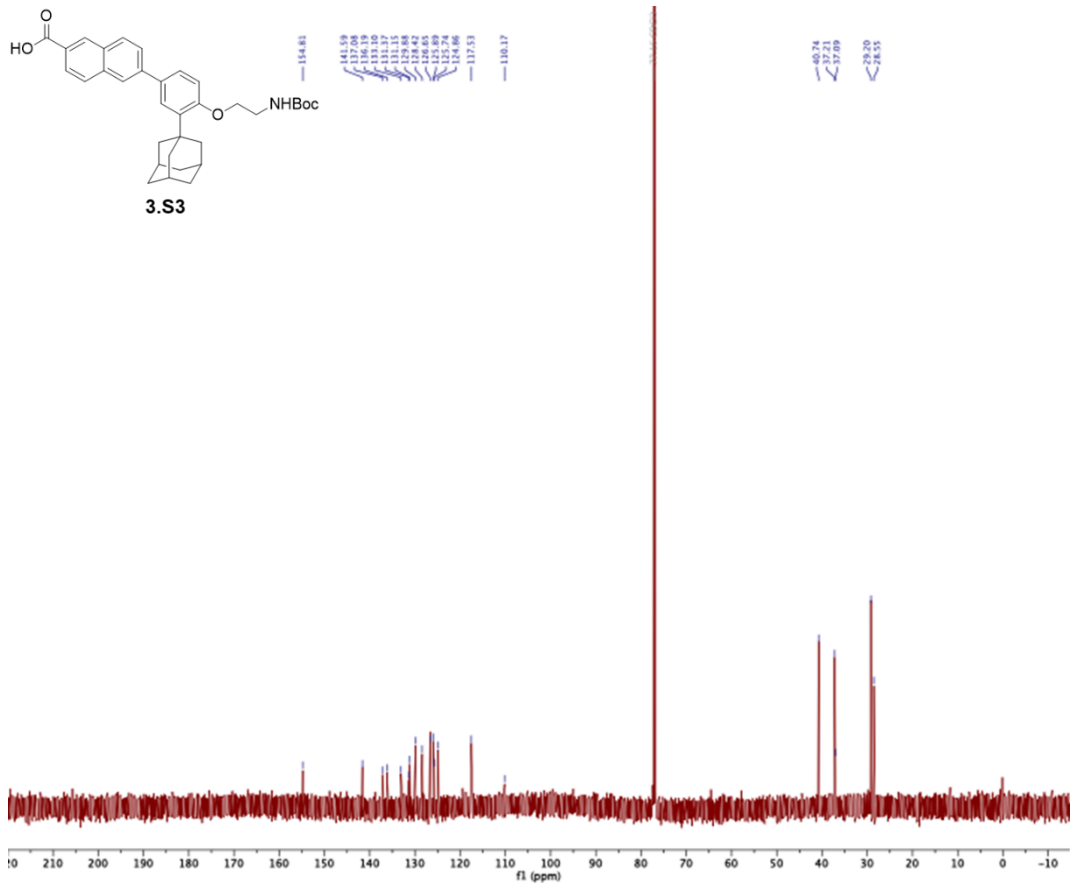
HO
O
NHBoc
3.S3
154.81
141.59
137.08
132.19
133.10
131.37
131.15
129.88
128.42
126.65
125.89
125.74
124.86
117.53
110.17
80.74
37.21
37.09
29.20
28.55
f1 (ppm)

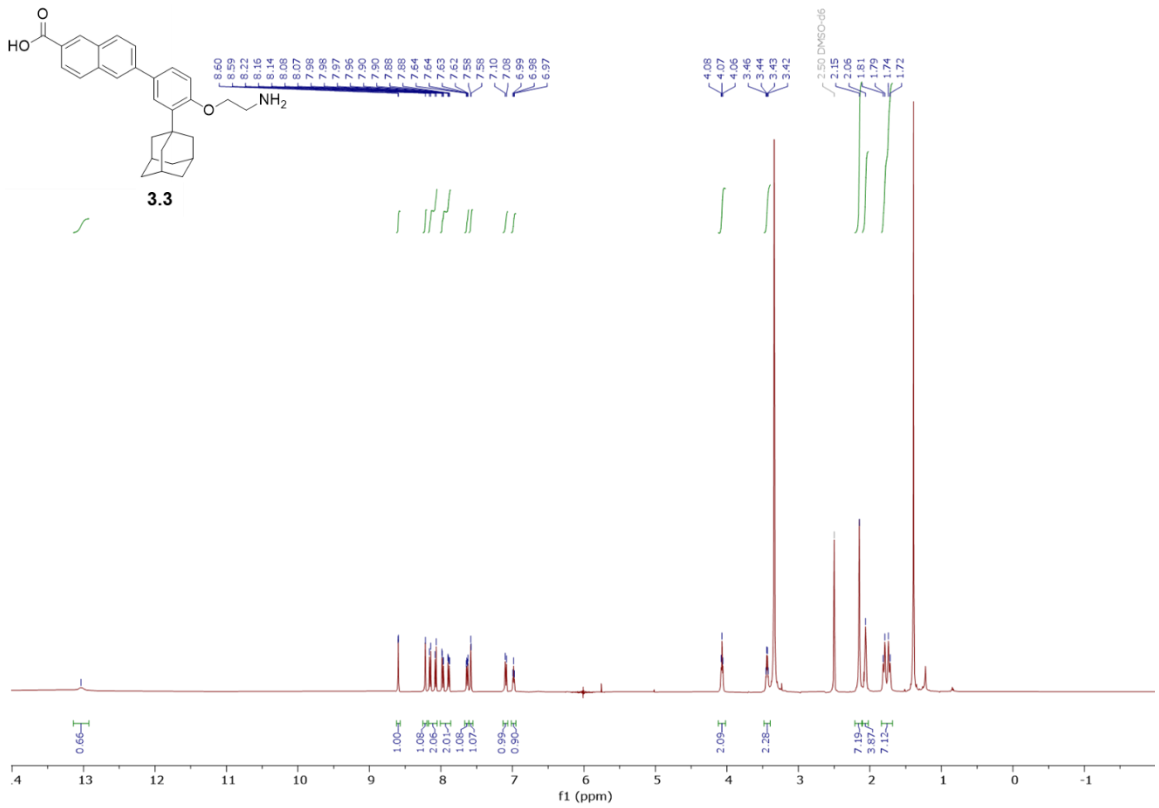
HO
O
NH2
3.3
f1 (ppm)

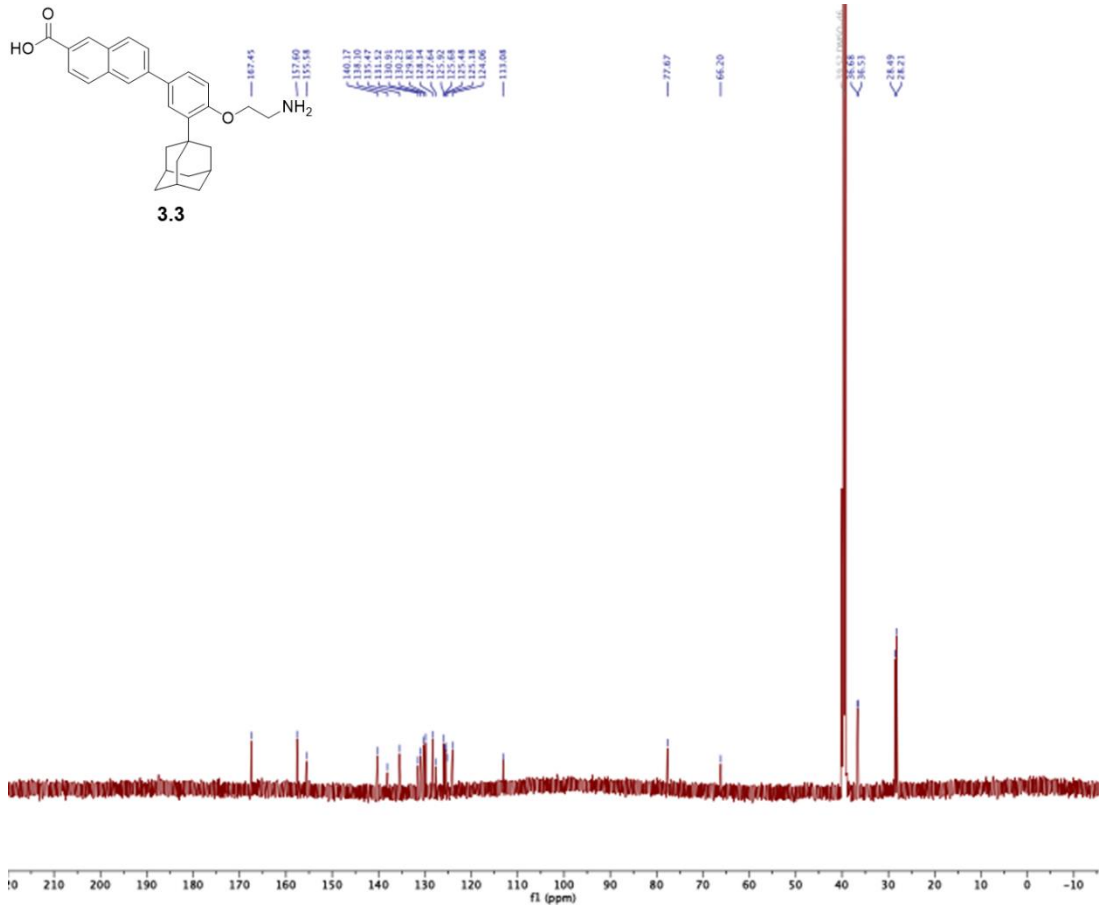
HO
O
NH2
3.3
f1 (ppm)

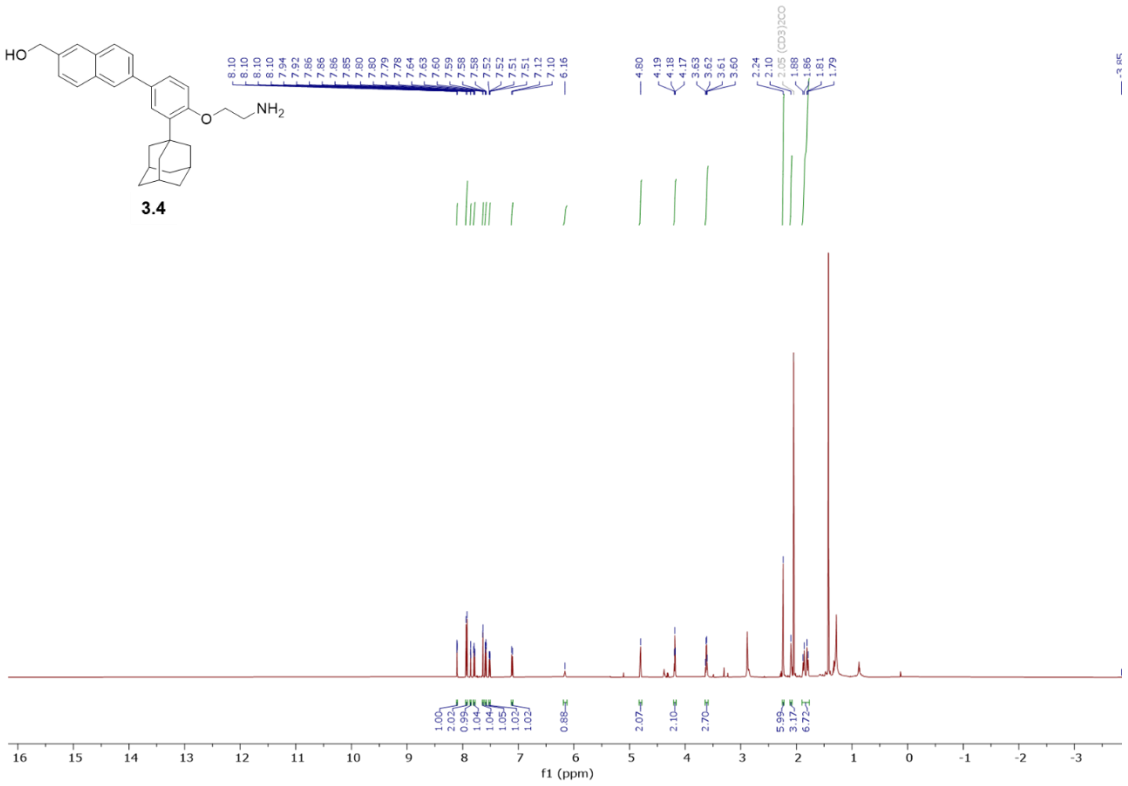
HO
O
NH2
3.4
f1 (ppm)

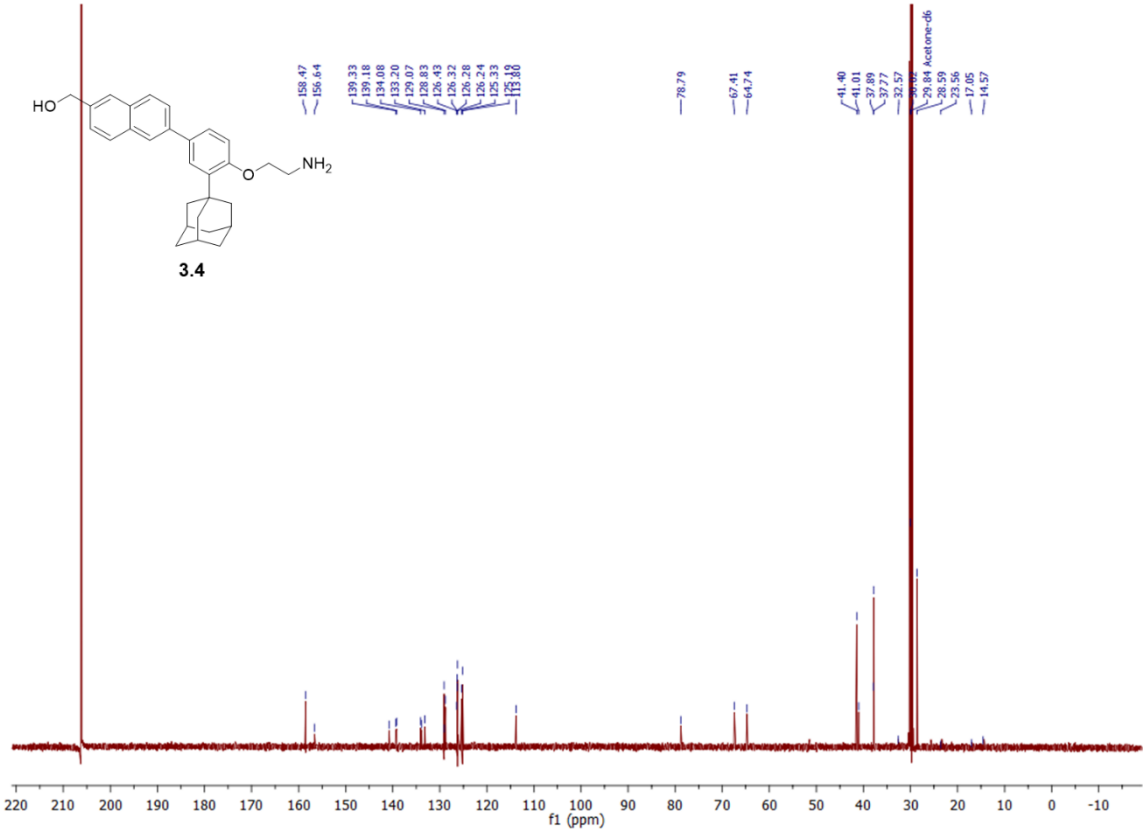
HO
O
NH2
3.4
f1 (ppm)

Chapter 3 Supporting Information

Biology

Biology was completed by Michael Cory.

[SI]

Chemistry

Chemistry was completed by Ana V. Cheng.

General Methods: NMR spectra were recorded using the following spectrometers: Varian INOVA 600, INOVA500, INOVA400, two VNMRS400, two Mercury300, Bruker AVANCE III HD 600, Bruker NANO HD III 400, Bruker AVANCE 600 WB SSNMR, and Bruker AVANCE III 300 WB SSNMR. Chemical shifts are quoted in ppm relative to the indicated solvents. The following abbreviations are used to describe splitting: s (singlet), d (doublet), t (triplet), q (quartet), m (multiplet), and dd (doublet of doublets). Accurate mass spectra were recorded using a Thermo LTQ-FTMS. Non-aqueous reactions were performed using flame-dried glassware under an atmosphere of Argon with HPLC-grade solvents purified on a Pure Process Technology solvent purification system. Brine refers to a saturated solution of sodium chloride, sat. Na_2CO_3 to a saturated aqueous solution of sodium carbonate, sat. $NaHCO_3$ to a saturated solution of sodium bicarbonate, and Na_2SO_4 to magnesium sulfate. Column chromatography was performed using a Biotage® flash chromatography purification system. Chemicals were used as received from Oakwood, Sigma-Aldrich, Alfa Aesar, or AK Scientific. All final compounds were assessed for >95% purity using either ^1H NMR integrations or an Agilent Technologies 1100 Series HPLC with the following parameters: 5µm 9.4 x 250mm FLOW column, a mobile phase gradient of water-acetonitrile dosed with 0.1% formic acid, and a MWD UV/Vis Detector.

Table S2. Base-catalyzed click troubleshooting

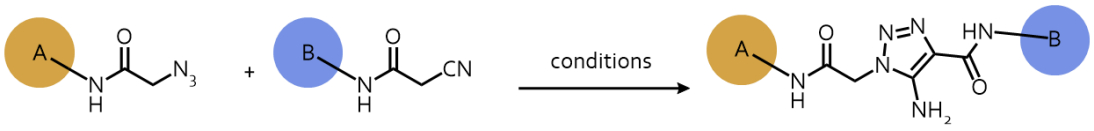

A	B	Conditions	Notes
4-ethoxyphenyl	Ph	EtONa, EtOH 40 °C, 4 h	One pot azide formation and click Dihydropyrrolone product (3% yield)
4-ethoxyphenyl	Ph	EtONa, EtOH RT 1 d then 40 °C 4 h	Dihydropyrrolone (7% yield)
4-ethoxyphenyl	2,4,6-trichlorophenyl	EtONa, EtOH 40 °C 24 h	Monitored by TLC—no new spots observed No product, recovered starting material
4-ethoxyphenyl	2,4,6-trichlorophenyl	EtONa, EtOH 40 °C, 3 d	Increased base eq. (from 1.2 to 2.1) Monitored by TLC—no new spots observed No product, recovered starting material
4-ethoxyphenyl	2,4,6-trichlorophenyl	EtONa, EtOH 40 °C, 4 h	Made EtONa fresh with Na° Monitored by TLC—no new spots observed No product, recovered starting material
4-ethoxyphenyl	2,4,6-trichlorophenyl	$CsCO_3$, $DMSO/H_2O$ RT, 24 h	Monitored by TLC—no new spots observed No product, recovered starting material
4-ethoxyphenyl	Ph	K_2CO_3, MeCN 80 °C, 3 h	Product in 53% yield

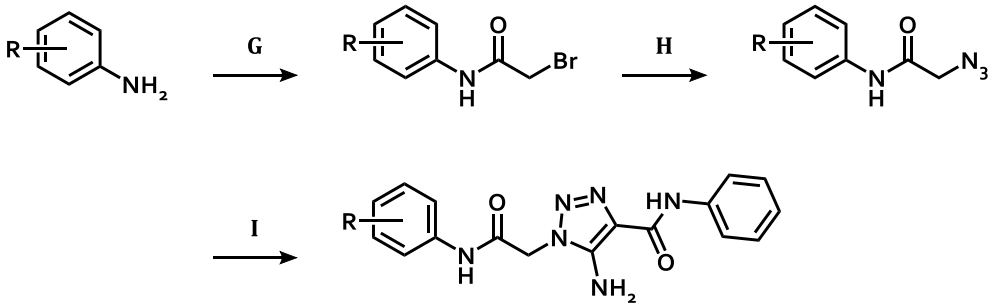

Figure S5. General synthesis of LexA inhibitors.

General procedure G: To a solution of substituted aniline in dichloromethane (1.0 eq) was added triethylamine (1.1 eq) followed by 2-bromoacetyl bromide (1.0 eq). The solution stirred at room temperature for 3-5 hours at room temperature during which a darkening of color was observed. Reaction progress was monitored via TLC (eluent: 4:1 hexanes:ethyl acetate). Upon consumption of starting material, the solution was washed with water, brine, then dried over Na_2SO_4. The organic layer was filtered through a silica plug which was then rinsed with ethyl acetate. The resultant solution was concentrated to yield pure amide product (typically a white or yellow solid).

General procedure H: Substituted 2-bromoacetamides (1.0 eq) were combined with sodium azide (1.2 eq) in EtOH and heated to reflux. Reaction progress was monitored via TLC (eluent: 4:1 dichloromethane:ethyl acetate). Upon consumption of starting material, the reaction solution was concentrated and suspended in water. The aqueous layer was extracted 3x with ethyl acetate. The organic layer was washed with brine, dried over Na_2SO_4, and concentrated. The product was purified via column chromatography (hexanes/ethyl acetate) to yield a yellow solid.

General procedure I: Substituted 2-azidoacetamides (1.0 eq) were combined with **4.S13** (1.7 eq) and K_2CO_3 (6.0 eq) in acetonitrile. The resultant suspension was stirred at reflux for 3-5 hours. Reaction progress was monitored via TLC (eluent: 4:1 dichloromethane:ethyl acetate). Upon consumption of the limiting reagent (and appearance of a more polar spot that stained with ninhydrin), the mixture was concentrated and suspended in water. The aqueous layer was extracted 3x with ethyl acetate. The organic layer was washed with brine, dried over Na_2SO_4, and concentrated. The product was purified via column chromatography (hexanes/ethyl acetate) and then further purified via HPLC for biological testing.

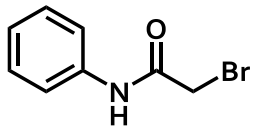

2-bromo-*N*-phenylacetamide. 4.*S*1 was prepared from aniline using general procedure G (94% yield). Structure was confirmed by comparison to published data.[172,173] **^{1}H NMR** (400 MHz, Chloroform-d) δ 8.18 (s, 1H), 7.53 (d, J = 7.5 Hz, 2H), 7.41 – 7.31 (m, 2H), 7.17 (t, J = 7.4 Hz, 1H), 4.02 (s, 2H).

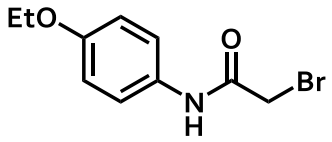

2-bromo-*N*-(4-ethoxyphenyl)acetamide. 4.*S*2 was prepared from 4-ethoxyaniline using general procedure G (81% yield). Structure was confirmed by comparison to published data.[174] **^{1}H NMR** (400 MHz, Chloroform-*d*) δ 8.05 (s, 1H), 7.41 (d, *J* = 9.0 Hz, 2H), 6.87 (d, *J* = 9.0 Hz, 2H), 4.02 (q, J = 7.0 Hz, 2H), 4.02 (s, 2H) 1.41 (t, *J* = 7.0 Hz, 3H).

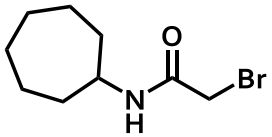

2-bromo-N-cycloheptylacetamide. 4.*S*3 was prepared from cycloheptylamine using general procedure G (57% yield). Structure was confirmed by comparison to published data.[175] **^{1}H NMR** (400 MHz, Chloroform-d) δ 6.46 (s, 1H), 4.00 – 3.87 (m, 1H), 3.86 (s, 2H), 2.00 – 1.38 (m, 12H).

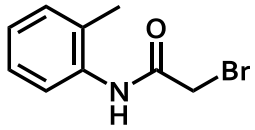

2-bromo-*N*-(*o*-tolyl)acetamide. 4.*S*4 was prepared from *o*-toluidine using general procedure G (89% yield). Structure was confirmed by comparison to published data.[174] **^{1}H NMR** (400 MHz, Chloroform-d) δ 8.15 (s, 1H), 7.85 (dd, J = 7.9, 1.4 Hz, 1H), 7.26 – 7.19 (m, 2H), 7.12 (td, J = 7.5, 1.3 Hz, 1H), 4.08 (s, 2H), 2.31 (s, 3H).

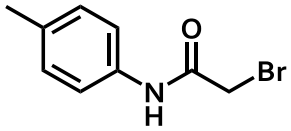

2-bromo-*N*-(*p*-tolyl)acetamide. 4.*S*5 was prepared from *p*-toluidine using general procedure G (91% yield). Structure was confirmed by comparison to published data.[173,174] **^{1}H NMR** (400 MHz, Chloroform-d) δ 8.13 (s, 1H), 7.40 (d, J = 8.5 Hz, 2H), 7.15 (dd, J = 8.7, 0.8 Hz, 2H), 4.01 (s, 2H), 2.33 (s, 3H).

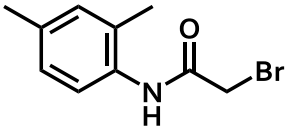

2-bromo-N-(2,4-dimethylphenyl)acetamide. 4.S6 was prepared from 2,4-dimethylaniline using general procedure G (96% yield). Structure was confirmed by comparison to published data.[176] **^{1}H NMR** (400 MHz, Chloroform-d) δ 8.07 (s, 1H), 7.64 (d, J = 8.8 Hz, 1H), 7.05 – 6.98 (m, 2H), 4.06 (s, 2H), 2.30 (s, 3H), 2.26 (s, 3H).

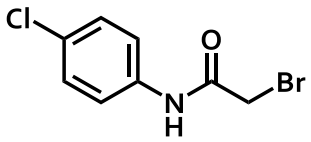

2-bromo-N-(4-chlorophenyl)acetamide. 4.S7 was prepared from 2,4-dimethylaniline using general procedure G (88% yield). Structure was confirmed by comparison to published data.[173] **^{1}H NMR** (400 MHz, Chloroform-d) δ 8.15 (s, 1H), 7.49 (d, J = 8.9 Hz, 2H), 7.32 (d, J = 8.9 Hz, 2H), 4.02 (s, 2H).

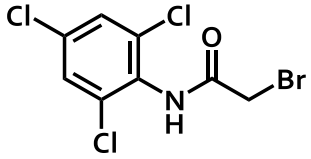

2-bromo-*N*-(2,4,6-trichlorophenyl)acetamide. 4.S8 was prepared from 2,4,6-trichloroaniline using general procedure G (99% yield). Structure was confirmed by comparison to published data.[177] **^{1}H NMR** (400 MHz, Acetone-d6) δ 9.36 (s, 1H), 7.61 (s, 2H), 4.15 (s, 2H).

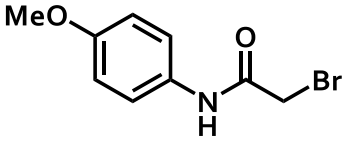

2-bromo-*N*-(4-methoxyphenyl)acetamide. 4.S9 was prepared from 4-methoxyaniline using general procedure G (72% yield). Structure was confirmed by comparison to published data.[173,174] **^{1}H NMR** (400 MHz, Chloroform-d) δ 8.07 (s, 1H), 7.42 (d, J = 9.0 Hz, 2H), 6.88 (d, J = 9.0 Hz, 2H), 4.01 (s, 2H), 3.80 (s, 3H).

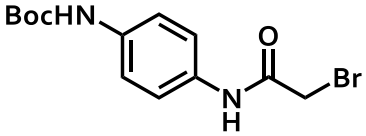

2-bromo-*N*-(*N*-Boc-4-aminophenyl)acetamide. 4.S10 was prepared from *N*-Boc-4-aminoaniline (obtained in 99% yield from *p*-phenylenediamine)[178] using general procedure

G (96% yield). Structure was confirmed by comparison to published data.[179] **^{1}H NMR** (400 MHz, Acetone-d6) δ 9.40 (s, 1H), 8.36 (s, 1H), 7.57 (d, J = 9.1 Hz, 2H), 7.51 (d, J = 9.1 Hz, 2H), 4.01 (s, 2H), 1.48 (s, 9H).

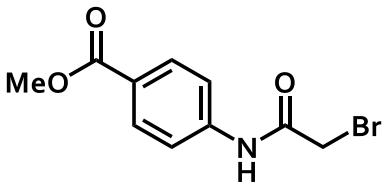

Methyl 4-(2-bromoacetamido)benzoate. 4.S11 was prepared from methyl 4-aminobenzoate using general procedure G (94% yield). Structure was confirmed by comparison to published data.[174] **^{1}H NMR** (400 MHz, Chloroform-d) δ 8.28 (s, 1H), 8.04 (d, J = 8.8 Hz, 2H), 7.63 (d, J = 8.7 Hz, 2H), 4.04 (s, 2H), 3.91 (s, 3H).

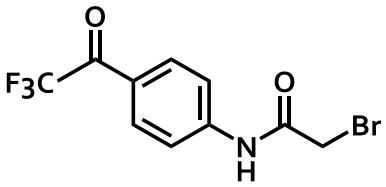

2-bromo-*N*-(4-(trifluoroacetyl)phenyl)acetamide. 4.S12 was prepared from 4-trifluoroacetylaniline (obtained over 2 steps in 94% yield)[180] using general procedure G (99% yield). **^{1}H NMR** (600 MHz, Chloroform-d) δ 8.35 (s, 1H), 8.10 (d, J = 8.5 Hz, 2H), 7.76 (d, J = 8.8 Hz, 2H), 4.06 (s, 2H). **^{13}C NMR** (151 MHz, CDCl3) δ 179.60, 179.37, 179.14, 178.91, 163.89, 143.36, 131.98, 126.35, 119.75, 119.46, 117.82, 115.89, 113.96, 29.33. **HRMS** Accurate mass (APCI+): found 309.96876 (0.83 ppm), $C_{10}H_8O_2N^{79}BrF_3$ ($M+H^+$) requires 309.9685.

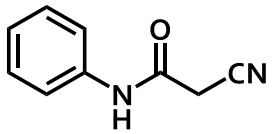

2-cyano-N-phenylacetamide 4.S13. To **4.S1** (2.206 g, 10.31 mmol, 1.0 eq) in dimethylformamide (10 mL) was added potassium cyanide (1.410g, 21.65 mmol, 2.1 eq). The mixture was stirred at room temperature overnight. Reaction progress was monitored by TLC (eluent: 4:1 dichloromethane:ethyl acetate). Upon consumption of starting material, the mixture was concentrated, suspended in water, and extracted with ethyl acetate 3x. The organic layer was washed with brine, dried over Na_2SO_4, and concentrated. The resultant crude mixture was purified via column chromatography in a gradient of hexanes/ethyl acetate (product eluted at 30% ethyl acetate) to yield the product as a pale orange solid (95% yield). Structure was confirmed by comparison to published data.[181] **^{1}H NMR** (400 MHz, Acetone-d6) δ 9.49 (s, 1H), 7.61 (dd, J = 8.5, 1.1 Hz, 2H), 7.33 (dd, J = 8.5, 7.5 Hz, 2H), 7.11 (t, J = 7.4 Hz, 1H), 3.82 (s, 2H).

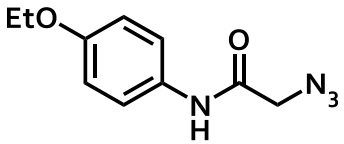

2-azido-*N*-(4-ethoxyphenyl)acetamide. 4.S14 was prepared from **4.S2** using general procedure H. Product was carried on without full characterization. **^{1}H NMR** (400 MHz, Chloroform-d) δ 7.96 (s, 1H), 7.41 (d, J = 9.0 Hz, 2H), 6.86 (d, J = 9.0 Hz, 2H), 4.11 (s, 2H), 4.00 (q, J = 6.9 Hz, 2H), 1.40 (t, J = 7.0 Hz, 3H).

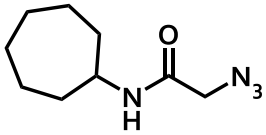

2-azido-N-cycloheptylacetamide. 4.S15 was prepared from **4.S3** using general procedure H (91% yield). **^{1}H NMR** (600 MHz, Chloroform-d) δ 6.26 (s, 1H), 3.96 – 3.91 (m, 1H), 3.91 (s, 2H), 1.94 – 1.39 (m, 12H). **^{13}C NMR** (151 MHz, CDCl3) δ 165.25, 52.83, 50.55, 35.01, 28.00, 24.05. **HRMS** Accurate mass (APCI+): found 197.13943 (-1.33 ppm), $C_9H_{17}ON_4$ ($M+H^+$) requires 197.13969.

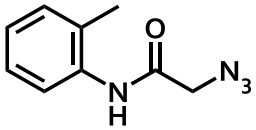

2-azido-*N*-(*o*-tolyl)acetamide. 4.S16 was prepared from **4.S4** using general procedure H. Product was carried on without full characterization. **^{1}H NMR** (600 MHz, Chloroform-d) δ 7.97 (s, 1H), 7.84 (d, J = 8.1 Hz, 1H), 7.23 – 7.18 (m, 2H), 7.11 (t, J = 7.2 Hz, 1H), 4.15 (s, 2H), 2.28 (s, 3H).

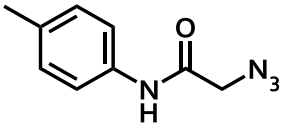

2-azido-*N*-(*p*-tolyl)acetamide. 4.S17 was prepared from **4.S5** using general procedure H (96% yield). Structure was confirmed by comparison to published data.[182] **^{1}H NMR** (600 MHz, Chloroform-d) δ 8.01 (s, 1H), 7.41 (d, J = 8.4 Hz, 2H), 7.14 (d, J = 8.3 Hz, 2H), 4.10 (s, 2H), 2.32 (s, 3H).

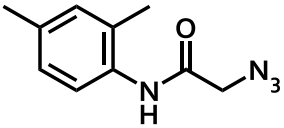

2-azido-N-(2,4-dimethylphenyl)acetamide. 4.S18 was prepared from **4.S6** using general procedure H. Product was carried on without full characterization. **^{1}H NMR** (600 MHz, Chloroform-d) δ 7.88 (s, 1H), 7.65 (d, J = 8.7 Hz, 1H), 7.05 – 6.97 (m, 2H), 4.15 (s, 2H), 2.30 (s, 3H), 2.24 (s, 3H).

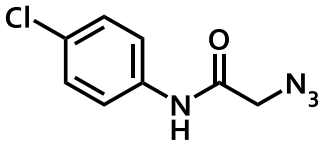

2-azido-N-(4-chlorophenyl)acetamide. 4.S19 was prepared from **4.S7** using general procedure H. Product was carried on without full characterization. **^{1}H NMR** (400 MHz, Chloroform-d) δ 8.04 (s, 1H), 7.50 (d, J = 8.8 Hz, 2H), 7.31 (d, J = 8.8 Hz, 2H), 4.14 (s, 2H).

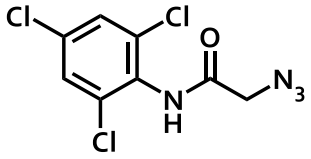

2-azido-*N*-(2,4,6-trichlorophenyl)acetamide. 4.S20 was prepared from **4.S8** using general procedure H (79% yield). **^{1}H NMR** (600 MHz, Chloroform-d) δ 7.83 (s, 1H), 7.40 (s, 2H), 4.20 (s, 2H). **^{13}C NMR** (151 MHz, CDCl3) δ 165.13, 134.35, 134.28, 130.03, 128.69, 52.77. **HRMS** Accurate mass (APCI+): found 278.95977 (-1.45 ppm), $C_8H_6ON_4{}^{35}Cl_3$ ($M+H^+$) requires 278.96017.

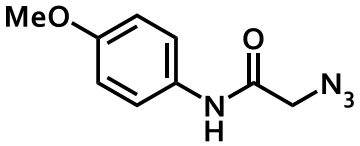

2-azido-*N*-(4-methoxyphenyl)acetamide. 4.S21 was prepared from **4.S9** using general procedure H (99% yield). Structure was confirmed by comparison to published data.[183] **^{1}H NMR** (400 MHz, Chloroform-d) δ 8.02 (s, 1H), 7.42 (d, J = 9.0 Hz, 2H), 6.86 (d, J = 9.0 Hz, 2H), 4.08 (s, 2H), 3.78 (s, 3H).

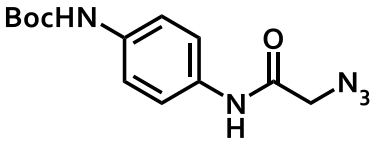

2-azido-*N*-(*N*-Boc-4-aminophenyl)acetamide. 4.S22 was prepared from **4.S10** using general procedure H (91% yield). **^{1}H NMR** (600 MHz, Chloroform-d) δ 8.04 (s, 1H), 7.43 (d, J = 8.9 Hz, 2H), 7.32 (d, J = 8.4 Hz, 2H), 6.61 (s, 1H), 4.09 (s, 2H), 1.50 (s, 9H). **^{13}C NMR** (151 MHz, CDCl3) δ 164.46, 152.87, 135.56, 132.08, 121.04, 119.25, 53.11, 31.07, 28.48. **HRMS** Accurate mass (ESI+): found 314.12228 (-0.26 ppm), $C_{13}H_{17}O_3N_5{}^{23}Na$ ($M+Na^+$) requires 314.12236.

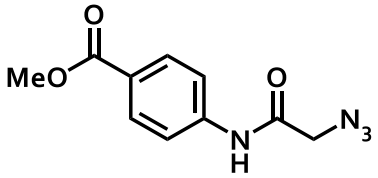

Methyl 4-(2-azidoacetamido)benzoate. 4.S23 was prepared from **4.S11** using general procedure H. Product was carried on without full characterization. **^{1}H NMR** (400 MHz, Chloroform-d) δ 8.21 (s, 1H), 8.02 (d, J = 8.8 Hz, 2H), 7.64 (d, J = 8.8 Hz, 2H), 4.17 (s, 2H), 3.90 (s, 3H).

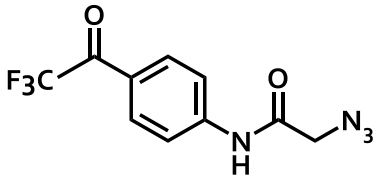

2-azido-*N*-(4-(trifluoroacetyl)phenyl)acetamide. 4.S24 was prepared from **4.S12** using general procedure H (91% yield). **^{1}H NMR** (600 MHz, Chloroform-d) δ 8.31 (s, 1H), 8.08 (d, J = 8.5 Hz, 2H), 7.76 (d, J = 8.8 Hz, 2H), 4.21 (s, 2H). **^{13}C NMR** (151 MHz, CDCl3) δ 179.60, 179.37, 179.14, 178.91, 165.11, 143.24, 131.98, 126.17, 119.75, 119.54, 117.82, 115.89, 113.96, 53.08. **HRMS** Accurate mass (APCI+): found 273.05905 (-1.24 ppm), $C_{10}H_8O_2N_4F_3$ ($M+H^+$) requires 273.05939.

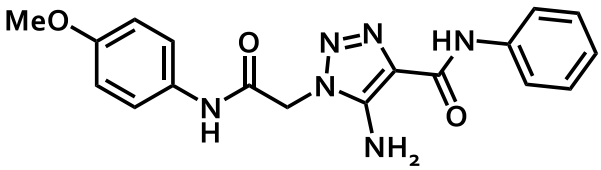

5-Amino-*N*-(4-methoxyphenyl)-4-[(phenylamino)carbonyl]-1*H*-1,2,3-triazole-1-acetamide 4.S25 was prepared from **4.S21** using general procedure I (68% yield). **^{1}H NMR** (600 MHz, Acetone-d6) δ 9.93 (s, 1H), 9.58 (s, 1H), 8.35 (d, J = 7.5 Hz, 2H), 8.00 (d, J = 9.1 Hz, 2H), 7.79 (dd, J = 8.6, 7.3 Hz, 2H), 7.53 (t, J = 7.4 Hz, 1H), 7.34 (d, J = 9.1 Hz, 2H), 6.63 (s, 2H), 5.60 (s, 2H), 4.22 (s, 3H). **^{13}C NMR** (151 MHz, Acetone) δ 164.47, 161.79, 157.31, 147.45, 140.00, 132.48, 129.52, 124.09, 123.29, 121.97, 120.45, 114.78, 55.66, 50.02. **HRMS** Accurate mass (APCI+): found 367.15062 (-1.89 ppm), $C_{18}H_{19}O_3N_6$ ($M+H^+$) requires 367.15131.

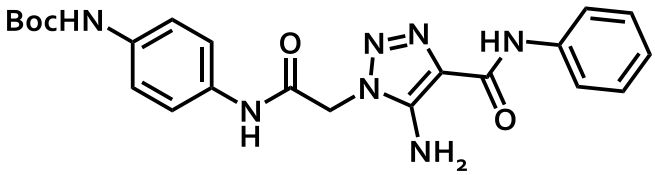

5-Amino-*N*-(*N*-Boc-4-aminophenyl)-4-[(phenylamino)carbonyl]-1*H*-1,2,3-triazole-1-acetamide 4.S26 was prepared from **4.S22** using general procedure I (18% yield). **^{1}H NMR** (400 MHz, Acetone-d6) δ 9.55 (s, 1H), 9.13 (s, 1H), 8.38 (s, 1H), 7.91 (d, J = 8.8 Hz, 2H), 7.59 – 7.48 (m, 4H), 7.34 (dd, J = 8.6, 7.4 Hz, 2H), 7.08 (t, J = 7.4 Hz, 1H), 6.24 – 6.17 (s, 2H), 5.17

(s, 2H), 1.47 (s, 9H). **^{13}C NMR** (151 MHz, DMSO) δ 163.63, 160.79, 152.80, 146.50, 139.06, 135.31, 133.00, 128.46, 122.94, 119.91, 119.60, 78.89, 48.40, 28.13. **HRMS** Accurate mass (ES+): found 474.18554 (-1.02 ppm), $C_{22}H_{25}O_4N_7{}^{23}Na$ ($M+Na^+$) requires 474.18602.

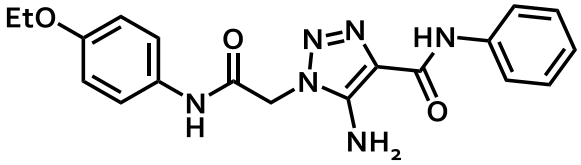

5-Amino-*N*-(4-ethoxyphenyl)-4-[(phenylamino)carbonyl]-1*H*-1,2,3-triazole-1-acetamide 4.1 was prepared from **4.S14** using general procedure I (49% yield over 2 steps). **^{1}H NMR** (600 MHz, DMSO-d6) δ 10.31 (s, 1H), 10.03 (s, 1H), 7.83 (d, J = 7.4 Hz, 2H), 7.49 (d, J = 9.1 Hz, 2H), 7.30 (t, J = 7.9 Hz, 2H), 7.04 (t, J = 7.3 Hz, 1H), 6.89 (d, J = 9.1 Hz, 2H), 6.56 (s, 2H), 5.10 (s, 2H), 3.98 (q, J = 7.0 Hz, 2H), 1.30 (t, J = 7.0 Hz, 3H). **^{13}C NMR** (151 MHz, DMSO) δ 163.53, 160.79, 154.67, 146.48, 139.05, 131.62, 128.46, 122.94, 121.24, 120.61, 119.90, 114.49, 63.06, 48.38, 14.67. **HRMS** Accurate mass (ES+): found 381.16684 (-0.33 ppm), $C_{19}H_{21}O_3N_6$ ($M+H^+$) requires 381.16697.

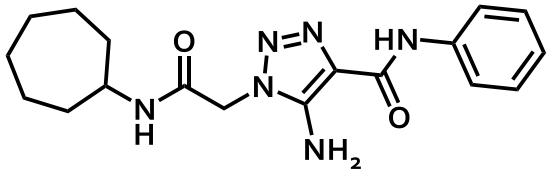

5-Amino-*N*-cycloheptyl-4-[(phenylamino)carbonyl]-1*H*-1,2,3-triazole-1-acetamide 4.2 was prepared from **4.S15** using general procedure I (62% yield). **^{1}H NMR** (600 MHz, DMSO-d6) δ 10.00 (s, 1H), 8.20 (d, J = 7.8 Hz, 1H), 7.82 (d, J = 7.4 Hz, 2H), 7.30 (t, J = 7.9 Hz, 2H), 7.04 (t, J = 7.4 Hz, 1H), 6.45 (s, 2H), 4.85 (s, 2H), 3.83 – 3.65 (m, 1H), 1.86 – 1.31 (m, 12H). **^{13}C NMR** (151 MHz, DMSO) δ 163.97, 160.78, 146.36, 139.04, 128.45, 122.94, 121.30, 119.90, 49.93, 47.97, 34.19, 27.81, 23.62. **HRMS** Accurate mass (APCI+): found 357.20296 (-1.08 ppm), $C_{18}H_{25}O_2N_6$ ($M+H^+$) requires 357.20335.

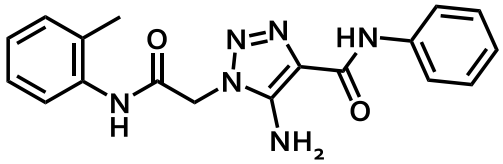

5-Amino-*N*-(*o*-tolyl)-4-[(phenylamino)carbonyl]-1*H*-1,2,3-triazole-1-acetamide 4.3 was prepared from **4.S16** using general procedure I (77% yield over 2 steps). **^{1}H NMR** (600 MHz, DMSO-d6) δ 10.03 (s, 1H), 9.68 (s, 1H), 7.83 (d, J = 7.5 Hz, 2H), 7.47 (d, J = 7.6 Hz, 1H), 7.30 (t, J = 7.9 Hz, 2H), 7.23 (d, J = 7.4 Hz, 1H), 7.17 (t, J = 7.4 Hz, 1H), 7.10 (t, J = 7.1 Hz, 1H), 7.04 (t, J = 7.4 Hz, 1H), 6.57 (s, 2H), 5.18 (s, 2H) 2.26 (s, 3H). **^{13}C NMR** (151 MHz, DMSO) δ 164.24, 160.79, 146.46, 139.05, 135.67, 131.34, 130.40, 128.46, 126.01, 125.34, 124.56, 122.95, 121.30, 119.91, 48.27, 17.83. **HRMS** Accurate mass (APCI+): found 351.15596 9-1.24 ppm), $C_{18}H_{19}O_2N_6$ ($M+H^+$) requires 351.1564.

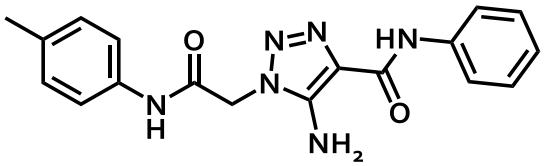

5-Amino-*N*-(*p*-tolyl)-4-[(phenylamino)carbonyl]-1*H*-1,2,3-triazole-1-acetamide 4.4 was prepared from **4.S17** using general procedure I (83% yield). **^{1}H NMR** (600 MHz, DMSO-d6) δ 10.29 (s, 1H), 10.03 (s, 1H), 7.83 (d, J = 7.4 Hz, 2H), 7.48 (d, J = 8.5 Hz, 2H), 7.30 (t, J = 7.9 Hz, 2H), 7.14 (d, J = 8.3 Hz, 2H), 7.04 (t, J = 7.4 Hz, 1H), 6.56 (s, 2H), 5.10 (s, 2H), 2.26 (s, 3H). **^{13}C NMR** (151 MHz, DMSO) δ 163.81, 160.79, 146.50, 139.06, 136.05, 132.55, 129.26, 128.46, 122.95, 121.24, 119.91, 119.10, 48.44, 20.43. **HRMS** Accurate mass (ES): found 351.15597 (-1.24 ppm), $C_{18}H_{19}O_2N_6$ ($M+H^+$) requires 351.1564.

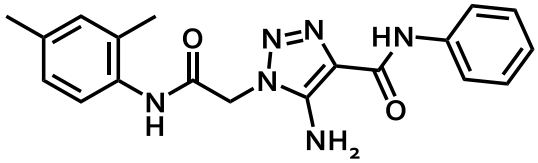

5-Amino-*N*-(2,4-dimethylphenyl)-4-[(phenylamino)carbonyl]-1*H*-1,2,3-triazole-1-acetamide 4.5 was prepared from **4.S18** using general procedure I (29% yield over 2 steps). **^{1}H NMR** (600 MHz, DMSO-d6) δ 10.02 (s, 1H), 9.61 (s, 1H), 7.83 (d, J = 7.6 Hz, 2H), 7.33 – 7.28 (m, 3H), 7.07 – 7.01 (m, 2H), 6.97 (d, J = 8.0 Hz, 1H), 6.56 (s, 2H), 5.15 (s, 2H), 2.24 (s, 3H), 2.21 (s, 3H). **^{13}C NMR** (151 MHz, DMSO) δ 164.18, 160.79, 146.44, 139.05, 134.44, 133.07, 131.31, 130.90, 128.46, 126.50, 124.62, 122.94, 121.30, 119.90, 48.23, 20.45, 17.75. **HRMS** Accurate mass (APCI+): found 365.17174 (-0.85 ppm), $C_{19}H_{21}O_2N_6$ ($M+H^+$) requires 365.17205.

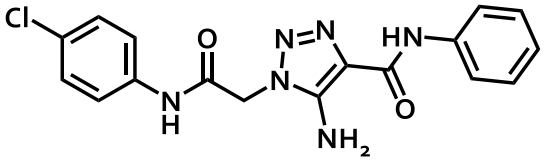

5-Amino-*N*-(4-chlorophenyl)-4-[(phenylamino)carbonyl]-1*H*-1,2,3-triazole-1-acetamide 4.6 was prepared from **4.S19** using general procedure I (47% yield over 2 steps). **^{1}H NMR** (600 MHz, DMSO-d6) δ 10.53 (s, 1H), 10.03 (s, 1H), 7.83 (d, J = 8.0 Hz, 2H), 7.62 (d, J = 8.9 Hz, 2H), 7.40 (d, J = 8.8 Hz, 2H), 7.30 (t, J = 7.9 Hz, 2H), 7.04 (t, J = 7.4 Hz, 1H), 6.58 (s, 2H), 5.13 (s, 2H). **^{13}C NMR** (151 MHz, DMSO) δ 164.25, 160.77, 146.49, 139.05, 137.53, 128.82, 128.46, 127.16, 122.95, 121.22, 120.67, 119.90, 48.47. **HRMS** Accurate mass (APCI+): found 371.10186 (0.22 ppm), $C_{17}H_{16}O_2N_6{}^{35}Cl$ ($M+H^+$) requires 371.10178.

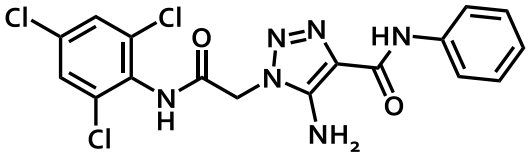

5-Amino-*N*-(2,4,6-trichlorophenyl)-4-[(phenylamino)carbonyl]-1*H*-1,2,3-triazole-1-acetamide 4.7 was prepared from **4.S20** using general procedure I (43% yield). **^{1}H NMR**

(600 MHz, DMSO-d6) δ 10.34 (s, 1H), 10.02 (s, 1H), 7.82 (dd, J = 8.5, 1.1 Hz, 2H), 7.79 (s, 2H), 7.30 (dd, J = 8.6, 7.3 Hz, 2H), 7.04 (t, J = 7.4 Hz, 1H), 6.57 (s, 2H), 5.23 (s, 2H). **^{13}C NMR** (151 MHz, DMSO) δ 164.53, 160.73, 146.45, 139.01, 134.20, 132.67, 131.63, 128.46, 128.38, 122.97, 121.27, 119.92, 47.68. **HRMS** Accurate mass (APCI+): found 439.024 (0.38 ppm), $C_{17}H_{14}O_2N_6{}^{35}Cl_3$ ($M+H^+$) requires 439.02383.

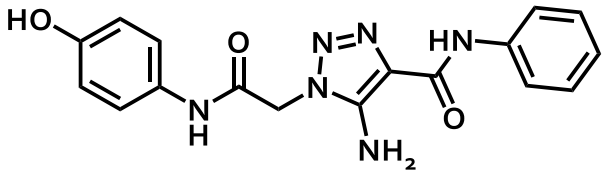

5-Amino-*N*-(4-hydroxyphenyl)-4-[(phenylamino)carbonyl]-1*H*-1,2,3-triazole-1-acetamide 4.8 was prepared from **4.S25**. **4.S25** (60 mg, 0.164 mmol, 1.0 eq) was dissolved in dichloromethane and treated with BBr_3 (1.0 M in DCM, 4.0 eq) at room temperature. Addition of BBr_3 was accompanied by a color change from scarlet red to a dark wine red. Reaction progress was monitored via TLC (eluent: 4:1 dichloromethane:ethyl acetate). Upon consumption of starting material, the solution was diluted with ethyl acetate, washed with saturated $NaHCO_3$, water, and brine. The organic layer was dried over Na_2SO_4 and concentrated. The resulting crude mixture was purified via column chromatography in a gradient of hexanes/ethyl acetate. The product was obtained as red solid and was further purified via HPLC to yield a white solid (39.4 mg, 68% yield). **^{1}H NMR** (600 MHz, DMSO-d6) δ 10.18 (s, 1H), 10.02 (s, 1H), 9.32 (s, 1H), 7.83 (d, J = 7.4 Hz, 2H), 7.37 (d, J = 8.9 Hz, 2H), 7.30 (t, J = 7.9 Hz, 2H), 7.04 (t, J = 7.4 Hz, 1H), 6.71 (d, J = 8.9 Hz, 2H), 6.55 (s, 2H), 5.07 (s, 2H). **^{13}C NMR** (151 MHz, DMSO) δ 163.32, 160.80, 153.61, 146.47, 139.06, 130.18, 128.46, 122.94, 121.25, 120.83, 119.90, 115.19, 48.36. **HRMS** Accurate mass (APCI+): found 353.13566 (-0.01 ppm), $C_{17}H_{17}O_3N_6$ ($M+H^+$) requires 353.13566.

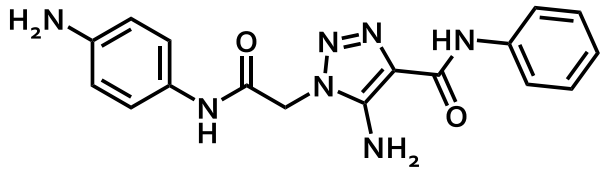

5-Amino-*N*-(4-aminophenyl)-4-[(phenylamino)carbonyl]-1*H*-1,2,3-triazole-1-acetamide 4.9 was prepared from **4.S26. S26** (195 mg, 0.433 mmol) was dissolved in 4.0 M HCl in dioxane (5 mL) at room temperature for 2 hours. The reaction was monitored via TLC. Upon completion, the solution was quenched with saturated Na_2CO_3 then diluted in water. The aqueous layer was extracted with ethyl acetate (3x). The resultant organic layer was washed with brine, dried over Na_2SO_4, and concentrated. The product was obtained as a red solid and purified via HPLC to yield a white solid (126 mg, 83% yield). **^{1}H NMR** (400 MHz, DMSO-d6) δ 10.06 (s, 1H), 10.05 (s, 1H), 7.83 (d, J = 7.5 Hz, 2H), 7.34 – 7.26 (m, 2H), 7.23 (d, J = 8.8 Hz, 2H), 7.04 (t, J = 7.3 Hz, 1H), 6.56 (s, 2H), 6.51 (d, J = 8.8 Hz, 2H), 5.05 (s, 2H), 4.92 (s, 2H). **^{13}C NMR** (101 MHz, DMSO) δ 163.02, 160.85, 146.51, 145.13, 139.09, 128.51, 127.70,

123.00, 121.29, 120.81, 119.95, 113.89, 48.41. **HRMS** Accurate mass (APCI-): found 350.1368 (-0.84 ppm), $C_{17}H_{16}O_2N_7$ (M^-) requires 350.1371.

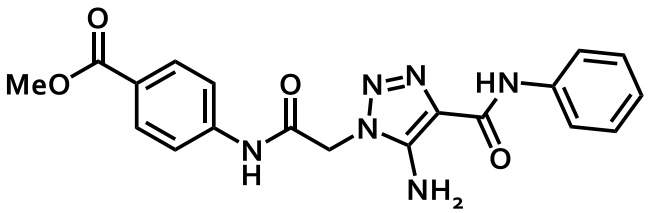

Methyl 4-(2-(5-amino-4-(phenylcarbamoyl)-1H-1,2,3-triazol-1-yl)acetamido) benzoate 4.10 was prepared from **4.S23** using general procedure I (56% yield over 2 steps). **^{1}H NMR** (400 MHz, DMSO-d6) δ 10.81 (s, 1H), 10.05 (s, 1H), 7.95 (d, J = 8.8 Hz, 2H), 7.83 (d, J = 8.6 Hz, 2H), 7.74 (d, J = 8.8 Hz, 2H), 7.35 – 7.26 (m, 2H), 7.04 (t, J = 7.4 Hz, 1H), 6.60 (s, 2H), 5.75 (s, 2H), 3.82 (s, 3H). **^{13}C NMR** (101 MHz, DMSO) δ 165.79, 164.77, 160.81, 146.54, 142.99, 139.08, 130.46, 128.51, 124.35, 123.00, 121.25, 119.94, 118.61, 51.97, 48.65. **HRMS** Accurate mass (APCI+): found 395.14635 (0.3 ppm), $C_{19}H_{19}O_4N_6$ ($M+H^+$) requires 395.14623.

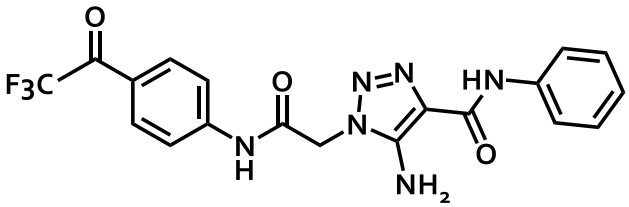

5-amino-1-(2-oxo-2-((4-(2,2,2-trifluoroacetyl)phenyl)amino)ethyl)-N-phenyl-1H-1,2,3-triazole-4-carboxamide 4.11 was prepared from **4.S24** using general procedure I (83% yield). **^{1}H NMR** (400 MHz, DMSO-d6) δ 10.58 (s, 1H), 10.05 (s, 1H), 7.83 (d, J = 7.4 Hz, 2H), 7.59 (d, J = 9.0 Hz, 2H), 7.52 (d, J = 8.7 Hz, 2H), 7.34 – 7.26 (m, 2H), 7.04 (t, J = 7.4 Hz, 1H), 6.59 (s, 2H), 5.14 (s, 2H). **^{13}C NMR** (101 MHz, DMSO) δ 164.25, 160.81, 146.52, 139.08, 138.47, 132.12, 128.49, 127.30, 122.97, 121.25, 119.92, 118.50, 46.84. **HRMS** Accurate mass (APCI+): found 433.12332 (0.63 ppm), $C_{19}H_{16}O_3N_6F_3$ ($M+H^+$) requires 433.12305.

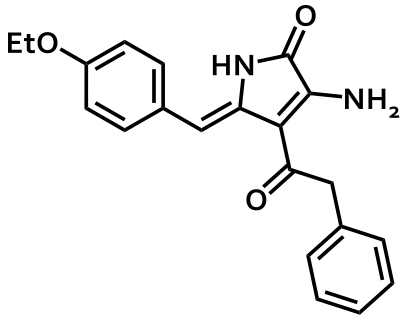

(*Z*)-3-amino-5-(4-ethoxybenzylidene)-4-(2-phenylacetyl)-1,5-dihydro-2*H*-pyrrol-2-one. 4.12. To a solution of **4.S2** (220 mg, 0.851 mmol, 1.0 eq) in ethanol (10 mL) was added sodium azide (66 mg, 1.02 mmol, 1.2 eq). The mixture was heated to reflux for 2 hours.

Separately, **4.S13** (150 mg, 0.936 mmol, 1.1 eq) was dissolved in a solution of sodium ethoxide (70 mg, 1.02 mmol, 1.2 eq) in ethanol (10 mL) and stirred for 10 minutes at room temperature. The two solutions were combined, sonicated for 20 seconds, then heated to 40 °C for 5 hours. The reaction solution was concentrated, suspended in water, and extracted with ethyl acetate (3x). The organic layer was washed with brine, dried over Na_2SO_4, and concentrated. The resultant solid was purified via column chromatography in a gradient of hexanes and ethyl acetate. **4.12** was obtained as a yellow solid (10 mg, 0.029 mmol, 3% yield). **^{1}H NMR** (600 MHz, Chloroform-d) δ 10.56 (s, 1H), 7.62 (d, J = 7.6 Hz, 2H), 7.53 (s, 1H), 7.40 (s, 1H), 7.33 (t, J = 7.9 Hz, 2H), 7.09 (t, J = 7.4 Hz, 1H), 6.95 (d, J = 8.9 Hz, 2H), 6.92 (d, J = 9.0 Hz, 2H), 5.74 (s, 2H), 4.04 (q, J = 6.9 Hz, 2H), 1.44 (t, J = 7.0 Hz, 3H). **^{13}C NMR** (151 MHz, CDCl3) δ 165.32, 162.82, 156.79, 149.98, 148.56, 139.57, 138.30, 129.10, 124.09, 122.88, 120.03, 115.65, 97.15, 63.98, 14.98. **HRMS** Accurate mass (APCI+): found 351.14443 (1.7 ppm), $C_{19}H_{19}O_3N_4$ ($M+H^+$) requires 351.14517.

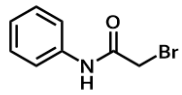

4.S1

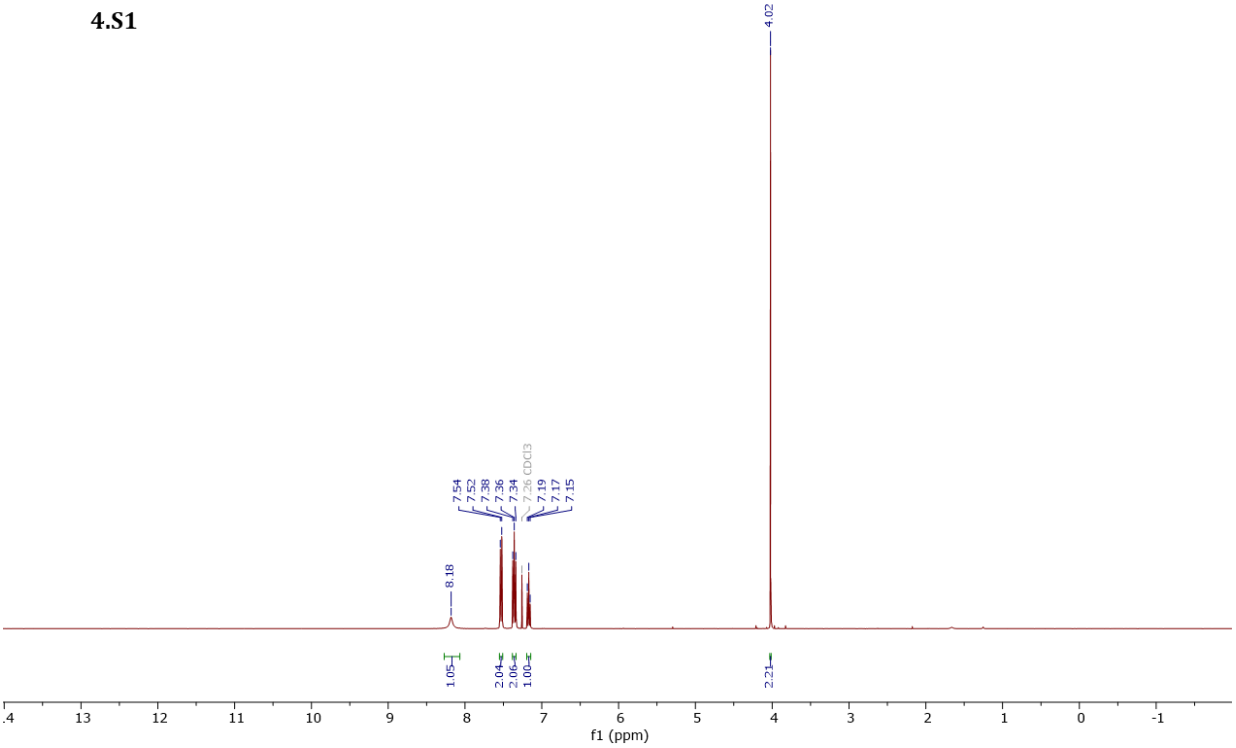
4.02
7.54
7.52
7.38
7.36
7.34
7.26 CDCl3
7.19
7.17
7.15
8.18
1.05
2.04
2.06
1.00
2.21
f1 (ppm)

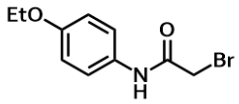

4.S2

4.04
4.03
4.02
4.01
3.99
1.42
1.41
1.39
7.42
7.40
7.26 CDCl3
6.89
6.86
8.05
1.00
2.14
2.20
4.16
3.07
f1 (ppm)

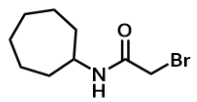

4.S3

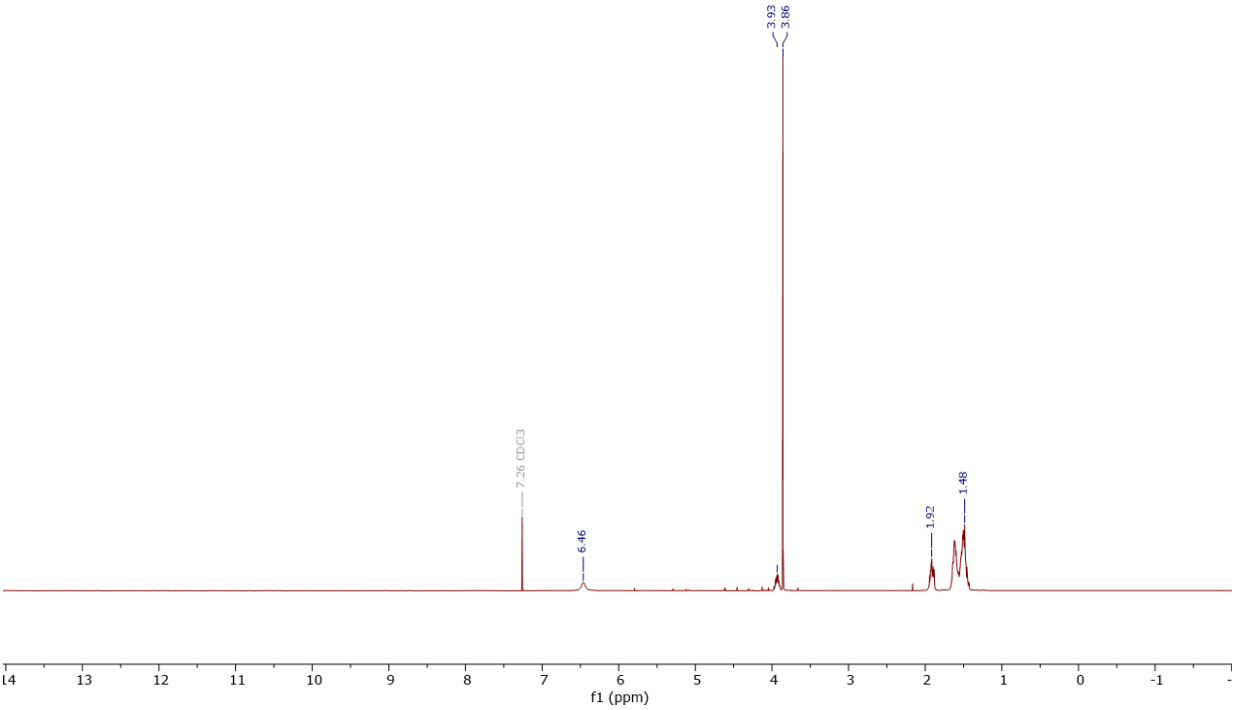
3.93
3.86
7.26 CDCl3
6.46
1.92
1.48
f1 (ppm)

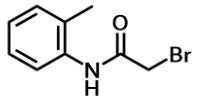

4.S4

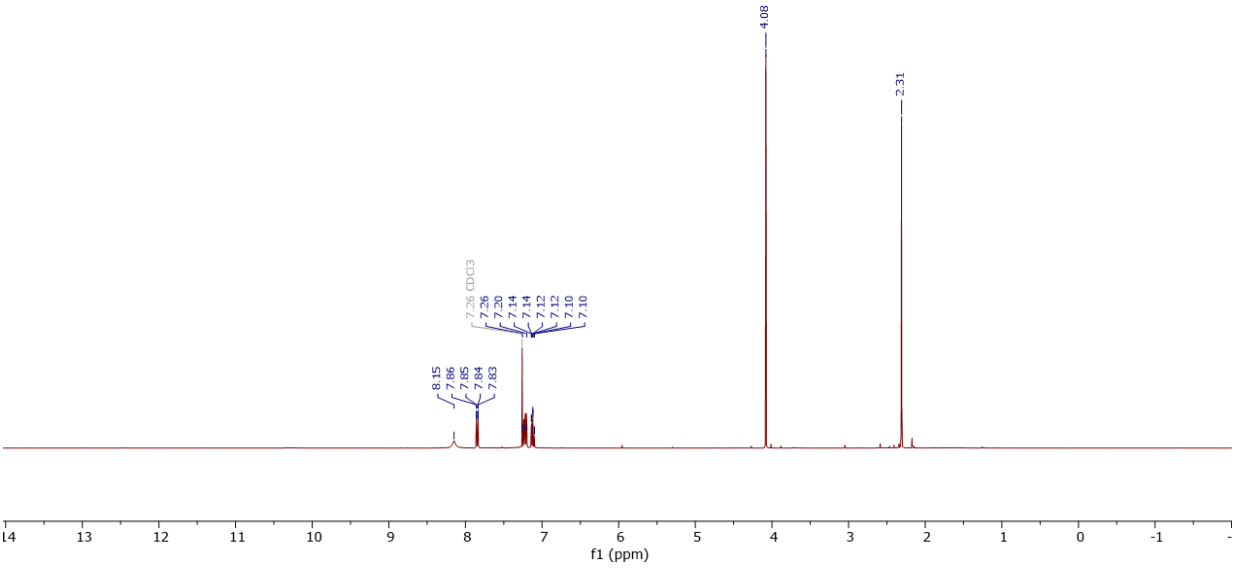
4.08
2.31
7.26 CDCl3
7.26
7.20
7.14
7.14
7.12
7.12
7.10
7.10
8.15
7.86
7.85
7.84
7.83
f1 (ppm)

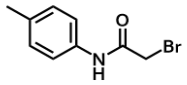

4.S5

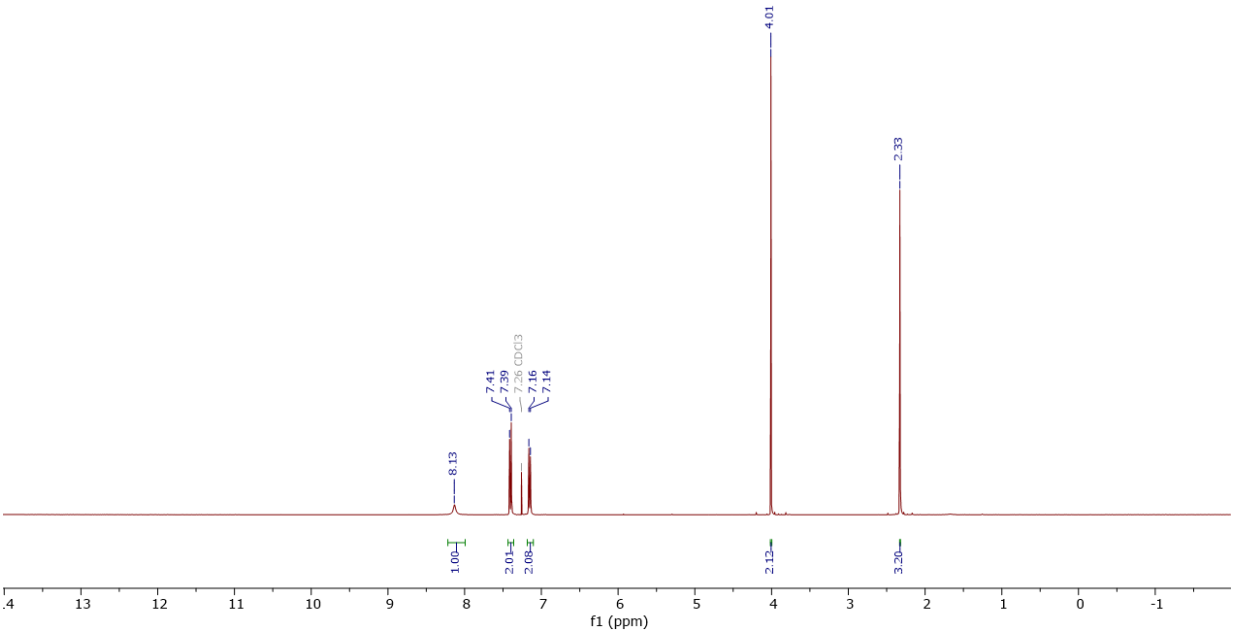
4.01
2.33
7.41
7.39
7.26 CDCl3
7.16
7.14
8.13
1.00
2.01
2.08
2.13
3.20
f1 (ppm)

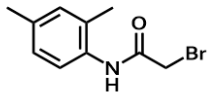

4.S6

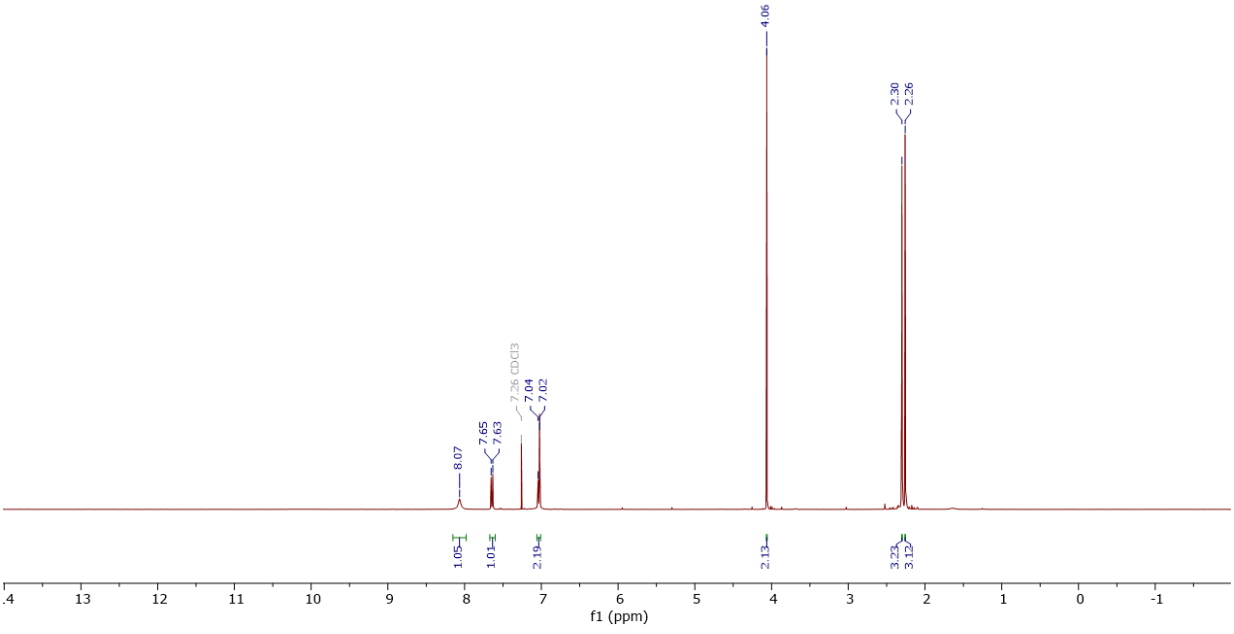
4.06
2.30
2.26
7.26 CDCl3
7.65
7.63
7.04
7.02
8.07
1.05
1.01
2.19
2.13
3.23
3.12
f1 (ppm)

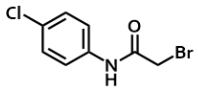
Cl
O
N
H
Br

4.S7

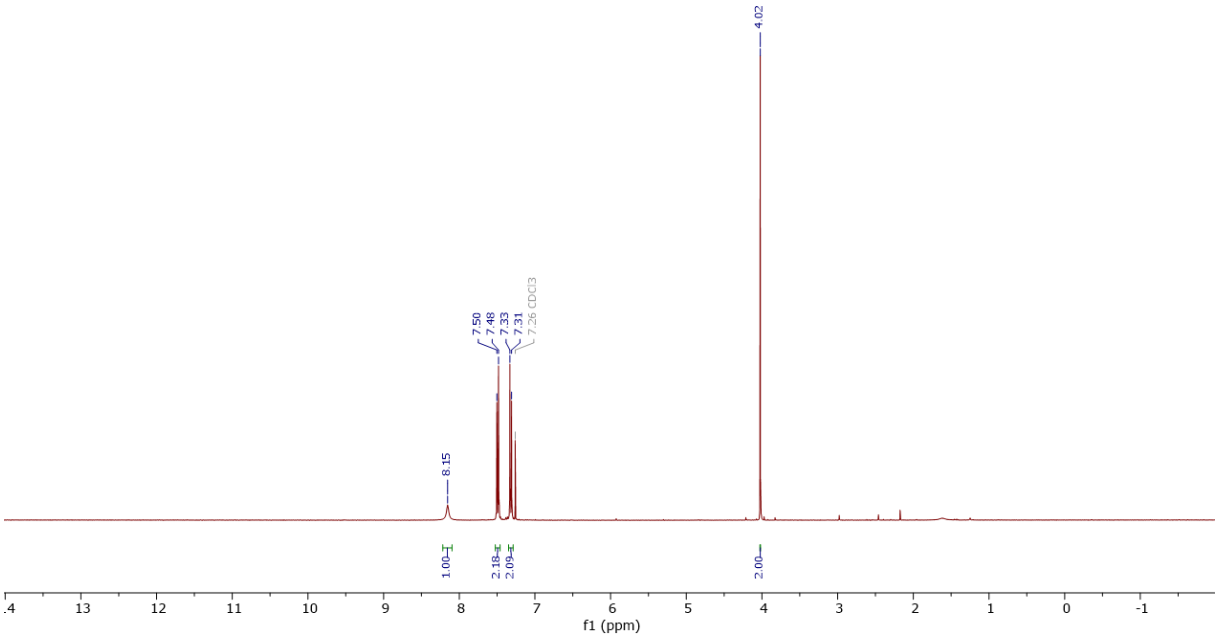
4.02
7.50
7.48
7.33
7.31
7.26 CDCl3
8.15
1.00
2.18
2.09
2.00
f1 (ppm)

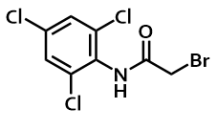
Cl
Cl
O
N
H
Br
Cl

4.S8

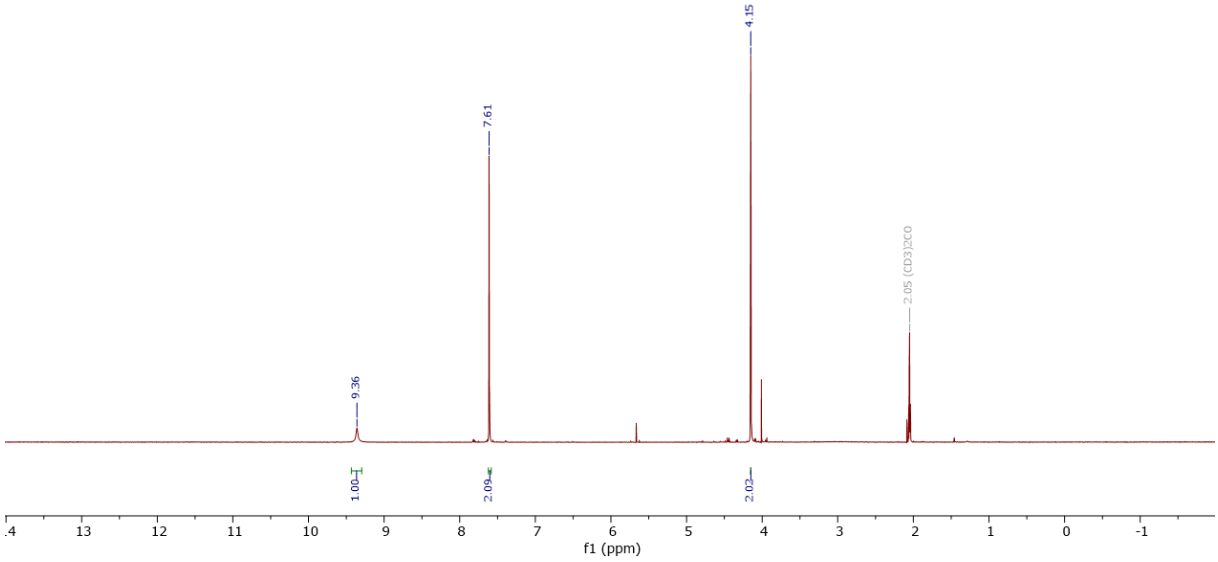
4.15
7.61
2.05 (CD3)2CO
9.36
1.00
2.09
2.02
f1 (ppm)

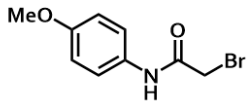
MeO
O
N
H
Br

4.S9

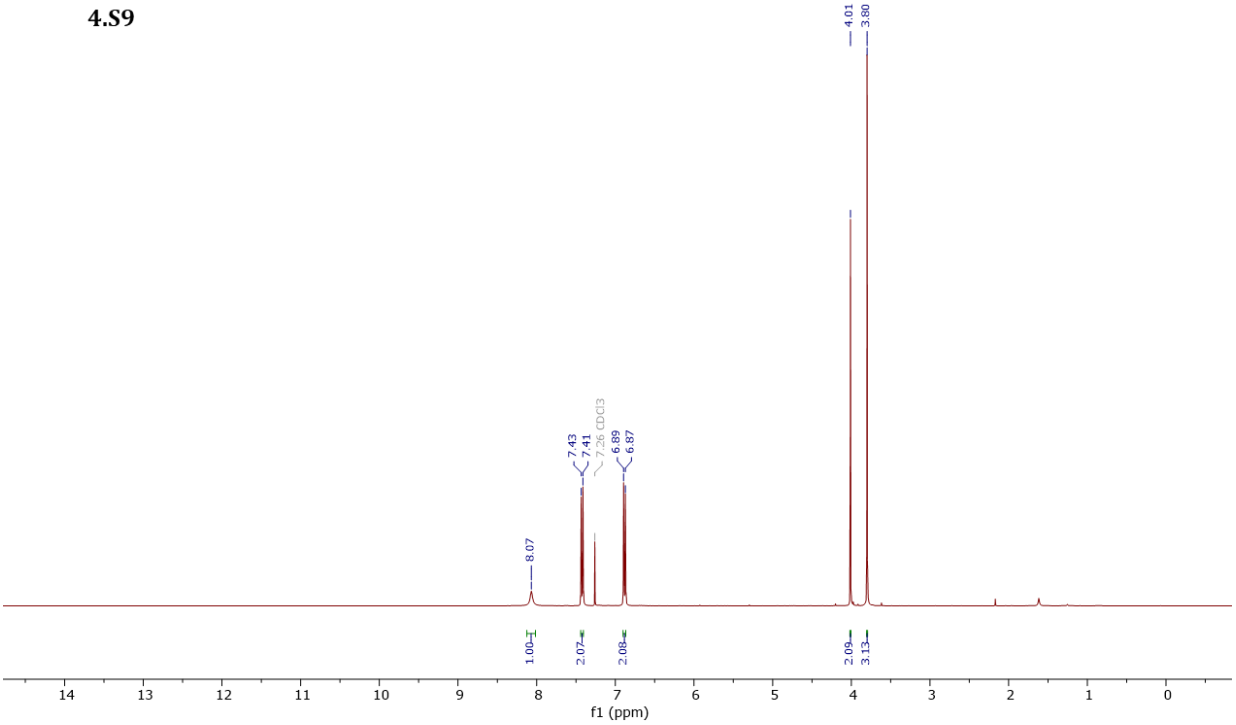
4.01
3.80
7.43
7.41
7.26 CDCl3
6.89
6.87
8.07
1.00
2.07
2.08
2.09
3.13
14 13 12 11 10 9 8 7 6 5 4 3 2 1 0
f1 (ppm)

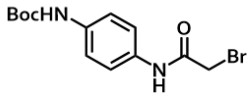
BocHN
O
N
H
Br

4.S10

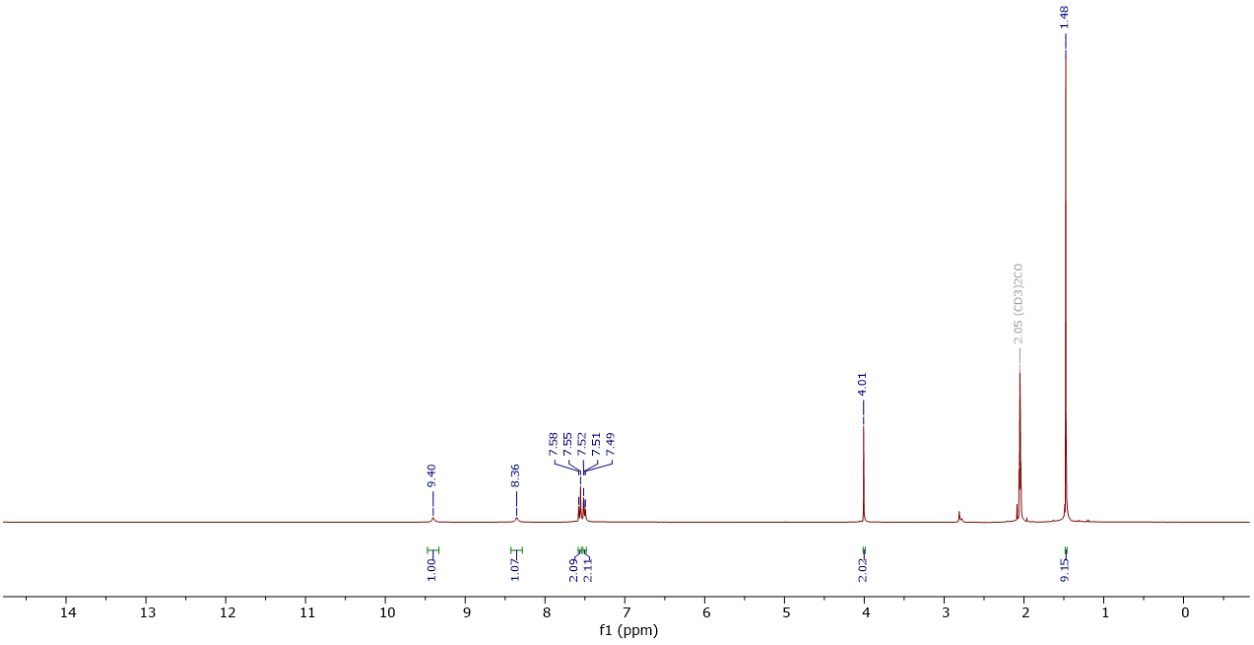
1.48
2.05 (CD3)2CO
4.01
7.58
7.55
7.52
7.51
7.49
9.40
8.36
1.00
1.07
2.09
2.11
2.02
9.15
14 13 12 11 10 9 8 7 6 5 4 3 2 1 0
f1 (ppm)

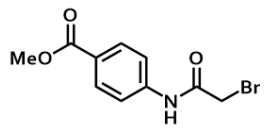
MeO
O
O
N
H
Br

4.S11

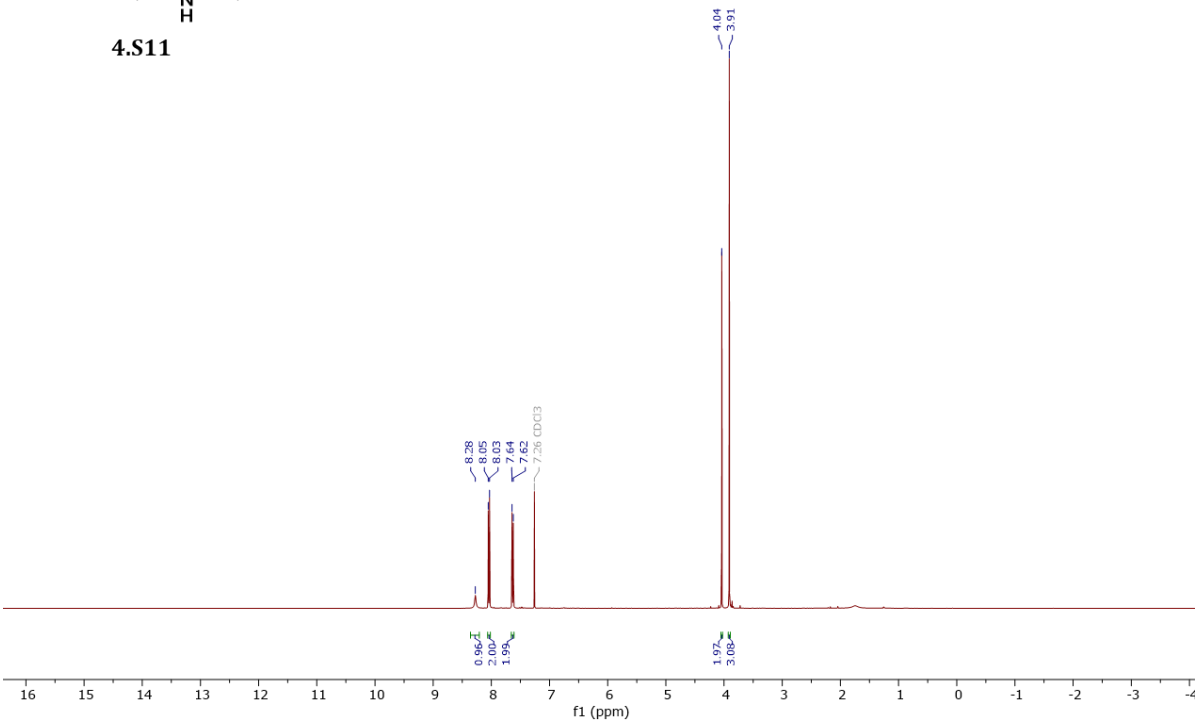
8.28
8.05
8.03
7.64
7.62
7.26 CDCl3
4.04
3.91
0.96
2.00
1.99
1.97
3.08
16
15
14
13
12
11
10
9
8
7
6
5
4
3
2
1
0
-1
-2
-3
f1 (ppm)

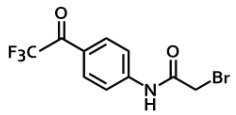

4.S12

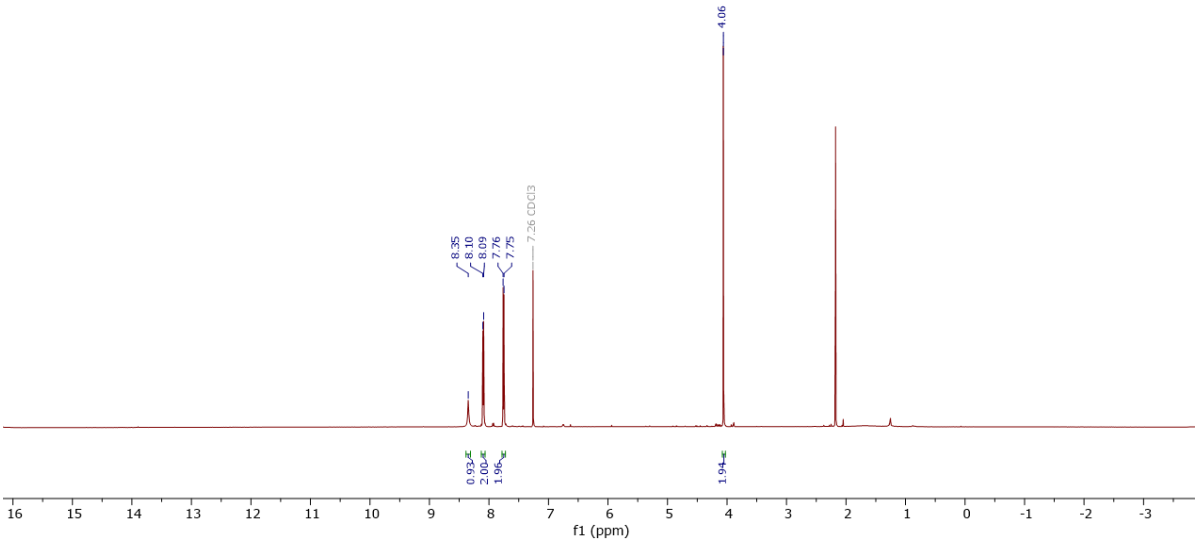
4.06
8.35
8.10
8.09
7.76
7.75
7.26 CDCl3
0.93
2.00
1.96
1.94
f1 (ppm)

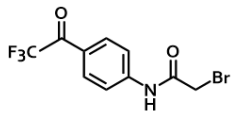

4.S12

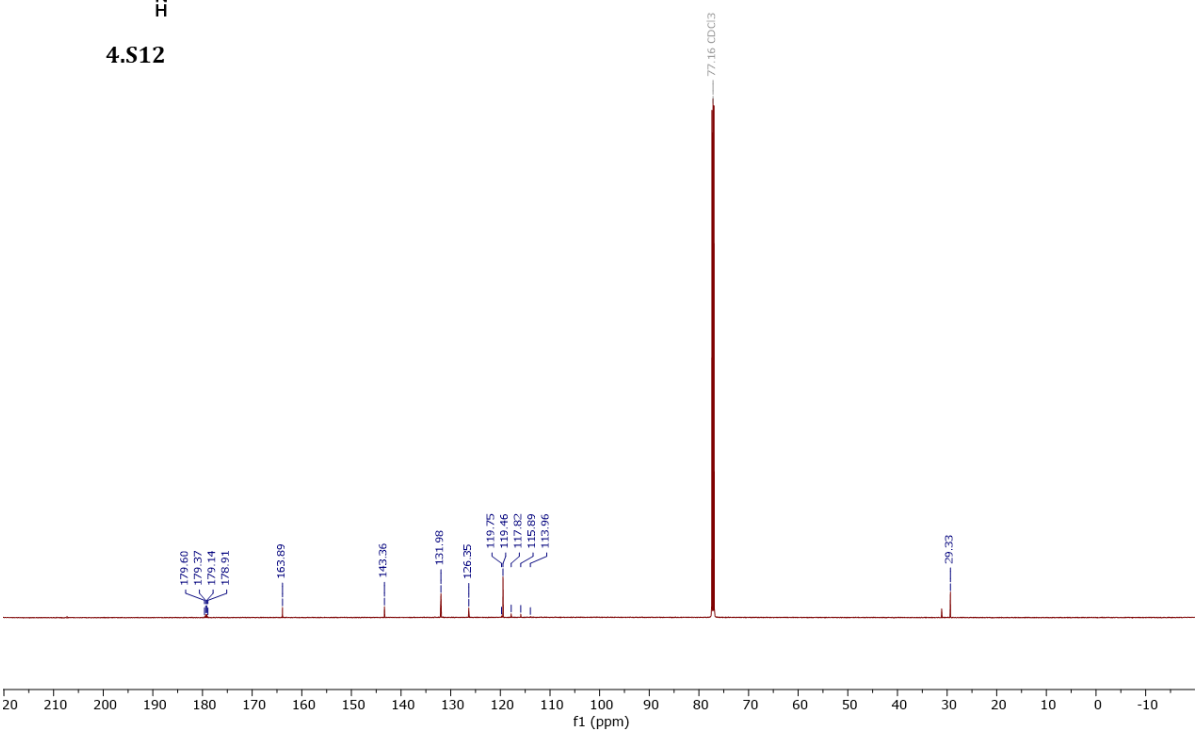
77.16 CDCl3
179.60
179.37
179.14
178.91
163.89
143.36
131.98
126.35
119.75
119.46
117.82
115.89
113.96
29.33
f1 (ppm)

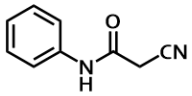
O
N
H
CN

4.S13

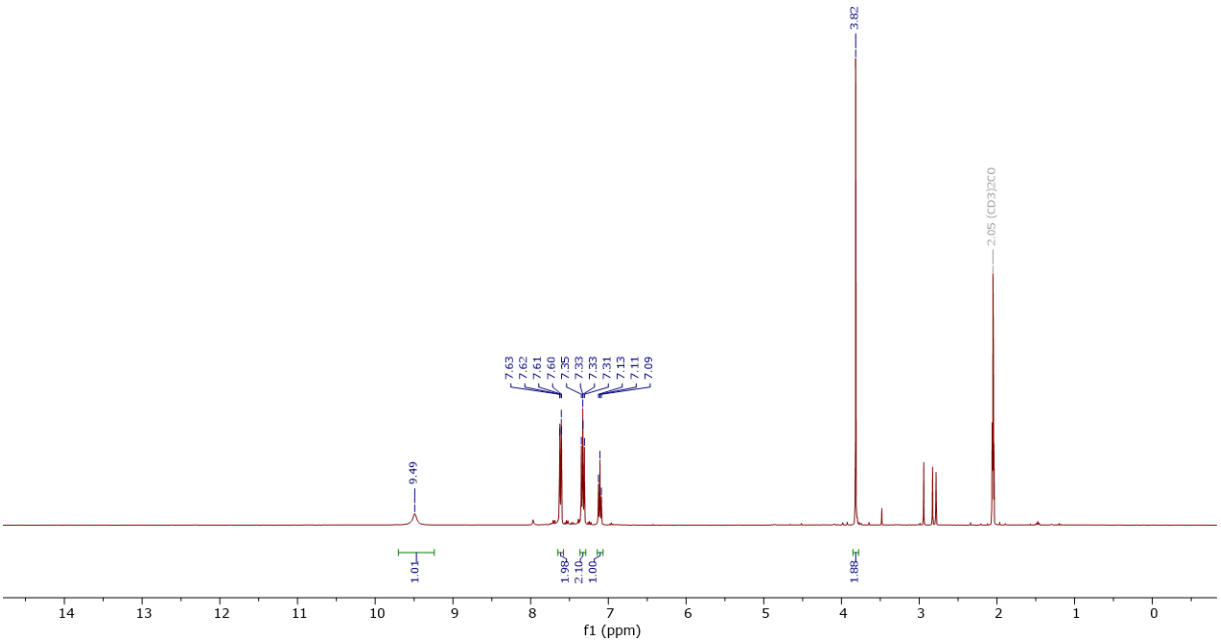
3.82
2.05 (CD3)2CO
7.63
7.62
7.61
7.60
7.35
7.33
7.33
7.31
7.13
7.11
7.09
9.49
1.01
1.98
2.10
1.00
1.88
14
13
12
11
10
9
8
7
6
5
4
3
2
1
0
f1 (ppm)

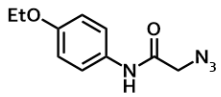
EtO
O
N
H
N3

4.S14

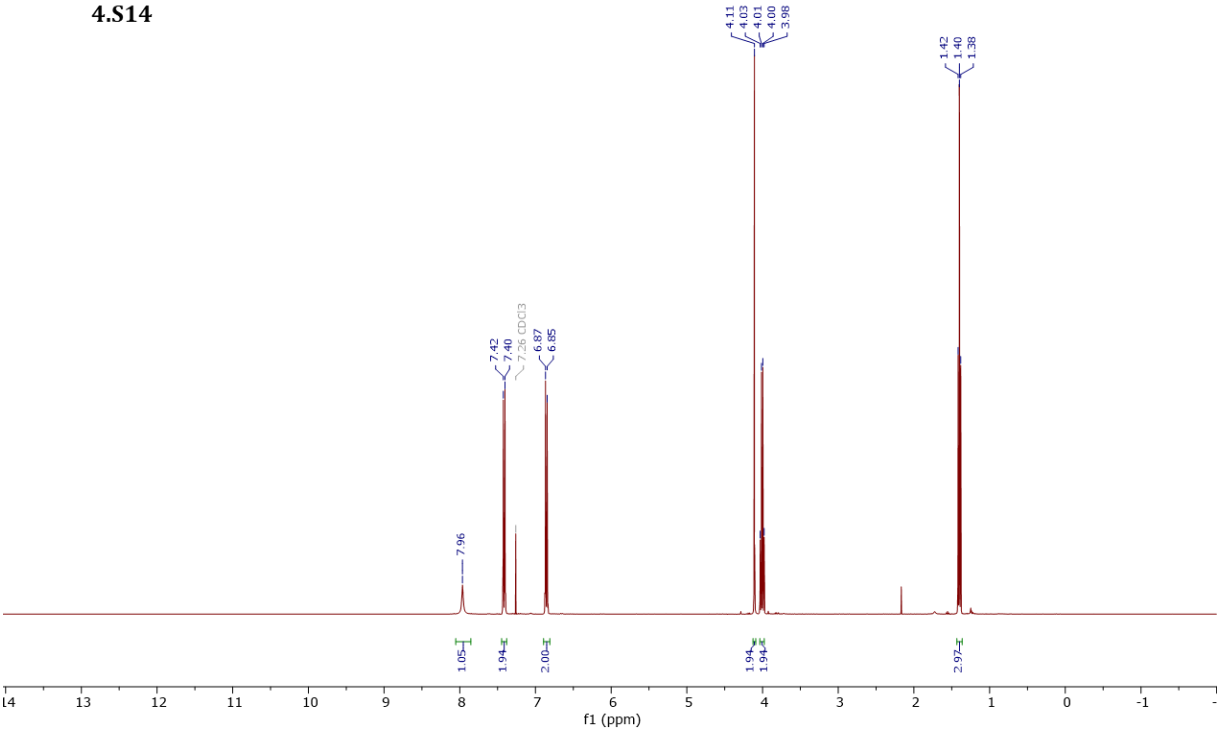
4.11
4.03
4.01
4.00
3.98
1.42
1.40
1.38
7.42
7.40
7.26 CDCl3
6.87
6.85
7.96
1.05
1.94
2.00
1.94
1.94
2.97
14
13
12
11
10
9
8
7
6
5
4
3
2
1
0
-1
f1 (ppm)

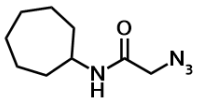

4.S15

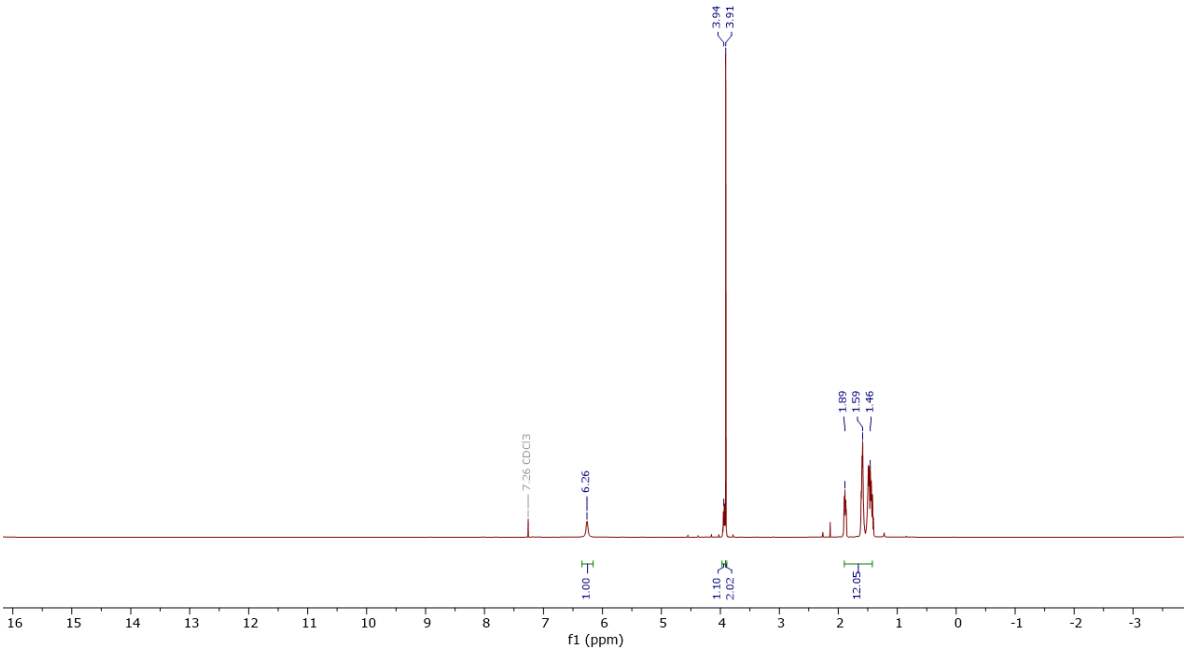
3.94
3.91
1.89
1.59
1.46
7.26 CDCl3
6.26
1.00
1.10
2.02
12.05
f1 (ppm)

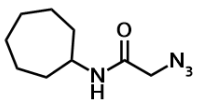

4.S15

35.01
28.00
24.05
52.83
50.55
77.16 CDCl3
165.25
f1 (ppm)

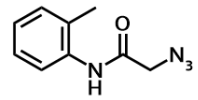

4.S16

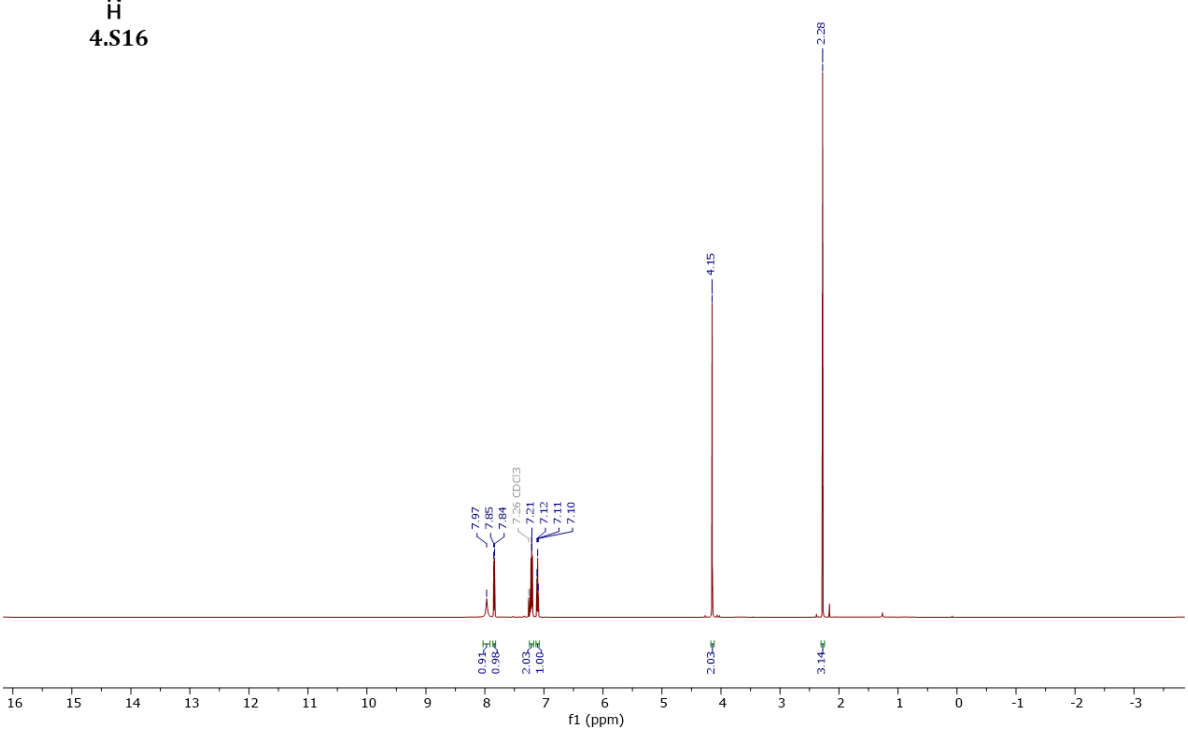
2.28
4.15
7.97
7.85
7.84
7.26 CDCl3
7.21
7.12
7.11
7.10
0.91
0.98
2.03
1.00
2.03
3.14
f1 (ppm)

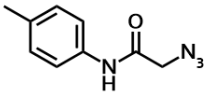

4.S17

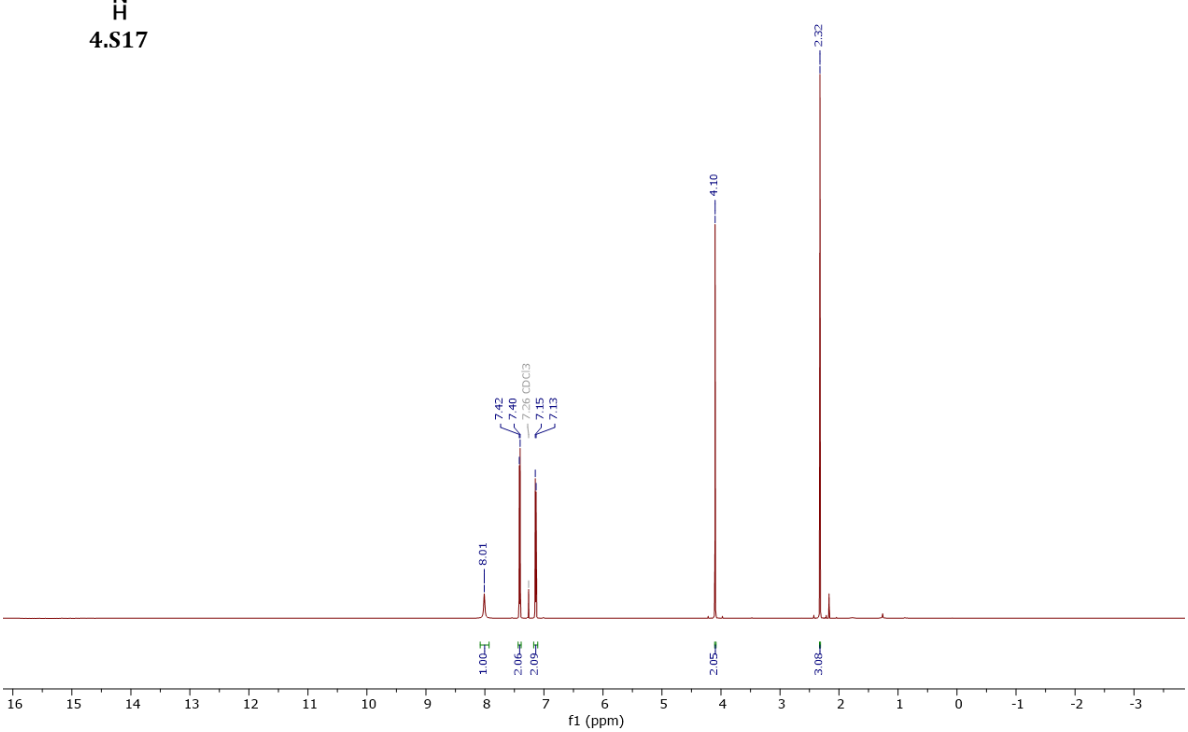
2.32
4.10
8.01
7.42
7.40
7.26 CDCl3
7.15
7.13
1.00
2.06
2.09
2.05
3.08
f1 (ppm)

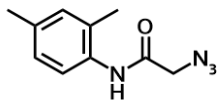

4.S18

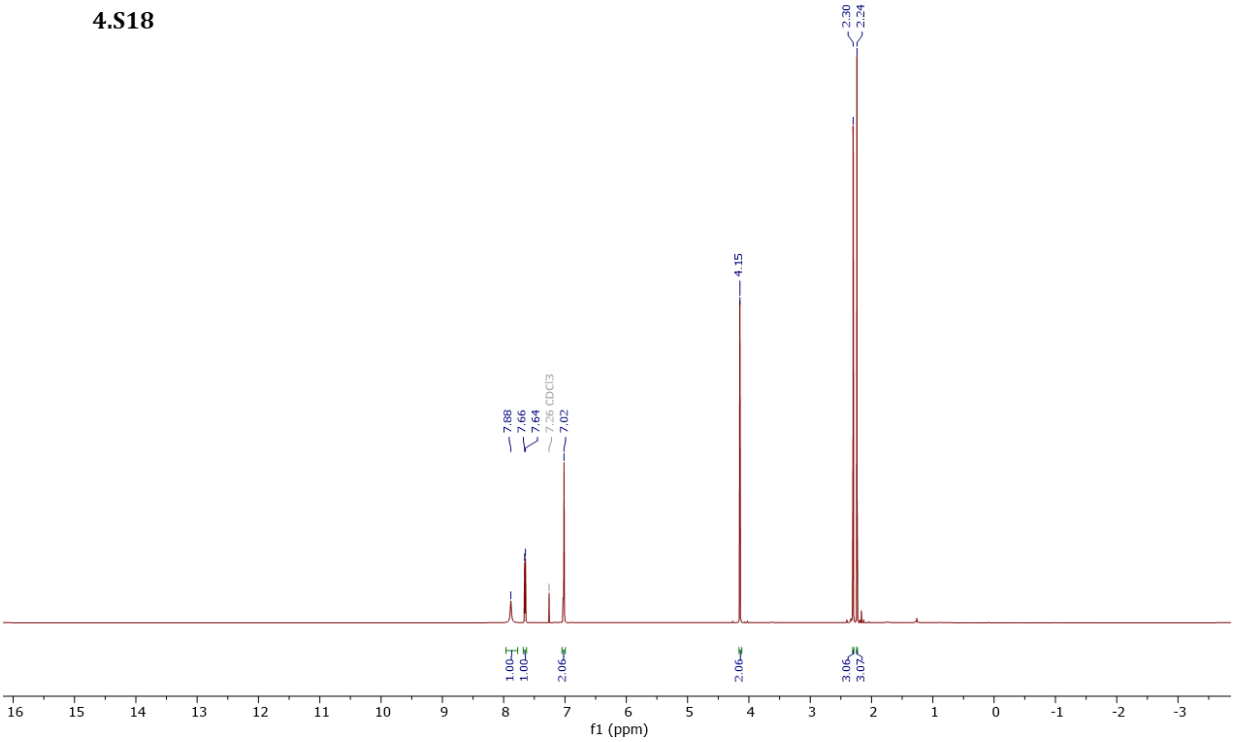
2.30
2.24
4.15
7.88
7.66
7.64
7.26 CDCl3
7.02
1.00
1.00
2.06
2.06
3.06
3.07
f1 (ppm)

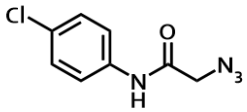

4.S19

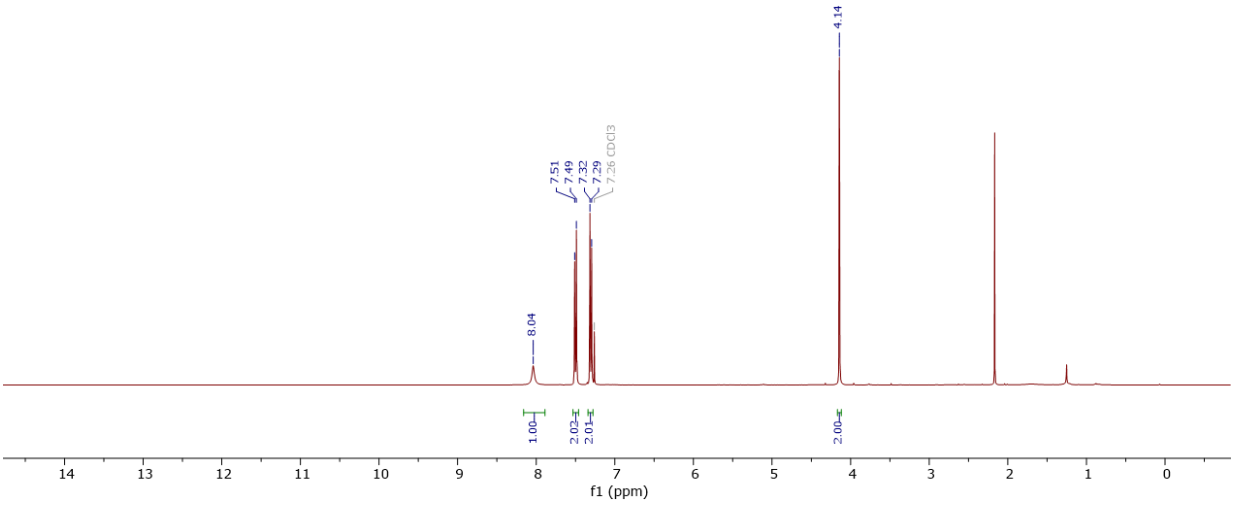
4.14
7.51
7.49
7.32
7.29
7.26 CDCl3
8.04
1.00
2.02
2.01
2.00
f1 (ppm)

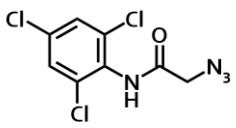

4.S20

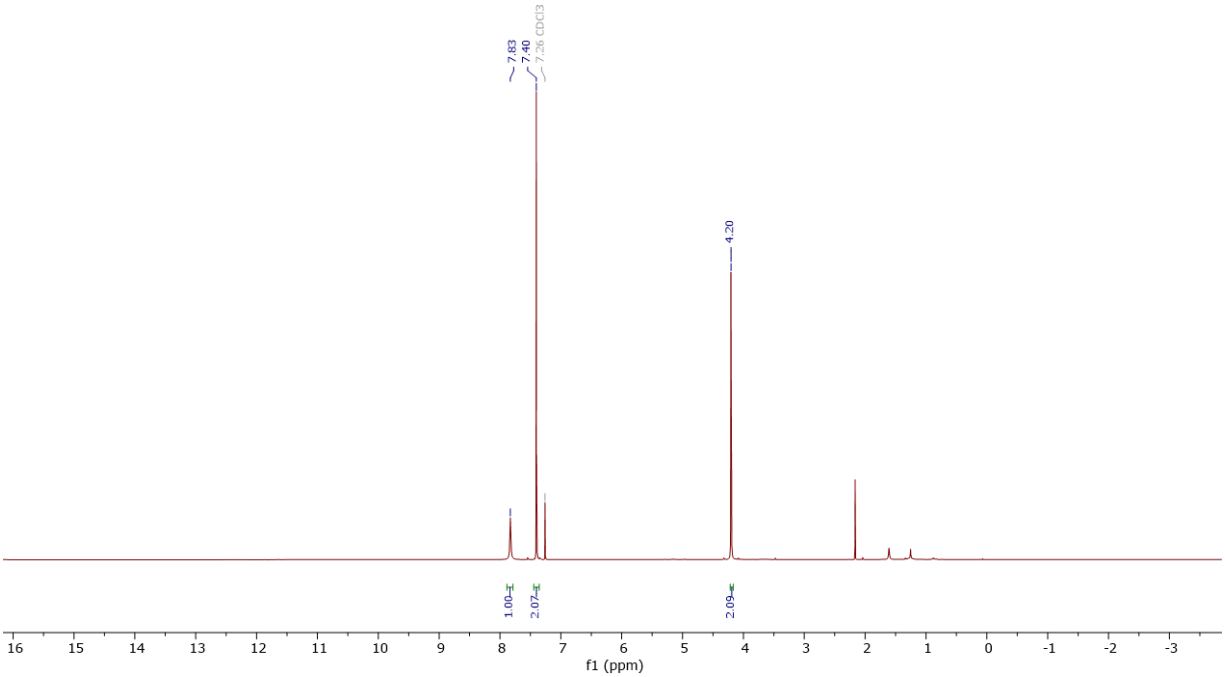
7.83
7.40
7.26 CDCl3
4.20
1.00
2.07
2.09
f1 (ppm)

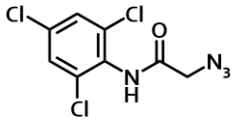

4.S20

134.35
134.28
130.03
128.69
165.13
52.77
f1 (ppm)

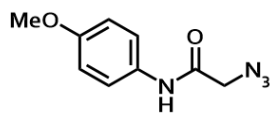
MeO
O
N
H
N3

4.S21

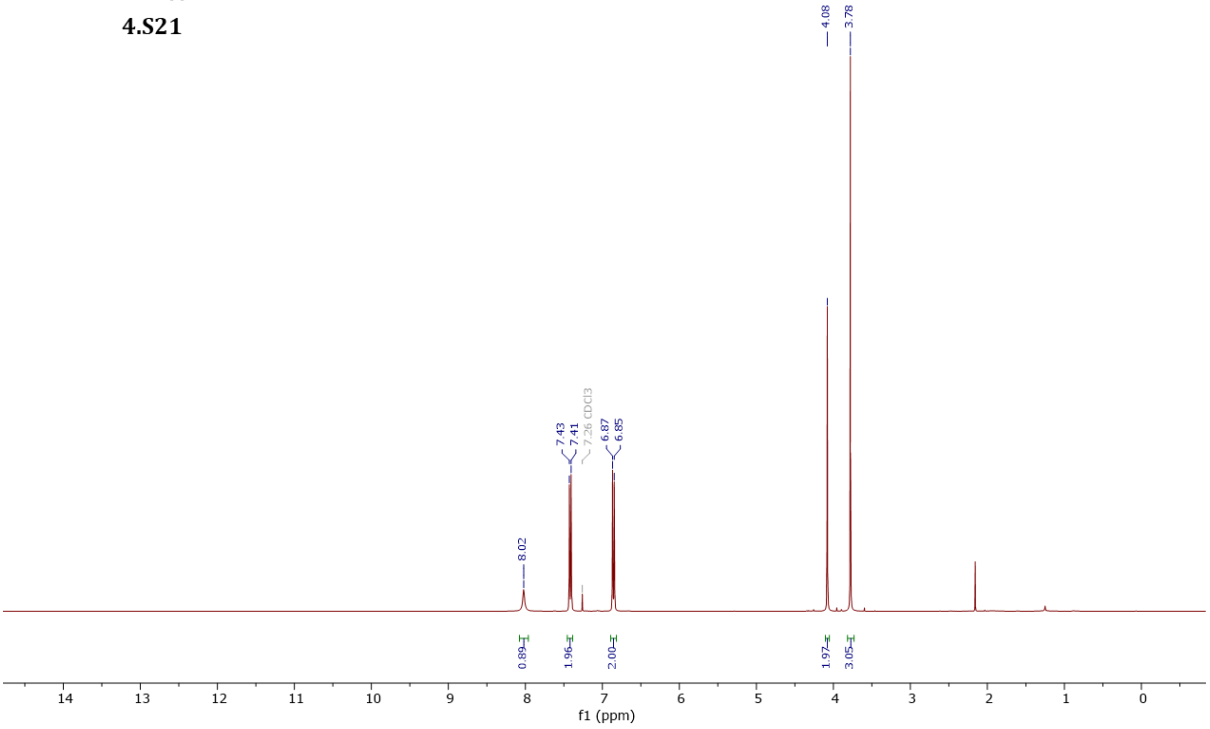
4.08
3.78
7.43
7.41
7.26 CDCl3
6.87
6.85
8.02
0.89
1.96
2.00
1.97
3.05
14
13
12
11
10
9
8
7
6
5
4
3
2
1
0
f1 (ppm)

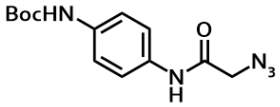
BocHN
O
N
H
N3

4.S22

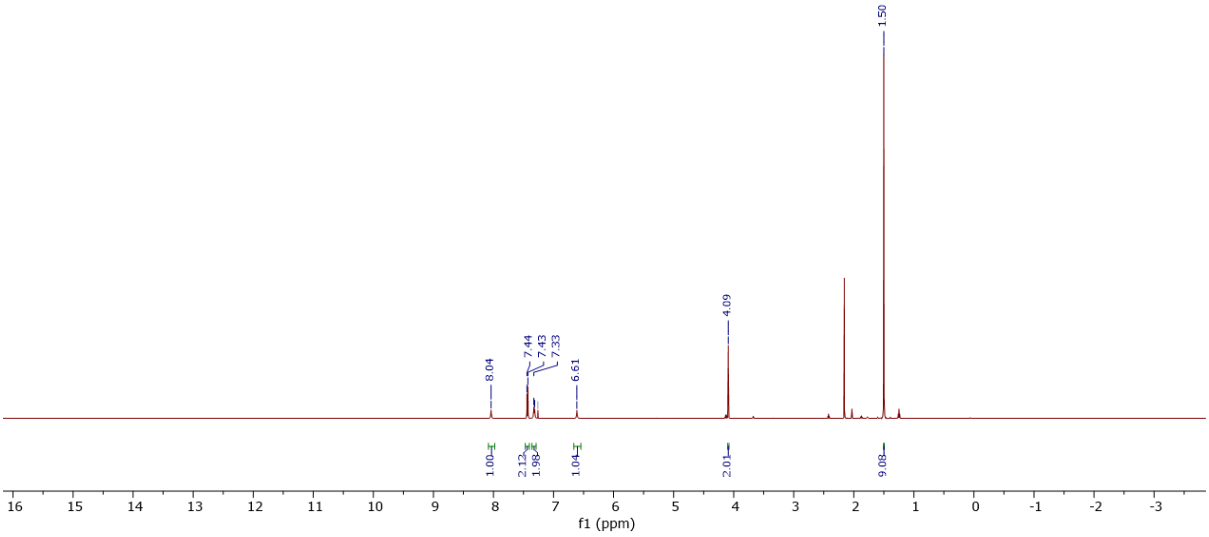
1.50
4.09
8.04
7.44
7.43
7.33
6.61
1.00
2.12
1.98
1.04
2.01
9.08
16 15 14 13 12 11 10 9 8 7 6 5 4 3 2 1 0 -1 -2 -3
f1 (ppm)

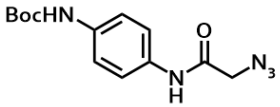
BocHN
O
N
H
N3

4.S22

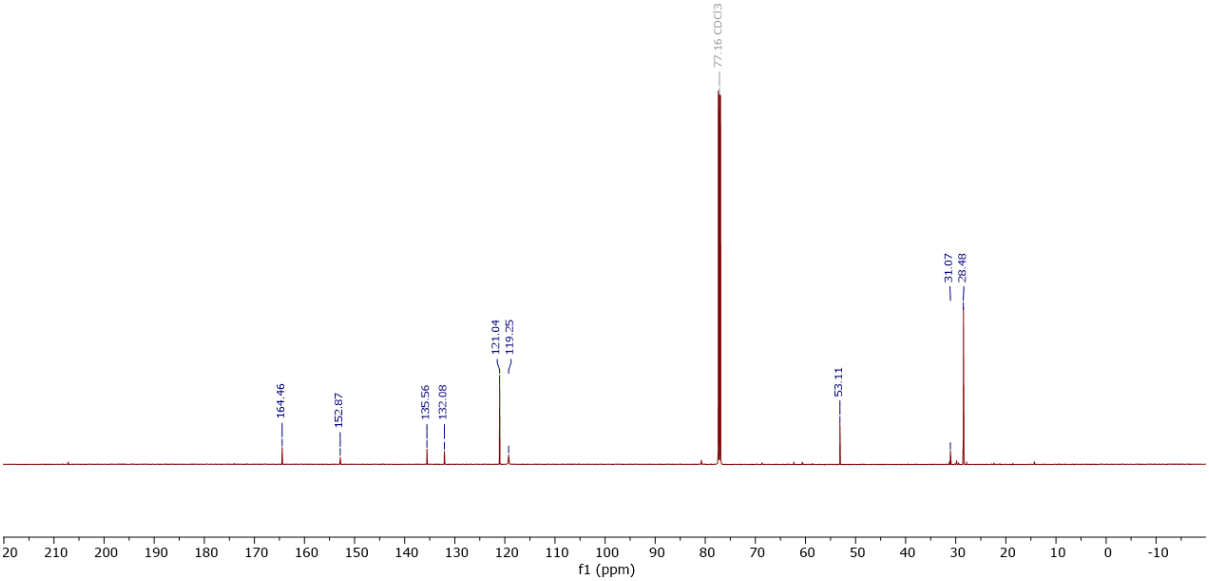
77.16 CDCl3
164.46
152.87
135.56
132.08
121.04
119.25
53.11
31.07
28.48
20 210 200 190 180 170 160 150 140 130 120 110 100 90 80 70 60 50 40 30 20 10 0 -10
f1 (ppm)

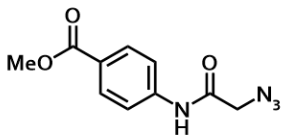
MeO
O
O
N
H
N3

4.S23

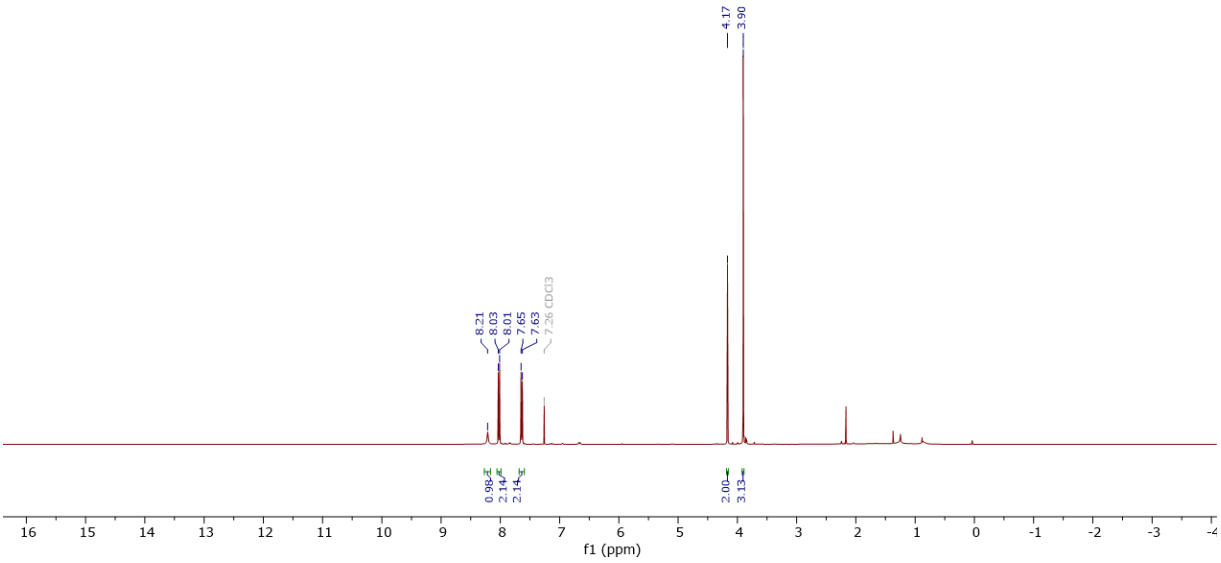
8.21
8.03
8.01
7.65
7.63
7.26 CDCl3
4.17
3.90
0.98
2.14
2.14
2.00
3.13
16
15
14
13
12
11
10
9
8
7
6
5
4
3
2
1
0
-1
-2
-3
f1 (ppm)

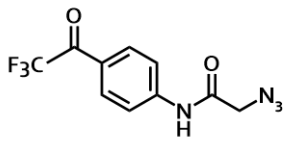

4.S24

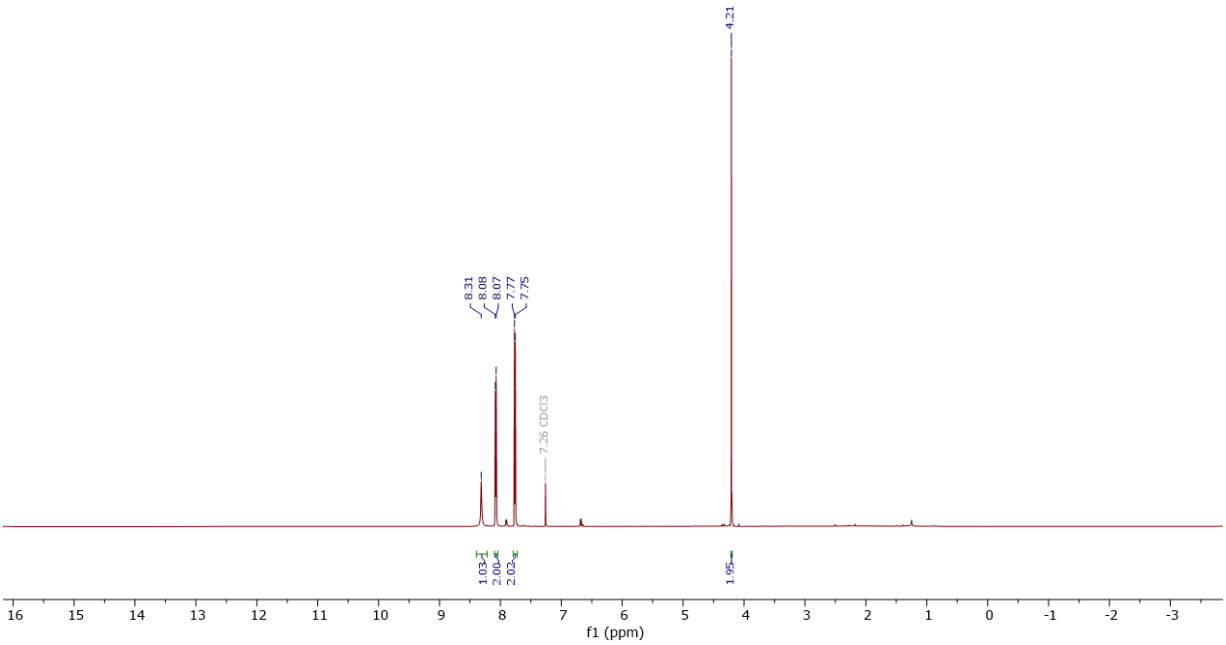
4.21
8.31
8.08
8.07
7.77
7.75
7.26 CDCl3
1.03
2.00
2.02
1.95
16 15 14 13 12 11 10 9 8 7 6 5 4 3 2 1 0 -1 -2 -3
f1 (ppm)

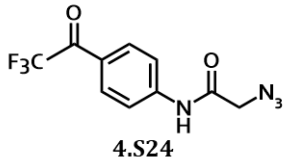

4.S24

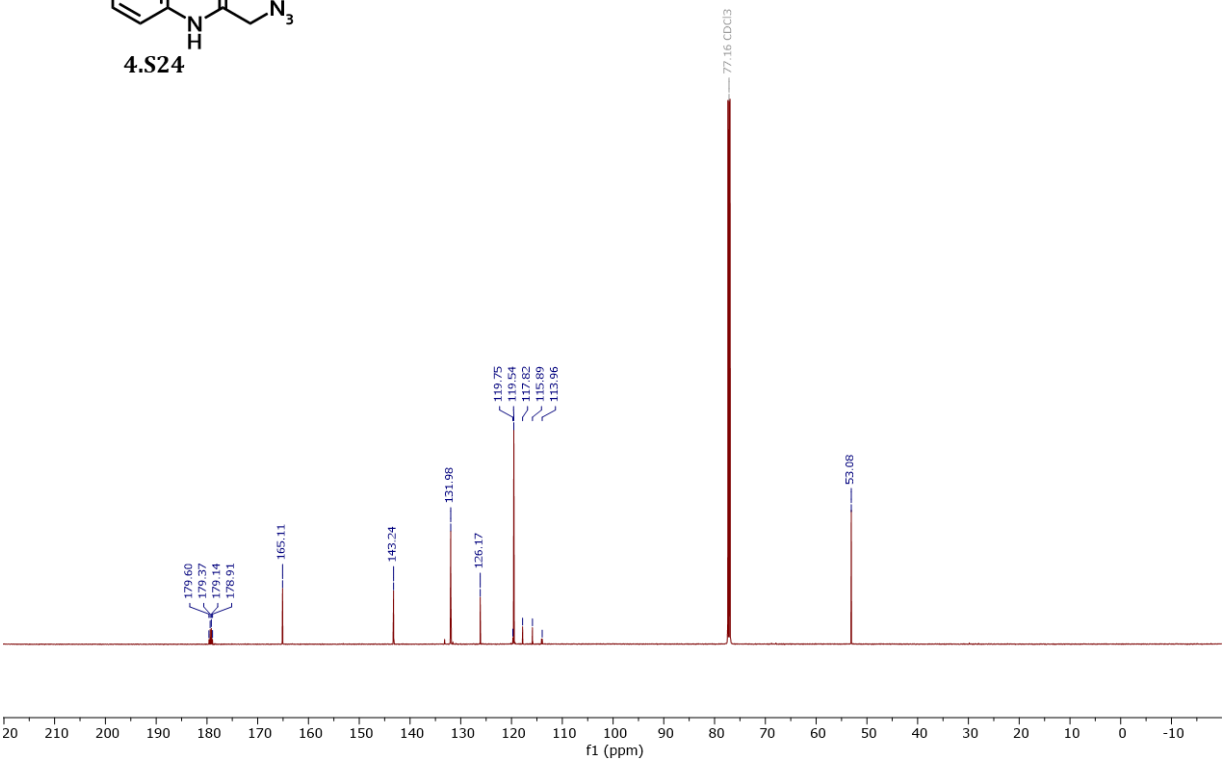
77.16 CDCl3
119.75
119.54
117.82
115.69
113.96
131.98
126.17
165.11
143.24
179.60
179.37
179.14
178.91
53.08
20 210 200 190 180 170 160 150 140 130 120 110 100 90 80 70 60 50 40 30 20 10 0 -10
f1 (ppm)

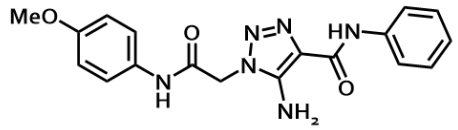

4.S25

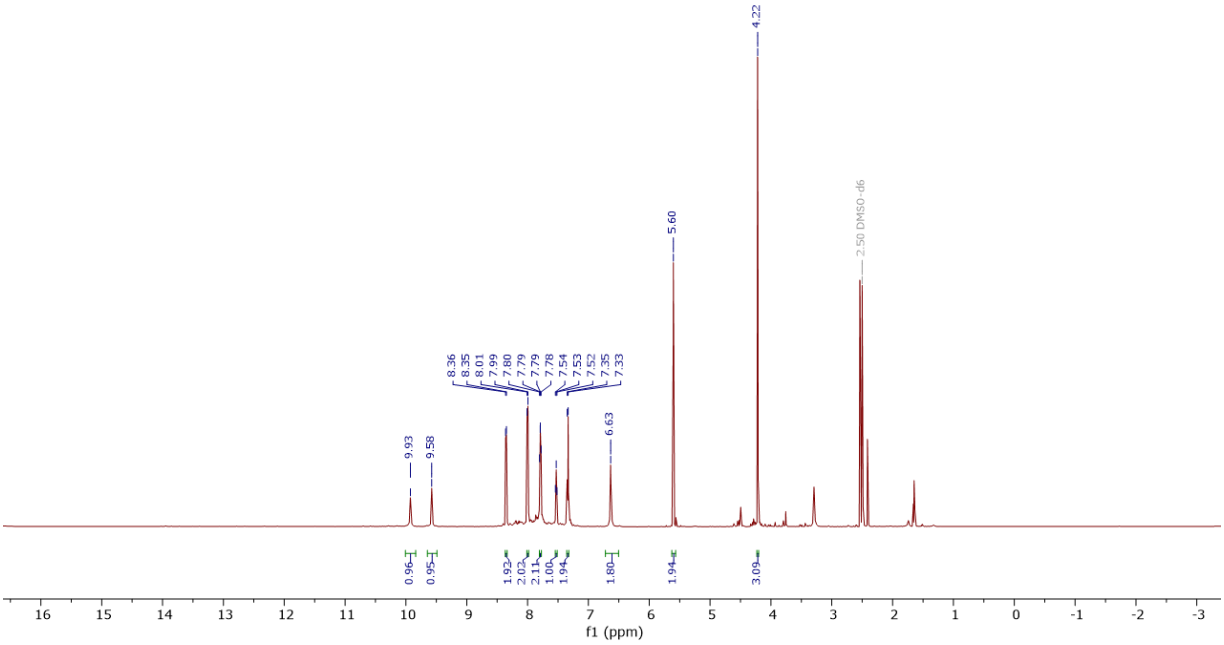
4.22
5.60
2.50 DMSO -d6
8.36
8.35
8.01
7.99
7.80
7.79
7.79
7.78
7.54
7.53
7.52
7.35
7.33
6.63
9.93
9.58
0.96
0.95
1.92
2.02
2.11
1.00
1.94
1.80
1.94
3.09
f1 (ppm)

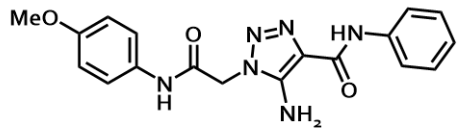

4.S25

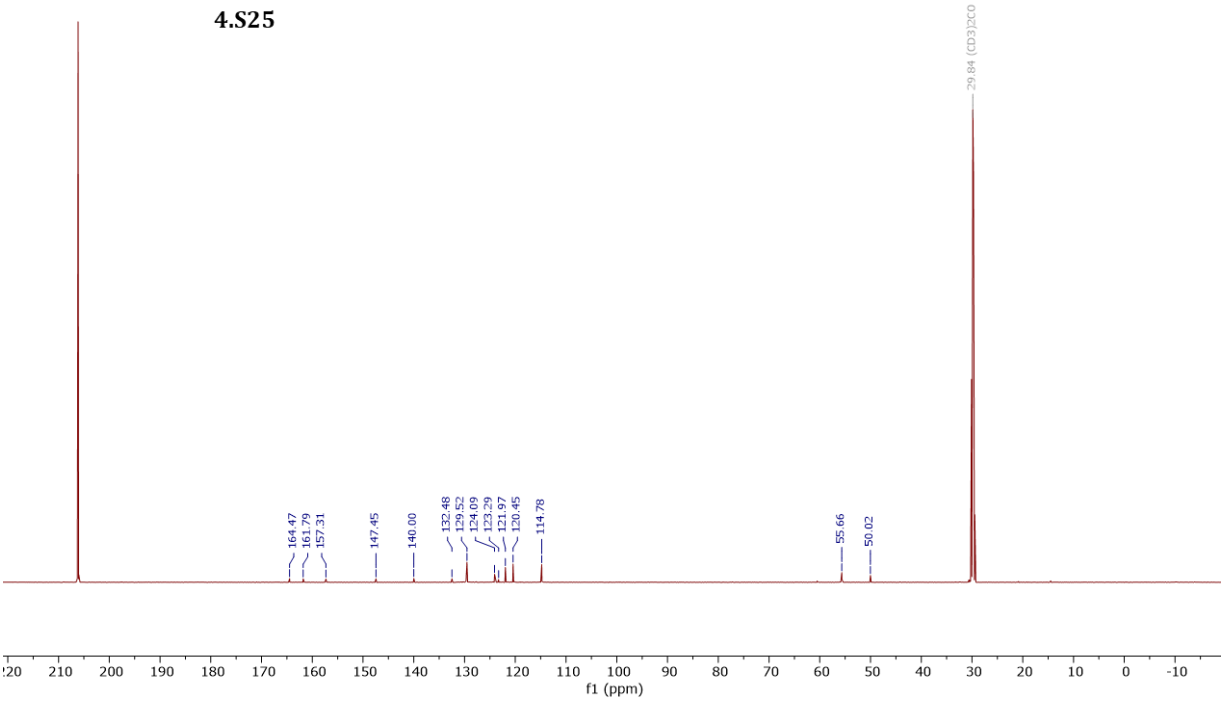
29.84 (CD3)2CO
164.47
161.79
157.31
147.45
140.00
132.48
129.52
124.09
123.29
121.97
120.45
114.78
55.66
50.02
f1 (ppm)

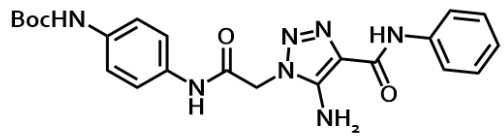
BocHN
O
N
H
N=N
N
HN
O
NH2

4.S26

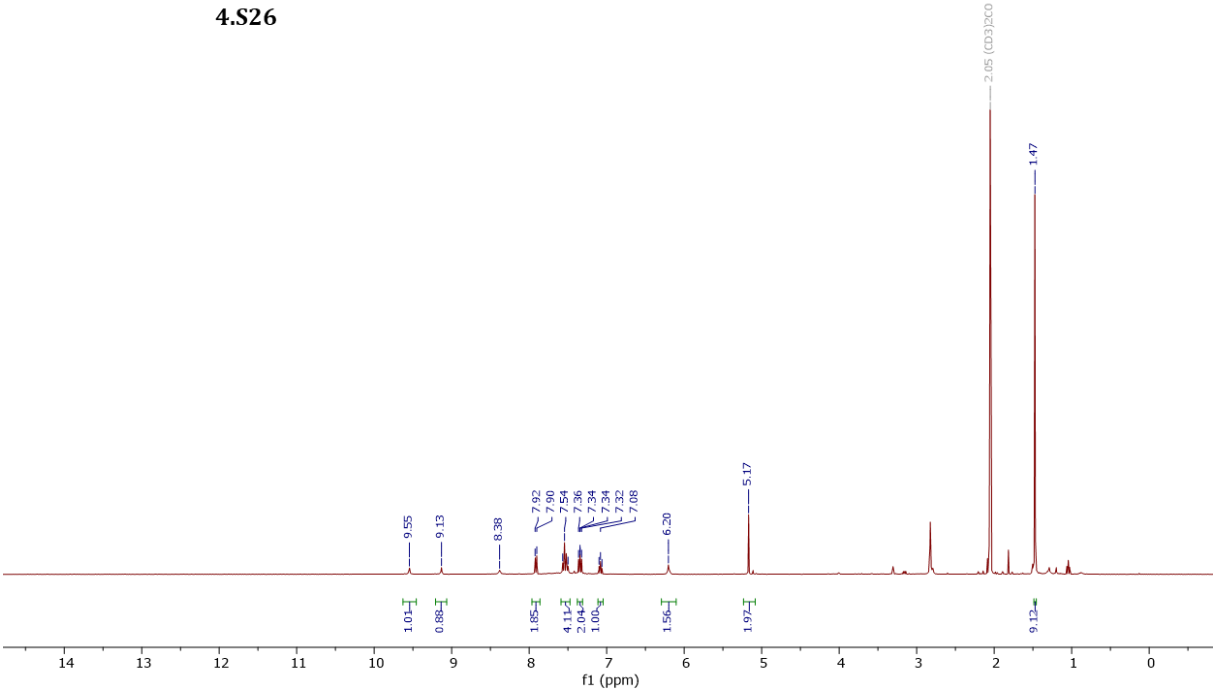
2.05 (CD3)2CO
1.47
5.17
9.55
9.13
8.38
7.92
7.90
7.54
7.36
7.34
7.34
7.32
7.08
6.20
1.01
0.88
1.85
4.11
2.04
1.00
1.56
1.97
9.12
f1 (ppm)

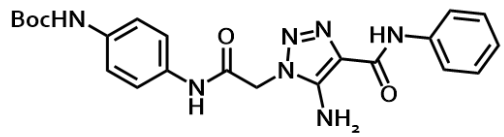
BocHN
O
N
H
N=N
N
HN
O
NH2

4.S26

163.63
160.79
152.80
146.50
139.06
135.31
133.00
128.46
122.94
119.91
119.60
78.89
48.40
28.13
f1 (ppm)

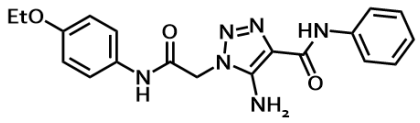
EtO
O
N
H
N=N
N
HN
O
NH2

4.1

2.50 DMSO-d6
10.31
10.03
7.83
7.82
7.50
7.49
7.31
7.30
7.29
7.05
7.04
7.03
6.90
6.88
6.56
5.10
4.00
3.99
3.98
3.96
1.32
1.30
1.29
16 15 14 13 12 11 10 9 8 7 6 5 4 3 2 1 0 -1 -2 -3
f1 (ppm)

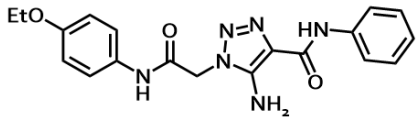
EtO
O
N
H
N=N
N
HN
O
NH2

4.1

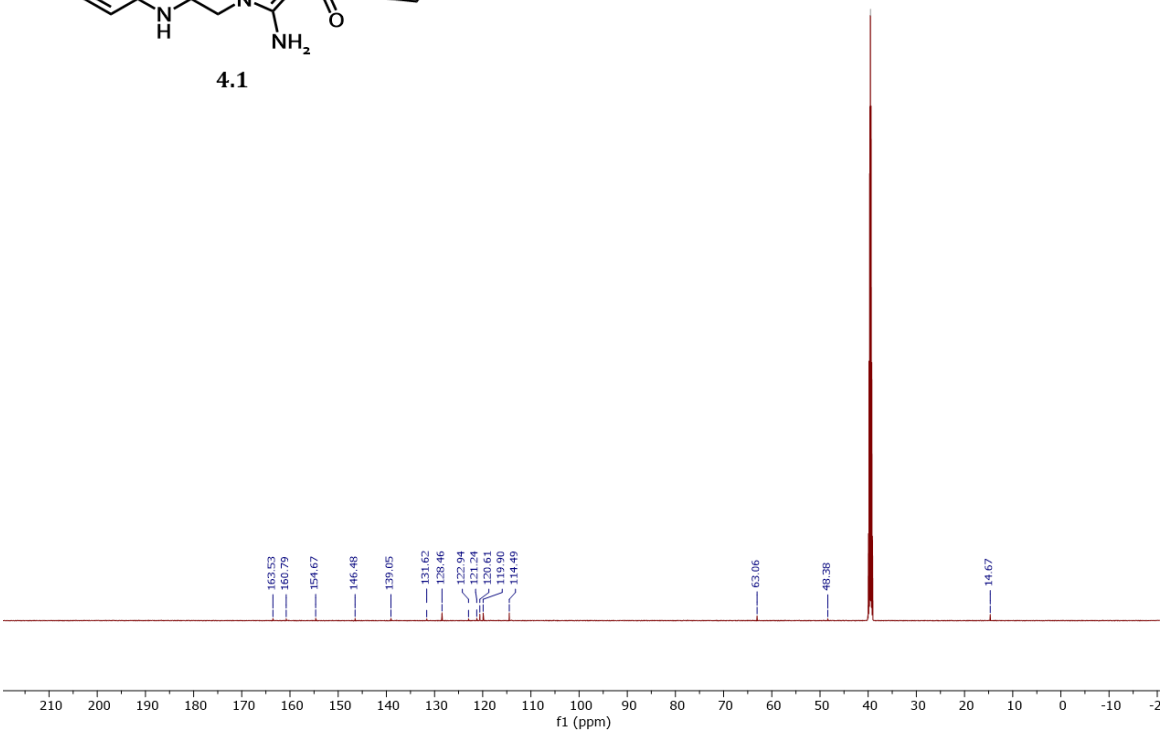
163.53
160.79
154.67
146.48
139.05
131.62
128.46
122.94
121.24
120.61
119.90
114.49
63.06
48.38
14.67
210 200 190 180 170 160 150 140 130 120 110 100 90 80 70 60 50 40 30 20 10 0 -10 -2
f1 (ppm)

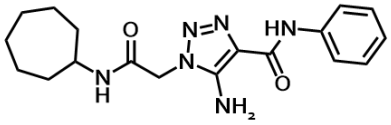

4.2

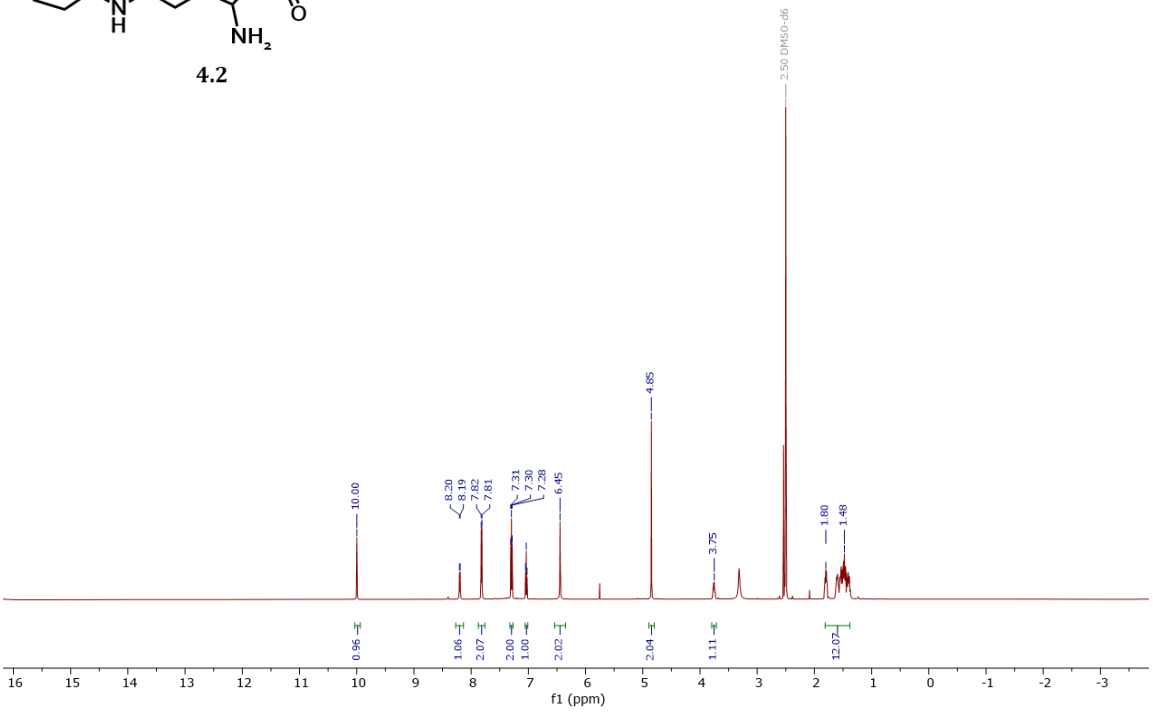
2.50 DMSO-d6
10.00
8.20
8.19
7.82
7.81
7.31
7.30
7.28
6.45
4.85
3.75
1.80
1.48
0.96
1.06
2.07
2.00
1.00
2.02
2.04
1.11
12.07
f1 (ppm)

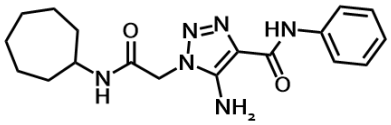

4.2

39.52 DMSO-d6
34.19
163.97
160.78
146.36
139.04
128.45
122.94
121.30
119.90
49.93
47.97
27.81
23.62
f1 (ppm)

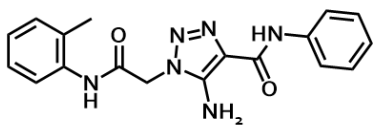

4.3

2.50 DMSO-d6
2.26
10.03
9.68
7.84
7.82
7.48
7.46
7.31
7.30
7.29
7.24
7.23
7.19
7.17
7.16
7.11
7.10
7.09
7.05
7.04
7.03
6.57
5.18
0.99
0.95
1.96
0.92
1.97
0.94
1.01
0.98
1.00
1.97
1.92
2.86
f1 (ppm)

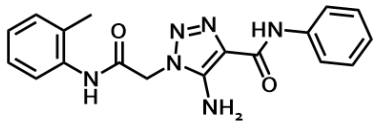

4.3

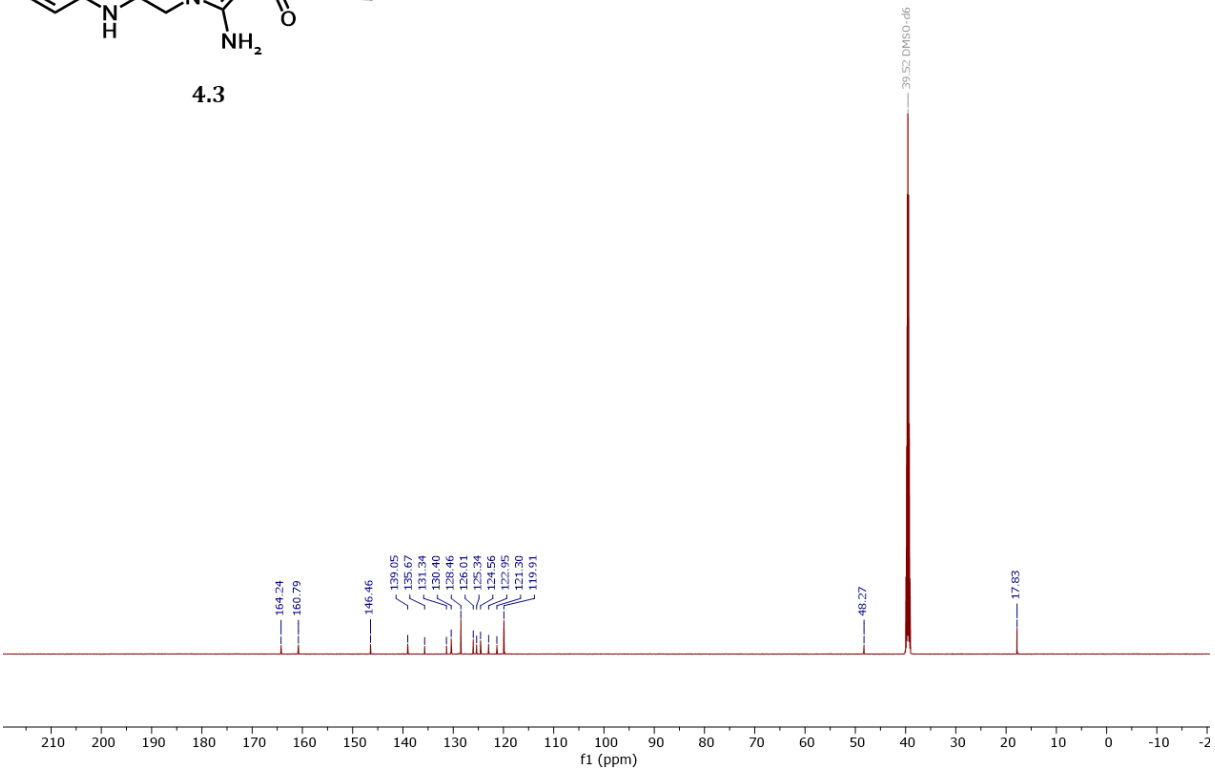
39.52 DMSO-d6
164.24
160.79
146.46
139.05
135.67
131.34
130.40
128.46
126.01
125.34
124.56
122.95
121.30
119.91
48.27
17.83
f1 (ppm)

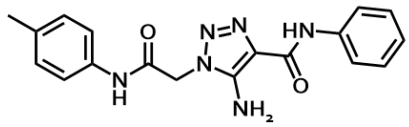

4.4

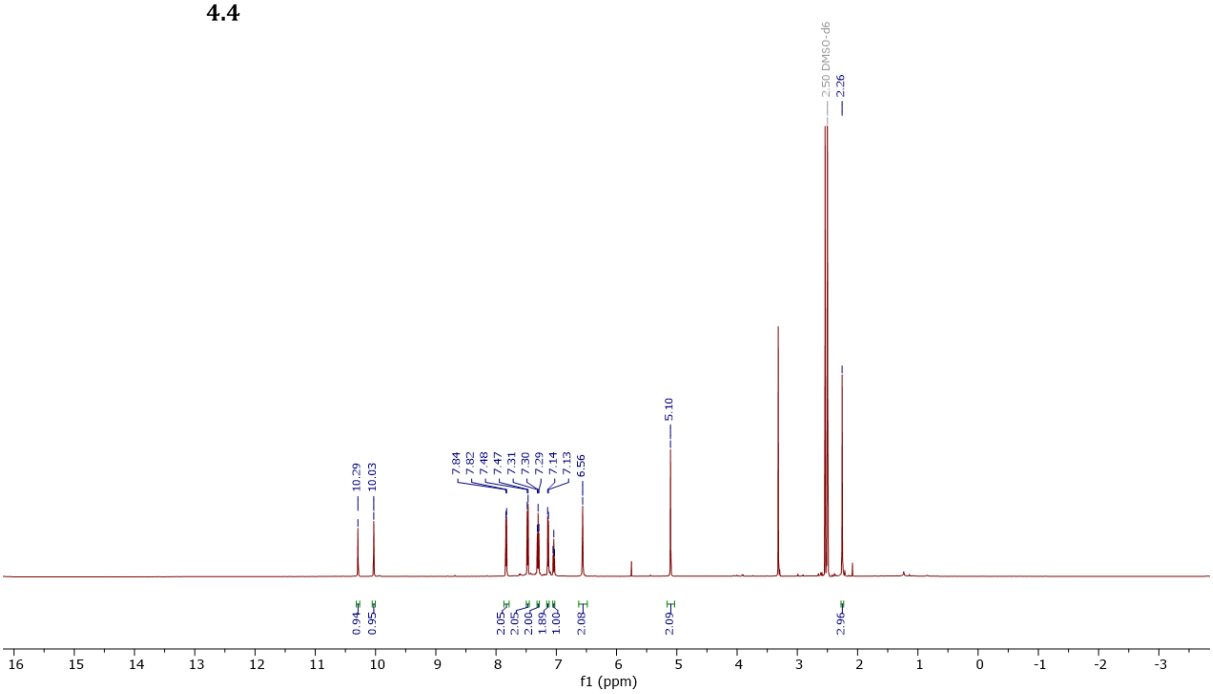
2.50 DMSO-d6
2.26
10.29
10.03
7.84
7.82
7.48
7.47
7.31
7.30
7.29
7.14
7.13
6.56
5.10
0.94
0.95
2.05
2.05
2.00
1.88
1.00
2.08
2.09
2.96
f1 (ppm)

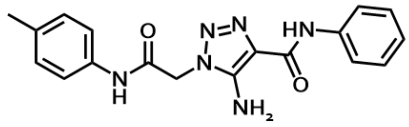

4.4

39.52 DMSO-d6
163.81
160.79
146.50
139.06
136.05
132.55
129.26
128.46
122.95
121.24
119.91
119.10
48.44
20.43
f1 (ppm)

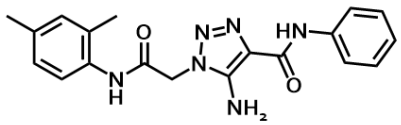

4.5

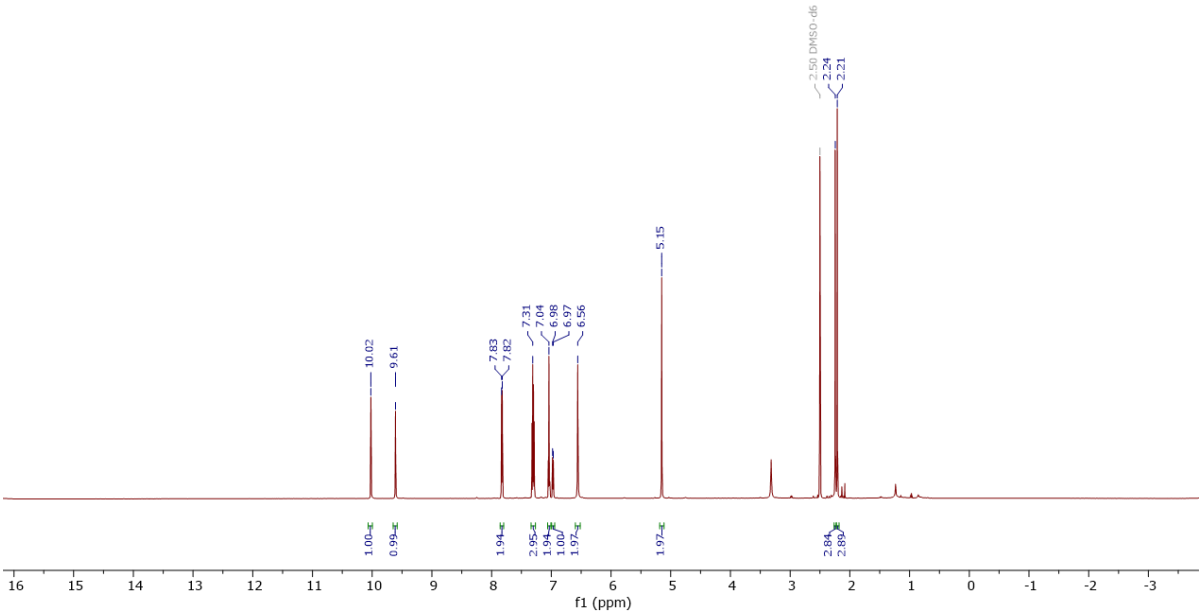
2.50 DMSO-d6
2.24
2.21
5.15
10.02
9.61
7.83
7.82
7.31
7.04
6.98
6.97
6.56
1.00
0.99
1.94
2.95
1.94
1.00
1.97
1.97
2.84
2.89
f1 (ppm)

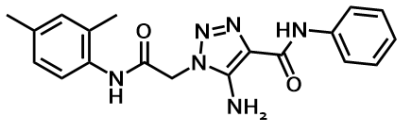

4.5

39.52 DMSO-d6
164.18
160.79
146.44
139.05
134.44
133.07
131.31
130.90
128.46
126.50
124.62
122.94
121.30
119.90
48.23
20.45
17.75
f1 (ppm)

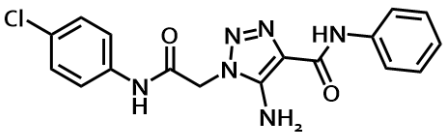

4.6

2.50 DMSO-d6
10.53
10.03
7.84
7.82
7.63
7.61
7.41
7.39
7.31
7.30
7.29
7.05
7.04
7.03
6.58
5.13
0.96
0.98
2.02
2.18
2.11
2.05
1.00
1.92
2.02
f1 (ppm)

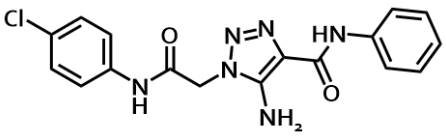

4.6

39.52 DMSO-d6
164.25
160.77
146.49
139.05
137.53
128.82
128.46
127.16
122.95
121.22
120.67
119.90
48.47
f1 (ppm)

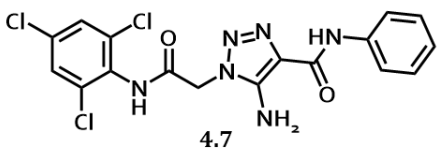

4.7

2.50 DMSO-d6
10.34
10.02
7.82
7.82
7.81
7.81
7.79
7.31
7.30
7.30
7.28
7.05
7.04
6.57
5.23
0.88
1.03
2.00
1.72
2.19
1.17
1.70
2.01
f1 (ppm)

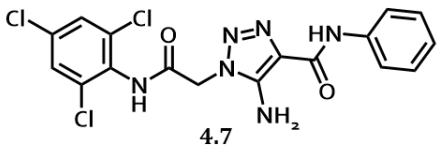

4.7

164.53
160.73
146.45
139.01
134.20
132.67
131.63
128.46
128.38
122.97
121.27
119.92
47.68
f1 (ppm)

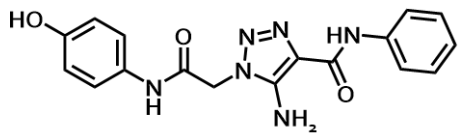

4.8

2.50 DMSO-d6
10.18
10.02
9.32
7.83
7.82
7.38
7.37
7.31
7.30
7.29
7.05
7.04
6.72
6.71
6.55
5.07
0.94
0.93
0.71
2.02
2.03
2.01
1.00
2.01
1.80
1.96
f1 (ppm)

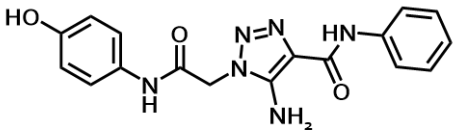

4.8

163.32
160.80
153.61
146.47
139.06
130.18
128.46
122.94
121.25
120.83
119.90
115.19
48.36
f1 (ppm)

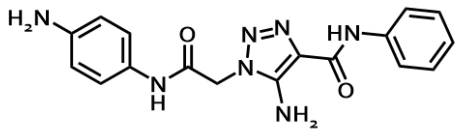

4.9

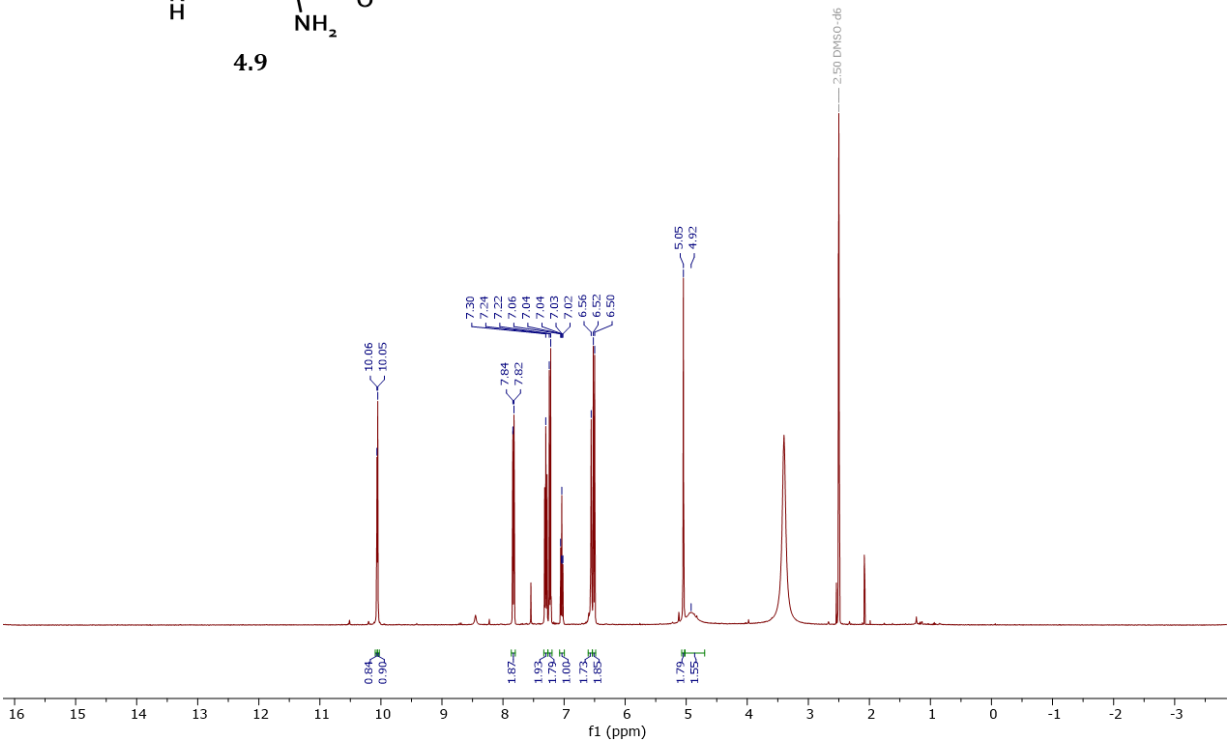
2.50 DMSO-d6
10.06
10.05
7.84
7.82
7.30
7.24
7.22
7.06
7.04
7.04
7.03
7.02
6.56
6.52
6.50
5.05
4.92
0.84
0.90
1.87
1.93
1.79
1.00
1.73
1.85
1.79
1.55
f1 (ppm)

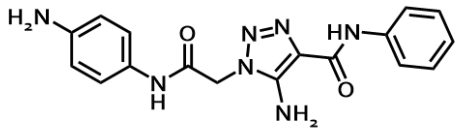

4.9

39.52 DMSO-d6
163.02
160.85
146.51
145.13
139.09
128.51
127.70
123.00
121.29
120.81
119.95
113.89
48.41
f1 (ppm)

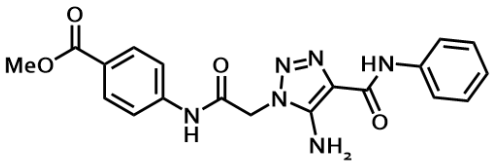

4.10

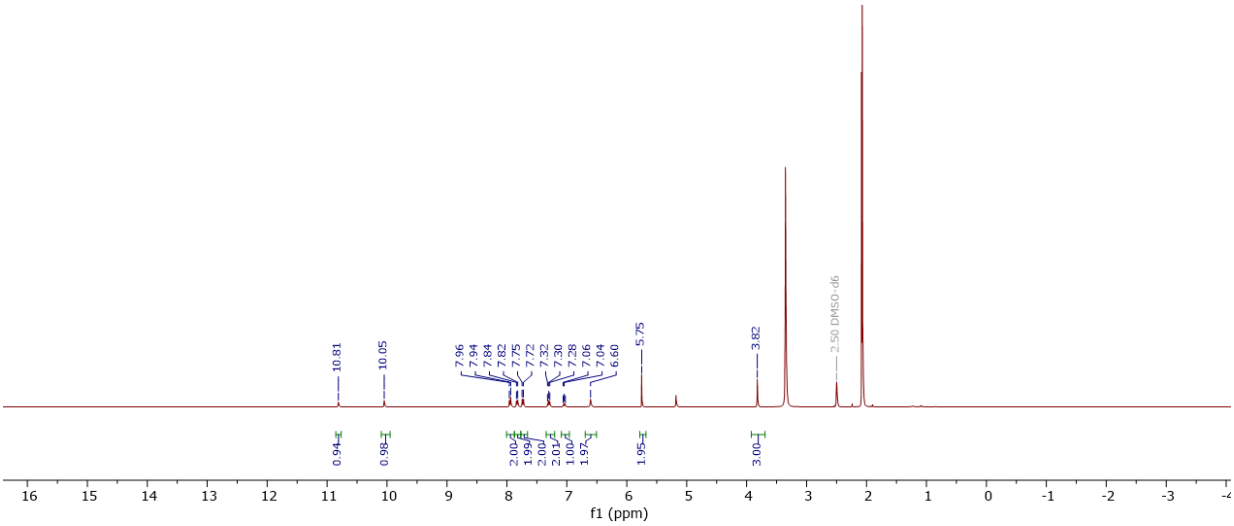
10.81
10.05
7.96
7.94
7.84
7.82
7.75
7.72
7.32
7.30
7.28
7.06
7.04
6.60
5.75
3.82
2.50 DMSO-d6
0.94
0.98
2.00
1.99
2.00
2.01
1.00
1.97
1.95
3.00
f1 (ppm)

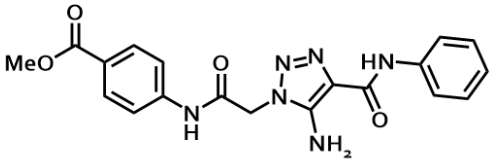

4.10

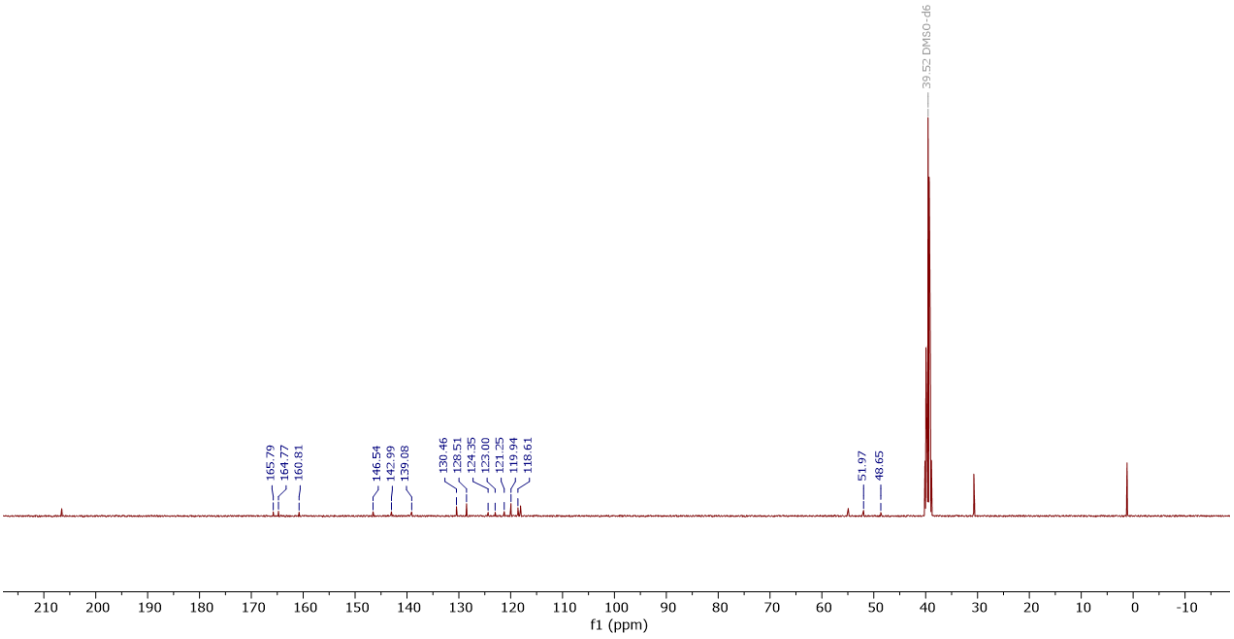
39.52 DMSO-d6
165.79
164.77
160.81
146.54
142.99
139.08
130.46
128.51
124.35
123.00
121.25
119.94
118.61
51.97
48.65
f1 (ppm)

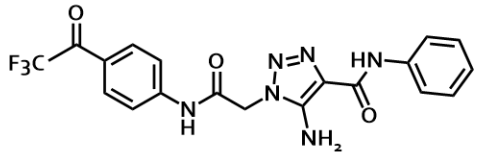

4.11

10.58
10.05
7.84
7.82
7.60
7.58
7.53
7.51
7.32
7.30
7.38
7.06
7.04
7.02
6.59
5.14
2.50 DMSO-d6
0.95
0.99
1.96
1.96
2.00
2.02
1.00
2.00
1.93
f1 (ppm)

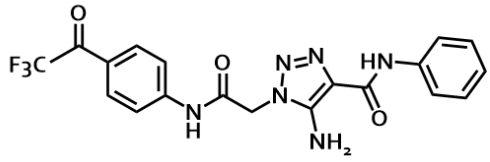

4.11

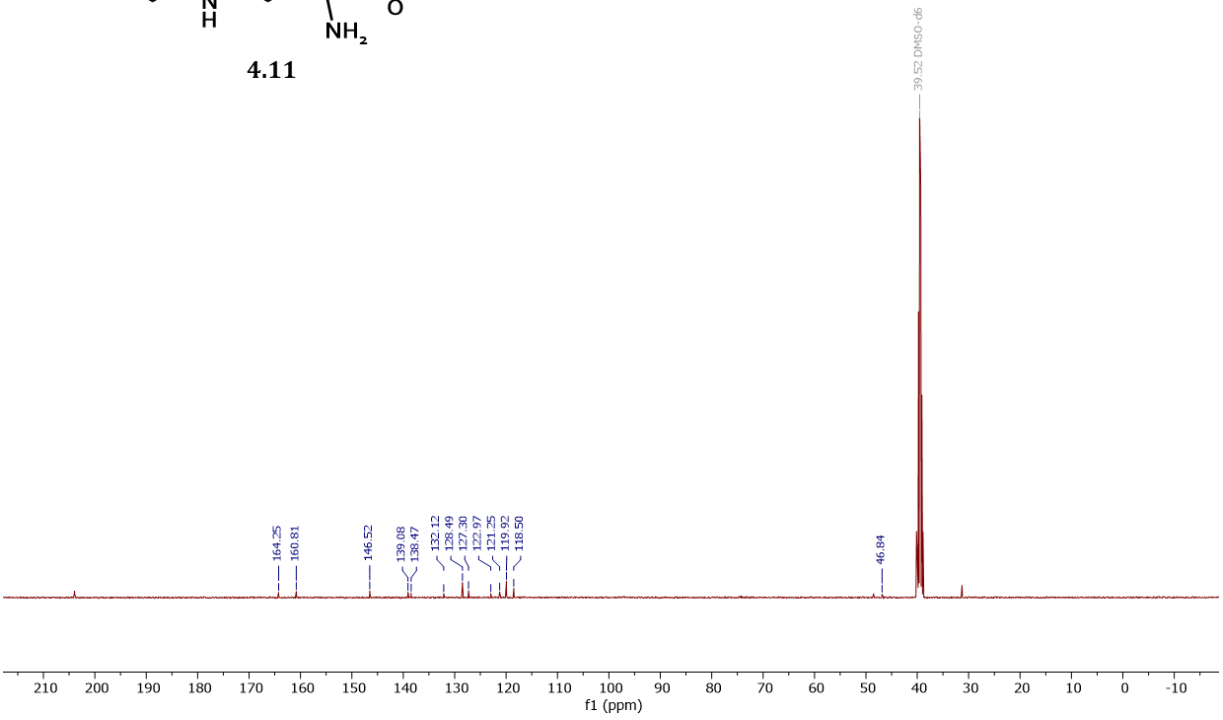
164.25
160.81
146.52
139.08
138.47
132.12
128.49
127.30
122.97
121.25
119.92
118.50
46.84
39.52 DMSO-d6
f1 (ppm)

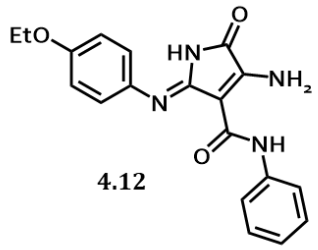
EtO
HN
O
NH2
N
O
NH

4.12

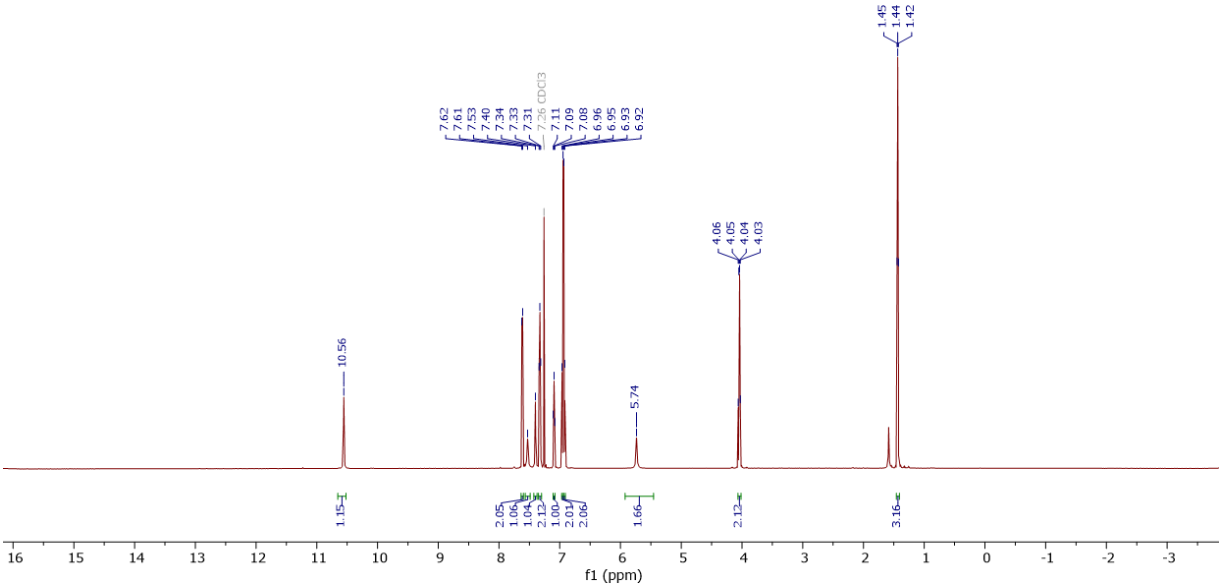
7.62
7.61
7.53
7.40
7.34
7.33
7.31
7.26 CDCl3
7.11
7.09
7.08
6.96
6.95
6.93
6.92
4.06
4.05
4.04
4.03
1.45
1.44
1.42
10.56
5.74
1.15
2.05
1.06
1.04
2.12
1.00
2.01
2.06
1.66
2.12
3.16
f1 (ppm)

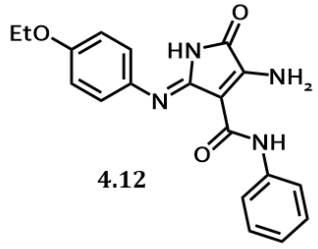
EtO
HN
O
NH2
N
O
NH

4.12

77.16 CDCl3
165.32
162.82
156.79
149.98
148.56
139.57
138.30
129.10
124.09
122.88
120.03
115.65
97.15
63.98
14.98
f1 (ppm)

4.12

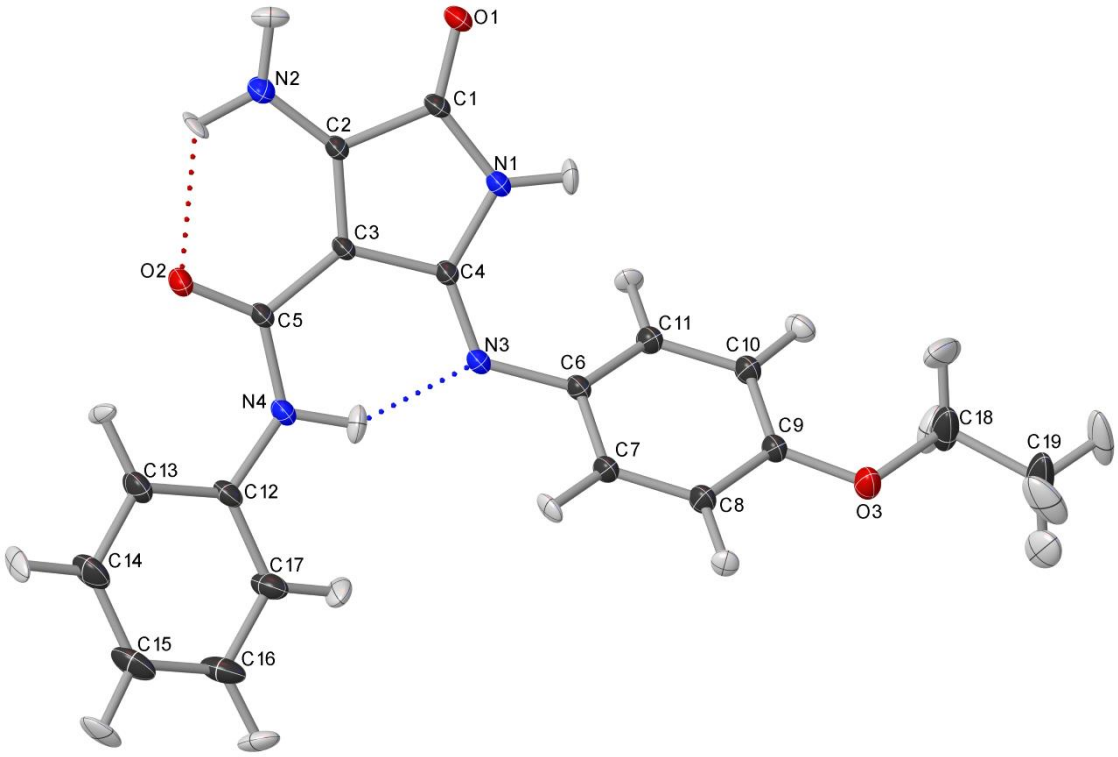

Crystallographic study performed by John Bacsa.

Table 1 Crystal data and structure refinement for 4.12.

Identification code	4.12
Empirical formula	$C_{19}H_{18}N_4O_3$
Formula weight	350.380
Temperature/K	100.0(2)
Crystal system	monoclinic
Space group	I2/a
a/Å	15.3981(5)
b/Å	8.65781(19)
c/Å	26.5131(8)
α/°	90
β/°	95.216(3)
γ/°	90
Volume/Å^3	3519.94(17)
Z	8
ρ_{calc}g/cm^3	1.322
μ/mm^{-1}	0.755
F(000)	1476.3
Crystal size/mm^3	0.454 × 0.369 × 0.05
Radiation	Cu Kα (λ = 1.54184)

2Θ range for data collection/°	6.7 to 140.58
Index ranges	-17 ≤ h ≤ 18, -10 ≤ k ≤ 7, -32 ≤ l ≤ 32
Reflections collected	14790
Independent reflections	3270 [R_{int} = 0.0407, R_{sigma} = 0.0256]
Data/restraints/parameters	3270/27/398
Goodness-of-fit on F^2	1.083
Final R indexes [I>=2σ (I)]	R_1 = 0.0366, wR_2 = 0.1004
Final R indexes [all data]	R_1 = 0.0390, wR_2 = 0.1021
Largest diff. peak/hole / e $Å^{-3}$	0.25/-0.21

Table 2 Fractional Atomic Coordinates (×10⁴) and Equivalent Isotropic Displacement Parameters (Å²×10³) for 4.12. U_{eq} is defined as 1/3 of of the trace of the orthogonalised U_{IJ} tensor.

Atom	*x*	*y*	*z*	U(eq)
O2	9187.9(6)	9023.5(11)	2853.7(4)	18.8(2)
O1	8559.7(6)	3207.2(11)	2375.7(4)	20.8(2)
O3	4855.0(7)	3138.6(11)	4533.6(4)	21.6(2)
N1	7645.2(8)	4453.1(13)	2894.4(4)	16.3(3)
N4	7981.0(7)	9230.4(13)	3304.3(4)	16.2(3)
N3	7075.0(7)	6490.7(12)	3405.6(4)	15.1(3)
N2	9459.3(8)	6152.9(15)	2370.6(5)	18.4(3)
C2	8752.4(8)	5902.7(15)	2610.0(5)	14.0(3)
C5	8522.4(9)	8466.3(15)	3013.1(5)	14.3(3)
C4	7583.9(8)	5953.4(15)	3091.2(5)	13.7(3)
C1	8328.0(9)	4339.2(15)	2601.5(5)	15.7(3)
C8	5850.5(9)	5129.0(16)	4441.4(5)	17.7(3)
C11	5952.2(9)	4423.3(15)	3423.1(5)	15.9(3)
C6	6469.7(8)	5602.0(15)	3648.4(5)	14.6(3)
C7	6389.4(9)	5968.8(15)	4156.3(5)	17.2(3)
C3	8280.5(8)	6867.6(14)	2893.6(5)	13.5(3)
C9	5360.6(9)	3901.3(15)	4219.7(5)	16.2(3)
C10	5402.6(9)	3565.1(16)	3709.0(5)	17.0(3)
C12	8124.9(9)	10637.8(15)	3562.7(5)	17.0(3)
C13	8887.4(10)	11509.2(16)	3557.2(6)	22.6(3)
C17	7473.0(10)	11131.6(17)	3858.3(6)	23.7(3)
C15	8351.7(11)	13313.1(18)	4153.6(6)	29.8(4)
C16	7588.1(11)	12452.2(18)	4154.7(6)	28.6(4)
C14	8993.5(11)	12837.4(18)	3852.3(6)	28.5(4)

C18	4420.3(14)	1778(2)	4351.9(7)	38.1(5)
C19	3952.5(18)	1117(3)	4778.2(8)	55.7(7)

Table 3 Anisotropic Displacement Parameters ($Å^2×10^3$) for 4.12. The Anisotropic displacement factor exponent takes the form: $-2π^2[h^2a^{*2}U_{11}+2hka^*b^*U_{12}+...]$.

Atom	U_{11}	U_{22}	U_{33}	U_{12}	U_{13}	U_{23}
O2	17.6(5)	11.3(5)	28.5(5)	-2.5(4)	6.9(4)	-1.5(4)
O1	22.1(5)	11.4(5)	30.2(6)	-1.7(4)	8.8(4)	-5.5(4)
O3	24.5(5)	19.5(5)	21.4(5)	-8.0(4)	6.0(4)	-3.5(4)
N1	17.8(6)	9.9(6)	21.6(6)	-1.6(5)	5.0(5)	-2.2(4)
N4	17.0(6)	10.0(5)	21.8(6)	-1.9(4)	3.3(5)	-2.4(4)
N3	16.6(6)	9.7(5)	19.3(6)	-1.1(4)	4.2(4)	-1.3(4)
N2	18.3(6)	12.4(6)	25.1(6)	1.4(5)	6.1(5)	-0.4(5)
C2	14.7(6)	9.1(6)	18.5(6)	-0.3(5)	3.6(5)	-0.8(5)
C5	15.4(6)	8.9(6)	18.7(6)	-0.8(5)	2.9(5)	-1.7(5)
C4	13.2(6)	10.0(6)	18.4(6)	-0.5(5)	3.4(5)	-0.7(5)
C1	17.1(7)	9.2(6)	21.2(7)	0.4(5)	4.3(5)	-2.6(5)
C8	19.9(7)	15.5(7)	18.1(7)	-4.4(5)	3.4(5)	-3.5(5)
C11	15.9(6)	15.2(6)	16.9(7)	-2.3(5)	2.3(5)	-2.0(5)
C6	14.9(6)	11.4(6)	17.8(7)	-1.8(5)	2.3(5)	-2.3(5)
C7	18.7(7)	13.7(6)	19.8(7)	-4.1(5)	4.9(5)	-4.2(5)
C3	14.3(6)	8.4(6)	18.1(6)	-0.9(5)	3.0(5)	-1.8(5)
C9	17.0(6)	13.6(6)	18.2(7)	-2.8(5)	3.1(5)	-1.7(5)
C10	17.9(7)	15.1(6)	18.1(7)	-3.8(5)	2.4(5)	-2.7(5)
C12	18.2(7)	9.8(6)	22.6(7)	0.6(5)	0.4(5)	-2.9(5)
C13	23.9(8)	14.0(7)	30.1(8)	-5.1(6)	3.0(6)	-5.3(6)
C17	20.4(8)	18.5(7)	32.2(8)	1.4(6)	2.8(6)	-10.0(6)
C15	33.1(9)	18.2(8)	36.4(9)	2.2(6)	-6.7(7)	-13.0(6)
C16	28.3(8)	23.0(8)	34.0(9)	6.6(6)	-0.7(7)	-14.0(7)
C14	32.0(9)	17.1(7)	35.8(9)	-4.8(7)	-0.7(7)	-10.1(6)
C18	54.2(12)	35.9(10)	26.7(9)	-29.7(9)	16.4(8)	-10.1(7)
C19	82.1(17)	52.4(14)	36.4(11)	-50.6(13)	26.8(12)	-16.4(10)
H00C	39(12)	38(12)	23(11)	-7(10)	-2(9)	-8(9)
H00D	56(14)	39(12)	16(4)	-2(10)	7(3)	-6(2)
H00F	34(11)	20(9)	54(13)	-10(5)	-7(7)	-11(6)
H00K	38(13)	52(15)	62(15)	-25(11)	31(12)	-40(12)
H00I	48(13)	35(12)	50(13)	-6(11)	1(11)	-13(11)
H005	38(12)	50(14)	56(16)	-20(6)	8(8)	16(9)
H004	62(17)	38(14)	65(18)	-32(14)	22(14)	0(13)
H00M	110(20)	31(9)	57(13)	-4(10)	-6(13)	-30(6)

H00N	46(14)	79(18)	50(14)	5(13)	16(12)	-37(14)
H00a	38(14)	6(11)	100(20)	3(11)	12(14)	-6(12)
H00b	52(16)	47(15)	42(15)	15(13)	8(13)	-17(13)
H00h	79(12)	81(16)	80(20)	-42(6)	17(9)	-44(12)
H00O	24(12)	31(13)	130(20)	-16(11)	18(14)	-9(14)
H00e	140(20)	69(16)	80(19)	18(9)	76(13)	12(11)
H00j	180(30)	57(18)	69(11)	-36(17)	-27(8)	-22(10)
H00L	52(16)	47(15)	120(20)	0(13)	59(16)	1(15)
H00g	66(12)	100(20)	44(11)	-35(10)	5(6)	19(9)
H00p	220(30)	84(12)	67(19)	-115(10)	40(20)	-28(10)

Table 4 Bond Lengths for 4.12.

Atom	Atom	Length/Å	Atom	Atom	Length/Å
O2	C5	1.2411(16)	C4	C3	1.4677(17)
O1	C1	1.2187(16)	C8	C7	1.3793(19)
O3	C9	1.3612(16)	C8	C9	1.4014(19)
O3	C18	1.4174(18)	C11	C6	1.3953(18)
N1	C4	1.4062(16)	C11	C10	1.3999(19)
N1	C1	1.3662(17)	C6	C7	1.3999(19)
N4	C5	1.3585(17)	C9	C10	1.392(2)
N4	C12	1.4055(17)	C12	C13	1.397(2)
N3	C4	1.2821(17)	C12	C17	1.396(2)
N3	C6	1.4085(17)	C13	C14	1.392(2)
N2	C2	1.3267(17)	C17	C16	1.389(2)
C2	C1	1.5025(17)	C15	C16	1.392(2)
C2	C3	1.3750(18)	C15	C14	1.388(2)
C5	C3	1.4606(17)	C18	C19	1.507(2)

Table 5 Bond Angles for 4.12.

Atom	Atom	Atom	Angle/°	Atom	Atom	Atom	Angle/°
C18	O3	C9	118.29(11)	C7	C6	N3	115.83(11)
C1	N1	C4	111.02(11)	C7	C6	C11	118.74(12)
C12	N4	C5	128.43(12)	C6	C7	C8	121.19(13)
C6	N3	C4	124.60(11)	C5	C3	C2	123.88(12)
C1	C2	N2	120.97(12)	C4	C3	C2	107.90(11)
C3	C2	N2	131.28(12)	C4	C3	C5	127.86(12)
C3	C2	C1	107.74(11)	C8	C9	O3	115.30(12)
N4	C5	O2	124.93(12)	C10	C9	O3	124.96(12)

C3	C5	O2	119.77(12)	C10	C9	C8	119.72(13)
C3	C5	N4	115.29(11)	C9	C10	C11	119.97(13)
N3	C4	N1	129.94(12)	C13	C12	N4	123.96(13)
C3	C4	N1	106.84(11)	C17	C12	N4	116.73(12)
C3	C4	N3	123.11(12)	C17	C12	C13	119.25(13)
N1	C1	O1	127.74(12)	C14	C13	C12	119.74(15)
C2	C1	O1	125.84(12)	C16	C17	C12	120.56(15)
C2	C1	N1	106.42(11)	C14	C15	C16	119.20(14)
C9	C8	C7	119.84(13)	C15	C16	C17	120.24(15)
C10	C11	C6	120.41(13)	C15	C14	C13	121.00(15)
C11	C6	N3	125.43(12)	C19	C18	O3	107.69(14)

Table 6 Torsion Angles for 4.12.

A	B	C	D	Angle/°	A	B	C	D	Angle/°
O2	C5	N4	C12	-13.23(18)	N4	C12	C13	C14	-175.72(15)
O2	C5	C3	C2	0.25(16)	N4	C12	C17	C16	175.42(13)
O2	C5	C3	C4	172.49(12)	N3	C4	C3	C2	173.94(14)
O1	C1	N1	C4	-179.84(15)	N3	C4	C3	C5	0.71(16)
O1	C1	C2	N2	-1.99(17)	N3	C6	C11	C10	176.87(13)
O1	C1	C2	C3	178.19(15)	N3	C6	C7	C8	-176.70(12)
O3	C9	C8	C7	179.51(12)	N2	C2	C3	C5	-3.50(18)
O3	C9	C10	C11	-179.57(13)	N2	C2	C3	C4	-177.06(16)
N1	C4	N3	C6	3.50(18)	C8	C7	C6	C11	3.89(16)
N1	C4	C3	C2	-2.59(12)	C8	C9	C10	C11	1.87(15)
N1	C4	C3	C5	-175.82(10)	C12	C13	C14	C15	0.02(18)
N1	C1	C2	N2	177.89(11)	C12	C17	C16	C15	1.03(18)
N1	C1	C2	C3	-1.93(12)	C13	C14	C15	C16	-0.67(19)
N4	C5	C3	C2	-179.10(11)	C17	C16	C15	C14	0.16(19)
N4	C5	C3	C4	-6.86(15)					

Table 7 Hydrogen Atom Coordinates (Å×10⁴) and Isotropic Displacement Parameters (Å²×10³) for 4.12.

Atom	*x*	*y*	*z*	U(eq)
H00C	5783(13)	5400(20)	4843(7)	34(5)
H00D	5971(13)	4180(20)	3026(7)	37(5)
H00F	6790(12)	6920(20)	4334(8)	37(5)
H00K	9397(14)	11150(30)	3307(9)	49(7)
H00I	5024(14)	2630(20)	3511(8)	44(5)

H005	7493(15)	8500(30)	3421(9)	48(6)
H004	7233(17)	3570(30)	2945(10)	54(7)
H00M	8421(18)	14340(20)	4403(9)	68(8)
H00N	7065(14)	12800(30)	4386(8)	58(7)
H00a	9745(15)	7250(20)	2422(10)	46(7)
H00b	9778(15)	5260(30)	2216(9)	47(6)
H00h	3430(20)	1880(30)	4864(11)	80(8)
H00O	9617(13)	13530(20)	3838(11)	61(8)
H00e	4870(20)	980(30)	4201(11)	93(10)
H00j	4350(20)	1080(30)	5137(11)	103(11)
H00L	6884(16)	10470(30)	3865(11)	70(8)
H00g	3964(17)	2140(30)	4025(9)	71(8)
H00p	3670(30)	20(40)	4676(11)	124(12)

Experimental

Single crystals of $C_{19}H_{18}N_4O_3$ (**4.12**) were recrystallized from acetonitrile. A suitable crystal was selected and **[]** on a **XtaLAB Synergy, Dualflex, HyPix** diffractometer. The crystal was kept at 100.0(2) K during data collection. Using Olex2 [1], the structure was solved with the ShelXT [2] structure solution program using Intrinsic Phasing and refined with the ShelXL [3] refinement package using Least Squares minimisation.

1. Dolomanov, O.V., Bourhis, L.J., Gildea, R.J, Howard, J.A.K. & Puschmann, H. (2009), J. Appl. Cryst. 42, 339-341.
2.
3. Sheldrick, G.M. (2015). Acta Cryst. C71, 3-8.

Crystal structure determination of 4.12

Crystal Data for $C_{19}H_{18}N_4O_3$ (M =350.380 g/mol): monoclinic, space group I2/a (no. 15), a = 15.3981(5) Å, b = 8.65781(19) Å, c = 26.5131(8) Å, β = 95.216(3)°, V = 3519.94(17) Å^3, Z = 8, T = 100.0(2) K, μ(Cu Kα) = 0.755 mm^{-1}, $Dcalc$ = 1.322 g/cm^3, 14790 reflections measured (6.7° ≤ 2Θ ≤ 140.58°), 3270 unique (R_{int} = 0.0407, R_{sigma} = 0.0256) which were used in all calculations. The final R_1 was 0.0366 (I>=2u(I)) and wR_2 was 0.1021 (all data).

Refinement model description

Number of restraints - 27, number of constraints - 0.
Details:
1. Rigid body (RIGU) restrains
C11, H00D
with sigma for 1-2 distances of 0.003 and sigma for 1-3 distances of 0.003
C19, H00p
with sigma for 1-2 distances of 0.005 and sigma for 1-3 distances of 0.005
C19, H00h
with sigma for 1-2 distances of 0.005 and sigma for 1-3 distances of 0.005
H005, N4

with sigma for 1-2 distances of 0.005 and sigma for 1-3 distances of 0.005
C18, H00e
with sigma for 1-2 distances of 0.005 and sigma for 1-3 distances of 0.005
C15, H00M
with sigma for 1-2 distances of 0.005 and sigma for 1-3 distances of 0.005
H00j, C19
with sigma for 1-2 distances of 0.005 and sigma for 1-3 distances of 0.005
C7, H00F
with sigma for 1-2 distances of 0.005 and sigma for 1-3 distances of 0.005
C18, H00g
with sigma for 1-2 distances of 0.005 and sigma for 1-3 distances of 0.005